

1. Report No. FHWA/IN/JTRP-2003/7	2. Government Accession No.	3. Recipient's Catalog No.	
4. Title and Subtitle Beta Testing Implementation of the Purdue Time Domain Reflectometry (TDR) Method for Soil Water Content and Density Measurement		5. Report Date August 2003	
7. Author(s) Vincent P. Drnevich, Xiong Yu, and Janet E. Lovell		6. Performing Organization Code 8. Performing Organization Report No. FHWA/IN/JTRP-2003/7	
9. Performing Organization Name and Address Joint Transportation Research Program 1284 Civil Engineering Building Purdue University West Lafayette, IN 47907-1284		10. Work Unit No. 11. Contract or Grant No. SPR-2489	
12. Sponsoring Agency Name and Address Indiana Department of Transportation State Office Building 100 North Senate Avenue Indianapolis, IN 46204		13. Type of Report and Period Covered Final Report 14. Sponsoring Agency Code	
15. Supplementary Notes Prepared in cooperation with the Indiana Department of Transportation and Federal Highway Administration.			
16. Abstract The Purdue TDR method is a new technology for simultaneously measuring soil water content and dry density insitu. An ASTM standard for using TDR to measure soil water content and dry density based on Purdue TDR method was approved during the time span of this project and is designated ASTM D6780. The primary objective of this study was to take the Purdue TDR Method to the point where it is widely field tested by users on a broad spectrum of soils around the country. This goal was achieved by involving researchers at other universities and practitioners in federal and state agencies and in private practice firms. The results and feedback was obtained from Beta Partners by Purdue University for evaluation and further analysis. Major achievements in this research include: 1) Involvement of Beta Partners - Six Beta partners including two universities, two private firms and two state DOTs were involved in this project and instructions were provided to each Beta Partners. Involving these Beta partners provided a large span of field applications and research feedback. Results from testing performed were compared with existing technologies and provided the basis for the precision and bias statements needed for ASTM D6780. Based on feedback from extensive field tests, testing procedures were improved. Meanwhile, the testing equipment was refined and integrated, which made the testing system both more robust and easier to handle. The overall cost of the testing system has also been significantly reduced, which made it more economically competitive for mass production. 2) Testing automation - A new generation of electronics was identified and incorporated into the Purdue TDR test, the new TDR100 by Campbell Scientific, Inc. Corresponding software for automation was designed and systematically improved. This provided a user friendly interface and facilitated performance of TDR testing process. Preliminary feedback from using the computer software is satisfactory. The efforts and achievements on testing automation also built up the basis for a developing a more compact package in the future. 3) One step method for TDR testing - A simplified procedure to that described by ASTM D6780 to measure soil water content and dry density was discovered, which is an important product of this project. The simplified procedure is called the one-step method since it only requires one field TDR reading. The one-step method achieved this simplification by incorporating information of bulk electrical conductivity from TDR signal in addition to the apparent dielectric constant used by previous TDR test. A scheme to account for the difference between field conditions and laboratory situations was developed, which serves as the basis of the one step method. A simplified temperature compensation scheme was also designed which makes it possible for the one-step method to deal with complex field situations. Computer software was developed to automate the performance of one-step method in the field. TDR for non-conventional materials - The discoveries in developing the one step method as well as the advancement in software development significantly expanded the application domain of the TDR system. More potential new applications for TDR technology in civil engineering practice were identified. One of these is the application of TDR to non-conventional materials such as fly ash, lime stabilized soil and Portland cement concrete. The range of applications for the TDR technology developed in this research is ever broadening and will have significant impact in the future on the testing of civil engineering materials.			
17. Key Words Time Domain Reflectometry, TDR, apparent dielectric constant, permittivity, conductivity, bulk electrical conductivity, soils, gravels, sands, silts, clays, water content, compaction, density, dry density.		18. Distribution Statement No restrictions. This document is available to the public through the National Technical Information Service, Springfield, VA 22161	
19. Security Classif. (of this report) Unclassified	20. Security Classif. (of this page) Unclassified	21. No. of Pages 237	22. Price

Final Report

FHWA/IN/JTRP-2003/7

**BETA TESTING IMPLEMENTATION OF THE
PURDUE TIME DOMAIN REFLECTOMETRY (TDR)
METHOD FOR SOIL WATER CONTENT AND
DENSITY MEASUREMENT**

Vincent P. Drnevich¹
Xiong Yu²
Janet Lovell³

School of Civil Engineering
Purdue University

Joint Transportation Program
Project No. 656-1284-0156
File No.: 6-6-21

Prepared in Cooperation with the
Indiana Department of Transportation and
The U.S. Department of Transportation
Federal Highway Administration

The contents of this report reflect the views of the authors who are responsible for the facts and the accuracy of the data presented herein. The contents do not necessarily reflect the official views or policies of the Federal Highway Administration and the Indiana Department of Transportation. This report does not constitute a standard, specification or regulation.

Purdue University
West Lafayette, Indiana
August 13, 2003

¹ Principal Investigator and Professor of Civil Engineering

² Graduate Assistant

³ Laboratory Manager, Geotechnical and Materials Laboratories

TABLE OF CONTENTS

	Page
LIST OF TABLES	v
LIST OF FIGURES	vii
 CHAPTER 1 – INTRODUCTION	
1.1 Background.....	1
1.2 Problem and Objective Statement.....	2
1.3 Scope of Work	2
1.5 Report Scheme.....	5
 CHAPTER 2 – BETA TESTING PARTNERS	
2.1 Statement of Objective.....	7
2.2 Description of Beta Partners	8
2.3 Interactions with Beta Partners	8
 CHAPTER 3 – TDR APPARATUS ASSEMBLY AND HARDWARE REFINEMENT	
3.1 Statement of Objective.....	10
3.2 TDR System Design and Refinement	10
3.2.1 Initial Purdue TDR System Design	10
3.2.2 Refinement in Subsequent Project.....	11
3.2.3 Updating TDR Hardware System in This Beta Test Project	12
3.3 Tool Case, Electronic Case and Wiring of TDR Testing System.....	28
3.4 Use of CSI Probes.....	33
 CHAPTER 4 – DEVELOPMENT OF SOFTWARE FOR TESTING AUTOMATION	
4.1 Statement of Objective.....	34
4.2 Algorithms for TDR Waveform Analysis.....	36
4.2.1 Reflection Model for TDR Waveform.....	37
4.2.2 Overview of Algorithms to Pick Reflection Points	39
4.2.3 Previous Algorithm Used at Purdue University	43
4.2.4 Objective for New Algorithm Development.....	43
4.2.5 Verification in Typical Conditions	47
4.3 Algorithm for Bulk Electrical Conductivity of Soil	53
4.3.1 Electrical Conductivity from Attenuation Analysis.....	53
4.3.2 Conductivity from Long Term TDR Response	56
4.4 TDR Software Development.....	60
4.4.1 Introduction to PMTDR Program	60
4.4.2 Introduction to PMTDR-RDR Program.....	63
4.4.3 Introduction to PMTDR-SM Program.....	65

CHAPTER 5 – TESTING PROCEDURES AND REFINEMENT

5.1	Progress of ASTM Standardization	80
5.2	Summary of Testing Procedures	80
	5.2.1 Field Testing Process: MRP insitu test and CMP mold test	81
	5.2.2 Data Reduction Process to Obtain Soil Water Content and Density from TDR Measurement	88
	5.2.3 Laboratory to Determine Soil Dependent Parameters <i>a</i> and <i>b</i>	89
5.3	Insulated Center Probe for Testing in Lossy Soil	92
	5.3.1 Principle of Energy Loss.....	93
	5.3.2 Mechanism of Insulation and Scheme for Data Reduction	94
	5.3.3 Procedure for Field Practice	98
5.4	Summary	101

CHAPTER 6 – ONE STEP METHOD FOR SOIL WATER CONTENT AND DRY DENSITY

6.1	Introduction.....	103
6.2	Basic Principles of One Step Method	103
	6.2.1 Soil Apparent Dielectric Constant and Bulk Electrical Conductivity from TDR Waveforms.....	103
	6.2.2 Calibration Relation for Soil Apparent Dielectric Constant.....	106
	6.2.3 Calibration Relation for Bulk Soil Electrical Conductivity.....	109
	6.2.4 The Soil Apparent Dielectric Constant-Bulk Electrical Conductivity Relationship	113
	6.2.5 Use of A Standard Pore Fluid to Calculate Soil Water Content and Dry Density	114
6.3	Application Procedure for One Step Method	117
6.4	Temperature Compensation for the One Step Method	122
6.5	The One-Step Method for Testing Large Particles and Highly Conductive Soils	125
6.5	Typical Results	127
6.6	Conclusions.....	129

CHAPTER 7 – RESULTS FROM PURDUE WORKING WITH BETA PARTNERS

7.1	University of South Florida and Florida DOT	131
	7.1.1 Experimental Results of Calibration Constants <i>a</i> and <i>b</i> of Sands around Florida	131
	7.1.2 Effects of Compaction Energy on the Values of the Soil Constants <i>a</i> and <i>b</i>	133
	7.1.3 Effects of the Accuracy of Constants <i>a</i> and <i>b</i> on the Resulting Moisture Content	134
	7.1.4 Accuracy of TDR Measurements	139
	7.2.5 Summary of the Results by the University of South Florida	139

7.2	GAI Consultants	141
	7.2.1 LPC Material	142
	7.2.2 Experiments on Class C Fly Ash.....	149
	7.2.3 Experiments on Harrison Fly Ash.....	152
	7.2.4 Conclusions	154
7.3	INDOT Site.....	154
	7.3.1 INDOT Division of Research.....	155
	7.3.2 I-70 Relocation Project near Indianapolis Airport.....	163
	7.3.3 Summary of Findings from INDOT.....	168
7.4	H.C. Nutting Company	169
	7.4.1 Maxwell Silo Ash	169
	7.4.2 Airport Site	172
	7.4.3 Brown County Soils.....	178
	7.4.4 Summary of H.C. Nutting Tests	182
7.4	Rutgers University	182

CHAPTER 8 – SUGGESTIONS FOR FUTURE IMPLEMENTATION

8.1	Improvement to Support Implementation of Original TDR Method.....	184
8.2	Laboratory Tests to Establish Soil Parameters for the One-Step Method	185
8.3	Quality Control in Construction Operation with the One-Step Method.....	189
8.4	Monitoring Performance.....	191
8.5	Movement of the Technology to the Market Place.....	192
	9.1.1 Discussions with Potential Firms to Manufacture, Market, and Service the TDR Method.....	192
	9.1.2 Interaction with the Management 451 Class in the Krannert School of Business to Obtain Marketing Plans.....	192

CHAPTER 9 – RECOMMENDATIONS FOR FUTURE RESEARCH

9.1	Application of TDR for Regional Soils	193
9.2	Stabilized Soils	194
	9.2.1 Chemically Stabilized Soils	194
	9.2.2 Mechanically Stabilized Soils.....	194
9.3	Other Civil Engineering Materials.....	195
	9.3.1 Asphalt	195
	9.3.2 Concrete	196
9.4	Future Research in the Frequency Domain.....	197
9.5	Summary of Recommendations for Future Research	198

CHAPTER 10 – SUMMARY AND CONCLUSIONS

ACKNOWLEDGMENTS

REFERENCES.....	202
------------------------	------------

APPENDICES

I.	Notation	207
II.	Comparison of PCTDR and PMTDR-RDR with CSI 605 Probe	208
III.	Database Management System Design.....	229

LIST OF TABLES

Table	Page
2-1 Initial List of Expected Participants.....	7
2-2 Up-to-date List of Beta Test Participants	8
3-1 Major Parameters of Tektronix 1502B	13
3-2 Campbell Scientific, TDR100 Time Domain Reflectometer.....	14
3-3 Commercially Available Metallic TDR Pulse Generators	15
5-1 Typical Values of Apparent Dielectric Constant for Air, Water, and Dry Soil and Rock	91
5-2 Range of Expected Valuea of a for Dry Soil	92
7-1 Values of Constants a and b for Various Florida Soil Types	131
7-2 Different Tests Performed to Study the Effect of Compaction Energy	133
7-3 Error Resulting from Changing the Constant a	135
7-4 Error resulting from Changing the Constant b	137
7-5 TDR Measured Results Using Default Settings versus Oven Dry Result	140
7-6 Typical compositions of Class F and Class C ashes as defined by ASTM (1997)....	149
7-7 TDR Measured Water Content, Dry Density versus Results by Nuclear Total Density and Stove-Top-Cooked Water Contents for INDOT I-70 Soils	168
7-8 Maxwell Silo Ash Data from HCN with PMTDR.....	170
7-9 Maxwell Silo Ash Data Reanalyzed with PMTDR-RDR.....	171
7-10 Compaction Data for Airport Site Soil	173
7-11 TDR Calibration Factors for Airport Soil.....	174
7-12 Comparison of Results for Airport Site	176

Table	Page
A2-1. Low Energy Hand Compaction, (9 lifts, 30 blows per lift) in Test Phase I	218
A2.2. Data for Calibration Factors a and b for INDOT Soil with Low Energy Hand Compaction Using 4-in. Dia. by 9-in. High TDR Mold with Purdue TDR Probe.....	219
A2.3. Data for Determination of a and b for INDOT Soil under Low Energy Hand Compaction from PMTDR-RDR with 6-in. Dia. by 12-in. Plastic Mold with CSI605 Probe.....	220
A2-4. Calibration Factors a and b Obtained from Low Energy Hand Compaction for INDOT Soil	221
A2-5. The comparison of gravimetric water contents from oven-dry method and those by PMTDR-RDR program with CSI605 probe	222
A2-7. Data to Calculate a and b for INDOT Soil under High Energy Hand Compaction from PMTDR-RDR with CSI 605 probe.....	225
A2-8. The Comparison of Volumetric Water Content by Different Programs.....	226
A3-1 Compaction Table with Sample Data	231
A3-2 A Part of Agency Table with Sample Data.....	231
A3-3 GSD Table with Sample Data.....	232
A3-4 Lab Table with Sample Data.....	232

LIST OF FIGURES

Figure	Page
3.1 Photo of : (a) Tektronix 1502B; (b) Campbell Scientific TDR 100	16
3.2 Comparison of TDR Waveforms on the Same Specimen with the Same Probe: (a)Tektronix 1502B; (b) Campbell Scientific TDR100	17
3.3 Old and New MRP heads (a) Old MRP Head (b) New MRP Head	18
3.4 Coaxial Cable with Impedance of 50 ohms	19
3.5 Manufactured Field Probe Rods (Spikes).....	21
3.6 Photos of Guide Template for the Multiple Rod Field Probes	22
3.7 Photo of Guide for Installing Center Rod.....	23
3.8 Photo of Compaction Mold with Height Twice That of the Standard Compaction Mold	23
3.9 Photo of Hand Tamper.....	24
3.10 Photo of Balance.....	24
3.11 Photo of Digital Thermometers: (a) Old Version; (b) New Version	25
3.12 Hammers: (a) Insitu Probe Rod Installation; (b) Mold Rod Installation	26
3.13 Power Drill with Bit.....	27
3.14 Supplementary Tools	27
3.15 Case 1 Containing TDR Measurement Equipment and Tools.....	29
3.16 TDR Electronics	30
3.17 Layout of TDR100 and Power Sources in Case	31
3.18 Pull Switch to Supply Power to TDR100 from PS12 Power Supply	31
3.19 Cables to MRP and Computer through Case Deck.....	32

Figure	Page
3.20 Wiring Diagram of Components in Case 2.....	32
4.1 Interface of TDR++ Program.....	34
4.2 TDR System using Tektronix 1502B Cable Tester	35
4.3 TDR System Schematic: a) Reflections in the TDR system and b) Resulting TDR Waveform	38
4.4 Two Methods to Manual Identify Second Reflection Point	40
4.5 Smoothing the Curve Improve the First Derivative Value	41
4.6 Measured and Predicted TDR Waveforms from the Reflection Models (Timlin and Pachepsky, 1996)	42
4.7 Typical TDR Waveforms likely to Be Encountered in Field	44
4.8 Noise Level in a TDR System: a) Standard Deviation of Ten Measurements; b) Noise-to-Signal Ratio across the Frequency Bandwidth	46
4.9 Analysis of TDR Measurement in Water (a) Deionized Water; (b) Tap Water	47
4.10 TDR Measured Dielectric Constant of Water.....	48
4.11 Comparison of Reflection Pattern at First Reflection Point a) Enlargement of the First Reflection of a Small 0.10 m Triple Wire Probe (Heimovaara, 1990); b) Enlargement of the First Reflection Measured by Purdue TDR Device	49
4.12 TDR Measurement and Analysis in Dry Ottawa Sand	50
4.13 TDR Signal Measured for Wet-to-Dry and Dry-to-Wet Cases	51
4.14 Locations of Reflection Points Picked by the Algorithm (a) Wet-over-Dry Case (First Point=1.923m Second Point 2.418, $K_a=4.64$) (b)Dry-over-Wet Case (First Point=1.930m Second Point 2.438 $K_a=4.88$).....	52
4.15 Likelihood of “Contaminated” Signal (Heimovarra, 1990).....	54
4.16 Definition of Voltage Levels in a TDR Waveform for Determining Bulk Electrical Conductivity.....	55

Figure	Page
4.17 Model for Long-term Static Response (a) Dynamic Model; (b) Equivalent Static Model for Long Term Response	57
4.18 Response of TDR System with Parameters $V_{in}=1.986$ V, $Z_s=R_s=50$ Ohms, $Z_L=R_L=1000$ Ohms, $L=0.25$ m (a) Step Pulse; (b) $Z_p=100$ Ohms; (c) $Z_p=500$ Ohms; (d) $Z_p=10$ Ohms	58
4.19 Interface of PMTDR Program (a) Screen for Field MRP test (b)Screen for Mold CMP Test	62
4.20 User Interface of the PMTDR-RDR Program: (a) Screen for Field (MRP) TDR Test; (b) Screen for Mold (CMP) TDR Test	64
4.21 MRP Screen for Field TDR Test	66
4.22 CMP Screen for Mold TDR Test	66
4.23 Set Measurement Parameters in Measurement Parameters Window	67
4.24 Two TDR Waveforms are Displayed on the Screen.....	68
4.25 Dialog Window Warning of a Hardware Connection Problem	69
4.26 Display after a Completed Analysis with PMTDR-SM	70
4.27 Save Test Results by Clicking File->Save Test Results Menu.....	71
4.28 Content in Configuration File	72
4.29 Click File->Load Configuration to Load Configuration Files.....	72
4.30 Calibration Toolbox	73
4.31 Content of Data File for Calibration	74
4.32 Use File->Open Menu to Load Calibration Data File	74
4.33 Data in Calibration Data File are Displayed in a Table on the Screen	75
4.34 Input Calibration Data Directly to the Data Table.....	76
4.35 Click Plot Calibration Data to Calculate Calibration Constants.....	76

Figure	Page
4.36 Remove Dad Data and Recalculated Calibration	77
4.37 Calibration Results Stored in Data File	78
4.38 Display Different TDR Waveforms for Comparison.....	79
5.1 Driving Probes through Template for Field Test.....	82
5.2 Remove Template to Expose Probes	82
5.3 Simulation of Coaxial Cable by Probes	83
5.4 Place MRP Head on Probe Rods	83
5.5 Computer Program to Obtain TDR Waveform and Make Analysis.....	84
5.6 Remove Soil with Power Drill.....	85
5.7 Compacting Soil into Compaction Mold	85
5.8 Measure the Mass of Soil with Balance.....	86
5.9 Drive the Center Pin through the Guide	86
5.10 Place MRP Head on Mold Using Adapter Ring.....	87
5.11 Obtain TDR waveform and Computer Soil Water Content and Dry density	87
5.12 Plot to Determine a and b Values	90
5.13 Information Contained in a Typical TDR Curve	93
5.14 TDR waveform in lossy soil	94
5.15 Waveform before and after Using Insulated Probe.....	95
5.16 Contours of Dimensionless Electrical Field Distribution Normal to Direction of Probe Insertion for a Material of Uniform Dielectric Constant (from Zegelin et al., 1989).....	96
5.17 Cross Section of the Insulated Probe	96
5.18 Calibration Curve for Insulated Probe.....	97

Figure	Page
5.19 Calibration Data for a Field Probe with an Insulated Center Rod	99
5.20 Calibration Data for a Mold Probe with an Insulated Center Rod.....	99
6.1 Influence of Soil Properties on TDR Waveform: (a) Same Dry Density, Different Gravimetric Water Content; (b) Same Gravimetric Water Content, Different Dry Density	104
6.2 TDR Measured Conductivity Versus Conductivity Meter Measurement	105
6.3 Calibration of Dielectric Constant Using Different Pore Fluid: (a) Clayey Soil, PL=20, LL=32; (b) ASTM Graded Sand.....	108
6.4 Relationship between Bulk Electric Conductivity and Gravimetric Water Content at Given Pore Fluid Conductivity using Data by Amenta et al. (2000).....	112
6.5 Schema of “Adjustment” Process: (a) Vertical Projection to “Adjust” Field Measurement; (b) Phase Diagram of Field Sample and “Adjusted” Sample Represented by Points in Fig. 6. 5(a).....	116
6.6 Mold test procedures (a) Driving Central Rod through a guide placed on the mold (b) Multiple Rod Probe Head ready for making TDR measurements.....	118
6.7 An Example of Calibration on ASTM Graded Sand: (a) Calibration of K_a ; (b) Calibration of EC_b ; (c) Calibration of K_a and EC_b	119
6.8 Field Test Procedures: (a) Spikes Being Driven through Template into Soil Surface; (b) Multiple Rod Probe Head on Spikes for Measurement.....	121
6.9 Schematic Presentation of Temperature Correction for One Step Method	123
6.10 Results by Simplified Temperature Correction Approach on ASTM Graded Sand.....	125
6.11 Comparison of TDR Water Contents with Oven-Dry Gravimetric Water Contents for Testing on Indiana 53. (Results are typically accurate to within +/- 1 percentage point.)	126
6.12 Comparison of TDR Water Contents with Oven-Dry Gravimetric Water Contents. (Results are typically accurate to within +/-0.01).....	128
6.13 Comparison of TDR Dry Density with Dry Density Determined from Total Density (direct measurement, sand cone, or nuclear) with Oven Drying for Water Content (Results are typically within +/- 3 percent.)	129

Figure	Page
7.1 Final Results of the TDR Tests in Mold for Various Soil Types	132
7.2 Effect of Compaction Energy on Constants a and b	133
7.3 Error Resulting from Changing the Constant a on the Predicted Moisture Content .	136
7.4 Results of Changing the Constant b on the Predicted Moisture Content	138
7.5 Rostraver LPC a and b Constants Using an Insulated Probe (performed on Mar 22, 2002)	143
7.6 Rostraver LPC a and b constant using insulated probe (performed on Mar 22, and May 05, 2002, respectively).....	144
7.7 Proposed bilinear calibration curve for LPC material using insulated probe	144
7.8 Calibration for a and b using Converted Soil Apparent Dielectric Constants.....	146
7.9 Difference in Conductivity of LPC at Low Water Content versus High Water Content	146
7.10 Compaction Curve of LPC.....	147
7.11 Relationship between Apparent Dielectric Constant and Water Content Using Short Probes in a Standard Compaction Mold	148
7.12 Relationship between Electrical Conductivity and Water Content Using Short Probes in a Standard Compaction Mold	148
7.13 Compaction Behavior of Class C Fly Ash Using Tap Water and Deionized Water	150
7.14 Fly Ash Apparent Dielectric Constant Calibrations Using Tap and Deionized Water	151
7.15 Fly Ash Bulk Electrical Conductivity Calibrations Using Tap and Deionized Water	151
7.16 Calibration Curve of Harrison Fly Ash.....	152
7.17 TDR Water Content versus Oven Dry Water Content.....	153
7.18 TDR Dry Density versus Dry Density Calculated by Total Density and Oven Dry Water Content.....	153

Figure	Page
7.19 Standard Compaction Curves of Glacial Till Subgrade Using Tap and Deionized Water for the INDOT, Div. of Research Test Pavement Site.....	156
7.20 Calibration Curves of Glacial Till using Tap and Deionized Water.....	157
7.21 Water Content versus Location by TDR, Nuclear and Oven Drying at INDOT Div. of Research Test Lane Site (Location 0 is on the East End of the Site.)	158
7.22 Dry Density versus Location by TDR and Nuclear Method at INDOT Div. of Research Test Lane Site (Location 0 is on the East End of the Site.)	158
7.23 Compaction Curve of Indiana 53 Used at INDOT, Div of Research Test Pavement Site	159
7.24 Calibration of Apparent Dielectric Constant for Indiana 53 Used at INDOT, Div of Research Test Pavement Site	160
7.25 Calibration of Bulk Electrical Conductivity for Indiana 53 Used at INDOT, Div of Research Test Pavement Site	160
7.26 Relationship between Apparent Dielectric Constant and Bulk Electrical Conductivity for Indiana 53 Used at INDOT, Div of Research Test Pavement Site	161
7.27 TDR Measured Water Contents and Oven Dry Water Contents at INDOT Div. of Research Test Lane Site (Location 0 is on the East End of the Site.)	162
7.28 Calibrations for Apparent Dielectric Constant Using All Five Data Points versus only Using First Four Points	163
7.29 Standard Compaction Curves for Virgin Soil and Lime Stabilized Soil (around 3~6% lime) for INDOT I-70 Relocation Site.....	165
7.30 Calibration Factor Determination for Apparent Dielectric Constant for INDOT I-70 Relocation Site	165
7.31 Calibration for Bulk Electrical Conductivity for Soil from INDOT I-70 Relocation Site	166
7.32 Monitoring of Lime Hydration Process for Soil from INDOT I-70 Relocation Site	166
7.33 Calibration of Apparent Dielectric Constant for Soils at the INDOT I-70 Site	167

Figure	Page
7.34 Calibration of Maxwell Silo Ash	170
7.35 TDR Measured Water Content and Dry Density of Maxwell Silo Ash	171
7.36 Screen Dumps of the TDR Data for Test 3 on Maxwell Silo Ash.....	171
7.37 Modified Compaction Test Results for Airport Soil	173
7.38 Plot to Obtain Calibration Factors <i>a</i> and <i>b</i> for Airport Soil	174
7.39 Plot to Obtain Calibration Factors <i>c</i> and <i>d</i> for Airport Soil.....	175
7.40 Plot to Obtain Calibration Factors <i>f</i> and <i>g</i> for Airport Soil	175
7.41 Dry Density versus Water Content from TDR Calibration Tests by H.C. Nutting	179
7.42 Calibration Curve for Brown Country Clay from Calibration Test at H.C. Nutting	180
8.1 Driving the Central Rod through the Rod Guide Placed on Mold.....	186
8.2 Placement of the MRP Head on the Mold using the Adaptor Ring.....	187
8.3 An Example of Calibration on ASTM Graded Sand: (a) Calibration of K_a ; (b) Calibration of EC_b ; (c) Calibration of K_a versus EC_b	188
8.4 Field Test Procedures: (a) Spikes Being Driven through Template into Soil Surface; (b) Multiple Rod Probe Head on Spikes for TDR Measurement	190
8.5 Program to Obtain TDR Waveform and Determine Water Content and Dry Density for One-Step Method.....	191
A2.1. CSI 605 Probe by Campbell Scientific, Inc.	209
A2.2. PCTDR Sample Screen.....	210
A2.3. PMTDR-RDR Sample Screen	210
A2.4. Case Containing TDR100 and Computer, CSI 605 Probe.....	211
A2.5. Hand Tools and Equipment Used	212
A2.6. Fully Embedded CSI 605 Probe	212

Figure	Page
A2.7. Algorithms of PCTDR to determine K_a	214
A2.8 Algorithms of PMTDR-RDR to determine K_a	214
A2.9. Calibration Parameters a and b for Ottawa Silica Sand in the 12-inch Plastic Mold.....	215
A2.10 TDR Test in a 4.0-in Diameter by 9-in. High Metal Compaction Mold	216
A2.11 Soil from INDOT that Passed No.4 Sieve	217
A2.12 Low Energy Hand Compaction Curves of INDOT Soil.....	219
A2.13. Plot to Determine Calibration Parameters a and b for INDOT Soil in the 4-in. Dia. by 9-in. TDR Mold with Purdue TDR Probe	220
A2.14. Plot to Obtain Calibration Parameters a and b for INDOT Soil under Low Energy Hand Compaction in the 6-in. Dia. by 12-in. High Plastic Mold with CSI605 Probe	221
A2.15 Gravimetric Water Content from PMTDR-RDR with CSI 605 Probe Using Default Calibration Factors ($a=1$, $b=9$).....	223
A2.16 Gravimetric Water Content from PMTDR-RDR with CSI 605 Probe Using INDOT Soil Calibration Factors ($a=1.07$, $b=9.929$).....	223
A2.17. Comparison of Volumetric Water Contents from Different Software with the Oven-Dried Method for Low Energy Hand Compaction of INDOT Soil	224
A2.18. Plots to Obtain Calibration Parameters a and b for INDOT Soil in the 6-in. Dia. by 12-in. High Plastic Mold (high energy hand compaction).....	226
A2.19. Comparison of Volumetric Water Contents from PCTDR and PMTDR-RDR software with the Oven-Dried Method (High Energy Hand Compaction)	227
A3.1 Database Design Elements.....	235
A3.2 Database Schema	236
A3.3 Database interface.....	237

1. Introduction

1.1 Background

This project is titled *Beta Testing Implementation of the Purdue Time Domain Reflectometry (TDR) Method for Soil Water Content and Density Measurement*. The purpose of the project is to take the Purdue TDR Method, a new technology for measuring water content and density of soil, to the point where it is widely field tested by users on a broad spectrum of soils. The project aims to involve researchers at several universities and practitioners in federal and state agencies and in firms in private practice. Results from all these tests will then be compared with existing technologies and help to establish a comprehensive database that will be the basis for the precision and bias statements needed in the ASTM Standard associated with this method. Based on feedback from the participants, the project also made improvements to the procedures for performing the test and increased the robustness of the equipment. A new generation of TDR electronics was incorporated into the Purdue TDR method to replace the existing electronics which are expensive and are no longer manufactured.

There were three previous projects on use of TDR for measuring properties of soil. The first was to examine its feasibility for measurement of soil water content in conjunction with field density testing for construction control. A major breakthrough occurred in this project; a technique was developed that made it possible to measure both water content and density. The procedure was written up, published, and is the source of three patents.

The second project focused on developing an automated procedure for this test and for creating a draft ASTM Standard for the method. The automated, computer-based procedure was called TDR⁺⁺ and a draft standard was developed. The second project also developed procedures to remove the effects of the apparatus and cables.

The third project focused on obtaining a rational mathematical model for the propagation of an electromagnetic wave in the soil specimen so that the model could be used to better understand the testing process and provide more information about the soil being tested. An extension to the third project focused on examining the effects of

temperature and establishing the validity of the method for soils with large particle sizes and for soils with additives like fly ash, lime, etc.

The TDR method developed at Purdue is totally new and a radical departure from the current procedures used in geotechnical practice for measuring water content and density for soil. All the other applications of TDR technology are direct transfer of the existing technologies that are used in areas such as agriculture science. This greatly limited the advantage of TDR technology in geotechnical engineering practice. The new TDR technology developed here needs to be put into the hands of technicians engaged in routine testing and have the results compared with the more traditional methods such as the sand cone method and the nuclear method. This Beta Testing project performed these tasks and paved the way for implementation of this technology on a larger scale.

1.2 Problem and Objective Statement

The Purdue TDR Method is a new technology for measuring water content and density of soil, which are two important indicators for earthwork compaction quality control. The technology is proving to be accurate, non-contaminating, and efficient. These are strong motivators to get this technology widely used in geotechnical practice. In order to do this, the technology must be widely field tested on a broad spectrum of soils. There is also a need for improvements to the methods for performing the test and for increased robustness of the equipment. Efforts of this project were successful in getting an ASTM Standard Method of Test (ASTM D6780) for the method. The Standard will have to be updated to include precision and bias statements that are based on test results.

1.3 Scope of work

This project took the Purdue TDR method to the point where it is widely field tested by users on a broad spectrum of soils. Results from this testing were compared with existing technologies and are part of a comprehensive database that will be the basis for the precision and bias statements of the method. Improvements to the methods for performing the test and increased robustness of the equipment occurred in the project. The project introduced a new generation TDR electronics for this method. Participants in

the project included researchers at other universities and practitioners in state agencies and in firms in private practice. Major tasks in this project are classified as the followings:

- **Task 1: Modernize Electronic Equipment** - The previously used electronic equipment, Tektronix 1502B, is bulky, expensive, and has been in existence for about 20 years. Newer technology is available that is more compact. Characteristics of the new electronics were evaluated to see whether they are fully suited to the demands of testing soil.
- **Task 2: Fabricate and Deliver Test Equipment to the Participants** - The PIs arranged for the fabrication and assembly of the test equipment for the participants. Modifications to the previously developed equipment were made. Some testing and evaluation of the modified equipment was performed before releasing it to the participants.
- **Task 3: Instruct Participant Personnel in Use of Equipment** - The PI, Co-PI, and students associated with the project traveled to participant's sites to instruct the staff of the participants in the use of this equipment. Part of this effort involves the drafting of a User's Manual for the procedures and equipment that complemented the ASTM Standard.
- **Task 4: Coordinate Testing Plans of Participants** - Participants utilized the Purdue TDR Method in a meaningful way on regular projects where soil water content and density measurements were made. Recommendations were made to the participants and a plan developed with them for use of the Purdue TDR Method to gather data for the project. Several of the participants chose to use the TDR Method on problem soils that other technologies gave inaccurate results. This posed an extra, unexpected challenge in this project.
- **Task 5: Collect and Analyze Data from Participants** - Procedures were established with the participants for reporting the data to Purdue as it is obtained. This data was incorporated into a master database and analyzed. The supplier of the data has access to the database and the results of the analyses.

- **Task 6: Establish Improvements to the Equipment and Procedures** - With any new procedure such as the Purdue TDR Method, improvements are likely in both equipment and procedures. Participants were invited to suggest improvements on a continuing basis. Special emphasis was made to simplify the testing process to reduce the time required to conduct the test so that it will be more competitive with other field-testing methods. Those suggestions were with other participants and evaluated for adoption.
- **Task 7: Refine the Draft ASTM Standard and Promote Adoption** - The draft ASTM Standard developed by a previous JTRP project (Ref. FHWA/IN/JTRP-98-4) was revised to be consistent with recently adopted ASTM requirements and to accommodate improvements in equipment and procedures developed as part of this project. The PI is a member of ASTM Committee D18.08 that has jurisdiction for these kinds of tests and was recently appointed as chair of *Task Committee D18.08.03 - New Technologies* that specifically will handle tests like the Purdue TDR Method. Standardization normally is a long and tedious process, but adoption of the Standard by ASTM occurred in little more than a year from introducing the first draft. Part of the out-of-state travel costs were for travel to the semi-annual ASTM Committee D-18 Meetings associated with the standardization process.
- **Task 8: Disseminate Findings through Publications and Presentations** - As with any new technology, acceptance depends on widespread dissemination of information and experiences with the technology. The participants in this project were encouraged to publish and make presentations on their experiences and findings. Publications by all participants that relate to work done on this project will be subject to the publication provisions in Section 5.2 of the USER'S MANUAL FOR RESEARCH AND IMPLEMENTATION (Rev. Aug. 1999).
- **Task 9: Generate Quarterly Reports, Other Required Reports, and a Final Report** - Procedures for these reports are outlined in the USER'S

MANUAL FOR RESEARCH AND IMPLEMENTATION (Rev. Aug. 1999).
Participants will be invited to contribute to and review these reports.

1.4 Report Scheme

The report is divided into 9 chapters.

- Chapter 2 introduces the Beta Testing partners of this project, gives basic information about them, and describes the interaction with them.
- Chapter 3 described the TDR apparatus assembly and hardware refinements. This is an important step in making the TDR technology accurate, efficient, easy to use, and economically competitive.
- Chapter 4 introduces the development of software for TDR automation. This includes the algorithm for picking reflection points which is used subsequently for computing soil apparent dielectric constant; this also includes the algorithm for computing bulk electrical conductivity which is another piece of important information contained in the TDR signal. Results of using these algorithms are evaluated and compared with existing technologies.
- Chapter 5 talks about the refining the TDR testing procedure. The standardization process is documented. The newly refined procedures are outlined. The physical significance of the calibration parameters are explained. Adjustments to the TDR method using an insulated center rod is introduced to handle the special situations where the soils have very high conductivities such as in fat clays at high water contents and some ash materials. These improvements make the technology more robust, accurate, and more widely applicable.
- Chapter 6 gives a comprehensive introduction on a One-Step Method for soil water content and dry density determination, which is an important advance made in this project. The One-Step Method makes use of measured apparent dielectric constant and bulk electrical conductivity to calculate directly, water content and dry density. This chapter includes the principles of the One-Step Method, the procedures for using this method,

and typical results. Application range and limitations of this method are also discussed in this chapter.

- Chapter 7 presents the results obtained from the Beta Testing Partners. It discusses the interaction with them to overcome the problems encountered. Work on sand soils in Florida was quite extensive and indicated that a single pair of calibration factors could provide accurate results for most of the sands used in Florida construction of road and highways. From other tests on stabilized waste materials, it was discovered that the measured bulk electrical conductivity is a strong indicator of hydration taking place in materials that have components that hydrate.
- Chapter 8 provides suggestions for further implementation of the findings, especially the One-Step Method. A separate ASTM Standard will be necessary for it. Experience gained in this project indicates that the methods developed herein are applicable to a wide variety of geotechnical and man made materials including chemically modified soils, waste materials, asphalt and cement.
- Chapter 9 provides suggestions for future research. The list includes stabilized soils, asphalt, and concrete. It also recommends further research in the frequency domain be done to extract additional information from the TDR data. A proposal to the National Science Foundation for this work was submitted, was recommended for funding, and will be funded if sufficient funds are available at NSF.
- Chapter 10 provides a summary of the project and gives some highlights of the research.

2. Beta Testing Partners

2.1 Statement of Objective

An important task of this Beta Testing program was to obtain information on how well the Purdue TDR Method would work on a variety of different soils when used by others in research and production settings. A secondary objective was to promote the awareness of the Purdue TDR method and encourage widespread application of this technology. Background of this technology can be found in the final report for the first project sponsored by the JTRP for this research, Report No. FHWA/IN/JTRP-95/9. The aim of the present project was to refine the technology and make it more robust and accurate. This aim was achieved by involving partners from around the country. The initial list of thirteen potential Beta Testing partners is shown in Table 2-1.

Table 2-1 Initial List of Expected Participants

No.	Agency/Firm/University	Location	Contact Person	Liaisons
1	Earth Exploration, Inc.	Indianapolis, IN	Dr. Shafiq Siddiqui, P.E.	Purdue University
2	GAI Consultants, Inc.	Pittsburgh, PA	Dr. Anthony DiGioia, P.E.	Carnegie Mellon U.
3	Geo Environmental Consultants, Inc.	Charlotte, NC	Christopher Hardin, P.E.	
4	H.C. Nutting Co., Inc.	Cincinnati, OH	Ronald Ebelhar, P.E.	Univ. of Cincinnati
5	INDOT	Indianapolis, IN	Dr. Kulanand Jha, P.E.	Purdue University
6	Petra Geotech, Inc.	Fullerton, CA	Dr. Soumitra Guha, P.E.	Caltrans
7	Purdue University	W. Lafayette, IN	Dr. Vincent Drnevich, P.E.	INDOT
8	Rutgers University	Piscataway, NJ	Dr. Ali Maher, P.E.	NJDoT
9	Somat Engineering	Detroit, MI	Richard Anderson, P.E.	
10	Univ. of South Florida	Tampa, FL	Dr. Alaa Ashmawy, P.E.	Florida DoT
11	Rieth-Riley Construction	Goshen, IN	Peter Capon	Purdue University
12	U.S. Army Corps of Engineers	Vicksburg, MS	Donald Yule	
13	U.S. Bureau of Reclamation	Denver, CO	Jeffrey Farrar, P.E.	

With the exception of INDOT and Purdue University, it was planned that each of the other participants would provide funding for the purchase of the equipment and for the testing of this new technology in their regions. They also would cover all of the expenses associated with use of the equipment in laboratory and field tests and in reporting the data. One set of equipment for Purdue University and for INDOT were covered by the budget in this project. The project covered training individuals from these organizations.

2.2 Description of Partners

A list of Beta Testing partners as of April 2003 is shown in Table 2-2. Overall, the process of engaging potential Beta Test partners went reasonably well. Some potential Beta Testing Partners, especially some of the private firms, decided not to join the program due to slow economic conditions.

Table 2-2 List of Beta Test Participants

Agency/Firm/University	Location	Contact Person	Liaisons
Purdue University	W. Lafayette, IN	Dr. Vincent Drnevich, P.E.	INDOT
Univ. of South Florida	Tampa, FL	Dr. Alaa Ashmawy, P.E.	Florida DOT
INDOT	Indianapolis, IN	Dr. Kulanand Jha, P.E.	Purdue University
Florida DOT	Florida	David Honhote, P.E.	U. of South Florida
GAI Consultants, Inc.	Pittsburgh, PA	Dr. Anthony DiGioia, P.E.	Carnegie Mellon U.
H.C. Nutting Co., Inc.	Cincinnati, OH	Ronald Ebelhar, P.E.	Univ. of Cincinnati
Rutgers University	Piscataway, NJ	Dr. Ali Maher, P.E.	NJDOT

2.3 Interactions with Partners

The PI as well as research personnel at Purdue have been interacting with Beta Partners. Typical communication flows between Purdue TDR group and Beta Partners are:

- 1) Make arrangement with Beta partners and set date for delivery;
- 2) Deliver equipment to Beta partners;
- 3) Give instructions to technical staff of Beta partners. This generally includes presentation of principles and laboratory and field demonstrations;
- 4) Communication with Beta partners to get feedback on TDR field applications;

- 5) Continued instructions to them on use of equipment and testing procedures, especially with updated methods and software; and
- 6) Help them to resolve problems encountered in testing.

Results and feedback obtained from Beta partners are summarized in Chapter 7.

3. TDR Apparatus Assembly and Hardware Refinement

3.1 Statement of Objective

Before the TDR equipment could be provided to Beta Testing Partners, many refinements were made in the equipment, procedures, and software. The direct objective of TDR equipment design was to increase the quality of the data, facilitate TDR field measurements, and reduce the manufacturing cost. Another important goal was to have the equipment nicely packaged and look good.

3.2 TDR System Design and Refinement

The work in this project built on the work of previous projects (Siddiqui and Drnevich (1995), Feng et al. (1998), Drnevich et al. (2001)). These refinements made the equipment and procedures easier and more user friendly.

3.2.1 Initial Purdue TDR System Design (Siddiqui and Drnevich (1995))

In the first research project (Siddiqui and Drnevich (1995)), important parameters influencing TDR measurements were systematically investigated. These are summarized below:

1) Configuration of Transmission Lines

This research compared the response of four parallel rods, consisting of a central rod and three outer rods (Fig. 5.3), with that of cylindrical coaxial system. It was found that the four parallel rods provide signals that were essentially the same as those with cylindrical outer conductors, further validating the work by Zeglin et al. (1989). Based on this similarity in system response, both coaxial type line probes and parallel rod probes are used to obtain data on soils in the TDR methods described in this report.

The coaxial line type probe is called the “Mold Probe” because a steel soil compaction molds nicely serves as the outer conductor. After soil is compacted in the mold, a guide is placed on the mold and a steel rod is driven into the compacted soil to form the inner conductor as shown in Fig. 5.9.

The parallel rod probe is called the “Multiple Rod Probe” and consists of four spikes driven into the soil through a template (Fig. 5.1). After removing the template, a “Probe

Head” is placed on the four spikes (Fig. 5.4) completing the probe. This probe is exceptionally robust and inexpensive. Spikes damaged by driving are discarded. The probe head is rugged, but is not subjected to any installation forces. Research from this and previous projects show that it gives excellent and repeatable results.

2) Length of Measurement Probes

The length of measurement probes affects the observed return signal. If probes are too long, the return signal reflected from the probe tip cannot be observed. If the probes are too short, accurate measurements cannot be made of the travel time in the probe. For testing most soils, the probe length should be 178 to 250 mm (7 to 10 in.) in length. Longer probes can be used for cohesionless soils with low conductivity to improve the accuracy. Shorter probes must be used to obtain clear reflections in highly conductive soils. In this project, probe lengths in the soil of 116 mm (4.6 in.) were used with good success. This shorter length works well in conventional compaction molds.

3) Ratio of Probe Radii

The ratio of the radius to the outer conductor, R_o , to the radius of the inner conductor, R_i , is important in probe design as the ratio affects the pattern of the reflected signals. Additionally, when the radius of the inner conductor is too small, air gaps adjacent to the inner conductor created by driving it into the soil will significantly affect the accuracy of the results. On the other hand, if the radius of the inner conductor is too large, the installation process affects the density of the soil adjacent to the rod. From the work of Siddiqui and Drnevich (1995) the ratio of R_o to R_i should be between 12 and 15.

3.2.2 Refinement in the Subsequent Project (Feng et al. (1998))

The second project focused on developing an automated procedure for the measurement of water content and density of soil by TDR and for creating a draft ASTM Standard for the method. The following modifications to the equipment were made during this phase of the study: A single probe head was used for both the TDR field test and the TDR mold test. A steel ring placed on the mold allowed the outer studs of the probe head to make contact with the metal mold. This reduced the amount of needed equipment and lowered overall cost of the apparatus.

- The ratio R_o/R_i was set as 12.8.
- The volume of the mold designed was 1650 cm³ (1/17 ft³).

- Lengths of the mold and field probe were set to be 234 mm (9.2 in) and 254 mm (10 in), respectively.

Another important factor considered in determining probe geometry is the volume of soil tested. The ASTM Standard for the Sand Cone Test (D 1556) provided guidance for this. The center-to-center spacing of the inner conductor and outer conductor was 66 mm (2.6 in.) and the length of the rods inside the soil was 223.5 mm (8.8 in.). This gives sampled volume of 3060 cm³ (0.113 ft³) which is larger than the maximum value of 2830 cm³ (0.1 ft³) set by ASTM D1556.

3.2.3 Updating TDR Hardware System in This Beta Test Project

Updating TDR system hardware was an important task for the Beta Testing program. The tasks focused on updating the electronics and testing equipment based on feedback from the Beta Testing Partners.

3.2.3.1 Selection of Electronics

Major components of TDR electronics include: pulse generator/sampler, power supply, cable, and data acquisition system. The pulse generator/sampler sends out a signal and the sampler records the reflected signal which contains the response of the material under measurement.

A Tektronix 1502B was used in all previous projects. It was found to be accurate, stable and reliable. Major parameters of this pulse generator/sampler are listed in Table 3-1. However, the Tektronix 1502B is no longer in produced. Thus a new pulse generator/sampler was needed for this project. Considerations in selecting a pulse generator/sampler are:

- 1) Rise Time - The rise time of the pulse generator determines the frequency content in the measurement;
- 2) Price - Price of pulse generator/sampler is a very large portion of the total price of the TDR system. A system with both high measurement capacity and low price is desirable;
- 3) Portability – The ability to take the pulse generator/sampler into the field and have it operate on battery power is important.

Table 3-1 Major Parameters of Tektronix 1502B

1502B Metallic TDR Cable Tester	
Test Signal	Step rise
Amplitude	300 mV nominal into 50 Ω load.
System Risetime	200 ps (1.15 in./2.92 cm)
Output Impedance	50 ohms \pm 1%
Electrostatic Discharge Protection	1 kV/500 pF capacitor/1 k resistance
DC Input Protection	\pm 1 A
Maximum Range	2,000 ft/500 meters
Distance Readout Resolution	0.12 in./0.30 cm
Noise Filtering	1 to 128 averages
Vertical Scale	0.5 to 500 m ρ /div
Dist/Div	0.1 to 200 ft/div; 0.025 to 50 m/div
Environmental	Meets capabilities of a Type III, Class 3, Style A instrument as prescribed by MIL-T-28800

More specifically, considerations in selecting pulse generator/sampler include:

- 1) Rise time, which determines the frequency contains in the measurement and thus determines the measurement capacity and accuracy;
- 2) Price, price of pulse generator comprises a very large portion of the total price of the TDR system. A system with the advantage of both high measurement capacity and low price will put the system more competitive;
- 3) Requirement of handle, the pulse generator/sample is desirable to be easy to handle. Properties such as light weight, low duration, utilizing conventional power supply are good in terms of field application capability.

At the start of the project, a prototype PCMCIA-card TDR system by CM Technologies, Inc, was evaluated. However, it did not perform according to claims and was not considered further.

After some review of available systems, the Model TDR100 manufactured by Campbell Scientific was selected. It has worked well. Table 3-2 provides the characteristics of this unit.

Table 3-2 Campbell Scientific, TDR100 Time Domain Reflectometer

TDR100 TDR Cable Tester	
Test Signal	Step rise
Amplitude	250 mV nominal into 50 Ω load.
System Risetime	<250 ps
Time Resolution	12.8 ps
Output Impedance	50 ohms \pm 1%
Electrostatic Discharge Protection	1 kV/500 pF capacitor/1 k resistance
DC Input Protection	electrostatic discharge protection
Maximum Range	-2~2100 meters
Power Supply	Internal clamping power supply 12 volt, 300 milliamps maximum
Noise Filtering	1 to 128 averages
Environmental	Temperature range -25 to 50 $^{\circ}$ C
Dimension	210mm x110 mm x 55mm
Weight	700 g

Table 3-3 Commercially Available Metallic TDR Pulse Generators (after Andrews, 1994)

Manufacturer	Type	Pulse Type	Pulse Ampl. (V)	Dimensions (mm)	Mass (kg)	Power Source
IWATSU	Oscilloscope/Sampling head	<45ps step				AC
LE-CROY	Oscilloscope/Sampling head	<150ps step				AC
HYPERLABS	TDR plug-in card	35 ps step		191*89*50	2	IBM PC
	TDR	200 ps step	0.3			battery
Tektronix	Oscilloscope/Sampling head	<35 ps step				
	TDR	200 ps step	0.3	127*315*436	9	Battery
Hewlett-Packard	Oscilloscope/Sampling Head	<45 ps step				AC
Picosecond	Pulser	18 ps step				AC
ESI	TDR	140 ps step	0.3	274*248*173	5	battery
Environmental Sensor, Inc.						
Soil Moisture Equipment Co.	TDR	200 ps step	1.5			battery
Easy Test Ltd.	TDR	200 ps needle shape		260*180*130	4	battery
CM Tech. Corp.	TDR plug-in card	200 ps step				IBM-PC
IMKO GmbH	TDR	200 ps step	1.0			battery
PermAlert ESP	TDR					AC
Riser-Bond Instrument	TDR	½ sin wave (2 to 4000 ns)		267*248*127	4	battery
Biddle Instruments	TDR	½ sin wave (30 to 1500 ns)		140*290*260	8	battery
Signal Tensor	TDR	200 ps step	0.6	266*241*114	3	battery
	TDR plug-in card	100 ps step				IBM-PC
Bicotest	TDR	½ sin wave (2 to 1200 ns)	2.5	75*183*300	3	battery



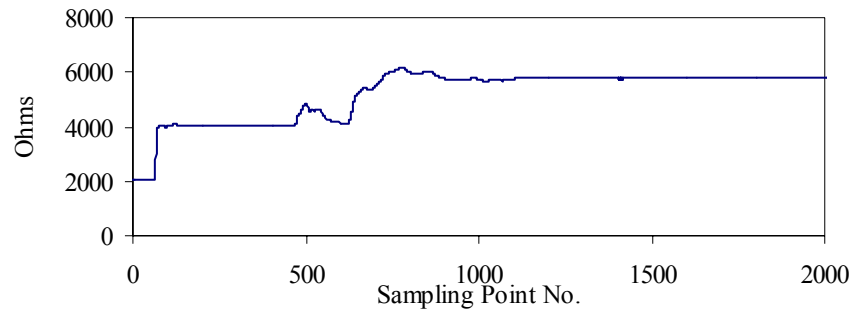
(a)



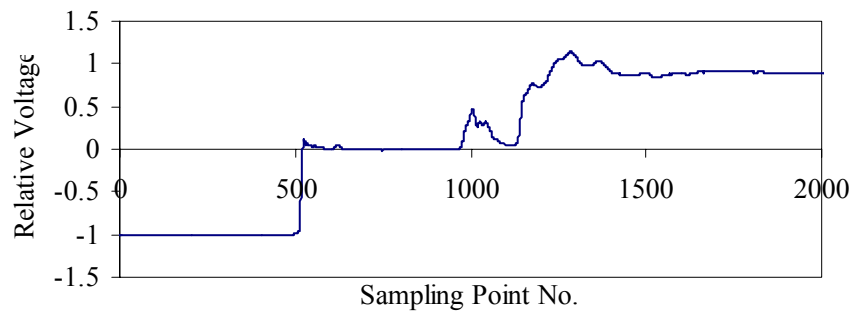
(b)

Fig. 3.1 Photo of: (a) Tektronix 1502B; (b) Campbell Scientific TDR 100

Compared with Tektronix 1502B, TDR100 has several advantages. Firstly, the dimension and weight of TDR100 is much smaller compared Tektronix. These make TDR100 easier to handle in the field. Secondly, the price of TDR100 is around \$3,800 which is just about 1/2 the price of Tektronix devices with similar capacity. This makes the TDR100 more economically viable. Thirdly, the TDR100 incorporates a processor and operating system to do some data reduction. The data can then be communicated to host device. This makes it more suitable for remote control and communication purpose. More importantly, measurements indicated that TDR100 has the similar accuracy compared with Tektronix device (Fig. 3.2).



(a)



(b)

Fig. 3.2 Comparison of TDR Waveforms on the Same Specimen with the Same Probe: (a) Tektronix 1502B; (b) Campbell Scientific TDR100

3.2.3.2 Refinement of TDR Hardware Equipment

TDR hardware was refined in this project based on field applications and feedback from Beta Testing Partners. The refinements make the hardware more robust and easier to handle in the field. Detailed improvements in hardware configuration are discussed below.

Multiple Rod Probe Head (MRPH)

Beginning with the previous project, the Multiple Rod Probe Head is used for both mold test and field test. Major improvements of MRPH in this project include:

- 1) Better wave transmission capacity - The MRP head is critical in forming a distinct 1st reflection point. The head geometry was improved for better wave transmission and to better protect the BNC connector.
- 2) Weight - Most of the MRPH is made from stainless steel, which makes it heavy compared to other existing TDR probes. One advantage of using large weight is to

ensure good contact between MRPH studs and rods. However, reducing the weight of MRPH makes it more portable. The newest design has a reduced thickness compared to earlier versions.

- 3) Contact Quality - Contact of MRPH with probes (spikes) or the adapter ring, especially the center probe, is critical for obtaining good TDR measurements. Changes to improve the contact quality include: A) The end of studs are slightly rounded; and B) The length of two of the three outer studs is fixed, while the remaining one is spring loaded. This helps to deal with the situation where the tops of the spikes are not perfectly on a horizontal plane.

A current version of MRP head is shown with the original version of MRP head (Fig. 3.3). The new head is much easier to handle and provides better signal quality.

(a)



(b)



Fig. 3.3 Old and New MRP Heads (a) Old MRP head; (b) New MRP head

Cable

The cable connects the pulse generator/sampler to the MRPH and is an important component of the coaxial configuration in the TDR measurement system. Factors that were considered in selecting cable include:

- 1) Length of cable. While a long cable allows for the pulse generator/sampler to be further away from the MHRP, e.g. in the cab of a pick up truck, it also results in reduced high frequency components of the TDR measurement because the cable acts like a low pass filter. On the other hand, a cable should not be too short, since this will limit measurement flexibility. Based on these considerations, a cable length of 1.8 meters is used for the current TDR testing system. To allow for easy replacements, we are using a cable available at Radio Shack, Part No. _____.
- 2) Impedance of cable. Impedance of cable is another important parameter to consider when selecting cables. The cable used need to match the internal impedance of pulse generator, which is generally 50 ohms. Otherwise, there will be undesirable reflections due to the impedance mismatch between the TDR100 and measurement cable. Based on these considerations, a 50 ohms coaxial cable with the length of around 1.8 m is used in the current TDR testing system. An example of the coaxial cable with BNC connector is shown in the Fig. 3.4.



Fig. 3.4 Coaxial Cable with Impedance of 50 ohms

Probes

The probes used in field testing are driven into the soil using a brass-headed hammer. They may encounter gravel-sized particles or be very hard to drive in densely compacted soils. It is important that they be:

- 1) Rugged – The rods (spikes) must withstand hammering without bending or breaking. After repeated use, the sides and pointed tips become worn. When this occurs, they should be discarded.
- 2) Inexpensive – For the Beta Testing Program, the rods (See Fig. 3.5) were manufactured from cold rolled steel to rather close tolerances, had heads welded to them, then were machined to keep the heads flat and lengths uniform, and finally, were zinc plated to keep them from rusting. Off-the-shelf spikes (3/8-in. Dia. with lengths 8-in., 10-in. or 12-in.) from a local hardware store may be used but require that manufacturing burrs be removed, the chisel points be changed to conical points, the top of the heads be flattened, and the shank just below the head be trimmed to the proper diameter and have a square shoulder. All spikes should have the same total length and same length from the cap to the tip so that they can be interchangeably used. Also, the oily film that results from the manufacturing process needs to be removed.
- 3) Length - The spikes need to be long enough so that a sufficient volume of soil is sampled in the test. Currently, the total length of field probe is 23 cm (9-in.) with 20 cm (7.9-in.) net length in the soil. The total length of central rod for mold test is around 26 cm (10.2-in.) with 23 cm (9-in.) net length in soil. These provide sufficient sampling volume of soils. For testing of cohesive soils or highly lossy materials, shorter rods can be used for both the field test and the mold test. The recommended minimum length for the field probes is 14.75 cm (5.8-in.) and for the mold probe is 14.15 cm (5.58-in.) to be used with the standard compaction mold that has a height of 11.64 cm (4.584-in.). When the standard compaction mold is used as the mold probe, the metal base plate must be replaced with a non-metallic plate.

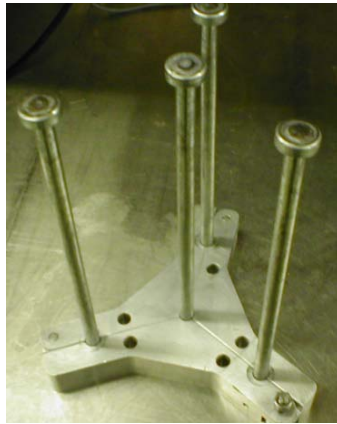


Fig. 3.5 Manufactured Field Probe Rods (Spikes)

Template

The template used to guide the driving of the probe rods (See Fig. 3.6) also needs to be rugged since it is used in conjunction with spikes. Hitting the template with the hammer when driving spikes can cause damages to the template. Considerations in updating the template design for field use were:

- 1) Rugged material - The material of the template needs to such that it is able to endure the inadvertent hitting by the hammer. While stainless steel might be the preferred material, aluminum was used to keep machining costs down and reduce equipment weight.
- 2) Hinge design - The hinge is one of the most fragile components of template and it is important component of the template ruggedness. Several hinge configurations were tried in the refining process. One is a conventional cabinet door type hinge, which was not sufficiently rugged. An integral hinge formed by machining is a more rugged hinge type and is being used at this time.
- 3) Removable pin design - The removable pin is inserted to holed the template in a closed position when driving the spikes. Subsequent to driving the spikes, it is removed to open the template for its removal before the MRPH is placed on the spikes. A tapered circular pin works reasonably well in field measurements. A ring and ball type chain (See Fig. 3.6) is used to keep the pin with the template to prevent it from being lost. The chain can also be helpful when removing the pin.



Fig. 3.6 Photo of Guide Template for the Multiple Rod Field Probes

Mold Rod Guide

Function of mold rod guide (See Fig. 3.7) is to facilitate the installation of central rod into the compaction mold when doing TDR test in the mold. Design criteria for the guide are:

- 1) Material - Originally, the guide was made of steel. The updated guide uses a plastic material called UHMW (Ultra High Molecular Weight) which is lighter weight, easy to machine, and durable.
- 2) Geometry - Critical dimensions of the guide include the diameter of guide hole, thickness, and inner diameter of shoulder that rests on the mold. The diameter of guide hole is designed such that it is slightly larger (typically 0.4 mm (1/64-in.) than diameter of central rod. The thickness is critical in that it establishes how much of the total rod length is within the soil. For the mold rod guide used in the Beta Testing Program, the thickness is kept at 25.4 mm (1.00-in.). The inner diameter of the shoulder needs to be large enough that the mold rod guide can easily be removed from the mold, but snug enough to keep the rod centered in the mold.



Fig. 3.7 Photo of Guide for Installing Center Rod

Compaction Mold

A compaction mold is used to compact soil and perform the TDR test in the mold. For cohesionless soils, a relative longer mold (such as mold with total length twice that of standard compaction mold) is recommended for testing cohesionless soils (Fig. 3.8). The large volume of compaction mold provides sufficient amount of representative sample to be tested. While for cohesive soils, a shorter mold such as standard compaction mold (ASTM D698) can be used.



Fig. 3.8 Photo of Compaction Mold with Height Twice That of the Standard Compaction Mold

Hand tamper

A hand tamper is needed to compact soil into the mold so that the soil density is evenly distributed in the compaction mold. An aluminum rod is used to serve this purpose (Fig. 3.9). The length of the rod is larger from previous design to accommodate the length of compaction

mold. It also is possible, even preferable, to compact the soil with the Standard Compaction Hammer (ASTM D698) or the Modified Compaction Hammer (ASTM D1557). Densities of compacted soil in the mold near the density of the soil insitu provides for more accurate measurements of insitu density.



Fig. 3.9 Photo of Hand Tamper

Balance

An electronic scale is used to measure the mass of soil in mold. The scale needs to be robust, durable and accurate. Several balances were tried in field tests during Beta test program. The balance selected is an A & D Company, Ltd., Model SK-10K that has a 10 kg (22 lbs) capacity, a resolution of 5 grams (0.01 lb), and nonlinearity within 10 grams (0.02 lb). It is shown in Fig. 3.10. It is battery operated with a life of about 1200 hours on a set of 6, size D batteries.



Fig. 3.10 Photo of Balance

Thermometer

A thermometer is used to measure temperature of the soil under test. The temperature is required by the data reduction program to adjust the values of apparent dielectric constant for temperature effects. Fig. 3.11 shows different digital thermometers used for this purpose.

(a)



(b)



Fig. 3.11 Photos of Digital Thermometers: (a) Old Version; (b) New Version

Supplementary Tools:

Hammer:

Hammers are needed to drive spikes and center rod. Field spikes can tolerate impact and some deformation of their thick and strong heads. This deformation is not a big problem since it does not influence template removal. To minimize the amount of deformation, a brass hammer is used to drive the field spikes because brass is softer than steel. For the mold test, deformation of center rod is not tolerable since the mold rod guide is removed by lifting it from the center rod. Thus a plastic hammer is used to drive the center rod for mold test.

(a)



(b)



Fig. 3.12 Hammers: (a) Insitu Probe Rod Installation; (b) Mold Rod Installation

Tools for Template Removal (Fig. 3.14)

Vice Grips - Removal of the template can be difficult when one or more of the spikes drift slightly due to impinging on a piece of rock or gravel. Several tools are included to help remove template. The removable pin can be pulled out in most cases with the aid of the attached ring. However, it is found sometimes that vice-grip type pliers must be used to grab the pin and pull it out. A pry bar, which was originally used for removing spikes from hard soils, can also be used for this purpose.

Screw driver - Screw driver is used to open the template so that it can be removed.

File. File is used to smooth damaged surfaces of template caused by inadvertent hits on it or from use of the screw driver to pry it apart.

Tools for digging soils

Power drill, spoon:

Power drill and “Nail Biter” wood bit (Fig. 3.13) and spoon are included in the TDR tool case. Power drill is used to loosen the soil and the spoon is used to excavate the loosened soil.

The power drill is especially useful for compacted stiff soils.



Fig. 3.13 Power Drill with Bit

Other supplementary tools (Fig. 3.14)

Screed is supplied to help trim the soil surface before placing the template on the soil for the insitu test and for trimming and smoothing the soil surface in the mold after it is compacted and the collar is removed.

Brush is provided to help clean up the mold from soil trimmings on the mold before determining its mass.



Fig. 3.14 Supplementary Tools

3.3 Tool Case, Electronics Case, and Wiring of TDR Testing System

TDR tool cases are designed to make the system more compact and easy to handle in the field. Several generations of tool cases have been updated by now. Each generation was significantly improved over previous ones and significantly increased efficiency in the field. Two cases are used in the Beta Test sets. One case contains the TDR Probes, molds, digital scale, and tools; the other case contains mostly electronic components. Apparatus stored in each case are summarized below:

Case 1 - Measurement Tools.

Case 1 (Fig 3.15) is a rugged travel case with wheels and a handle that contains all of the basic TDR equipment, accessories, spares, and tools for performing the test. When performing tests, all of the items, except spares are removed from the case and the case itself may be used as a work surface to hold Case 2 and the digital scale. If working from the bed of a pickup truck or a van, tools and accessories may be left in Case 1 until they are needed. A list of items in Case 1 includes:

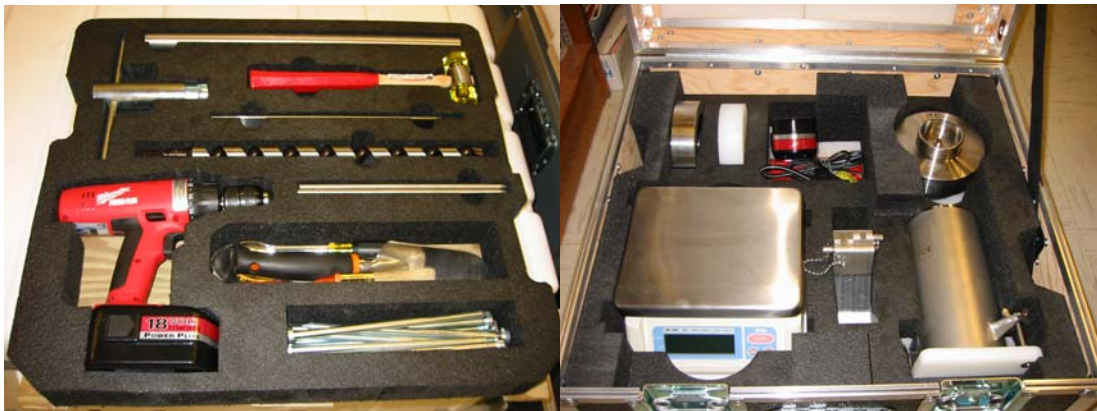
Insitu Test:

- 1 - Templates (plus 1 spare)
- 4 - Spikes (plus 4 spares)
- 1 - Brass Hammer for Driving Spikes
- 1 - Tool for Loosening Template
- 1 - Metal Rule for Measuring Length of Spikes above Ground
- 1 - Multiple Rod Probe Head
- 1 - Tool for Removing Spikes
- 1 - File
- 1 - Thermometer

Mold Test:

- 1 - Mold
- 1 - Mold Base

- 1 - Battery Operated Power Drill, Extra Battery, and Battery Charger (1 set)
- 1 - Auger bit for use power drill for loosening the soil
- 1 - Digging Tool for Excavating Soil
- 1 - Spoon for Removing Loose Soil from Hole
- 1 - Tamping Rod for Compacting Soil in Mold
- 1 - Guide for Installing Center Rod
- 1 - Center Rod (plus 1 spare)
- 1 - Acrylic Hammer for Driving Center Rod
- 1 - Metal Screed for Leveling Surface of Soil in Mold
- 1 - Brush for Removing Excess Soil from Mold Base before Placing on Scale
- 1 - Adapter Ring for Top of Mold
- 1 - Digital Scale for Measuring Mass of Mold before and after Filling



(a)

(b)

Fig. 3.15 Case 1 Containing TDR Measurement Equipment and Tools

Case 2 – TDR100 Generator/Sampler, Battery, Chargers, and Notebook Computer

Case 2 is a rugged, oversized briefcase (See Fig. 3.16) that contains the electronics for performing the TDR measurements, making the calculations, and storing the data. Specifically, it contains:

- 1 - Campbell Scientific, TDR100 Time Domain Reflectometer

- 1 - Campbell Scientific, PS12 Power Supply for TDR100
- 1 - Campbell Scientific, PN9591 120-Volt Charger for PS12
- 1 - Notebook Computer¹ with PMTDR Software
- 1 - Charger³ for Notebook Computer
 - 1 - BNC Cable to Connect TDR100 to MRP Head (Radio Shack part No. 980-0167, 50 ohm, 1.8 m (3 ft) long)
- 1 - Cable to Connect Chargers to 120V AC Source to Recharge Batteries

The wiring of the electronics is shown in Figs. 3.15 to 3.18.



Fig. 3.16 TDR Electronics

¹ This item is normally provided by the user and not included with the basic system.



Fig. 3.17 Layout of TDR100 and Power Sources in Case



Fig. 3.18 Pull Switch to Supply Power to TDR100 from PS12 Power Supply

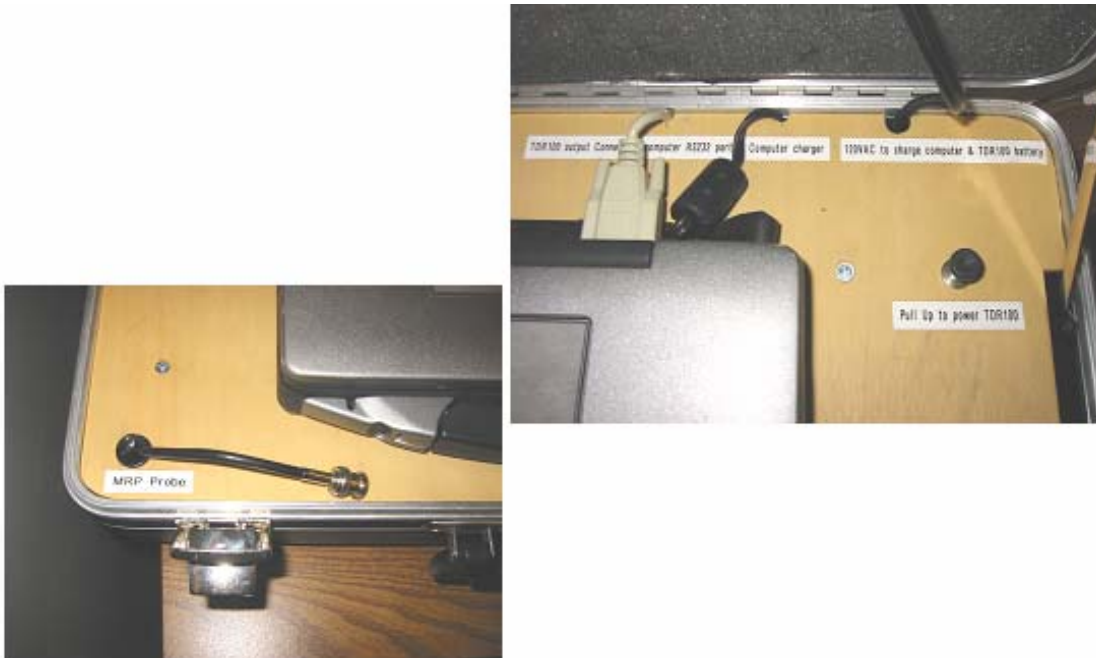


Fig. 3.19 Cables to MRP and Computer through Case Deck

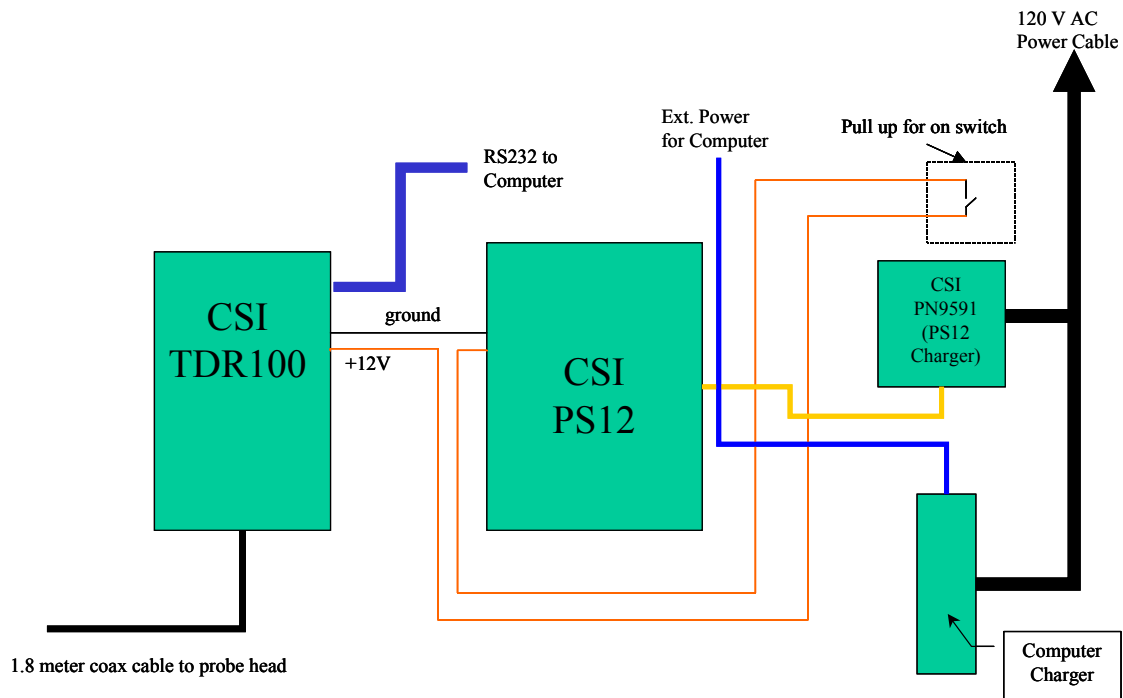


Fig. 3.20 Wiring Diagram of Components in Case 2

3.4 Use of CSI Probes

Beside the spikes designed at Purdue, the feasibility of Purdue TDR software to be used with Campbell Scientific CSI probes was also investigated. Results of this investigation are shown in **Appendix II**.

4. Development of Software for Testing Automation

4.1 Statement of Objective

For TDR measurements of soil water content and dry density to be widely accepted as a robust and convenient tool for routine construction quality inspection, automation of the testing process is necessary. Automation of the testing process is helpful not only for simplifying data acquisition and analysis process, but also for reducing the uncertainty and error associated with different test operators. For example, Topp et al., 1980 discovered that the major source of uncertainty in the calibration of TDR measurements was from the analysis of TDR waveform to get the travel time of the electromagnetic wave along the testing probes where manual operation induces significant error depending on the judgment of the operator.

In a previous research project by the PI, software called TDR++ was developed for testing automation using Tektronix 1502B system (Figs. 4.1 and 4.2). There are several problems

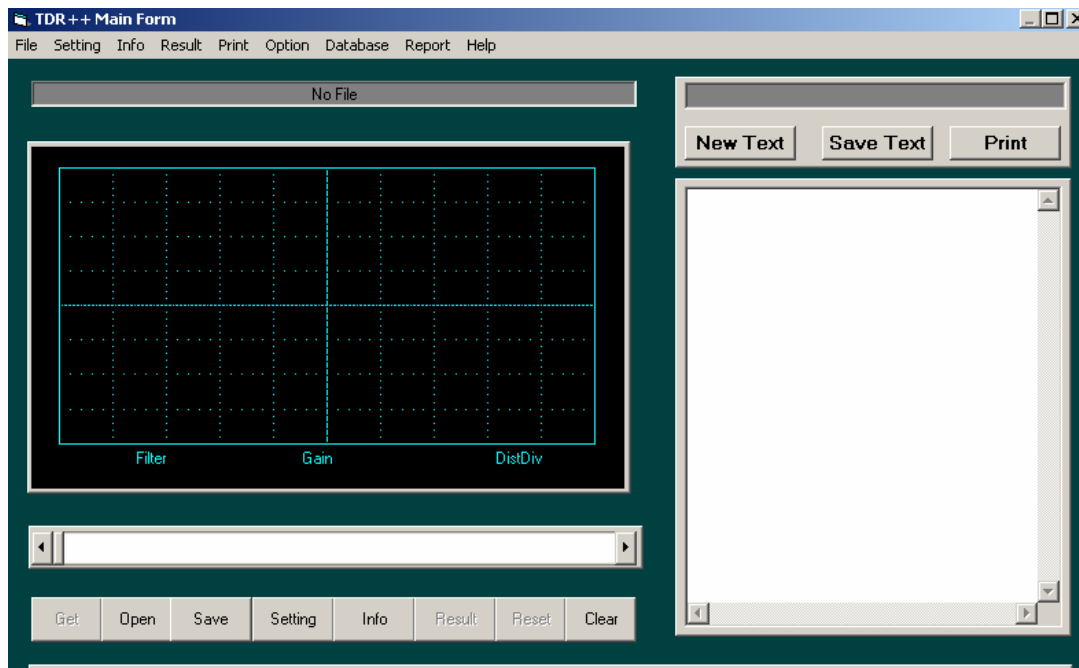


Fig. 4.1 Graphical User Interface of TDR++ Program

associated with the previously used Tektronix 1502B TDR system and TDR++ software, which

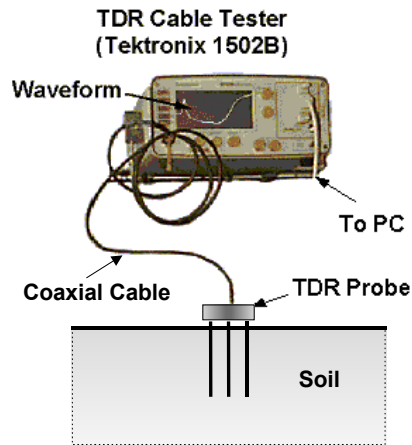


Fig. 4.2 TDR System using a Tektronix 1502B Cable Tester

are summarized below.

The existing data acquisition process is not truly automatic. For each test, manual operation on the Tektronix device is necessary. This includes manual setting of the starting position of cursor, selecting of the horizontal scale to maximize the accuracy of displaying TDR waveform, etc. Personal judgment of the operator is involved in this process. After making the settings, then the waveform currently displayed on the Tektronix screen is acquired by the computer using the TDR++ software.

TDR++ data sampling module only samples the current screen displayed on Tektronix 1502B screen, which consists of 250 data points. This is just a section of the whole TDR waveform. Generally, other important information associated with TDR testing such as final TDR waveform level could not be obtained. Although the function of TDR++ was later extended to obtain 2048 points, the data points are only stored as text files and no analytic module was provided to make analysis on the data obtained.

Additionally, the TDR++ software is rather complex and time consuming to use. It requires lengthy process of inputting the test information. It was not very applicable to field use.

The algorithm used by TDR++ has limited applicability, since it only makes analysis on a specific section of the TDR waveform. Also, it did not obtain a final voltage level which is used to obtain information on bulk electrical conductivity.

For the Beta Test Program, the Campbell Scientific TDR100 replaced the Tektronix 1502B as the generator/sampler and totally new software was developed. It simplified and speeded up the whole process, making it more suitable for application in field situation. The task of testing automation included the following objectives:

1) Automation of data acquisition, by which the intelligent device such as the computer and the associated software communicate with TDR tester to acquire data. It is also desirable to display the TDR waveform to identify possible errors associated with improper testing procedures;

2) Automation of TDR information analysis, in which the TDR waveform is automatically analyzed to obtain desired information such as apparent dielectric constant and bulk electrical conductivity. It is desirable to visual display relevant information such as reflection points, characteristic voltage levels for assisting in judging the quality of TDR waveform;

3) Automation of data deduction process, which includes computing the desired results of soil water content and dry density;

4) Functions for storing test data, including test information and results. Ability to recall old test data and reanalyze it;

5) Supplementary functions modules such as calibration and help documents etc. In addition to the above, it should look professionally done and be relatively bug free.

4.2 Algorithms for TDR Waveform Analysis

The automation of TDR data acquisition can be carried out following the proper communication protocols, and thus is relatively straightforward to perform. The task of developing the algorithm for analysis of the TDR waveform to obtain information such as soil apparent dielectric constant and bulk electrical conductivity is more cumbersome. This is due to the complexity of TDR waveforms obtained for the variety of soil types encountered in field situations. Our aims in developing the algorithm for TDR waveform analysis include:

- 1) Robustness - It needs to be applicable to various field situations;
- 2) Accurate - It needs to give results of dielectric constant and conductivity of given material that are consistent with measurement results by other technology; the

subsequently obtained results of measured soil water content and dry density are comparable to other established technology;

- 3) Repeatable – Results obtained must be the same from multiple measurements by the same and other operators.
- 4) Simple and Versatile – The algorithm needs to be simple and applicable to a wide variety of different field conditions.

4.2.1 Reflection Model for TDR Waveform

Understanding of the electromagnetic wave propagation phenomena in TDR systems and the resulting behavior of TDR waveforms are prerequisite for developing a robust algorithm for picking reflection points from TDR waveform analyses. As shown in Fig. 4.3, for a typical TDR system configuration, a pulse generator sends out a rapid rising step pulse, which travels down the transmission line. The changes of impedance by the geometry and materials cause reflections in the TDR signal. As the signal reaches the MRP head, a reflection takes place as indicated by a voltage increase. After passing through the MRP head, another reflection takes place due to the air/material interface, which causes an abrupt voltage drop in TDR signal. This results in a first “peak” in the TDR signal. Following the reflection, the transmitted signal continues to travel along the testing probe embedded in material under test. When the signal reaches the tapered end of probe, the change of impedance caused by the discontinuity and geometry changes cause a reflection of TDR signal, which then subsequently transmits through the material under test, the air/material interface, the probe head, and travels back into TDR device. This causes a rise in the TDR signal, with magnitude dependent upon the characteristics of the probe and material properties within the probe. The resulting curve is generally used to find the so-called second reflection point.

Multiple reflections will take place for low-lossy materials and the reflections continue until TDR waveform becomes stabilized. The process is illustrated in Fig.4.3 where the section numbers in part (a) relate to the resulting signal in part (b).

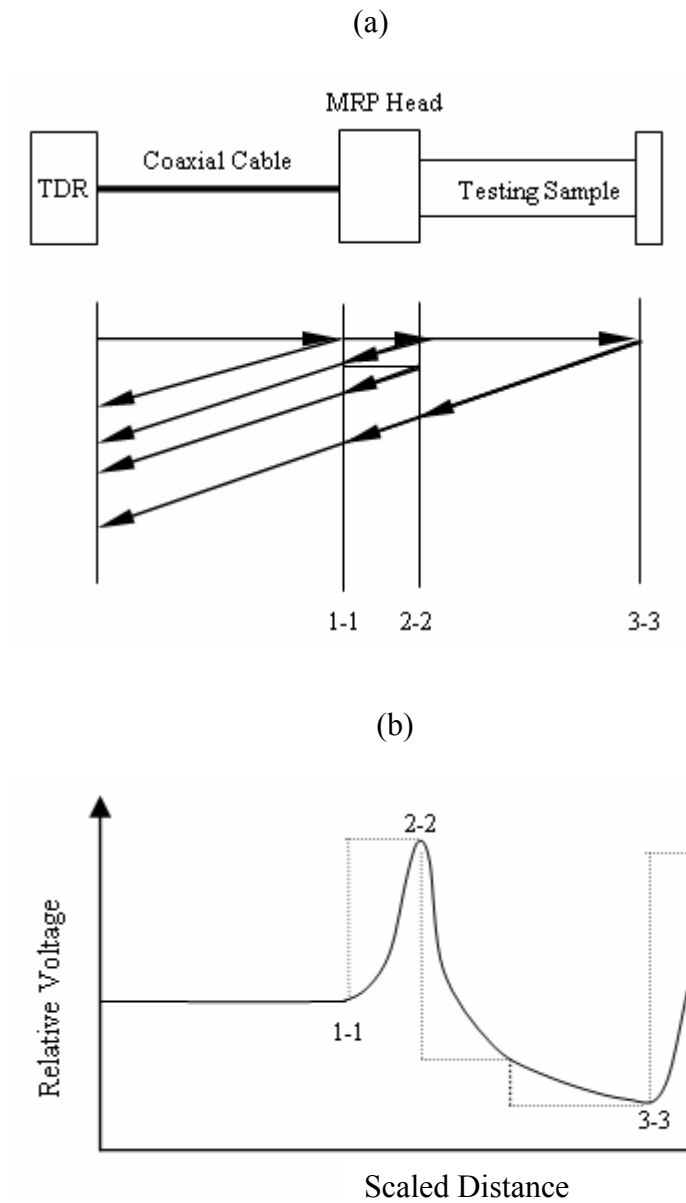


Fig. 4.3 TDR System Schematic: a) Reflections in the TDR system; and b) Resulting TDR waveform

The detailed reflection pattern not only depends on material under test, but also depends on the configuration of TDR system, which includes the signal generator, cables, and probe. This complexity makes almost all algorithms TDR system dependent. Algorithm developed under one TDR system generally needs to be verified and modified before it can be applied with confidence to other TDR systems.

4.2.2 Overview of Algorithms to Pick Reflection Points

The soil apparent dielectric constant, K_a , is a function of the travel time of the electromagnetic pulse along the waveguides. Currently, there are three commonly used methods to obtain the travel time from a recorded signal trace (Timlin and Pachepsky, 1996). They are: i) Measure the signal trace manually, ii) Use a computer algorithm to find the initial point and end point of the trace by searching characteristic slope changes, and iii) Inverse analysis of the TDR waveform to obtain the parameters of transmission line simulated by the TDR system (Yanuka et al., 1988)

The manual method generally uses the tangent line approach described by Topp et al. (1982) or the method by Baker and Allmaras (1990). The basic idea is to draw tangent lines from characteristic points along the TDR signal; the intersections of these tangent lines are regarded as the reflection points. The difference between the two approaches by Topp et al. and that by Baker and Allmaras is the criteria of selecting the characteristic points. The method proposed by Topp et al., uses two lines from linear sections of the TDR signal, while for the method by Baker and Allmaras, one line is from the linear section of the TDR signal and the other line is from a horizontal line through the point where the voltage is a local minimum (Fig. 4.4). The approach by Baker and Allmaras is also used at the initial stage of Purdue TDR research, in which the operator scrolls the cursor on the screen and identifies the location of first and second reflection points by empirical judgment. Although it could give satisfactory results in some case, it is more prone to be influenced by the operator's personal preference. Besides, the time and effort needs in the process of manual operating the cursor under field condition are intolerable. Thus a process that automation of the TDR waveform analysis is highly desirable.

The second approach for analysis of TDR signal is by computer algorithm. In this project, TDR waveform analysis was performed using an algorithm operating on the data within the computer program used to acquire, operate on, and store the data and calculated results. The algorithm generally follows the description provided above for the manual method of picking reflection points. It makes use of numerical differentiation, which calculates the first derivative and finds the location of the point with the largest first derivative. Of particular interest is the location where the slope of the tangent line is a maximum. The numerical slope of tangent line is calculated using

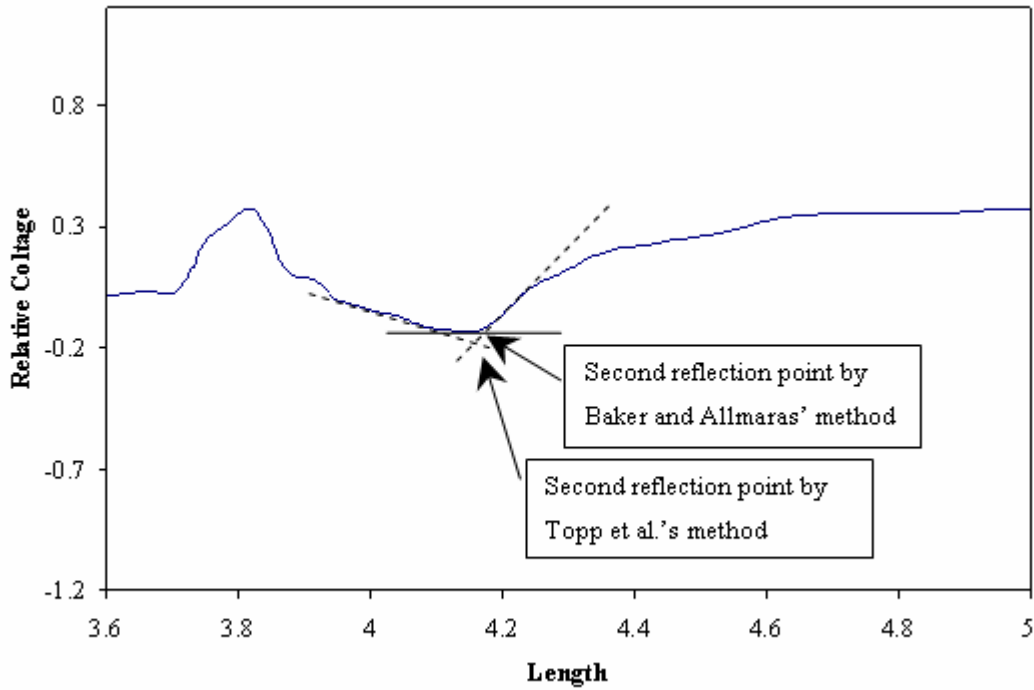


Fig. 4.4 Two Methods to Manually Identify the Second Reflection Point

$$s_i = \frac{d_{i+1} - d_{i-1}}{2\Delta} \quad (4-1)$$

where s_i is the approximate slope of tangent line at point i , d_{i-1} and d_{i+1} are measured voltage levels on the TDR signal at point $i+1$ and $i-1$, Δ is horizontal interval of the signal. TDR signals generally contain noise and effects of noise can be reduced by averaging multiple signals. This can be done at the sampling stage and TDR hardware generally provides this capability. The other approach commonly used is to use moving average before making analysis on the TDR signals. The methods generally utilize 5-point or 7-point averaging to smooth the curve and reduce noise effects (Fig. 4.5). The smoothed data is then used for further analysis and numerically computing the derivatives. As can be seen from Fig. 4.5, although the noise effects could not be completely eliminated by the moving average data points, the noise level has been significantly reduced.

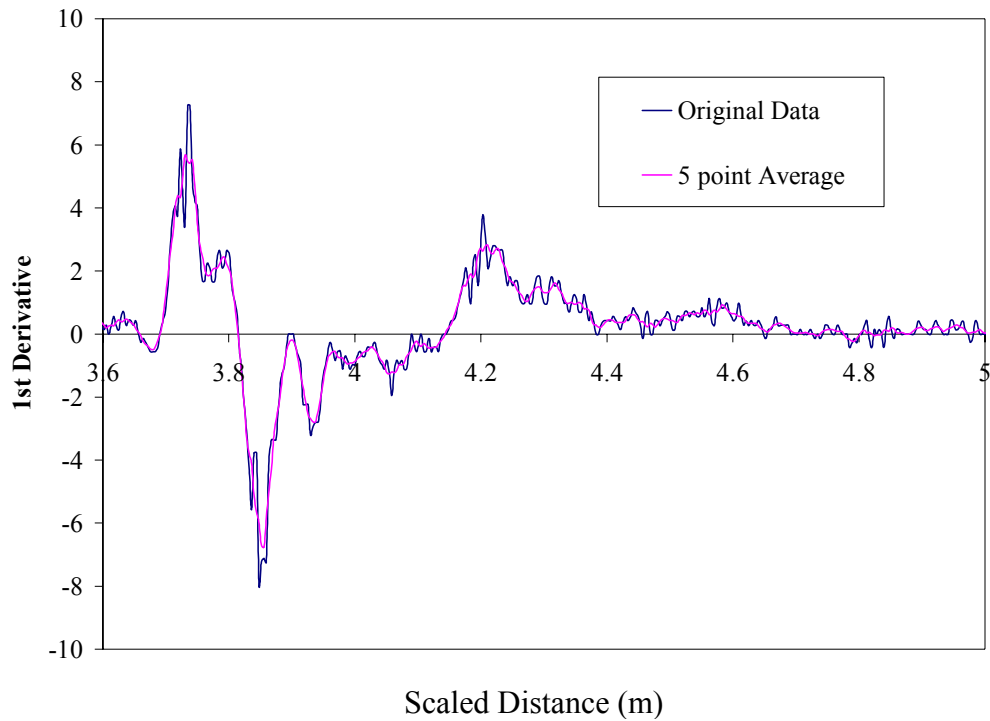


Fig. 4.5 Smoothing the Curve to Improve the First Derivative Values

Characteristic points include local maxima or minima points, points with maximal first derivative in the TDR signal can be identified. The locations and slopes at the characteristic points are then used to calculate the intersection and consequently locate the reflection points.

The third approach to analysis TDR signal is to apply inversion theory. Inversion theory is a science that studies parameter estimation of a system from given system responses. Inverse analysis of TDR waveforms is the most complicated method to identify soil properties. In this method, the parameters of a transmission line are first identified from inverse analysis of a TDR signal. Parameters of transmission line are then related to soil dielectric properties. Theoretically speaking, inverse analysis of TDR waveform is the most comprehensive approach since it physically describes the phenomena that happen in the TDR system. However, the complexity of the TDR system as well properties of soils makes it very difficult to simulate the actual behavior of the TDR system, nonetheless for the inverse analysis. Assumptions and simplifications generally have to be made before a solution can be obtained.

The model by Yanuka et al. (1988) is a simplified time domain model which accounts for the multiple reflections taking place in the TDR system. The model parameters are then inverse analyzed by making comparison of the predicted signal with that by actual measurement. Although Yanuka et al. obtained reasonably good results for certain soils they tested, they got poor results for cohesive soils. This is attributed to the over simplification of their model in that it does not account for relaxation or dispersion, finite rise time, and infinite reflections. Timlin and Pachepsky (1996) improved the model of Yanuka et al. by adding a model to account for the finite rise time of the cable tester. Results from laboratory tests are quite promising (Fig. 4.6). However, since this model is still a time domain model. It can not account for relaxation or dispersion of soil material. And thus it can not completely describe TDR system behavior.

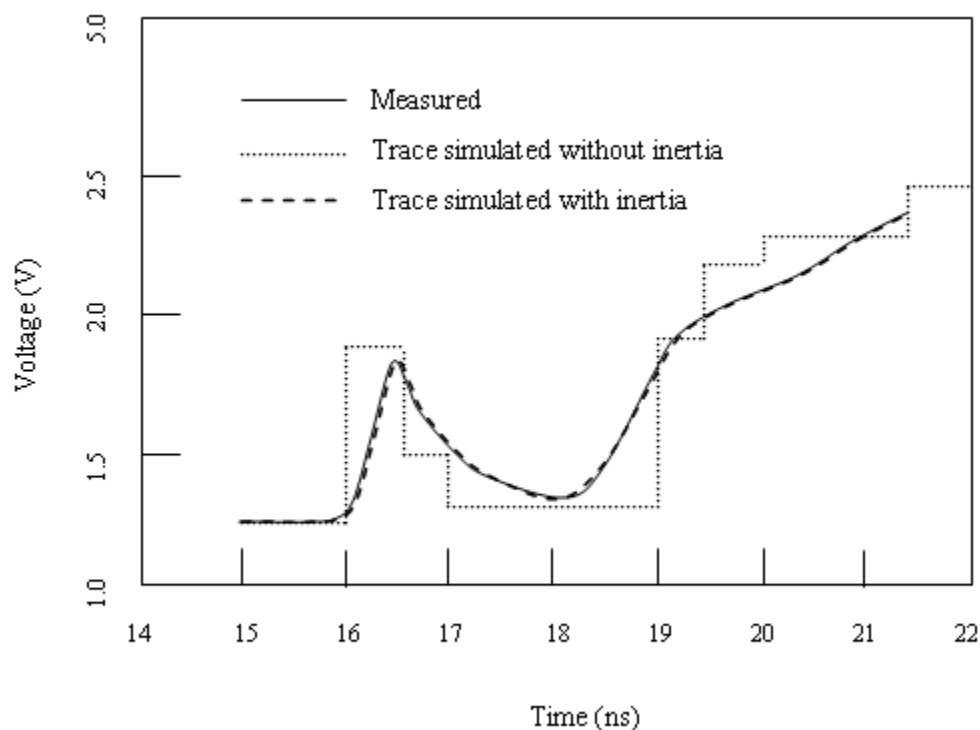


Fig 4.6 Measured and Predicted TDR Waveforms from the Reflection Models (Timlin and Pachepsky, 1996)

The model used by Feng, et al. (2000) and the model by Lin (2000) are by far the most sophisticated forward models for analysis of TDR systems. These models are built in the frequency domain. Thus they can accommodate the finite rise time of the TDR input pulse,

simulate dispersive behavior of materials, and account for multiple reflections in soil. Inverse analysis of these models is still under investigation to make it robust and accurate.

Comparison of the three approaches to analyze TDR signals indicates that the second approach, i.e., the automation of TDR waveform analysis, has the highest accuracy compared the results with the other two approaches (Timlin & Pachepsky, 1996). This is indicated by higher R-squared values of calibration curves obtained using this approach. This is attributed to the fact that it eliminated the possible errors caused by human operation and judgment.

4.2.3 Previous Algorithm Used at Purdue University

The computer algorithm previously used at Purdue University in TDR++ was developed by Feng et al. (1996). It uses smoothed curves and the first and second derivatives for locating the reflection points, which is an improvement over the method by Topp et al. (1982) and that by Baker and Allmaras (1990). It is a rather robust algorithm and can deal with a variety of different situations.

However, there are shortcomings with the algorithm when applied to dry soils or layered soil conditions. Also, the algorithm was developed for the Tektronix 1502B and is device dependent. Hence, a new algorithm was needed that overcomes the previous shortcomings and is less dependent on the TDR device.

4.2.4 Objective for New Algorithm Development

The objective of the new algorithm is an integral part of the objective of TDR testing automation. The criteria of the new algorithm includes: 1) Accurate - Which is demonstrated by factors such as improved calibration, improved accuracy of results of soil water content and dry density, consistent with known values for given material; 2) Easy to Implement - Can be described in terms of algorithms and implemented by computer code; 3) Robust - Which means that the algorithm needs to be applicable to various situations encountered. This includes conditions such as dry soil, soils with medium to high conductivity, layered soil conditions etc.

Fig. 4.7 shows the 6 typical different waveform shapes that are commonly measured in the field. The differences among those waveforms mostly lie in the distinct shape around the second reflection point. In Fig 4.7, the subplots indicate the following situations:

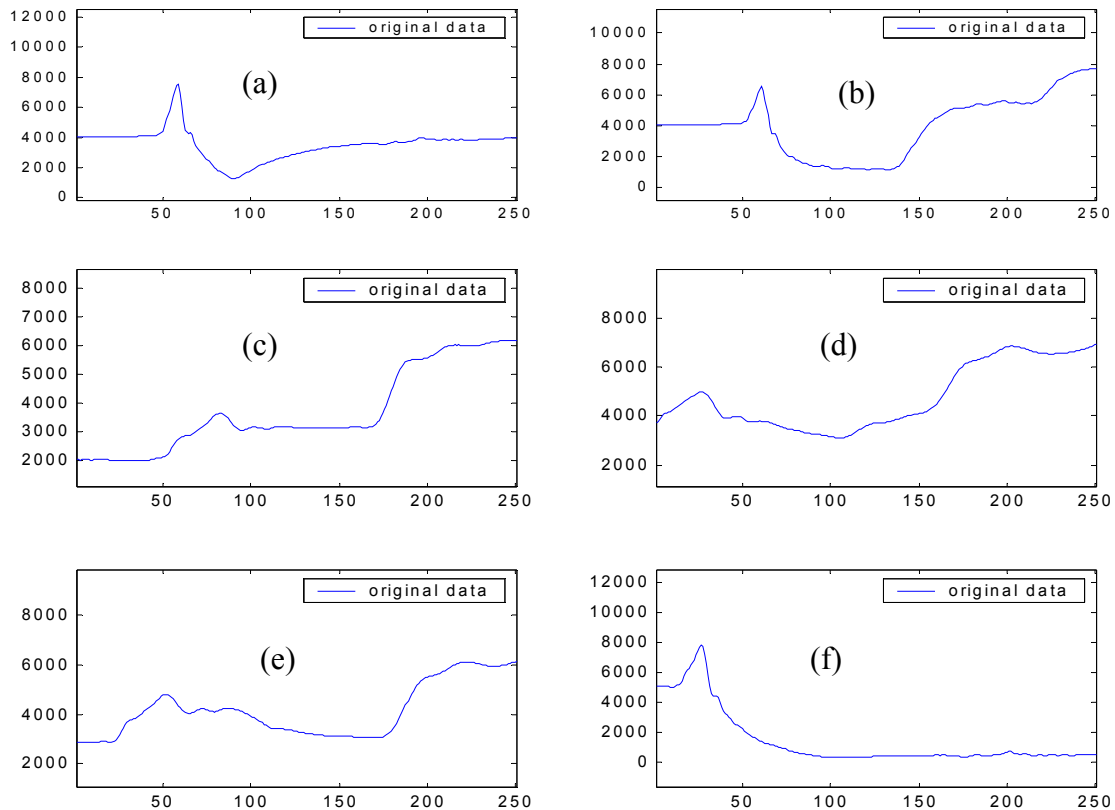


Fig. 4.7 Typical TDR Waveforms likely to be Encountered in the Field

- Plot a) is the typical waveform in clayey soil, which has relative slow rise after the second reflection point. This is mostly caused by energy loss in clay and scattering of electromagnetic energy by the dielectric relaxation of bound water.
- Plot b) is the typical waveform likely to be encountered in water or sandy soils with high water content. As conductive energy loss is relative small and the dielectric relaxation is not significant for free water, the TDR has a sharp rise in the second reflection point and high final the voltage level which indicate that there is no significant electromagnetic energy loss.
- Plot c) is the TDR signal likely to be encounter in soil with low water content, a characteristic in the waveform is the relative small drop in voltage after the first reflection. This causes problems in locating point with local minimum voltage level and thus the problem in locating the second reflection point.

- Plots d) and e) are more likely to be encountered in layered soil system. For plot d), it is likely that the soil evolves from wet to dry in the direction of electromagnetic wave propagation; while for the plot e), it is indication of soil evolving from dry to wet in the direction of electromagnetic wave propagation.
- Plot f) is the situation where there is significant energy loss caused by high conductivity of soils, which is demonstrated by the relative flat or non-existent rise after the second reflection point.

The commonly used tangent line method including the method previously used at Purdue determines the second reflection point by the intercept of the tangent line from the point with the largest first derivative and the horizontal line from the minimum point. Problems arise for the dry soils where the TDR signals rise up immediately after the first reflection point and no practical “minimum” point can be identified. Similar issue exists for layered soil conditions where soil profile goes from “wet” to “dry” with depth.

The algorithm developed in this project overcomes the shortcomings of its predecessors. Two important ideas implemented in the algorithm design include: noise reduction, curvature. The TDR signal is affected by variations in the soil being tested and by noise in the signal. The noise level can be measured by calculating the standard deviation of multiple measurements as well as calculating the noise-to-signal ratio in the frequency domain as demonstrated by Lin (1999). An example of this analysis is shown in fig. 4.8. Repeating and averaging TDR signals and 5-point or 7-point average of TDR data points helps to reduce the noise level. A curve fitting process can be used in the critical sections to further reduce the noise level.

Observations for the first reflection point include:

- It is the location where electromagnetic wave reaches the surface of mold;
- The point is a local maximum point on TDR signal;
- The position of first reflection is decided solely by the length of cable, its impedance, and the impedance of the head.

Observations for the second reflection point include:

- The second point lies after the first reflection point;
- It lies before the point with maximum first derivative;
- It is related to the section of sharp direction change in the curve.

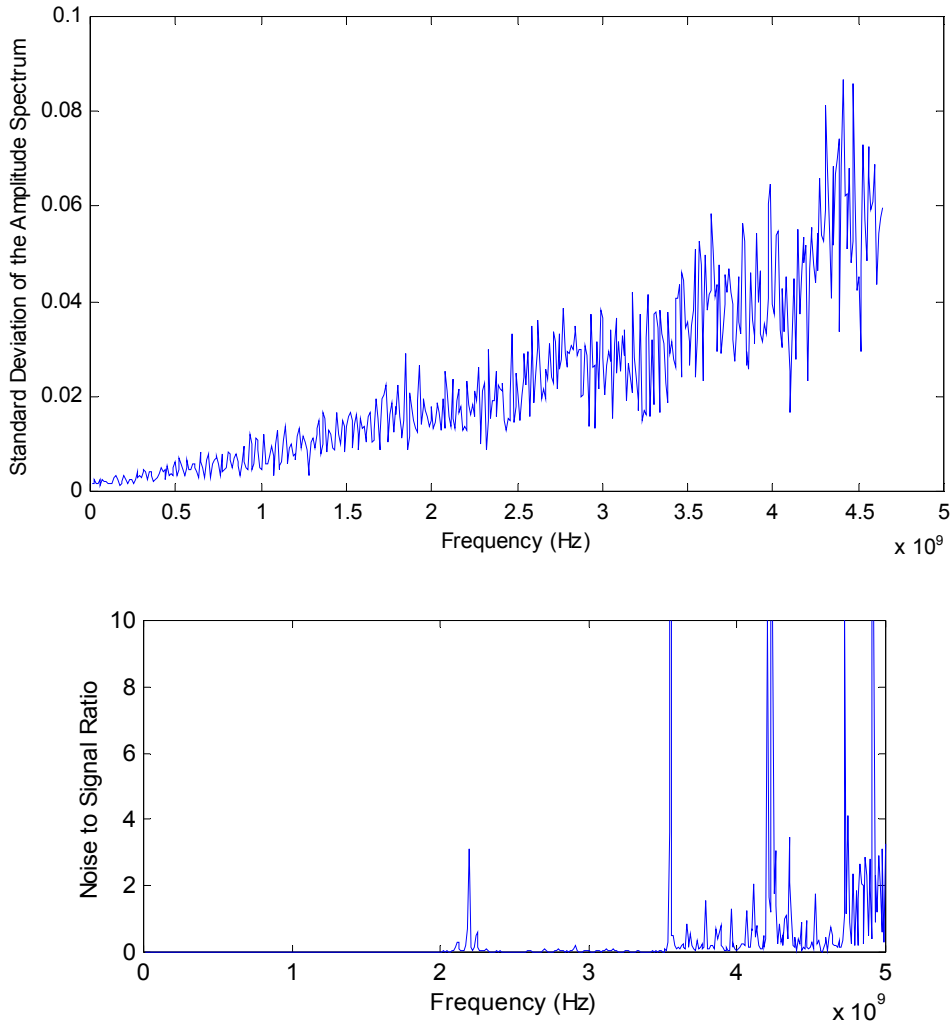


Fig. 4.8 Noise Level in a TDR System: a) Standard Deviation of Ten Measurements; b) Noise-to-Signal Ratio across the Frequency Bandwidth (Lin, 1999)

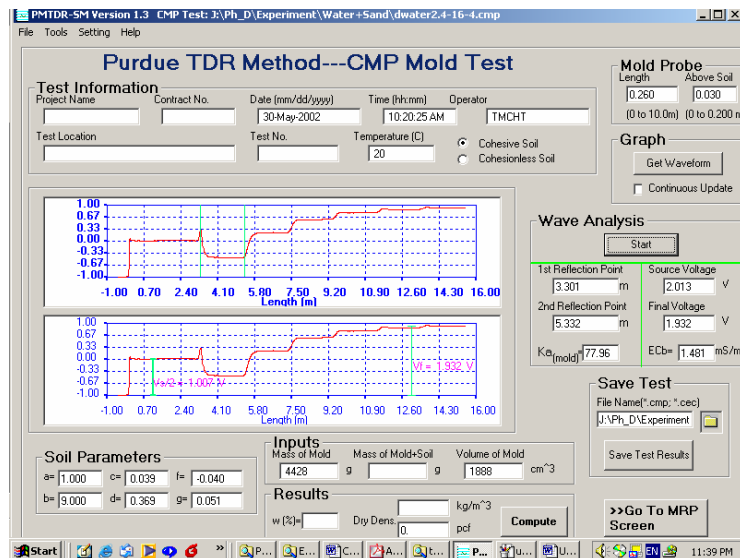
The algorithm is designed based on these observations. A second order polynomial is used for fitting the first reflection point. A third order polynomial is used for fitting the second reflection point. Details of the curve fitting process, locating of reflection points, and Matlab code are described in a copyrighted document (Drnevich and Yu, 2001).

4.2.5 Verification in Typical Conditions

Analysis of Measurements of Water

Water has an established dielectric constant of around 80 at 20° C. Measurements in water were conducted as part of the effort to validate the algorithm developed. The results of measurements in deionized water and in tap water are shown in Fig 4.9. From the analysis results, the dielectric constants obtained for deionized water and tap water were 77.9 and 80.7, respectively. Both of these values are close to the established values.

(a)



(b)

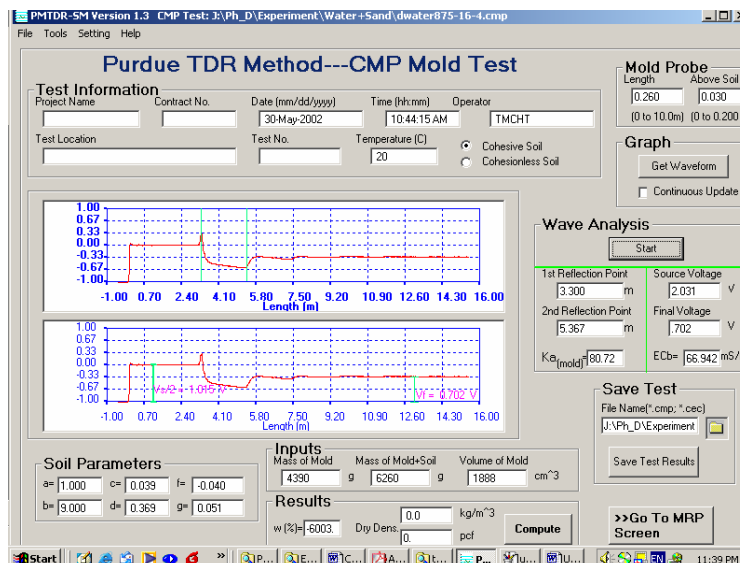


Fig. 4.9 Analysis of TDR Measurement in Water (a) Deionized Water; (b) Tap Water

Measurements of apparent electrical conductivity were made at other temperatures as shown in Fig. 4.10. The measurement was made with a Tektronix 1502B and then was converted into the format compatible with the newly designed algorithm and analyzed with it. The results look satisfactory compared to values published by Weast (1986) and Mitchell (1993).

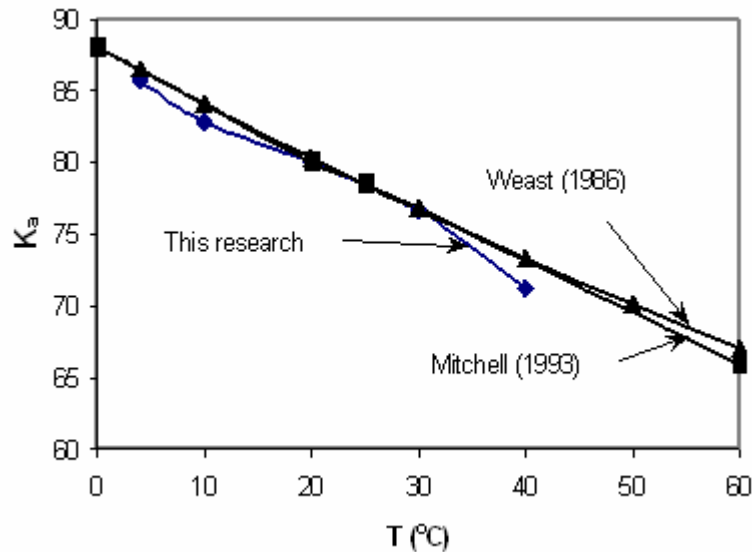


Fig. 4.10 TDR Measured Dielectric Constant of Water

Measurements in Dry Soil

Measurements in dry soil are challenging for TDR analysis, especially when using short probes. For example, Heimovaara (1993) discovered that primary reflection and the following reflections intermingle for probes shorter than 0.18 m with their TDR system. The intermingling of reflections makes it less accurate, if not impossible, to identify the reflection points accurately from TDR waveforms. The relative short travel time for electromagnetic wave to travel in dry soil condition makes it difficult to discern both the first and second reflection points.

The difficulty of picking first reflection point is overcome by the better hardware design of the Multiple Rod Probe head and rods developed in this research. The impedance discontinuity provided by Multiple Rod Probe Head results in a very clear reflection pattern around the first reflection point compared to other designs (Fig. 4.11). This reduces the difficulty in picking the first reflection point from TDR measurement in dry soil

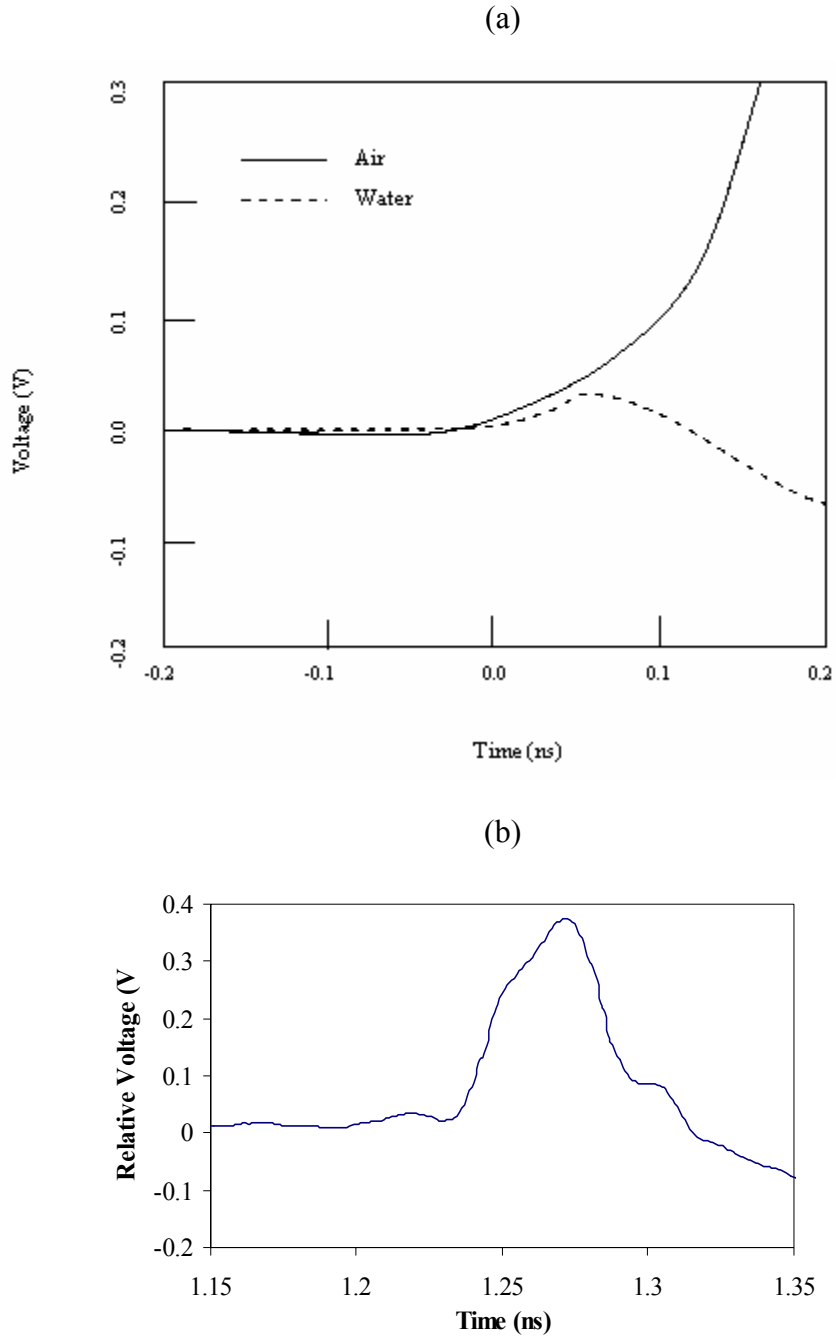


Fig. 4.11 Comparison of Reflection Pattern at First Reflection Point a) Enlargement of the First Reflection of a Small 0.10 m Triple Wire Probe (Heimovaara, 1990); b) Enlargement of the First Reflection Measured by Purdue TDR Device

Figure 4.12 shows the measurement and analysis results for dry Ottawa sand. The first reflection is relatively distinct. After the first reflection, the TDR signal drops slightly and then gradually rises rather than come to a valley with a minimum. Any algorithm that makes use of the minimum after the first arrival would not give accurate results for TDR curves like this. However, the concept of curvature used in the developed algorithm performs very well in this situation. As seen from the second vertical line in Fig. 4.12, the algorithm developed locates the second reflection point that provides an apparent dielectric constant for this soil that falls in the range provided by literature (Drnevich et al, 2002).

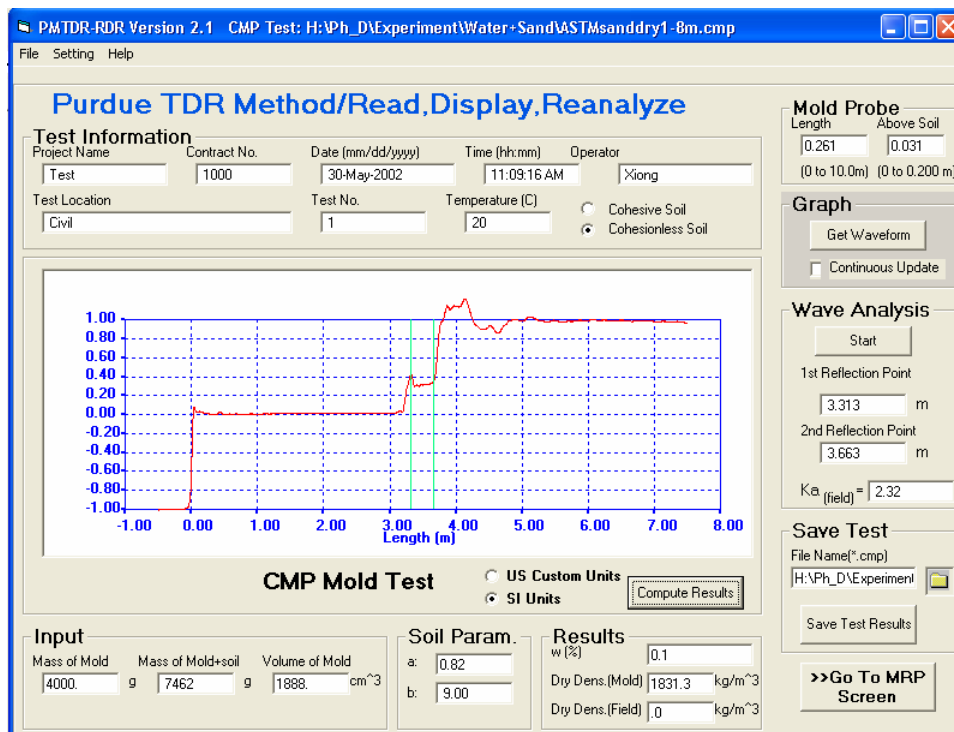


Fig. 4.12 TDR Measurement and Analysis in Dry Ottawa Sand

Layered Soil Conditions

Layered soil conditions, a situation frequently encountered in the field, provide another challenge for TDR measurement and can serve as a check on the robustness of the algorithm. A group of comparison tests were conducted to check the ability of TDR to measure layered soil conditions as well as check that TDR measures the average water content and dry density in the whole probe length.

A compaction test was conducted with two soil layers. One test had a wet soil above a dry soil (wet-over-dry) and the other with a dry soil above a wet soil (dry-over-wet). The material used was Ottawa sand compacted in mold with height of 26.3 cm. In the first test, 11.3cm of the mold was filled with sand having a water content of 1.3%. The remaining 12.0 cm was filled with wet sand with water content of 6.4%. In the second test, 11.9 cm of the mold was filled with wet sand having a water content of 6.8% and the remaining part was filled with sand having water content near 0%. The average water content for dry-over-wet case was around 4.1% and that of wet-over-dry case was around 3.7%. The total densities of these two samples were 1.725 g/cm^3 and 1.687 g/cm^3 , respectively.

Measured TDR waveforms for these tests are shown in Fig. 4.13. For the wet-over-dry case, after the first reflection the signal dips at a slower rate than that of dry-over-wet case. Then the signal suddenly becomes concaved downward, which is an indication of material with larger water content.

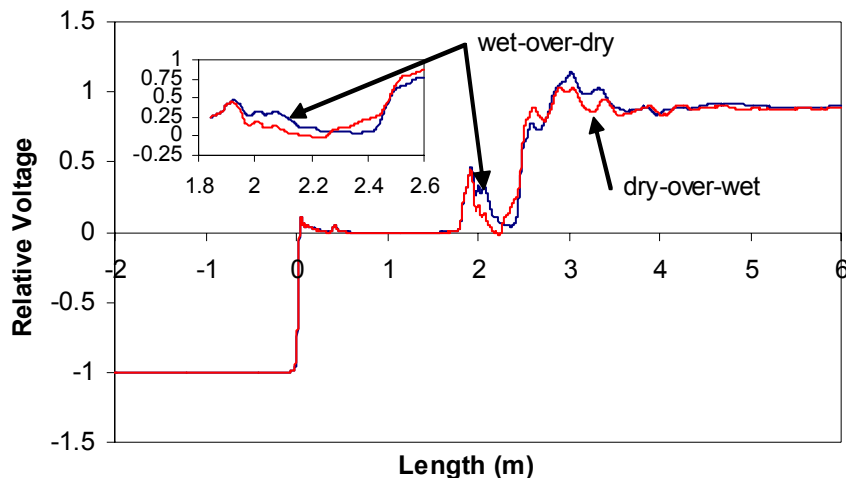


Fig. 4.13 TDR Signal Measured for Wet-to-Dry and Dry-to-Wet Cases

The locations that the algorithm picked up for first and second reflection points in these two cases are shown in the Fig. 4.14, respectively. The apparent dielectric constants measured are 4.88 and 4.64, respectively, which are close to each other. The calculated water content are 3.9% and 3.8%, respectively, using calibration constants $a=1.0$ and $b=8.5$, which gives values close to average water contents of 4.1% and 3.7%, respectively.

The change of TDR signal caused by changing material properties indicates that it might be possible to use TDR signal to tell the variation of soil physical properties in the ground.

Nevertheless, to do this, much more work is needed to develop the technology to make analysis and extract this piece of information. This could be a topic of interest for future investigations.

The ability to properly pick up the reflection points in these layered soil conditions also indicates that the algorithm developed here is robust for application to field situations.

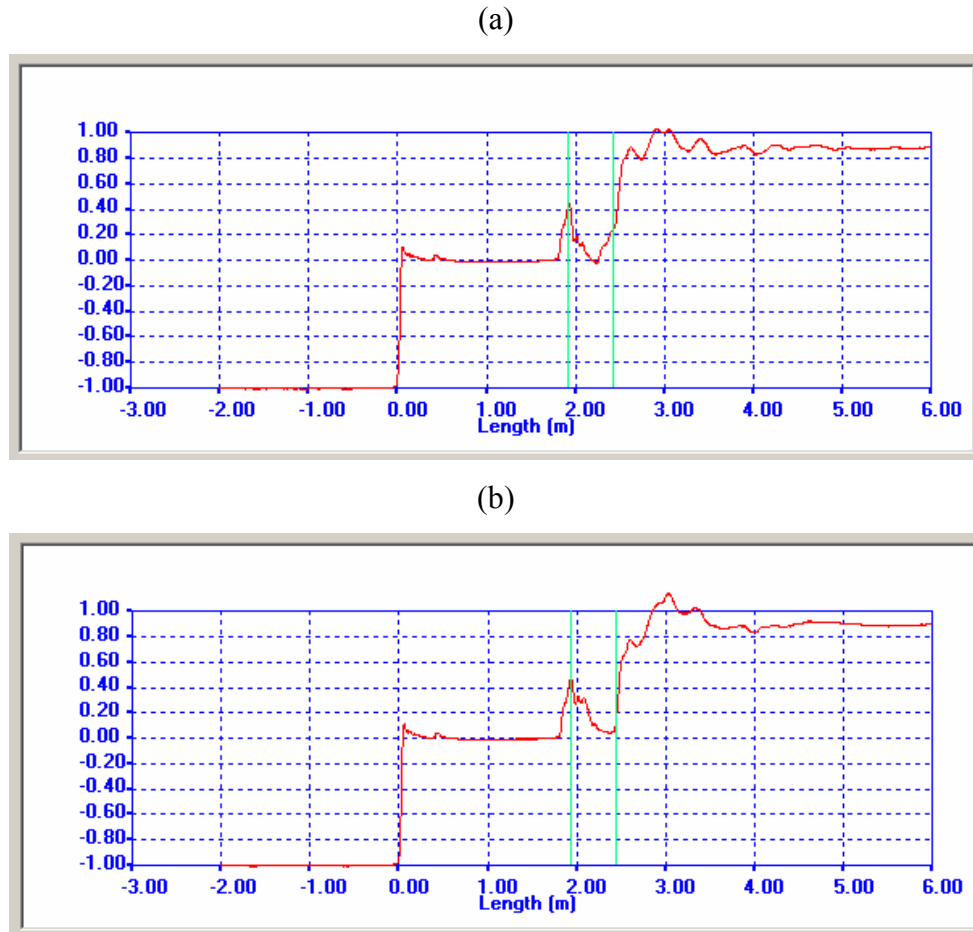


Fig. 4.14 Locations of Reflection Points Picked by the Algorithm (a) Wet-over-Dry Case (First Point=1.923m Second Point 2.418, $K_a=4.64$) (b) Dry-over-Wet Case (First Point=1.930m Second Point 2.438 $K_a=4.88$)

Lossy Conditions

Lossy is a term applied to the situation where electrical energy is dissipated as TDR signal travels through the sample, which is generally caused by dielectric relaxation (a mechanism in electrical systems similar to damping in a mechanical systems) or soil conductivity. This results in reduced magnitude of the reflected signal. Accuracy of TDR measurements are reduced for high lossy situations as the reduced level of the reflected signal makes it hard to accurately locate the second reflection point. Beside this, TDR is not applicable

to high lossy soils in which energy is totally lost and the second reflection can't be identified because of the flat signal after the first reflection point.

Multiple criteria are set in the developed algorithm. The algorithm gives a warning when a high lossy soil is encountered, i.e. when the voltage magnitude of the final reflection is less than 5% of TDR initial step voltage. This reminds the user to check the TDR signal and indicate that results might be erroneous. Another message will be given when the reflection level is less than 2% of TDR initial step voltage indicating that it is not possible to identify the second reflection point. Preliminary feedback from the Beta Test Partners is that the algorithm works reasonably well in most soils, but has difficulties in high lossy soils such as fat clays at high water contents or soils that have highly conductive pore fluids.

4.3 Algorithm for Bulk Electrical Conductivity of Soil

4.3.1 Electrical Conductivity from Attenuation Analysis

TDR measures both apparent dielectric constant (Topp et al., 1980) and bulk electrical conductivity (σ) (Dalton et al., 1984). Various algorithms have been proposed to obtain bulk electrical conductivity from measured TDR waveforms. Nadler et al. (1991) investigated most of these methods and concluded that the procedure by Dalton et al. (1984) is the most suitable for calculating σ from TDR measurement, including the case for layered soils, where TDR measures the average bulk electrical conductivity of the soil.

Dalton's approach to obtain bulk electrical conductivity is based on analysis of TDR voltage attenuation. The TDR signal exponentially decays as it travels along the measurement probe and is given by:

$$V_R - V_T = V_T \exp(-2\alpha L) \quad (4-2)$$

where V_T is the signal amplitude after partial reflection from the beginning of the probe, V_R is signal amplitude after reflection from the end of the probe, α is attenuation coefficient, L is the length of the measurement probe embedded in material under test. The attenuation coefficient is a function of the bulk electrical conductivity of the soil and apparent dielectric constant of the soil approximated by the equation

$$\alpha = \frac{60\pi\sigma}{\sqrt{K_a}} \quad (4-3)$$

where σ is the bulk electrical conductivity (also given in this report by the symbol EC_b) and K is the apparent dielectric constant. Combining these two equations, bulk electrical conductivity of the soil can be expressed as:

$$\sigma = \frac{\sqrt{K_a}}{120\pi L \ln\left(\frac{V_T}{V_R - V_T}\right)} \quad (4-4)$$

In analysis of a real TDR signals, characteristic voltages V_T , V_R can be obtained from measurement; information of apparent dielectric constant of the soil can be obtained as discussed earlier.

Reasonably good results of bulk electrical conductivity of soil are obtained by this approach. However, this approach has some problems. One is that it does not take into account multiple reflections measured by TDR waveforms (See Fig. 4.15). For signals measured with short probes or in materials with low apparent dielectric constants, the time for multiple reflections are relative short. These multiple reflections interfere with each other (Heimovarra, 1990) and make it difficult to pick the characteristic voltage from the TDR signal.

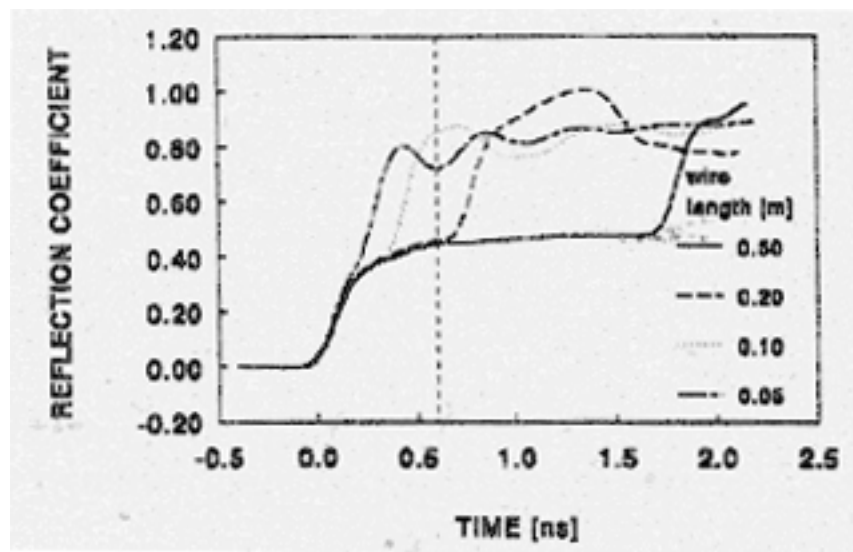


Fig. 4.15 Likelihood of “Contaminated” Signal (Heimovarra, 1990)

To compensate for the shortcomings of Dalton's approach, Yanuka (1988) introduced a multiple reflection model and used the amplitude of the signal after all reflections V_f to obtain bulk electrical conductivity. Zeglin et al. (1989) refined the expression Yanuka obtained for calculating conductivity as:

$$\sigma_{eff} = \frac{\sqrt{K_a}}{120\pi L} \ln\left(\frac{V_1 V_f - V_0 (V_1 + V_f)}{V_0 (V_1 - V_f)}\right) \quad (4-5)$$

where V_f is final signal amplitude after all reflections have occurred and the other qualities are defined as before and shown in the following figure.

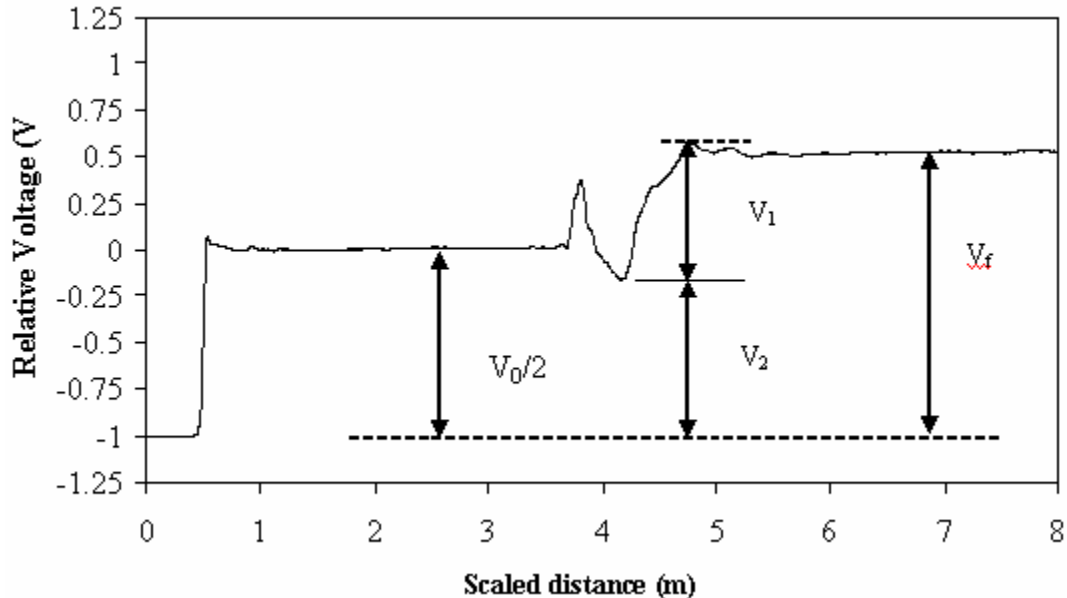


Fig. 4.16 Definition of Voltage Levels in a TDR Waveform for Determining Bulk Electrical Conductivity

Although the results using these different reflection models apply for certain cases and were observed to give consistent results, there are problems associated with these models, including the multiple reflection issue discussed above. Other difficulties include:

- 1) In the expressions, σ depends on K_a , which means that the error in the determination of K_a will be carried over in calculating σ . This would result in increased error;

- 2) It could be a difficult, if not impossible, to pick the characteristic voltages levels V_0, V_1, V_f , especially for materials with low apparent dielectric constant or short measurement probes;
- 3) As mentioned before, the expression used for attenuation factor is an approximation for the real attenuation factor, which could induce certain error.

4.3.2 Conductivity from Long Term TDR Response

A more sophisticated analysis to obtain bulk electrical conductivity from TDR signal is from analysis of the long term response of a TDR system using transmission line theory. This idea has been exploited as a result of using time domain solutions to provide some useful direct interpretation of the TDR waveforms (Giese and Tiemann, 1975). The transmission line theory indicates that the TDR system can be modeled with electrical circuit model and the long time response of TDR system is equivalent to response of the electrical circuit. In this approach, we don't need to trace the electromagnetic wave reflection process in the TDR system, the long term response is the only factor in which we have interest. To extract information from TDR waveforms, we only need to find the final voltage level of TDR signal, which is much easier to obtain. Detailed theoretical basis for TDR system analysis can be found in books dealing with transmission line theory (e.g. Ramo et al., 1994). Principles obtained from these analyses are:

- 1) TDR system can be represented by circuit model

Although the TDR system is a dynamic system and theoretically it should be modeled with a dynamic model (Fig. 4.17 (a)). A close inspection of the response in a transmission line indicates that it is possible to use a static model to represent the response of the TDR system (Fig. 4.17 (b)) since we are only interested in the long-term response.

In Fig. 4.17 (a), the dynamic response of TDR system is modeled with the following components: A pulse source, which generates the step pulse and has a characteristic impedance of Z_s . The coaxial line and measuring probe has length L_1 and L_2 respectively, impedance Z_p , the measurement sample has characteristic impedance of Z_L , which acts as the load impedance of the system. In Fig. 4.17(b), the static circuit model includes a static voltage source having a voltage equal to twice the pulse step generated by the dynamic model in Fig. 4.17 (a) and an inner resistance equal to that of characteristic impedance. The load is a resistor with resistance R_L equal to the load impedance of dynamic model.

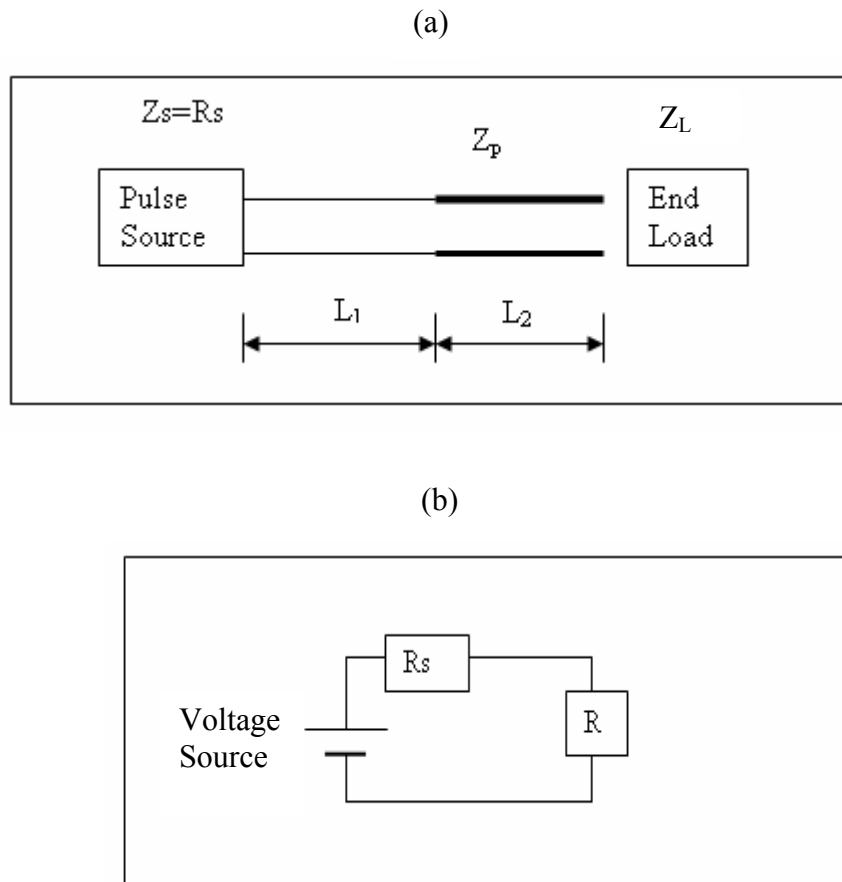


Fig. 4.17 Model for Long-term Static Response (a) Dynamic Model; (b) Equivalent Static Model for Long Term Response

A Matlab program was written for the dynamic response of model in Fig. 4.17(a). Model parameters were assumed to obtain the dynamic response as well as the long term response. The impedance of line was changed and the corresponding TDR system responses are shown in Fig. 4.18 below.

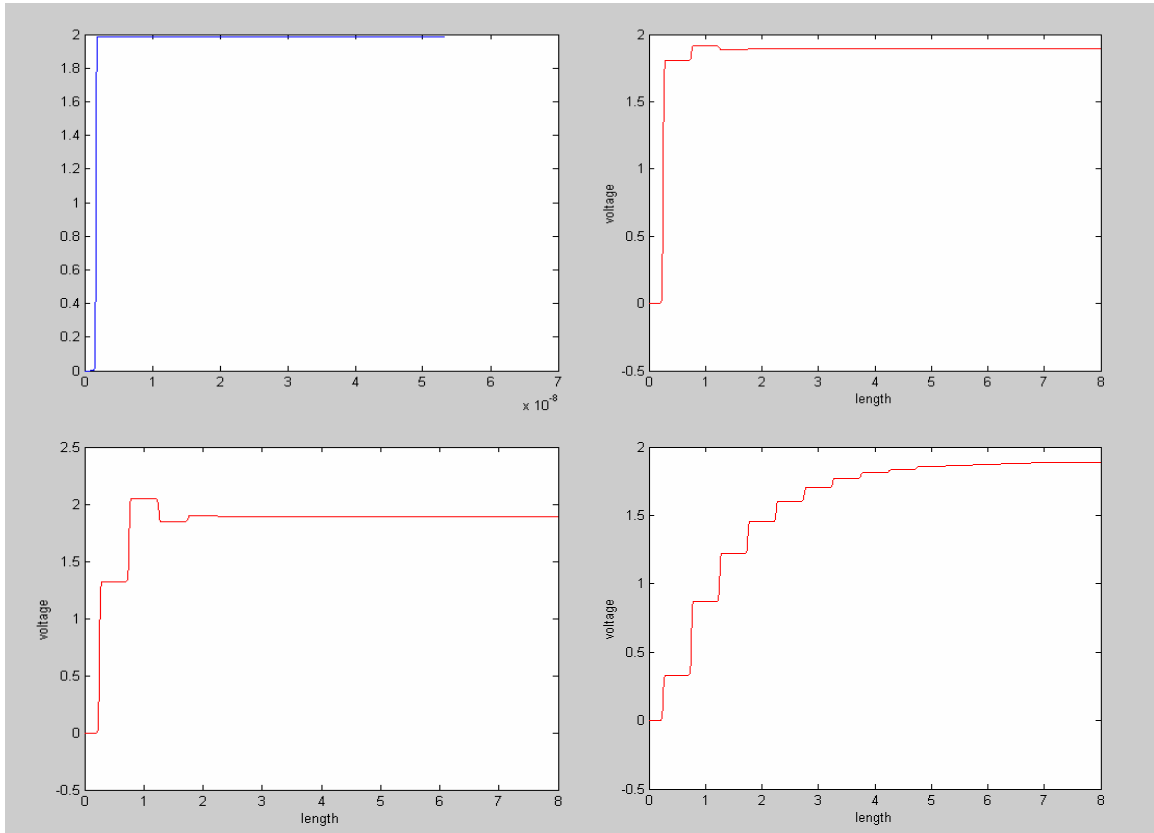


Fig. 4.18 Response of TDR System with Parameters $V_{in}=1.986$ V, $Z_s=R_s=50$ Ohms, $Z_L=R_L=1000$ Ohms, $L=0.25$ m (a) Step Pulse; (b) $Z_p=100$ Ohms; (c) $Z_p=500$ Ohms; (d) $Z_p=10$ Ohms

An interesting phenomenon is that although the parameters of the coaxial lines are different in each case shown in Fig. 4.18, the final voltage level is the same, 1.891 V.

A close inspection indicates that the following equation describes the model

$$V_f = V_s \frac{R_L}{R_s + R_L} = 1.986 \times \frac{1000}{1000 + 50} = 1.891 \quad (4-6)$$

Thus, the long term voltage level in the transmission line system is independent of the impedance of the connecting coaxial cable and is only dependent on the impedance of the pulse generator and load impedance. The voltage value is determined by the static circuit law, i.e., voltage distribution law. This means that the long term response of the TDR system can be obtained from the equivalent static circuit as shown in Fig. 4.18 (b).

In order to use Eq. 4-6, the following relationships are defined:

- 1) Step pulse generator provides the Voltage Source
- 2) TDR internal resistance is represented by the Resistor, R_s
- 3) TDR cable, probe head, probe is represented by conducting cable with no resistance
- 4) Soil sample or TDR test sample is represented by the Resistor, R

The remaining issue is how to relate the electrical conductivity of the sample under test to the resistance of the equivalent resistor. From static electromagnetic theory, for a sample with the geometry of inner diameter a , out diameter b , length L , and conductivity σ , the axial resistance can be obtained as:

$$R = \frac{V}{I} = \frac{1}{2\pi\sigma L} \ln\left(\frac{b}{a}\right) \quad (4-7)$$

Thus, final voltage level of the long term response of TDR system is

$$V_f = V_s \frac{R}{R + R_s} \quad (4-8)$$

$$\frac{V_s}{V_f} = 1 + \frac{R_s}{R} = 1 + \frac{2\pi LR_s}{\ln\left(\frac{b}{a}\right)} \sigma \quad (4-9)$$

Let $C = \frac{2\pi LR_s}{\ln\left(\frac{b}{a}\right)}$ then the electrical conductivity is obtained as

$$\sigma = \frac{1}{C} \left(\frac{V_s}{V_f} - 1 \right) \quad (4-10)$$

Thus, bulk soil electrical conductivity is a linear relationship to the measured ratio of $\frac{V_s}{V_f}$, with the slope, C , dependent upon geometry of the measurement probe and internal impedance of TDR pulse generator.

Compared with the analysis using the attenuation of electromagnetic waves in TDR systems, there are several advantages of using this relationship to obtain bulk soil electrical conductivity:

- This relationship is simple in form and has a sound theoretical basis;
- Compared with other relationships, it is easier to use;
- No K_a is involved in this expression.
- The long term TDR voltage level and voltage of pulse generator can be determined with greater accuracy since there are fewer factors influencing these variables.

This relationship is described as the algorithm and used the computer program PMTDR-SM described below.

4.4 TDR Software Development

Software development is an important for simplifying the TDR testing process. Three programs were developed for this research. One is called PMTDR, which was developed by Campbell Scientific, Inc. especially for the Purdue TDR method. PMTDR is the acronym of Purdue Method Time Domain Reflectometry. The other two programs are called PMTDR-RDR and PMTDR-SM and they were developed by Xiong Yu as part of this research. PMTDR-RDR was originally written to open data files previously stored by PMTDR to operate on them with updated calibration factors. The PMTDR program could not do this. Xiong Yu later incorporated “hand-shaking” functions into PMTDR-RDR to control the TDR100 signal generator/sampler and to acquire the TDR waveform data. After that, PMTDR was abandoned. Another program called PMTDR-SM was written to implement the one-step procedure for insitu measurement of water content and dry density.

4.4.1 Introduction to PMTDR Program

PMTDR is a program designed for automated TDR measurements of soil moisture content and density. The algorithms were designed by the TDR research group led by Prof. Drnevich. It is a Windows-based program with versatile functionality and a user-friendly interface. It features the following functionality:

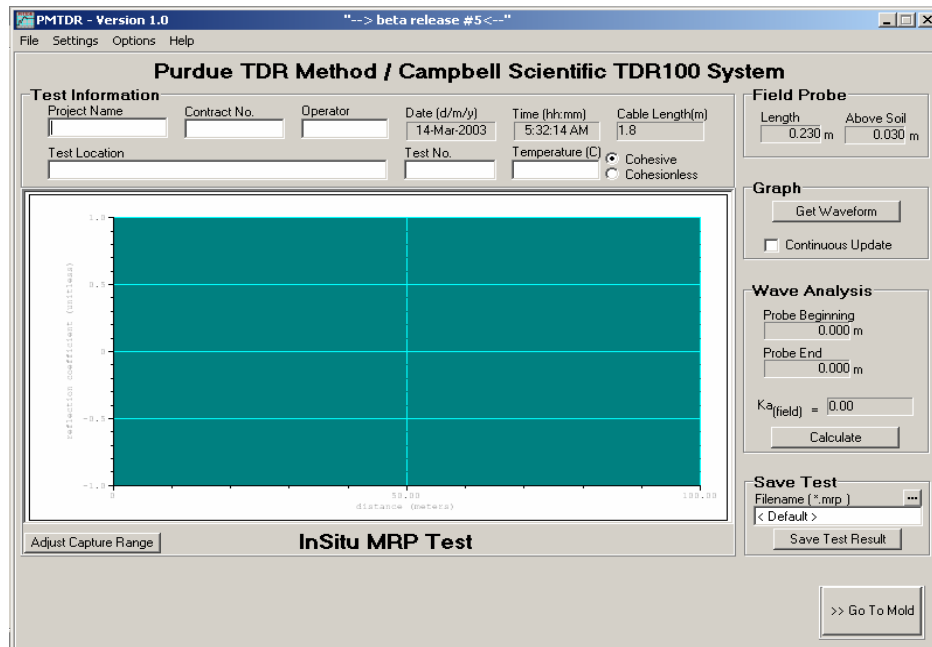
- Sampling parameter setting;
- Data acquisition;
- Signal displaying;
- TDR system information setting;

- TDR waveform analysis and display;
- Temperature effects correction;
- Insulated probe calibration;
- Soil water content and density calculation;
- TDR test information and waveform output;
- On-line help

A screen of this program is shown in Fig. 4.19. It is a product of TDR research at Purdue University. The program was written by Campbell Scientific Inc. The algorithm code used for PMTDR is developed by Dr. Drnevich and Xiong Yu.

The program is easy to operate and good in terms of communication with the TDR100 signal generator/sampler, however, it had some shortcomings. For example, a) it does not provide the function to open data files previously stored for purpose of reanalysis; b) although there is two screens in this program, only data obtained lastly is stored in the memory, which causes problems in some cases; and c) the function of unit conversion provided by this program is not very convenient. (It clears the input values for current units when switching to other units.) Thus an independent computer program called PMTDR-RDR was developed by Xiong at Purdue to overcome the shortcomings of the PMTDR program. Once it became functional, the program PMTDR was abandoned.

(a)



(b)

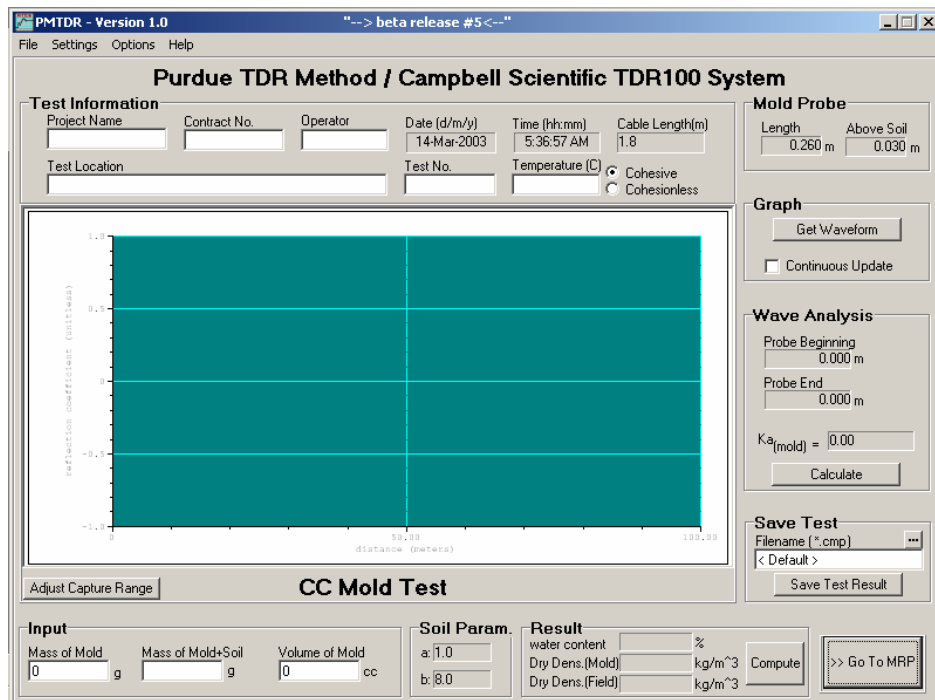


Fig. 4.19 Interface of PMTDR Program: (a) Screen for Field MRP Test; (b) Screen for Mold CMP Test

4.4.2 Introduction to PMTDR-RDR Program

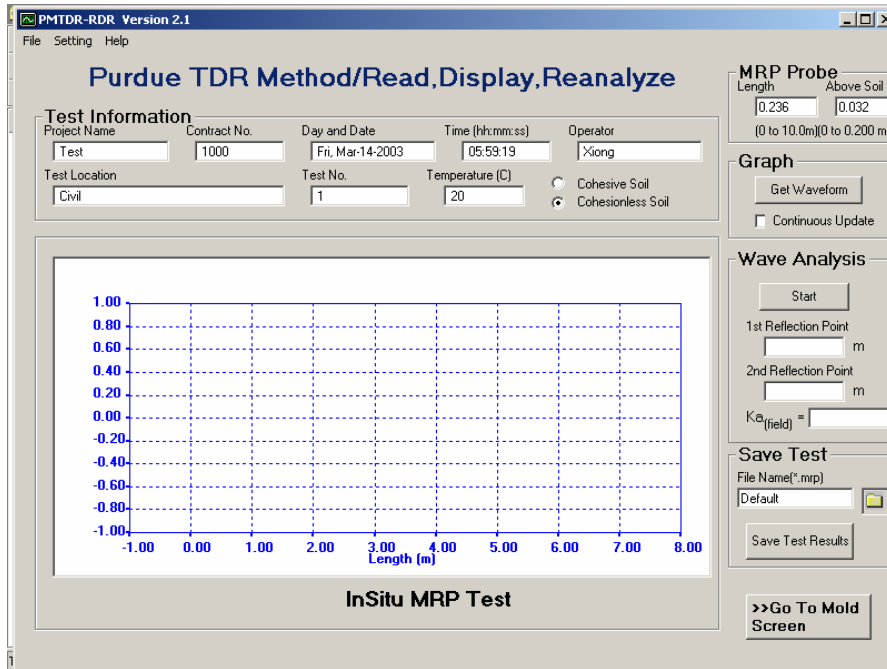
PMTDR-RDR is a program used for review, display and reanalysis of data by PMTDR. It was initially developed to supplement the program PMTDR. Its functions were expanded to acquire data and it was further improved based on feedback from various users in the Beta Testing program.

PMTDR-RDR is a Windows-based program with versatile functionality and a user-friendly interface. It features the following functionality:

- Sampling parameter settings
- Data acquisition
- Signal display
- TDR system information setting
- TDR waveform display and analysis
- Temperature effects correction
- Insulated probe calibration
- Soil water content and density calculation
- Units conversion
- TDR test information and waveform output
- Recall data saved by PMTDR and PMTDR-RDR
- Reanalyze data with new system information and calibration parameters
- Store analysis results
- On-line help

The program also uses two screens, one for field MRP test and the other for mold CMP test. Appearances of the screens of this program are shown in Fig. 4.20. Details on installation and operation of the program can be found in Purdue TDR Method User's Manual or the Help feature provided by the program.

(a)



(b)

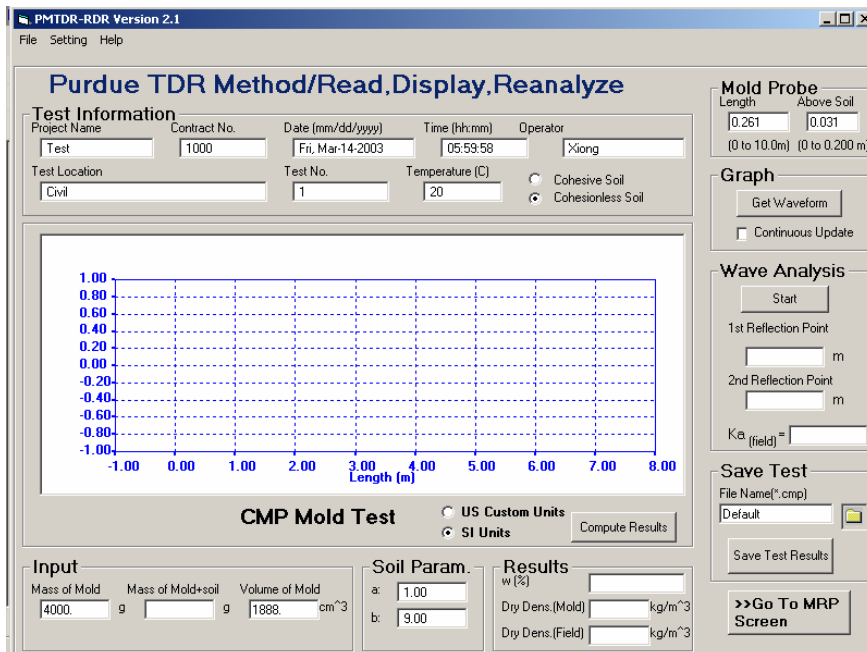


Fig. 4.20 User Interface of the PMTDR-RDR Program: (a) Screen for Field (MRP) TDR Test; (b) Screen for Mold (CMP) TDR Test

4.4.3 Introduction to PMTDR-SM Program

PMTDR-SM is the acronym of Purdue Method TDR - Simplified Method. It is the software used for automation of soil water content and dry density determination using the one-step TDR method described in the following chapters. It features the following functions:

- Operates the TDR100 to obtain desired TDR waveform;
- Graphic display of TDR waveforms on screen;
- Analysis of the TDR waveform to obtain apparent dielectric constant and bulk electrical conductivity of the soil;
- Computes soil water content and dry density using the one-step method;
- Logs information related to the TDR test and saves test results;
- Saves and loads test information as configuration files;
- Reads test results for reanalysis.
- In addition, it provides a module to facilitate the calibration process. The calibration constants obtained by this module are automatically uploaded to the testing screens.

PMTDR-SM currently has two screens, one is called MRP screen (Fig. 4.21) and one is called CMP screen (Fig.4.22). The MRP screen is used for field TDR tests and the CMP screen is used for mold TDR tests. The user can switch from one screen to the other by clicking on the button at the right-bottom of each screen. The appropriate screen needs to be activated for the type of test being performed. Then follow the instructions below to conduct the TDR test and perform the analysis to obtain the results.

4.4.3.1 Set test information

Test information related to the TDR test includes: Project Name, Contract No., Day and Date (automatically provided), Time (automatically provided), Operator, Test Location, Test No., Temperature, and soil type. This information goes in the ***Test Information*** section on the upper portion of the screen. It may be input on either the MPR or CMP screen and will be visible in both.

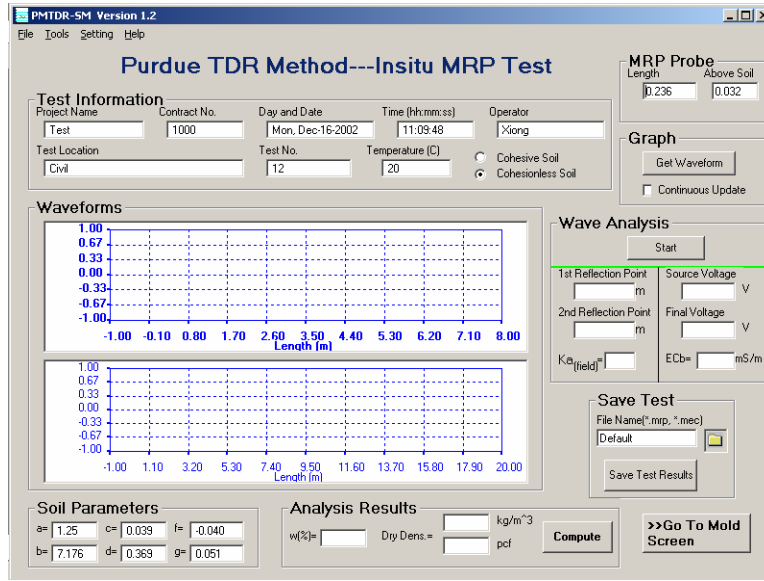


Fig. 4.21 MRP Screen for Field TDR Test

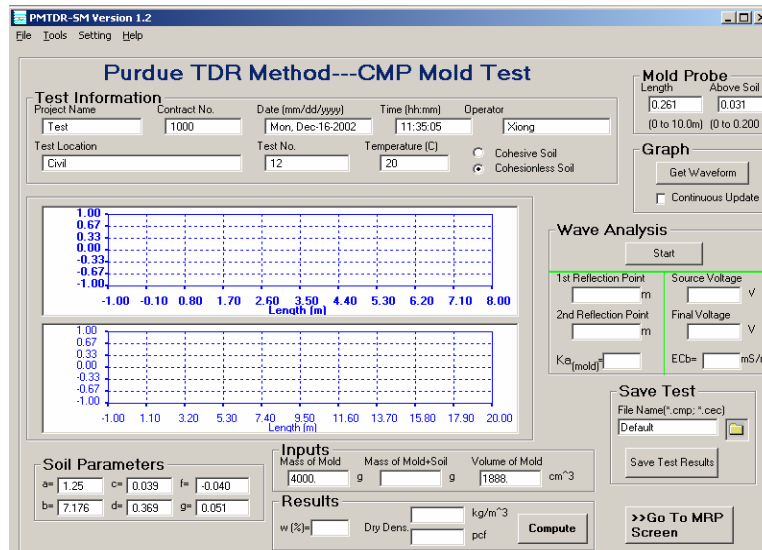


Fig. 4.22 CMP Screen for Mold TDR Test

Information about the TDR testing system includes the parameters for waveform sampling, probe information, and soil calibration parameters. These are displayed and can be set by click the menu *Setting->Measurement Parameters* (Fig. 4.23).

All the test information can be stored as a configuration (.cfg) file and can be loaded subsequently to save time, which is discussed in Section 4.4.3.1.

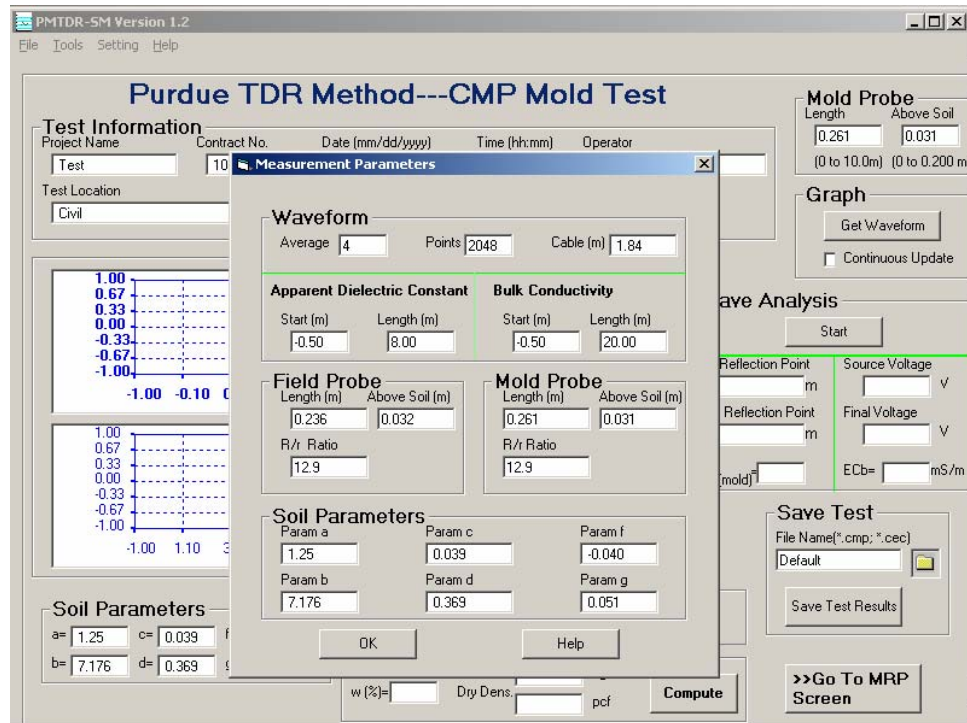


Fig. 4.23 Set Measurement Parameters in Measurement Parameters Window

4.4.3.2 Obtain TDR waveform

Click the button Get Waveform to obtain TDR waveform. It generally takes about 10 seconds to obtain and display two waveforms on the screen (Fig. 4.24). One will have a short scaled length to obtain apparent dielectric constant; the other with longer length to get bulk electrical conductivity.

The program automatically checks the connection of computer with the TDR100. If there is a problem with the connection, an error message appears saying: “Communication with TDR100 is not ready, please check on connection and plug” (Fig. 4.25). If this occurs, make sure the TDR100 power switch is pulled up and the connections of the RS232 cable with the computer are tight.

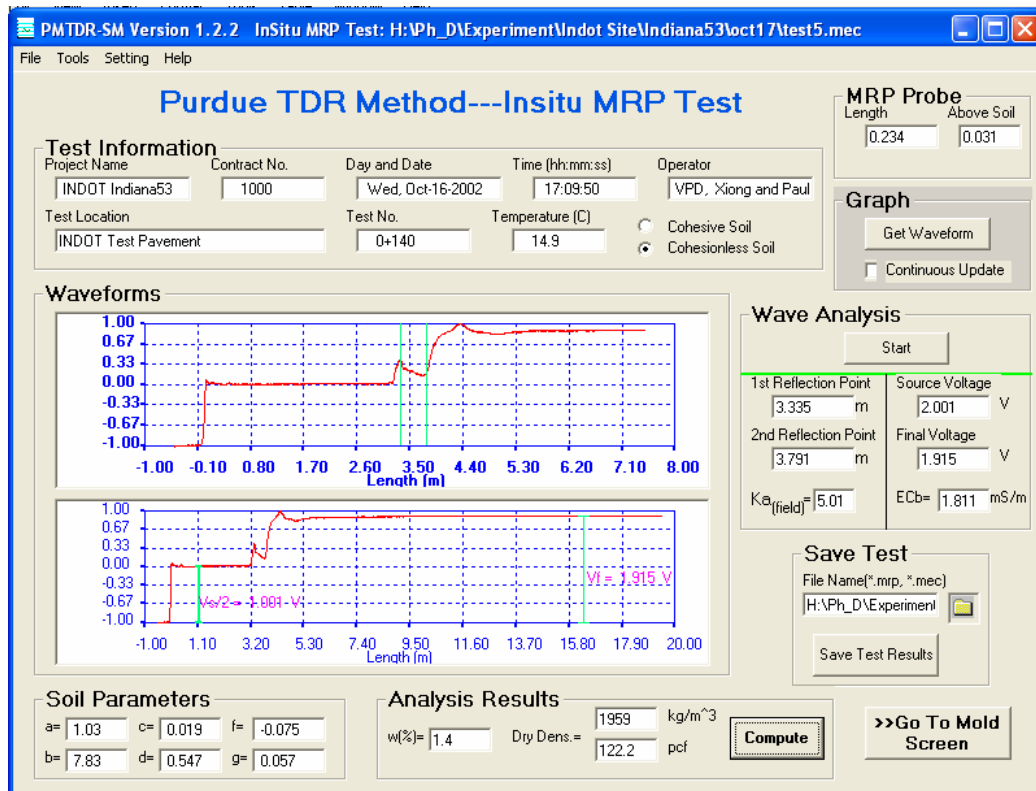


Fig. 4.24 Two TDR Waveforms are Displayed on the Screen

4.4.3.3 Analysis to Obtain Soil Water Content and Dry Density

- 1) Click the *Start* button to obtain apparent dielectric constant and bulk electrical conductivity from TDR waveforms;
- 2) Input the soil dependent calibration factors a, b, c, d, f, g . (these values can be obtained using regression analysis by known software like Excel or the calibration module discussed in session 4.3.4.2).
- 3) Click *Compute* button to make computations for soil water content and dry density.

An example of analysis results is shown in Fig. 4.26.

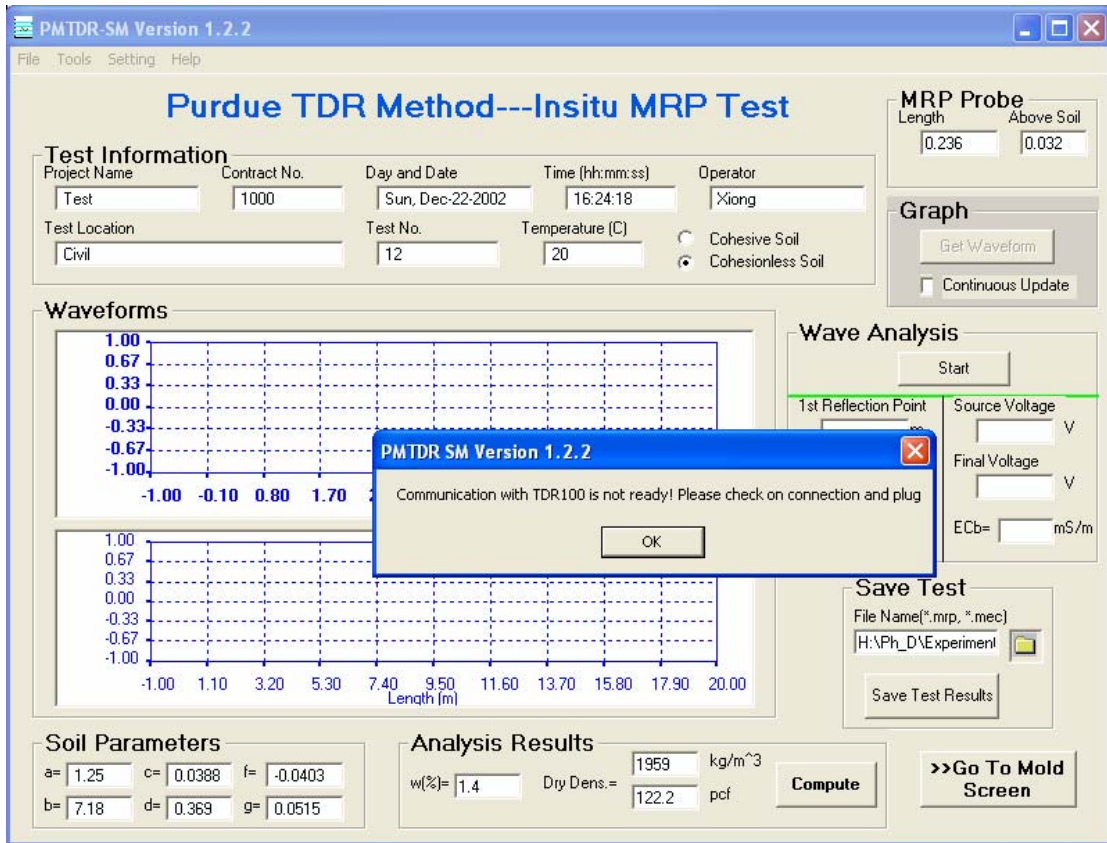


Fig. 4.25 Dialog Window Warning of a Hardware Connection Problem

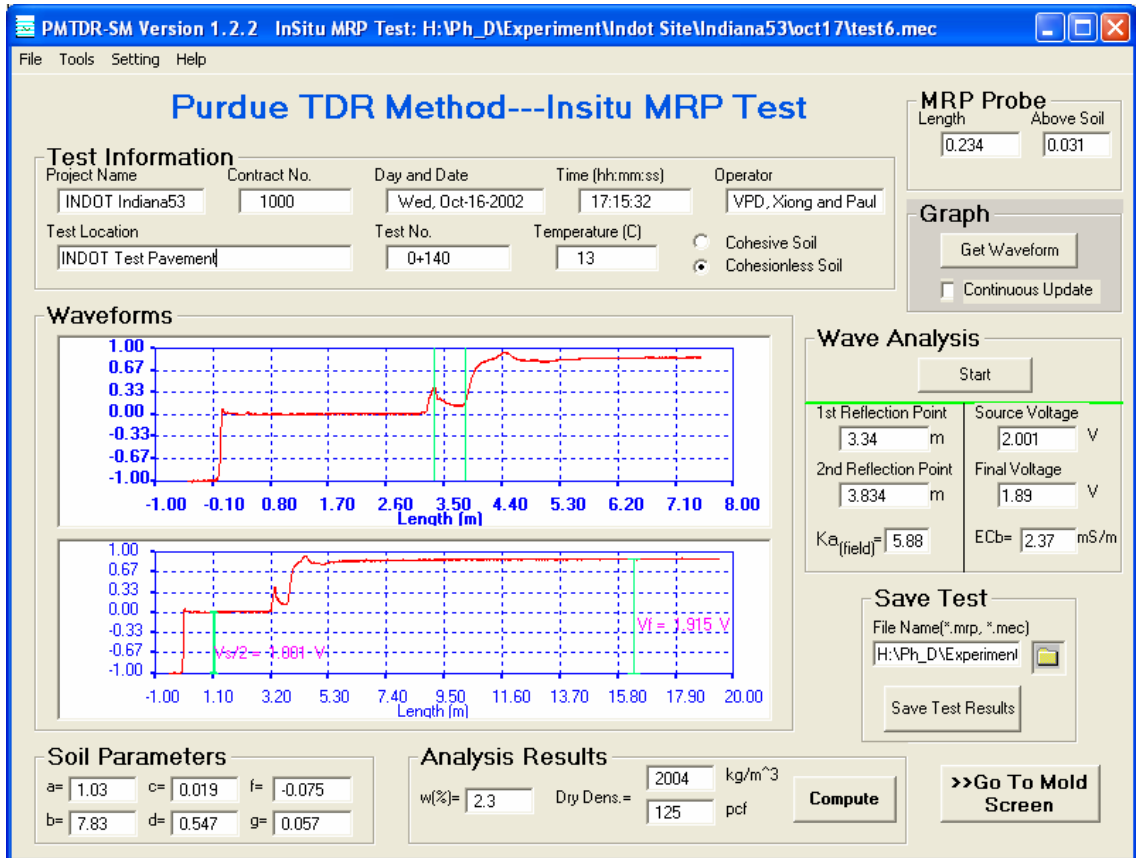


Fig. 4.26 Display after a Completed Analysis with PMTDR-SM

4.4.3.4 Store Test Results

Test results can be stored by clicking *File->Save Test Results menu* (Fig. 4.27). Information stored includes test information, TDR waveform data, and results of the analyses. For the MRP field test, two TDR waveforms are stored in files with postfixes “.mrp” and “.mec”, respectively. For the CMP mold test, the two TDR waveforms are stored in file with postfixes “.cmp” and “.cec”, respectively.

Test data can be recalled by click *File->Load Test Results* menu.

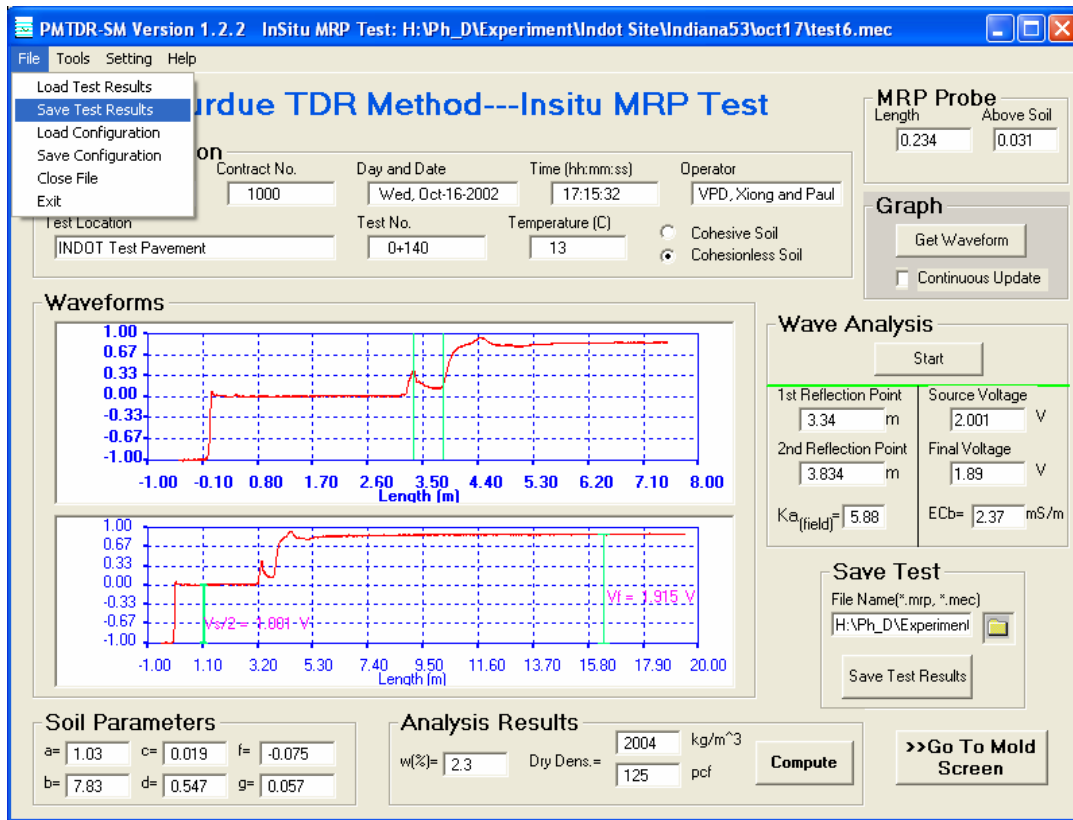


Fig. 4.27 Save Test Results by Clicking File->Save Test Results Menu

4.4.3.5 Useful Operation Skills

4.4.3.5.1 Save and Load Configuration

Test settings can be saved and then subsequently loaded for convenience. The configuration file is a text file with postfix “.cfg”. It stores project information, test parameters, and soil calibration constants. An example of the content in configuration file is shown in Fig. 4.28.

A default configuration file named PMTDR-SM.cfg is stored under the same directory as PMTDR-SM program when the program is installed. It is automatically loaded when program starts.

It is a good practice to create a configuration file for each project or soil under test. Then load the configuration by clicking **File->Load Configuration** (Fig. 4.29).

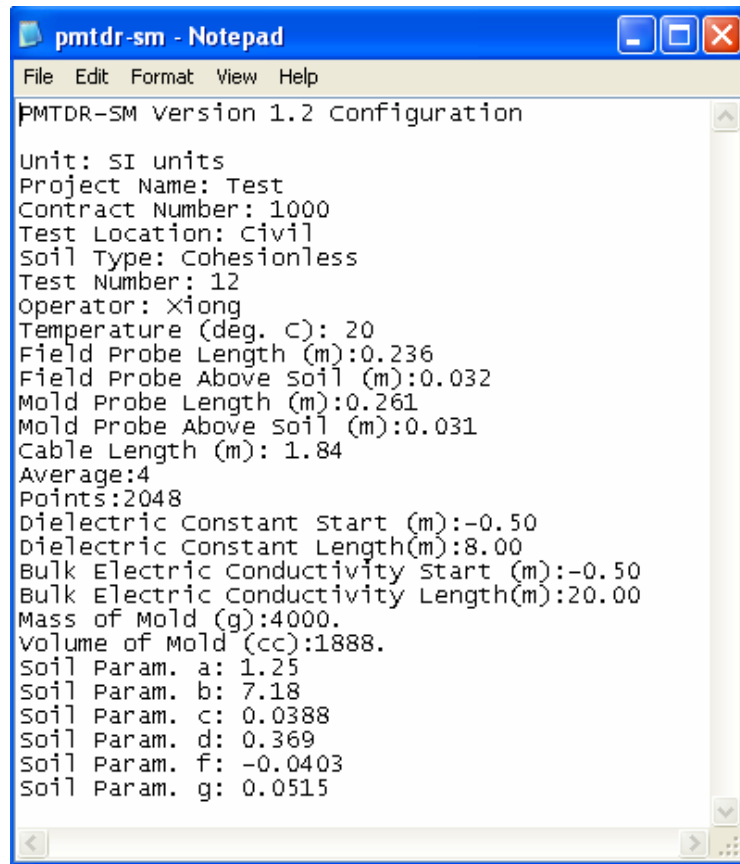


Fig. 4.28 Content in Configuration File

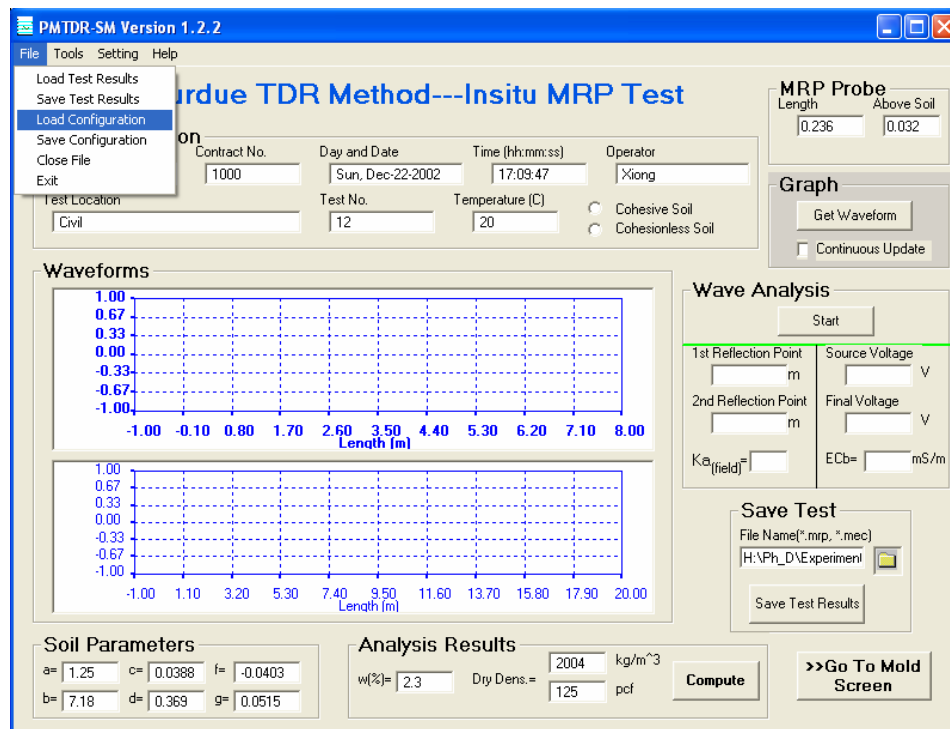


Fig. 4.29 Click File->Load Configuration to Load Configuration Files

4.4.3.5.2 Use calibration module

The PMTDR-SM program provides a calibration module to automate the calibration process to obtain soil specific calibration constants a, b, c, d, f, g needed for calculating soil water content and dry density.

The module is activated by click **Tools** menu (Fig.4.30).

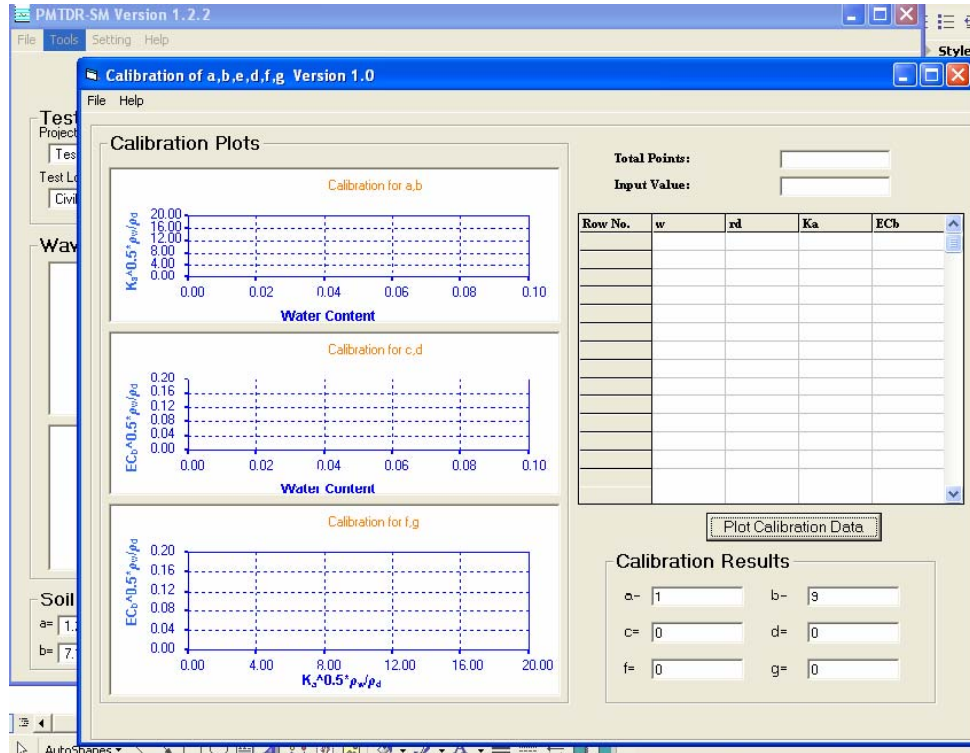


Fig. 4.30 Calibration Toolbox

Two approaches can be used for inputting data used for calibration. The first approach is to create a data file with postfix “.cal” according to the designated structure. Then read the data from the file. An example of the structure of the data file is shown in Fig. 4.31. The first line is the number of data sets in the calibration. Each data set consists of: soil water content (%), dry density (Mg/m^3), K_a , EC_b (mS/m). All are located on one line.

6				
4.3	1.787	6.470	9.16	
6.0	1.832	7.740	15.69	
8.0	1.825	10.248	26.96	
9.8	1.884	12.986	39.29	
12.4	1.956	16.640	55.15	
15.4	1.840	19.24	37.83	

Fig. 4.31 Content of Data File for Calibration

Use **File->Open** menu to load the calibration file (Fig. 4.32) and the data in the calibration file will be displayed in the table on the screen (Fig.4.33).

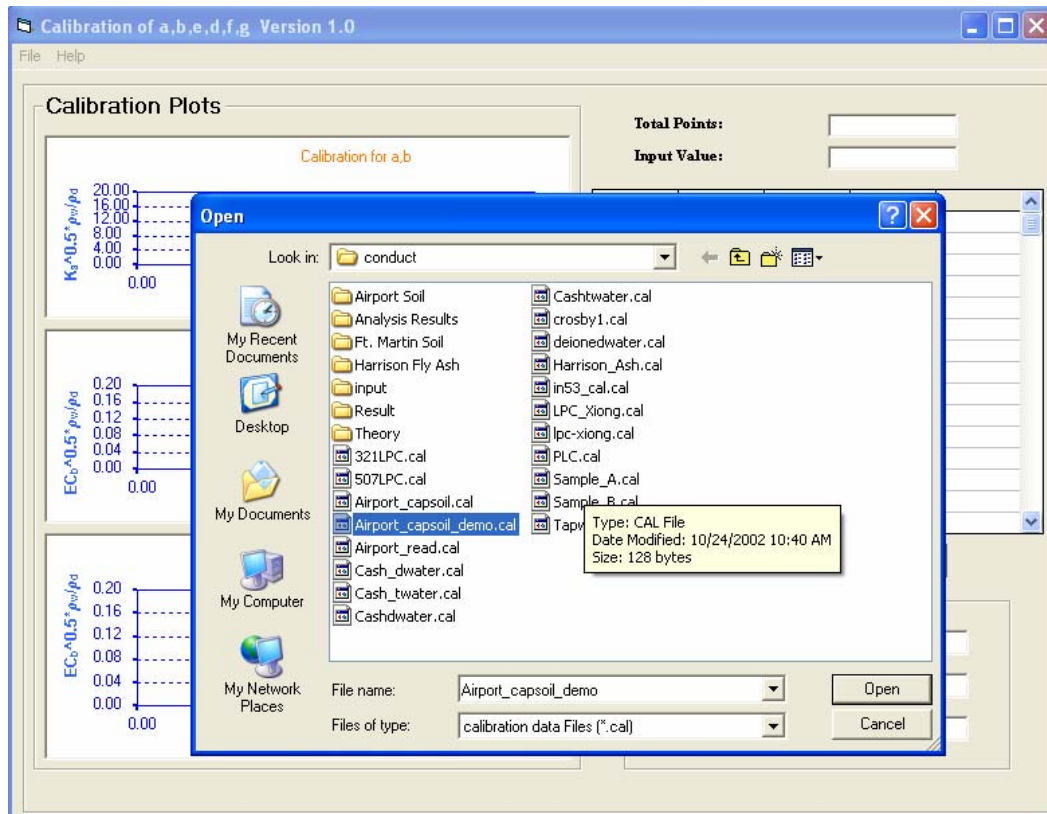


Fig. 4.32 Use File->Open Menu to Load Calibration Data File

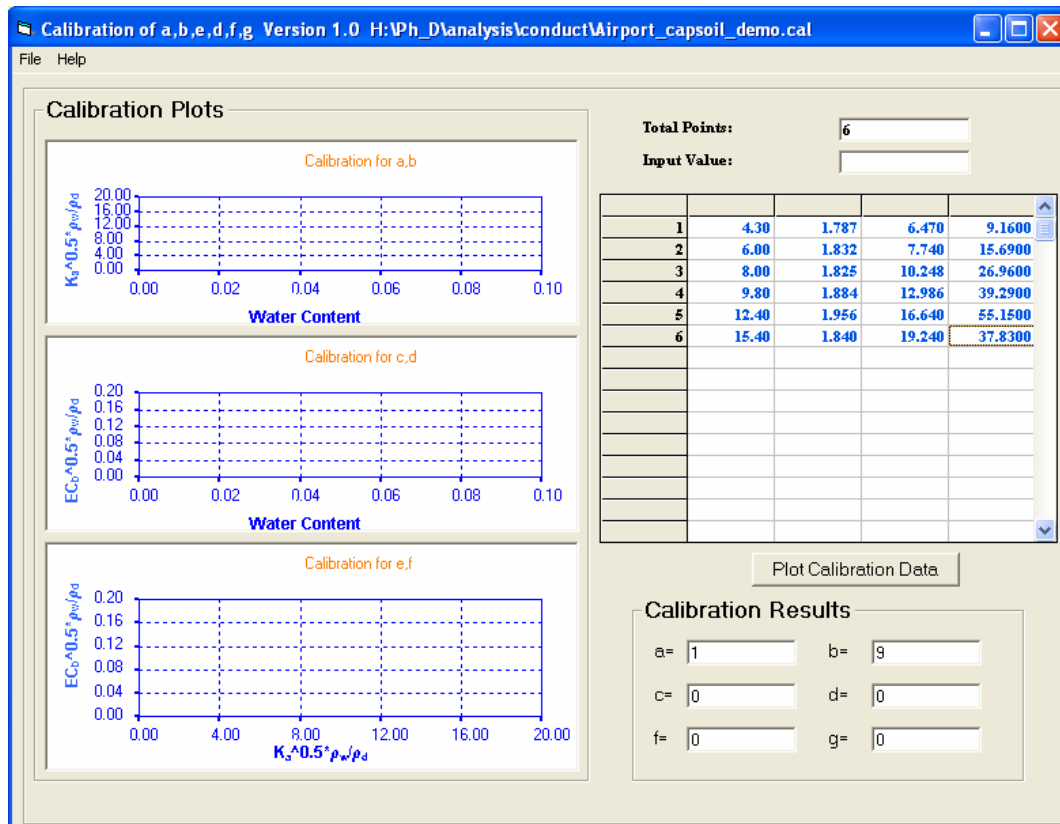


Fig. 4.33 Data in Calibration Data File are Displayed in a Table on the Screen

The other approach for inputting calibration data is to input data directly into data table. First, input total number of points in the **Total Points** textbox. Then, click on the cell and input the value from **Input Values** textbox (Fig. 4.34).

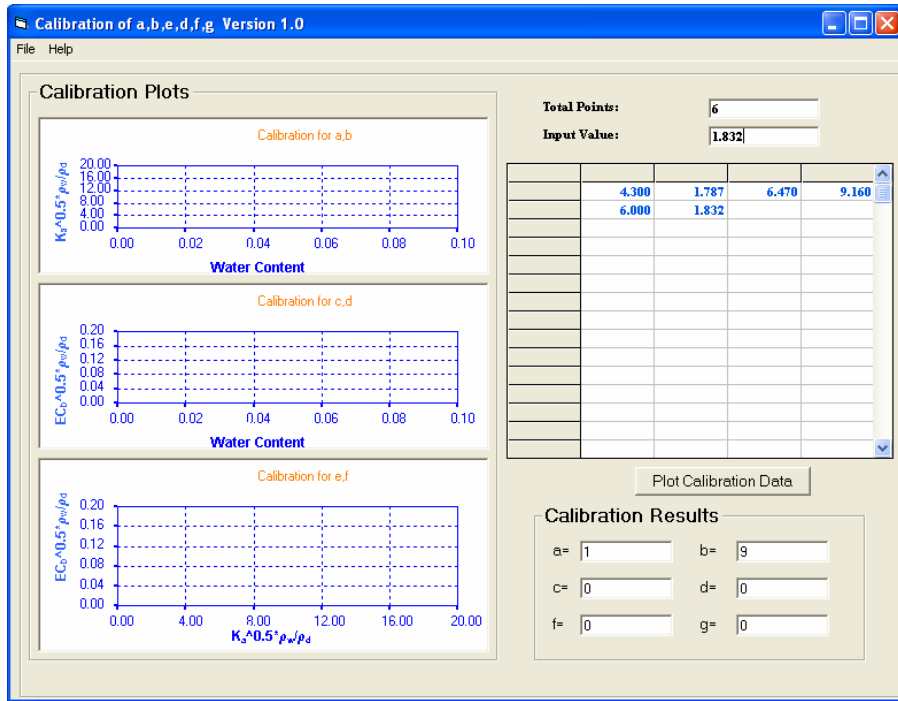


Fig. 4.34 Input Calibration Data Directly to the Data Table

After data are input by either approach, click **Plot Calibration Data** to calculate calibration constants (Fig. 4.35).

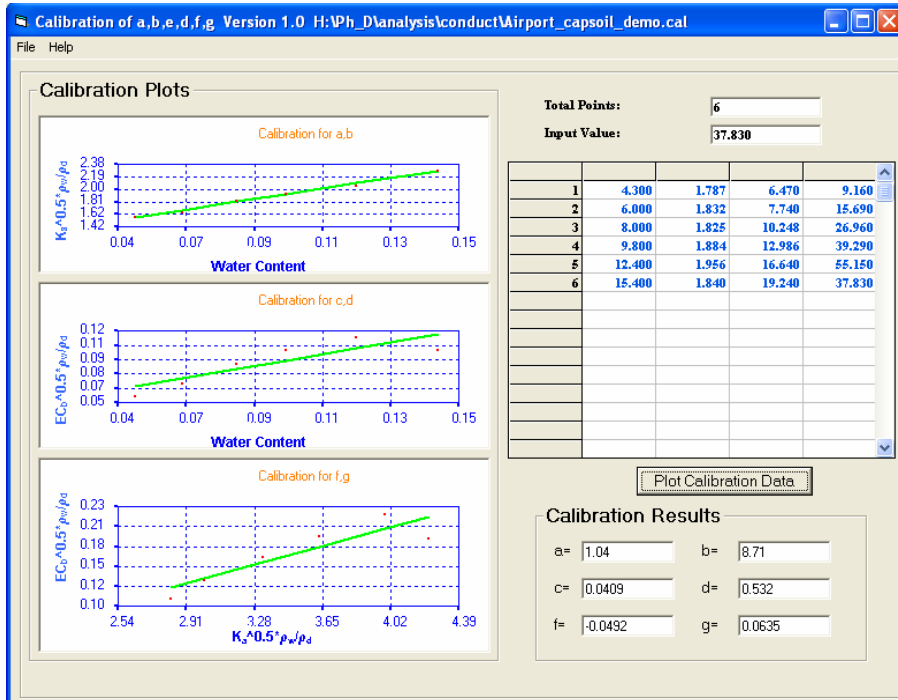


Fig. 4.35 Click Plot Calibration Data to Calculate Calibration Constants

A bad data point can be visualized and removed by double clicking on the corresponding data set number for the line, a “*” sign indicates that data in this line is removed from calibration analysis (Fig. 4.36). The calibration can be redone by clicking **Plot Calibration Data**. The removed data point can be restored by double clicking the corresponding data set number for the line again.

Results of calibration are automatically uploaded to the MRP screen and the CMP screen. Calibration results can also be stored by click **File->Save As** menu. The results stored in the calibration file (with postfix “.cal”) include number of data points stored, values of the data points used for calibration and the six calibration constants (Fig. 4.37).

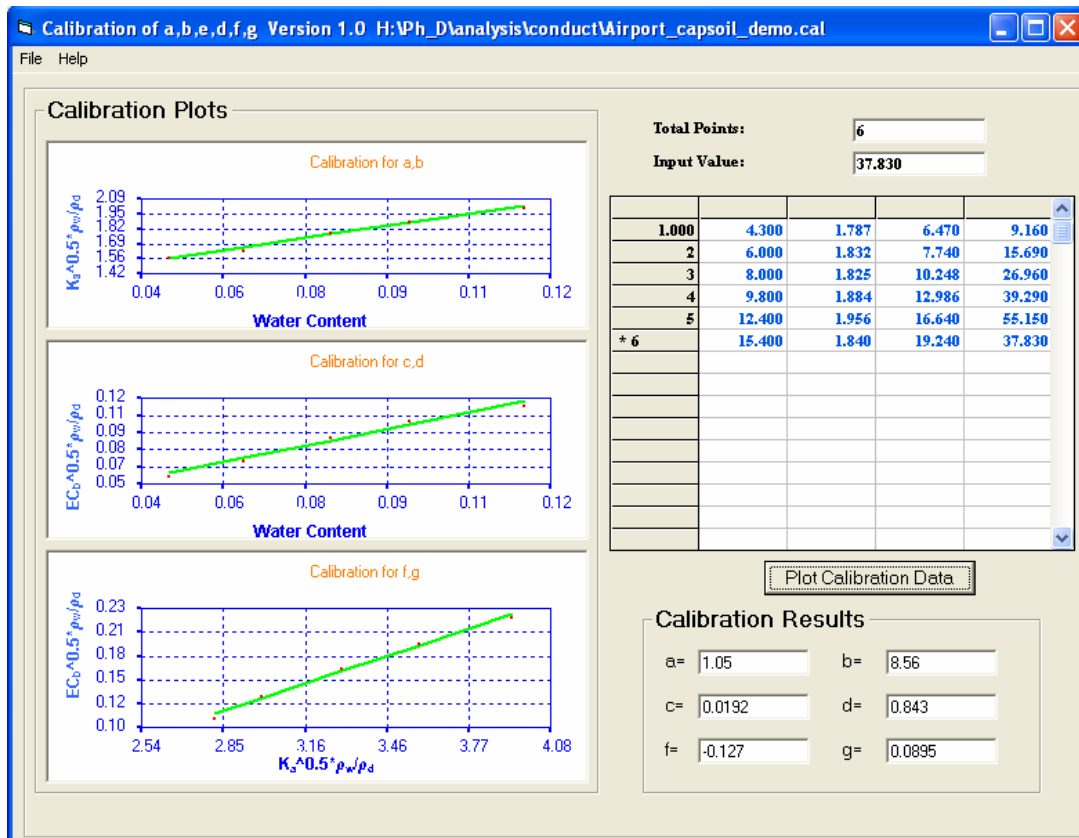


Fig. 4.36 Remove Dad Data and Recalculated Calibration

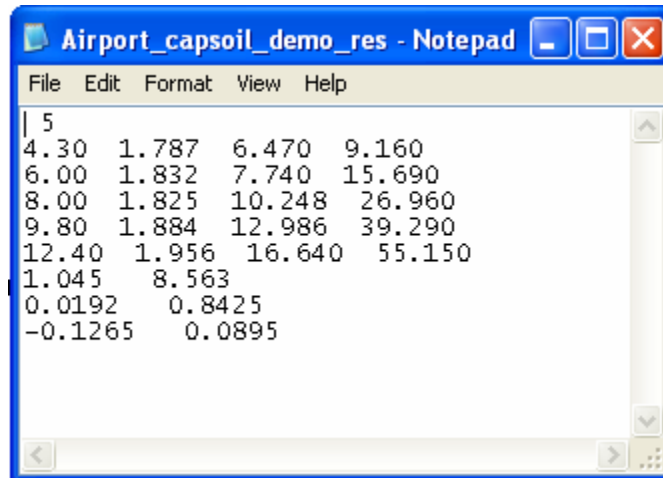


Fig. 4.37 Calibration Results Stored in Data File

4.4.3.5.3 Compare TDR Waveforms

Another useful utility for TDR analysis is the ability to simultaneously display different TDR waveforms to compare them.

To make a comparison of different TDR waveforms stored in data files, first click the checkbox *Continuous Update* under *Get Waveform* button. Then click *File->Load Test Results* to display a previously saved TDR waveform. It will be displayed with a different color (Fig. 4.38). It is also possible to click *Get Waveform* to compare the current TDR waveform display with the new TDR waveform obtained from TDR100.

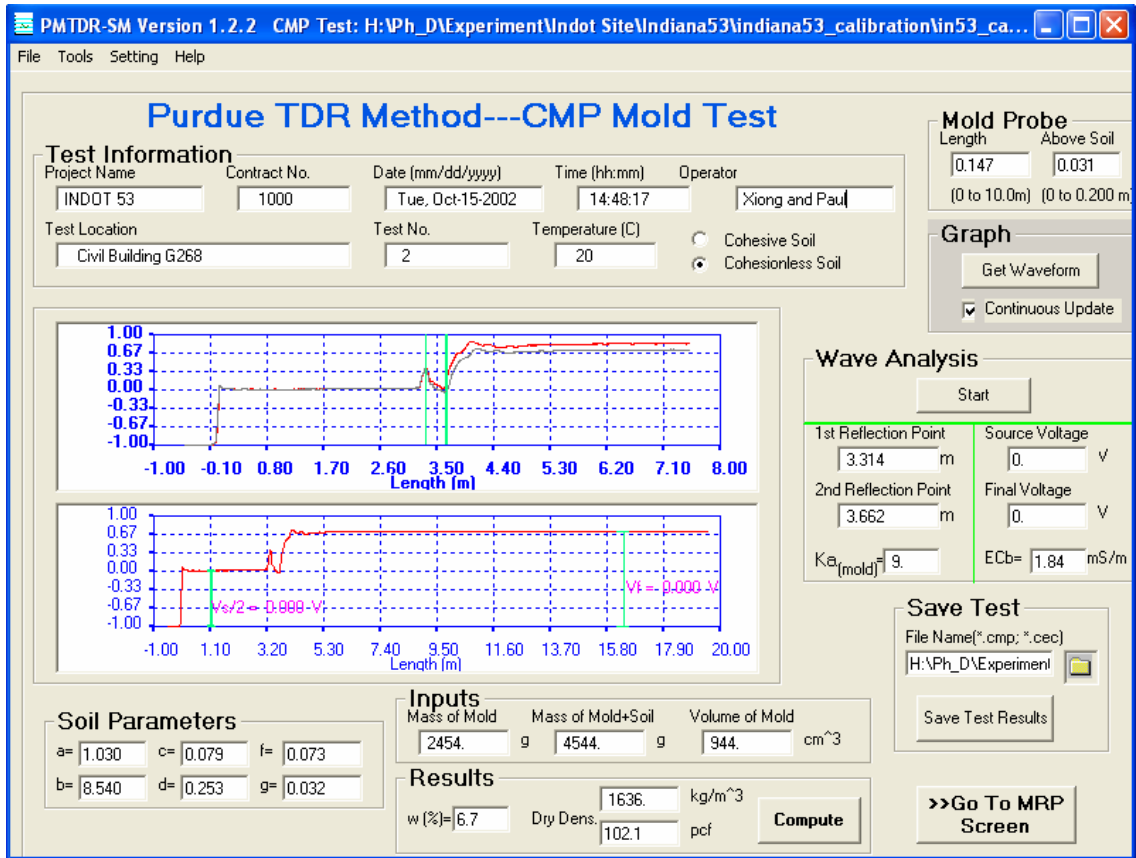


Fig. 4.38 Display Different TDR Waveforms for Comparison

5. Testing Procedures and Refinements

5.1 Process of ASTM Standardization

In a previous research project on automation and standardization of measuring moisture content and density using TDR (Feng et al. 1998), specifications were prepared to describe the equipment and the testing procedure in the format of both ASTM and AASHTO. Results of the study conducted at that stage were presented to the ASTM D18.08 committee in June, 1998. The committee was very receptive to the use of TDR for compaction quality control and suggested that it be considered for an ASTM Standard.

Since that time, the JTRP Projects (SPR-2201 and SPR-2489) generated many improvements in the testing procedure, equipment and accuracy of TDR test to obtain soil moisture content and density. Suggestions from the Beta Test partners were the source of many improvements. Most of the new discoveries and improvements were incorporated into the Draft ASTM Standard.

In spring 2001, the draft standard was submitted to ASTM Committee D18.08 committee for ballot. Some modifications were made to the draft based on ballot responses. The standard was officially approved in spring 2002 and was designated as ASTM D6780 with the title *Standard Test Method for Water Content and Density of Soil in Place by Time Domain Reflectometry (TDR)*. The standard is included in the 2003 Annual Book of ASTM Standards, Volume 04.09 and is available online from ASTM. A copy of the standard is attached with this report for reference purpose (Appendix IV).

5.2 Summary of Testing Procedures

The Purdue TDR Method for water content and density uses two “coaxial cables” where the “insulating” material between the “coaxial lead” and the “shield” is soil.

Driving four metal “spikes” into the soil surface in a pattern that simulates a cable creates the first “coaxial cable”. The length of the spikes driven into the soil determines the length of the cable, typically 20 cm (8-inches). Time Domain Reflectometry (TDR) is used to measure the travel time of an electromagnetic step pulse in this cable. The travel time allows for determining the “apparent dielectric constant” of the soil contained between the spikes. The word “apparent”

is used because the dielectric permittivity of soil is a complex, frequency-dependent function (Siddiqui and Drnevich (1995), Feng et al. (1999), Drnevich et al. (2001)).

The second “coaxial cable” consists of a soil-filled metal compaction mold and with a metal rod driven into the center for the center lead. The metal mold forms the “shield.” The compaction mold is placed on a non-metallic base to complete the simulation. Again, TDR is used to measure the travel time from which the “apparent dielectric constant” is determined. With the total density of the soil known in the compaction mold, the water content can be calculated for the soil using a simple equation. Water contents determined by this method compare exceptionally well with those obtained by oven drying. If the soil in the compaction mold is the same soil and has the same water content as tested in the first “cable” (insitu), then the density of the soil insitu is determined by a simple equation based on the ratio of dielectric constants measured insitu and in the compaction mold.

This process was conceived by the author and Dr. Shafiqul Siddiqui as part of his dissertation work at Purdue University and was enhanced and improved by faculty colleagues, Dr. Richard Deschamps and Dr. Robert Nowack, by former graduate students: Dr. Wei Feng, Dr. Chihping Lin, Weiyi Ma, Mr. Jie Zhang, Mr. Quanghee Yi, by current graduate student Mr. Xiong Yu and by the Geotechnical Laboratory Manager, Ms. Janet Lovell.

The current Beta Testing Program began in the fall of 2001 and involves various agencies/firms/universities. The purpose of the Beta Testing Program is to evaluate the method for a variety of different soils and with different users before making the equipment commercially available. Currently, the Beta Testing partners include: Indiana DOT Division of Materials and Test; University of South Florida, Florida DOT, GAI Consultants, Inc., H.C. Nutting Company, and Rutgers University. Feedback and input from Beta Partners have greatly facilitated the refinement of testing equipment and helped to refine the testing procedures.

5.2.1 Field Testing Process: MRP insitu test and CMP mold test

Insitu MRP Test:

An insitu MRP test is the first step of TDR testing to obtain water content and density. A “field cable” is first tested to measure the dielectric constant of soil in place ($K_{a,field}$). Four spikes are driven through a template into a smooth and level soil surface as shown in Fig. 5.1 to form

the “field cable.” The spikes have a nominal diameter of 9.5 mm (3/8 inch) and have a nominal length of 236 mm (9.3 inches).



Fig. 5.1 Driving Probes through Template for the Field Test

The template has a thickness of 25.4 mm (1 inch) so about 200 mm (8 inches) of the spikes are in the soil.

The template is removed from around the spikes as shown in Fig.5.2. This leaves an air



Fig. 5.2 Remove Template to Expose Spikes

gap of approximately 32 mm (1.3 inch) between the top of the spikes and the soil surface. The length of the spikes in the soil is the length of the “field cable” as shown in Fig. 5.3. Other length spikes could be used with the practical range of lengths ranging from 115 mm (4.5 inches) to 300 mm (12 inches), however, for lossy soils (in which electrical energy tends to dissipate as a result of dielectric relaxation damping or conductance) , the practical length may be limited to the lower end of this range. A specially designed multiple rod probe head is placed on the four

spikes as shown in Fig. 5.4. This head forms a transition unit between the spikes and the cable that connects to the TDR test device. All tests to date made use of either a Tektronix, model 1502B TDR Cable Tester or a Campbell Scientific, model TDR100. Both have serial ports that connect to a notebook computer. A computer program, TDR++, developed by Wei Feng et al. (1998) was used to control the Tektronix 1502B, acquire the data, perform calculations, and store

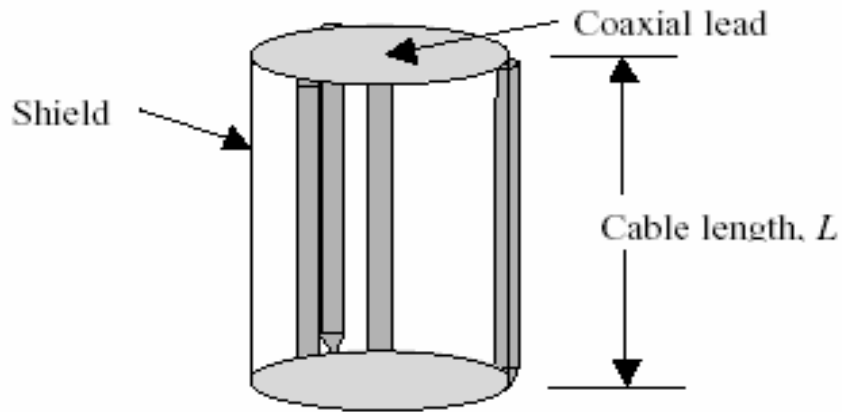


Fig. 5.3 Simulation of a Coaxial Cable by Probe Rods

test results along with other salient information about the apparatus, test, date, and location.

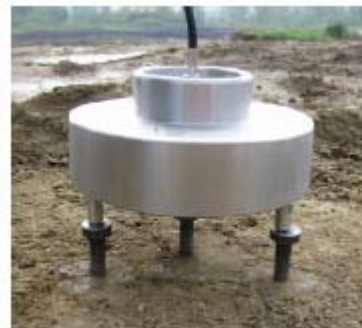


Fig. 5.4 Place MRP Head on Probe Rods

In 2001, the Campbell Scientific TDR100 replaced the Tektronix because Tektronix discontinued producing the 1502B. The software used with the TDR100 is called PMTDR-RDR, which is adapted from the software PCTDR developed by Campbell Scientific (Fig. 5.5). The adaptation by V.P. Drnevich, X. Yu, and J. Lovell includes a robust algorithm developed by the authors for identifying the wave reflections, which are used to determine the apparent dielectric, $K_{a, field}$.

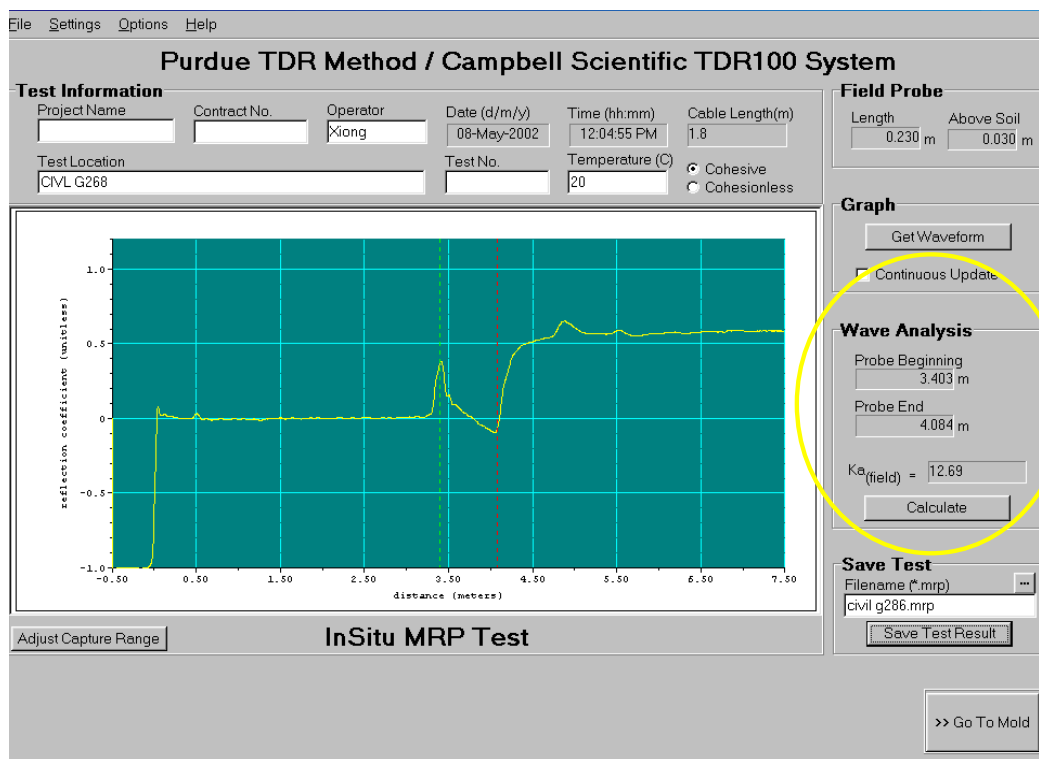


Fig. 5.5 Computer Program to Obtain TDR Waveforms and Make Analyses

Once the information is stored in the computer, the probe head is removed and the spikes are removed. The soil is then excavated from the space defined by the outer three spikes. A battery-operated power drill with a 26 mm (1-in) diameter “Nail Biter” wood auger bit works

well for loosening the soil for removal with a small hand scoop (Fig. 5.6). Unlike the sand cone test, disturbance of the soil adjacent to the excavated soil is not a problem.



Fig. 5.6 Remove Soil with Power Drill

Compaction Mold Testing:

A special compaction mold is used for these tests as shown in Fig. 5.7. It resembles the



Fig. 5.7 Place MRP Head on Mold Using Adapter Ring

conventional compaction mold specified by ASTM D698 except that it has twice the length and the bottom plate is made of a non-metallic material. The longer length allows for the transfer of most of the soil from the insitu test into the mold and it allows for more accurate measurements of the travel time. The diameter of center rod is optimized based on a sensitivity study (Siddiqui et al, 1995).

Soil is compacted into this mold using any desired compaction energy that produces a relatively uniform specimen in the mold. (An aluminum rod 38 mm (1.5 in) in diameter by 400 mm (16 in) in length works well as a hand tamper for routine field tests (Fig. 5.7)) A portable, battery operated electronic scale is used to measure the mass of the soil and mold (Fig. 5.8). The



Fig. 5.8 Measuring the Mass of Soil with Scale

total density of the soil in the mold, $R_{t,mold}$ is determined by subtracting the mass of the mold alone and dividing by the volume of the mold.

After the soil is compacted into mold, the mold containing soil is placed on a firm surface and a guide template is placed on the mold. A center rod is then driven into the mold (See Fig. 5.9) and the guide template is removed.



Fig. 5.9 Driving the Center Rod through the Rod Guide

A special adapter ring is then placed on the mold and the same probe head used for testing insitu is placed on the adapter ring as shown in Fig. 5.10.



Fig. 5.10 Placement of the MRP Head on the Adapter Ring

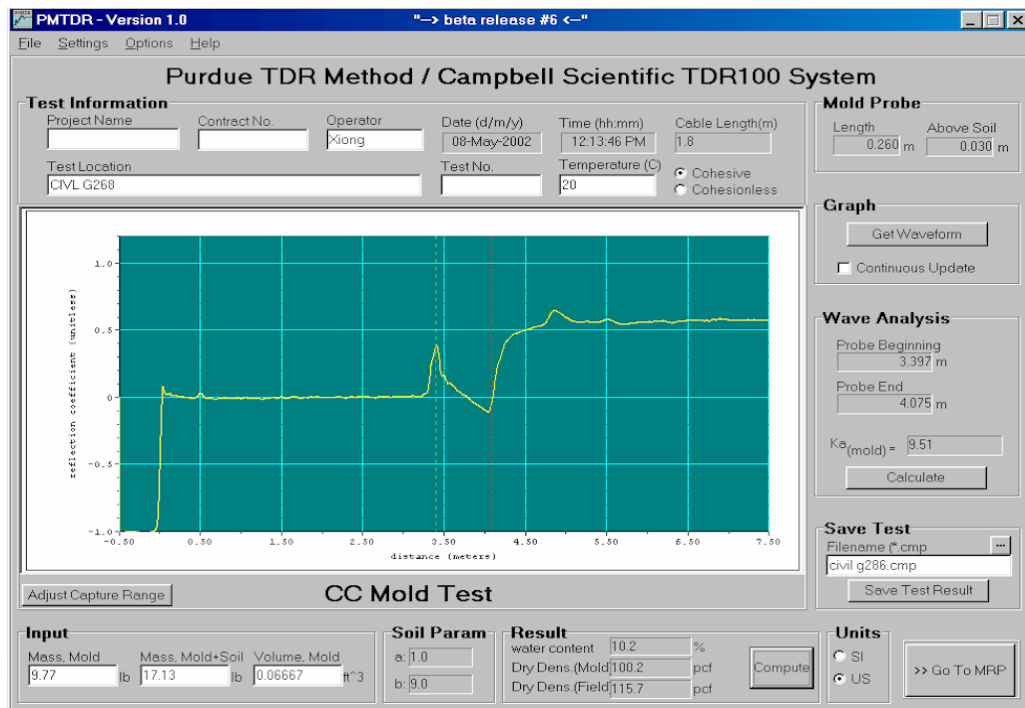


Fig. 5.11 Obtain TDR waveform and Computer Soil Water Content and Dry density

A TDR measurement gives the average apparent dielectric constant for the soil in the mold, $K_{a,mold}$. This together with a field measurement is then used to calculate soil water content and dry density. (Fig. 5.11)

5.2.2 Data Reduction Process to Obtain Soil Water Content and Density from TDR Measurement

The Siddiqui-Drnevich equation (Siddiqui et al, 1995) allows for the calculation of water content with the use of apparent dielectric constant and the soil dry density. The Siddiqui-Drnevich equation can be written for both the field test and the mold test as shown in Eqs. (5-1) and (5-2), respectively.

$$\sqrt{K_{a,field}} \frac{\rho_w}{\rho_{d,field}} = a + b w_{field} \quad (5-1)$$

$$\sqrt{K_{a,mold}} \frac{\rho_w}{\rho_{d,mold}} = a + b w_{mold} \quad (5-2)$$

The dry density of the soil in the mold, $\rho_{d,mold}$, is related to the total density, $\rho_{t,mold}$, through

$$\rho_{d,mold} = \frac{\rho_{t,mold}}{1 + w} \quad (5-3)$$

Substituting Eq. 5-3 into Eq. 5-2 and solving for w yields

$$w_{mold} = \frac{\sqrt{K_{a,mold}} - a \frac{\rho_{t,mold}}{\rho_w}}{b \frac{\rho_{t,mold}}{\rho_w} - \sqrt{K_{a,mold}}} \quad (5-4)$$

$$\rho_{d,mold} = \frac{\rho_{t,mold}}{1 + w_{mold}} \quad (5-5)$$

If the process of removal of the soil from the hole in the field and placement into the compaction mold is done quickly, it is valid to assume that the water contents in the mold and in the field test are identical.

$$w_{field} = w_{mold} \quad (5-6)$$

Substitute Eq. 5-6 into Eq. 5-1, the dry density of the soil in the field, $\rho_{d,field}$, may be calculated from:

$$\rho_{d,field} = \rho_{d,mold} \frac{\sqrt{K_{a,field}}}{\sqrt{K_{a,mold}}} \quad (5-7)$$

Hence, the accuracy of $\rho_{d,field}$ is dependent on the accuracy of the total density measurement in the compaction mold, the accuracy of the water content determination, and the accuracy in measuring the apparent dielectric constant in the field and in the compaction mold. With the use of the same probe head and procedures for data acquisition and reduction, there is potential for accurate measurement of these parameters.

5.2.3 Laboratory Calibration to Determine Soil Dependent Parameters a and b

1) Procedures for Calibration Tests

The Purdue TDR method requires values of a and b , which are soil-type dependent constants. The easiest way to determine values of a and b for a given soil is to run a series of tests in the compaction mold with different water contents.

Measure the total density and apparent dielectric constant and the water contents for each test by oven drying. Then plot $\sqrt{K_a} \frac{\rho_w}{\rho_d}$ versus w from the test results as shown in Fig. 5.12. Fit a straight line to the data. The value of a is the zero-intercept of the straight line and b is the slope of the line.

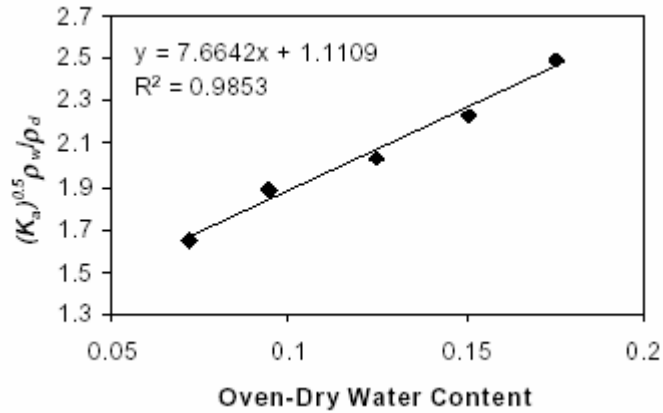


Fig. 5.12 Plot to determine a and b value

Experience from conducting hundreds of tests on different soils indicates that the value of a is typically near unity and the value of b is typically around eight to nine. The amount of compaction energy used in these tests, while important for obtaining the compaction curve, does not appear important for determining values of a and b for a given soil as long as the soil is relatively uniformly compacted in the mold.

2) Physical Significant of a and b Values

Recalling that the Siddiqui-Drnevich equation relates apparent dielectric constant, normalized by dry density with soil gravimetric water content, w , using the soil specific calibration constant a and b .

$$\sqrt{K_a} \frac{\rho_w}{\rho_d} = a + bw \quad (5-8)$$

(Note: Geotechnical engineers commonly work with the **gravimetric** water content of soil (mass of the water/mass of dry soil solids) and it is usually represented by the letter, w . While for more than 30 years, agronomists have been making extensive use of dielectric properties for measuring the **volumetric** water content of soil (volume of water as a percentage of the total volume of the soil). The volumetric water content is usually represented by the Greek letter θ . Both θ and w are expressed as percentages. Volumetric and gravimetric water contents are related by

$$w = \theta \frac{\rho_w}{\rho_d} \quad (5-9)$$

where ρ_d is the dry density of the soil and ρ_w is the density of water.

The significance of the a and b values can be obtained by expressing the Siddiqui-Drnevich equation using volumetric water content. Substituting (5-9) into (5-8) and solve for volumetric water content we can obtain:

$$\theta = \frac{1}{b} \sqrt{K_a} - \frac{a}{b} \frac{\rho_d}{\rho_w} \quad (5-10)$$

For a totally dry soil, θ is zero and Eq. 5-10 reduces to

$$a = \sqrt{K_{a, \text{dry soil}}} \frac{\rho_w}{\rho_d} \quad (5-11)$$

Typical values of K_a for dry soil for common minerals are on the order of 2 to 7 (See Table 5-1. adapted from Martinez and Burns, 2001) and the density of the dry soil $\rho_{d \text{ dry soil}}$ is typically about 1.5 to 2 times that of the density of water, ρ_w . Substitution of these values into Eq. 5-11 gives values of a that vary as shown in Table 5-2. Hence, values of a are expected to range from approximately 0.7 to 1.85, which compares well to values obtained from tests on soil.

Table 5-1 Typical Values of Apparent Dielectric Constant for Air, Water, and Dry Soil and Rock

Material	from Davis and Annan, 1989	from Daniels, 1996
Air	1	1
Distilled water	80	
Fresh water	80	81
Sea water	80	
Sand, dry	3-5	4-6
Sandstone, dry		2-3
Limestone, dry		7
Clay, dry		2-6
Soil, sandy dry		4-6
Soil, loamy dry		4-6
Soil, clayey dry		4-6
Coal, dry		3.5
Granite	4-6	
Granite, dry		5
Salt, dry	5-6	4-7

Table 5-2. Range of Expected Values of a for Dry Soil

$\frac{\rho_w}{\rho_d} \backslash \sqrt{K_a}$	Min 2	Mid 4	Max 7
0.7	0.99	1.40	1.85
0.6	0.85	1.20	1.59
0.5	0.71	1.00	1.32

Refer again to Eq. 5-10, let θ be equal 100%, which means that there are no soil solids, only water. The value of ρ_d becomes zero and Eq. 5-10 reduces to:

$$b = \sqrt{K_{a, \text{water}}} \quad (5-12)$$

For uncontaminated water, the value of $(K_a)_{\text{water}}$ is 81 at room temperature. Thus, the value of b should be about 9. Again, this is within the observed range of values for b observed, which typically varies from a low value of 7 to a high value of 12.

In summary, for use of Eq. 5-8, the value of a is related to both the soil dry density and the apparent dielectric constant of the soil solids and the value of b is related to the apparent dielectric constant of the pore fluid. Additional work is needed to more fully understand how and why values of a and b vary with different soils and pore water characteristics.

5.3 Insulated Center Rod for Testing in Lossy Soil

It was specified in the ASTM standard D6780 that the TDR method may not suitable for organic and highly plastic soils. The restraints on highly plastic soils are mostly due to their “lossy” behavior. The term “lossy” is defined as the electromagnetic energy dissipated as an electromagnetic wave propagates in the material. The lossy behavior of soils are caused by the

large imaginary part of dielectric permittivity which are mostly attributed to bulk soil electrical conductivity as discussed below.

5.3.1 Principle of Energy Loss

Two kinds of important information are obtained from TDR waveform analysis (Fig.5.13): 1) Apparent length (l_a), which is the distance between first and second reflection points. It is used to calculate soil apparent dielectric constant, which is then related to soil water content; 2) Long-time waveform level, which is related to soil conductivity. The long-time waveform level decreases with increasing soil conductivity.

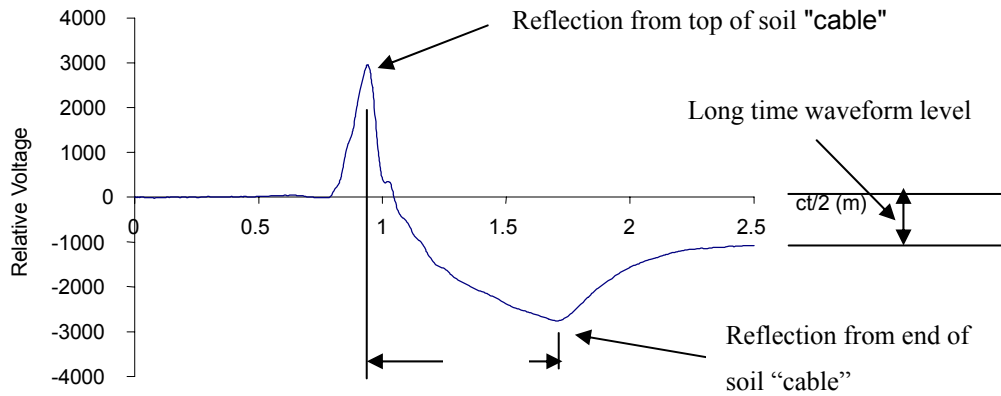


Fig. 5.13. Information Contained in a Typical TDR Curve

The TDR waveform is a visual representation of the electromagnetic properties of the material under test by the TDR measurement system. Analysis of material properties indicates that for uniform soil, the waveform characteristics are chiefly dependent upon the complex dielectric permittivity of soil:

$$\varepsilon = \varepsilon' - j\varepsilon'' = \varepsilon' - j\left(\varepsilon'' + \frac{\sigma}{2\pi f}\right) \quad (5-13)$$

Real part of permittivity is called apparent dielectric constant. Imaginary part of permittivity is the cause of energy loss and is made up of two terms. The term ε'' is loss caused by internal properties of the material, such as friction, collision among molecules. The term

$\frac{\sigma}{2\pi f}$ is energy loss caused by conductivity. For most lossy soils encountered, ϵ'' is very small and energy loss is mostly caused by conductivity.

One immediate result from lossy behavior is that the second reflection point becomes less distinct and more difficult to identify. As energy loss exceeds a certain level, the TDR waveform becomes totally absorbed and there is no effective means to extract information from TDR waveform analysis (Fig. 5.14).

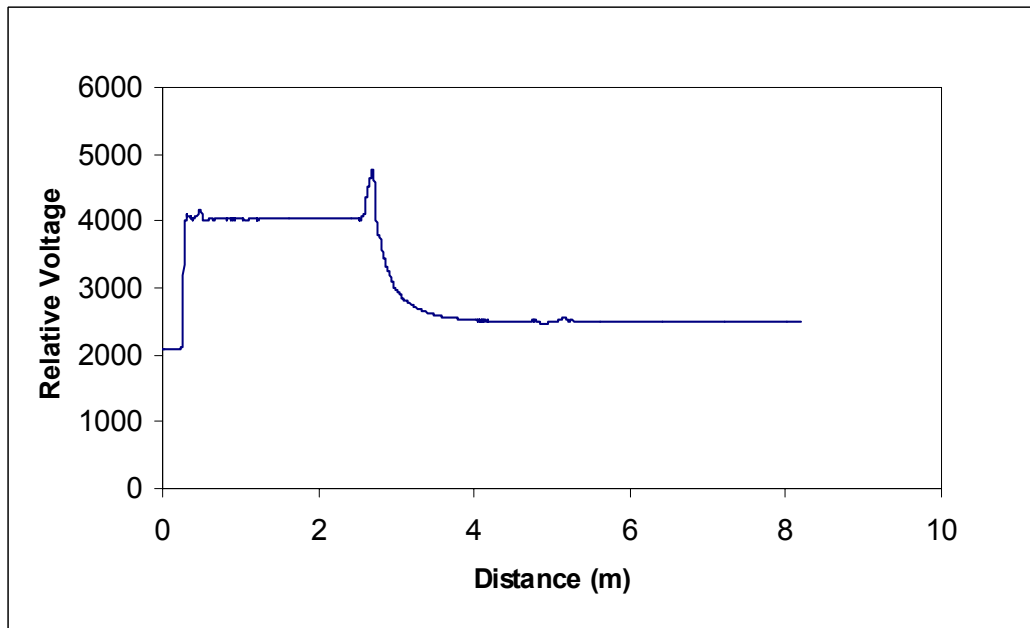


Fig. 5.14 TDR waveform in lossy soil

The unavailability of soil dielectric constant information for TDR waveforms prevents making a measurement of apparent dielectric constant on lossy soils including high plastic soils at high water contents, chemically stabilized soils and non-conventional soils such as fly ash, bottom ash, etc.

5.3.2 Mechanism of Insulation and Scheme for Data Reduction

1) Prevention of Energy Loss by Insulation

Because energy loss in a dielectric medium is mostly caused by conductivity, insulating the center rod of a TDR probe will reduce the lossy effects as shown in Fig. 5.15. Theoretical

analyses, as well as experimental results, show that satisfactory result can be obtained by simply insulating the center rod in the TDR probe coaxial configuration.

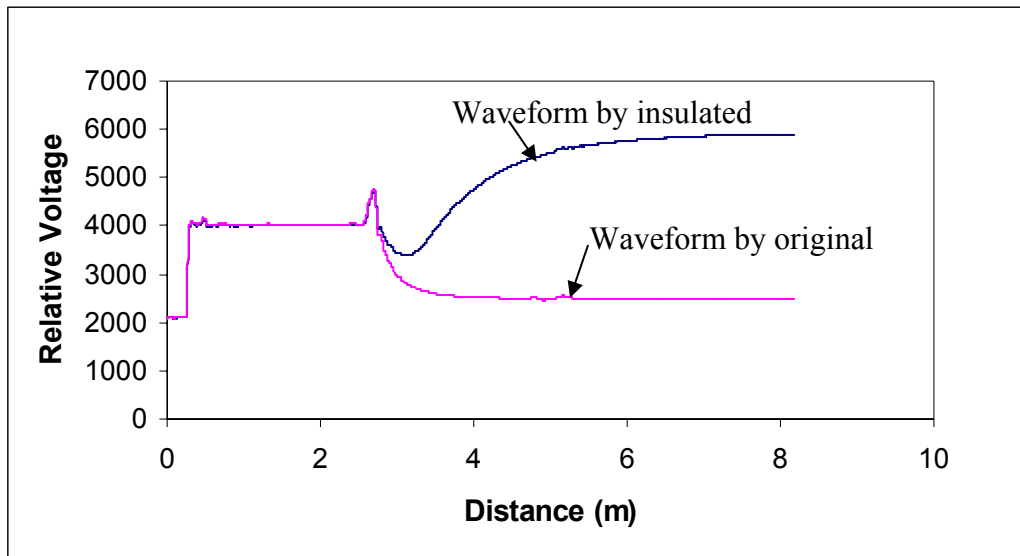


Fig.5.15 Waveform before and after Using Insulated Probe

2) Calibration of insulated center rod

Analysis on energy distribution in the TDR probe shows TDR waveform is sensitive to material around center rod of the probe (Figure 5.16). Thus, applying insulation to the center rod of a probe will affect the measured values of apparent dielectric constant.

Different approaches have been proposed to calibrate the effects of the insulating layer on the center rod. Most of them use empirical approach by fitting experimental data with some curve, for example a logarithmic equation that describes the measured data. We believe that an analytical approach would be more appropriate and more broadly applicable.

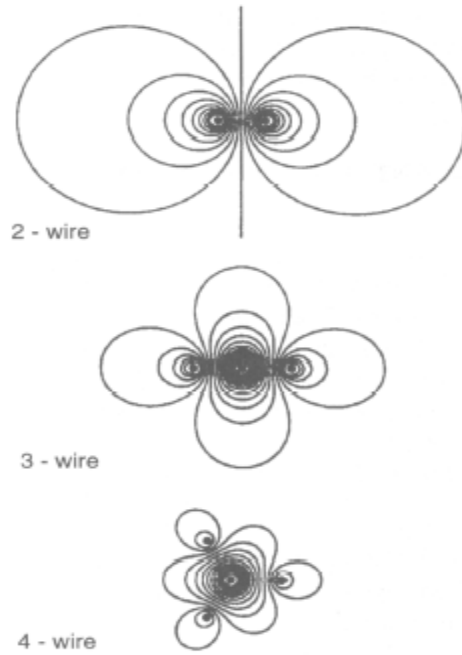


Fig. 5.16 Contours of Dimensionless Electrical Field Distribution Normal to Direction of Probe Insertion for a Material of Uniform Dielectric Constant (from Zegelin et al., 1989)

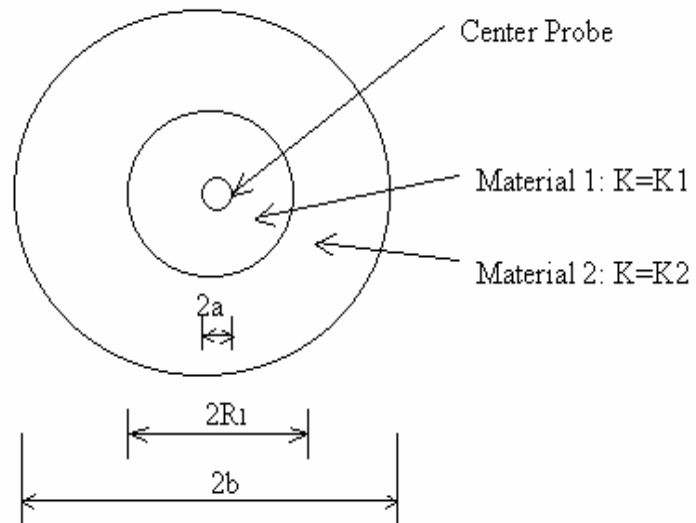


Fig. 5.17 Cross Section of the Insulated Probe

From theoretical viewpoint, insulating the center rod creates a composite material made up of the insulating material and the soil as shown in Fig. 5.17. The dielectric constant of composite dielectric medium can be expressed as Eq. 5-14:

$$\frac{\ln(b/a)}{K_a} = \frac{\ln(r_1/a)}{K_1} + \frac{\ln(b/r_1)}{K_2} \quad (5-14)$$

where a is the radius of the center rod, R_I is the radius of the center rod plus insulation thickness, b is the radius to the outer shield, K_1 is the apparent dielectric constant of the insulating material, and K_2 is the apparent dielectric constant of the soil.

This shows that reciprocal of apparent dielectric constant, K_a , measured by the insulated rod has a linear relationship to reciprocal of K_a by measured with the original probe. The equation can be applied as calibration curve. The basic idea for calibration is to make measurements using an uninsulated probe and an insulated probe on same material. The material used for calibration must have sufficiently low conductivity to obtain accurate values of apparent dielectric constant with the uninsulated probe (for example, clean Ottawa sand will work). Corresponding reciprocals of apparent dielectric constant values are then plotted, which give the calibration equation as shown in Fig. 5.18. In Fig. 5.18, reciprocals of corresponding K_a shows a fairly good linear relationship, which validates the theoretical prediction.

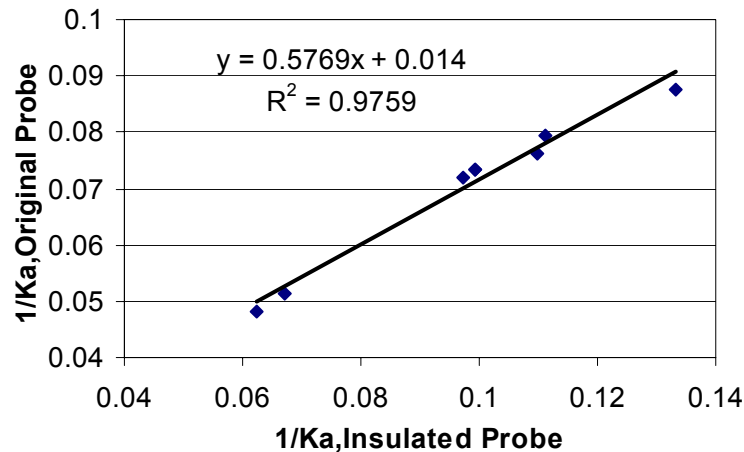


Fig. 5.18 Calibration Curve for Insulated Probe

By rearrangement of the calibration equation for the insulated center rod (Eq. 5-14), we can obtain the “true” dielectric constant of the soil from the dielectric constant measured with the insulated center rod which is a hyperbolic equation (an example is shown in (Eq. 5-15) for the calibration data in Fig. 5.18).

$$K_a = \frac{K_{a,insulated}}{0.5769 + 0.014K_{a,insulated}} \quad (5-15)$$

5.3.3 Procedure for Field Practice

5.3.1.1 Calibration Procedure

A typical calibration involves:

- 1) Material used - Low-conductive material, such as clean Ottawa sand
- 2) Apparatus - Calibration of insulated center rod can be conducted using the CMP mold; a special tank is needed to calibrate the insulated center rod of the MRP. The tank needs to have a diameter > 7.0 in. (180 mm), a depth > 8.5 in.(216 mm).
- 3) Procedure:
 - a) Weight sufficient amount of sand to fill up the tank used for calibration;
 - b) Choose a reasonable range of water contents and calculate amount of water that must be added to obtain each of the water contents;
 - c) Mix the water into the soil;
 - d) Put the soil into the tank and obtain the density of the soil-water mixture;
 - e) Using an uninsulated center rod, perform the MRP test in the tank and measure K_a ;
 - f) Remove uninsulated center rod and insert the insulated center rod;
 - g) Measure K_a using the insulated center rod;

Insulated center rod for the mold probe can be calibrated separately or in conjunction with calibrating the field probe with an insulated center rod. The additional steps include:

- h) Dig out the soil from the tank and compact it into the mold;
- i) Install the uninsulated center rod and take a TDR measurement;
- j) Remove center rod and install the insulated center rod;
- k) Make a TDR measurement with this center rod;

Repeat steps c) through k) for all designated water contents.

5.3.1.2 Calibration Results

The center rods were insulated with epoxy, with insulation thickness around 0.1mm and are calibrated following the procedure above. Calibration results of a field probe with an insulated center rod and a mold probe with an insulated center rod are shown in Figs. 5.19 and 5.20, respectively.

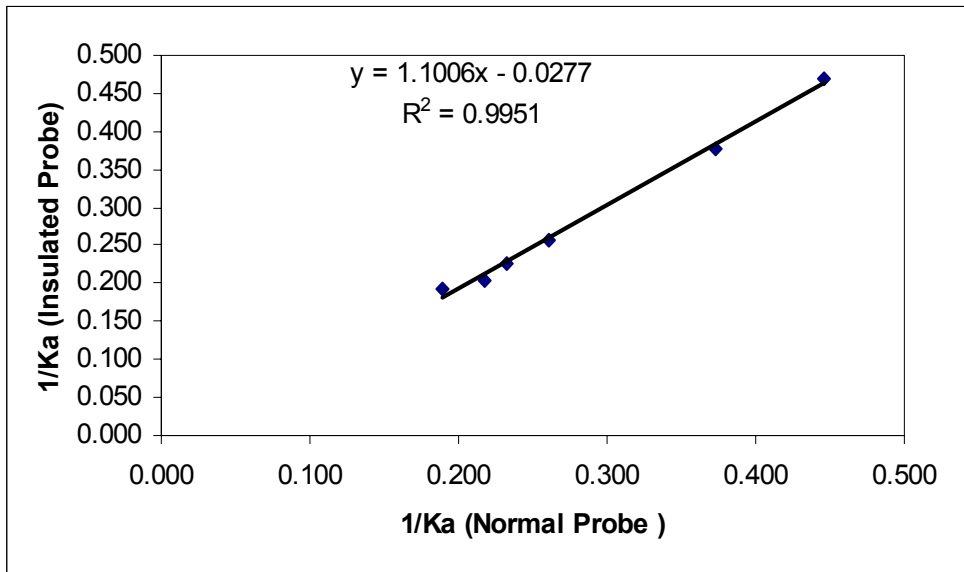


Fig. 5.19 Calibration Data for a Field Probe with Insulated Center Rod

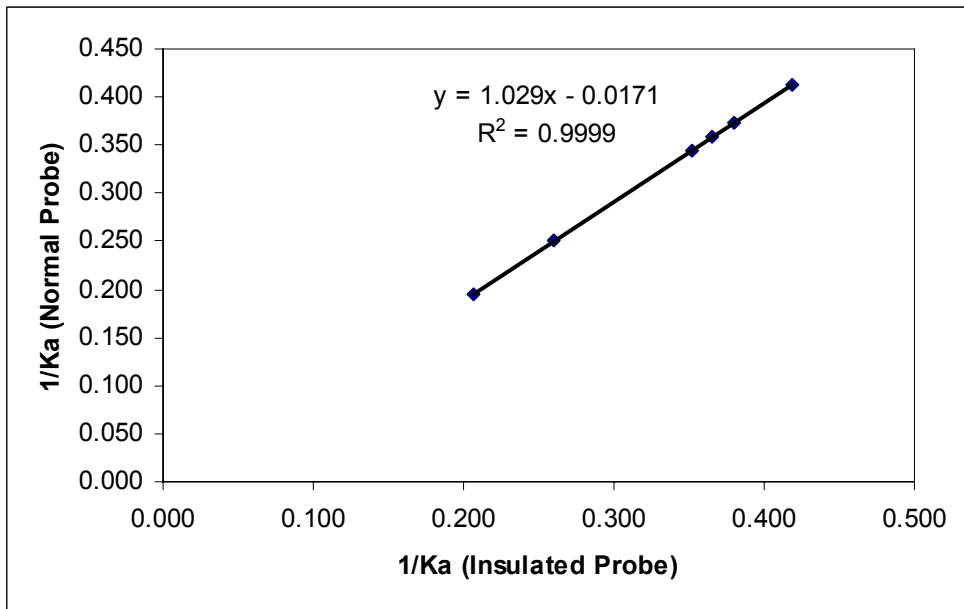


Fig. 5.20 Calibration Data for a Mold Probe with an Insulated Center Rod

From calibration results, equations for calculating the “true” soil dielectric constant from measured soil dielectric constant are:

$$K_{a,field} = \frac{K_{a,insulated,fieldprobe}}{1.1006 - 0.0277K_{a,insulated,fieldprobe}} \quad (5-16)$$

$$K_{a,mold} = \frac{K_{a,insulated,moldprobe}}{1.029 - 0.0171K_{a,insulated,moldprobe}} \quad (5-17)$$

5.3.1.3 Steps for Field Application of an Insulated Probe

Field procedures for using probes with insulated center rods are similar to those of using probes with uninsulated center rods. The extra steps in the process are listed below:

- 1) Try to perform the test with a conventional probe (no insulated center rod). If it is not possible to determine the second arrival, an insulated center rod will be needed;
- 2) Remove MRP head
- 3) Pull out center rod trying not to disturb the soil adjacent to the rod;
- 4) Direct the insulated rod into the hole left by original rod and drive it in until the head is at the same elevation as the outer rods. Be careful not to drive it too hard when the rod reaches the full depth to avoid damaging the insulation on the tip of the rod;
- 5) Carefully fill any gaps around the insulated rod before placing the MRP head on the rods and taking the TDR measurement;
- 6) Remove MRP head and remove all rods. Be careful not to scratch the insulation on the central rod;
- 7) Dig out the soil from the zone measured by the field probe and compact it into the mold using tools provided. Use the screed to level the soil at the top of mold and obtain the mass of mold plus soil;
- 8) Drive the uninsulated center rod into the mold using the rod guide;
- 9) Remove the center rod from the mold;
- 10) Direct the insulated center rod into the hole left by original probe and drive it to the appropriate depth. Be careful not to drive it too hard when the rod reaches the full depth to avoid damaging the insulation covering the tip of the rod;

11) Place the adapter ring on the mold and put the MRP head on the ring. Take a TDR measurement;

Note: procedures 7) through 11) used with the mold probe and insulated central rod also are used in the calibration process for finding the soil dependent parameters a and b .

The data reduction associated with probes with insulated center rods basically follows the same procedure as with the probes with uninsulated center rods. An extra step is to convert the K_a measured by the insulated probe to that of “true” soil dielectric constant by applying the calibration equation. Procedures for data reduction are listed below:

- 1) Convert measured K_a by probes with insulated center rods to corresponding actual soil K_a by applying insulated probe calibration equation (Eq. 5-16 for the field probe and Eq. 5-17 for the mold probe);
- 2) Calculate water content by Eqs. 5-4 and 5-6, which are repeated here for convenience:

$$w = \frac{\sqrt{(K_a)_{mold}} - a \left(\frac{\rho_{t,mold}}{\rho_w} \right)}{b \left(\frac{\rho_{t,mold}}{\rho_w} \right) - \sqrt{(K_a)_{mold}}} \times 100\% \quad (5-18)$$

- 3) Calculate soil dry density in the field by equation:

$$\rho_{d,field} = \frac{\sqrt{(K_a)_{field}}}{\sqrt{(K_a)_{mold}}} \frac{\rho_{t,mold}}{1 + \frac{w(\%)}{100\%}} \quad (5-19)$$

5.4 Summary

The development and refinement of the testing procedures for Purdue TDR Method is presented in this chapter. These provide the basis for the ASTM Standard D6780 adopted in spring 2002. The standard procedure to measure soil water content and density in the field with TDR include two steps: 1) a TDR test on the soil surface in the field using the field probe and 2)

a TDR test in the mold using the mold probe. Both probes use the same probe head and data reduction program. Calibration constants are determined in the laboratory in conjunction with standard compaction tests.

An insulated center rod has to be used for “lossy” soils where there is no discernible second reflection in TDR signal when using an uninsulated center rod. Calibration and testing procedures for using insulated center rod are also presented in this chapter.

6. One-Step Method for Soil Water Content and Dry Density

6.1 Introduction

The field procedure developed for the ASTM Standard D6780 consists of two tests: 1) a test in which a TDR reading is taken on four spikes driven into the soil; and 2) a test in a compaction mold on the same soil that was rapidly excavated from within the four spikes. Assuming the water content the same for both tests, apparent dielectric constant from the two TDR readings and the measured total density of the soil in the mold are used to calculate soil water content and dry density. This procedure only makes use of measured apparent dielectric constants (one insitu and one in the mold); it also requires digging out the soil and compacting it into the mold. This process requires about 10 to 15 minutes.

This chapter describes an improved method over that described above that makes use of bulk soil electrical conductivity in addition to apparent dielectric constant to obtain soil water content and dry density. This is accomplished with only one field TDR measurement. Thus no soil needs to be excavated and the testing time is reduced to a few minutes.

6.2 Basic Principles of One-Step Method

6.2.1 Soil Apparent Dielectric Constant and Bulk Electrical Conductivity from TDR Waveforms

TDR measures soil apparent dielectric constant through measuring the speed of an electromagnetic wave traveling in soil (Topp et al 1980). Apparent dielectric constant is given by

$$K_a = \left(\frac{L_a}{L_p} \right)^2 \quad (6-1)$$

where L_a is the distance between reflections (called apparent length) and L_p is the length of the probe. For TDR measurements in soil, electromagnetic reflections occur as the wave reaches the soil surface and again as the wave reaches the end of probe as shown in

Fig.6.1. The apparent length is the measured distance between these two reflections points. As water content or density increases, the apparent length also increases (Fig.6.1).

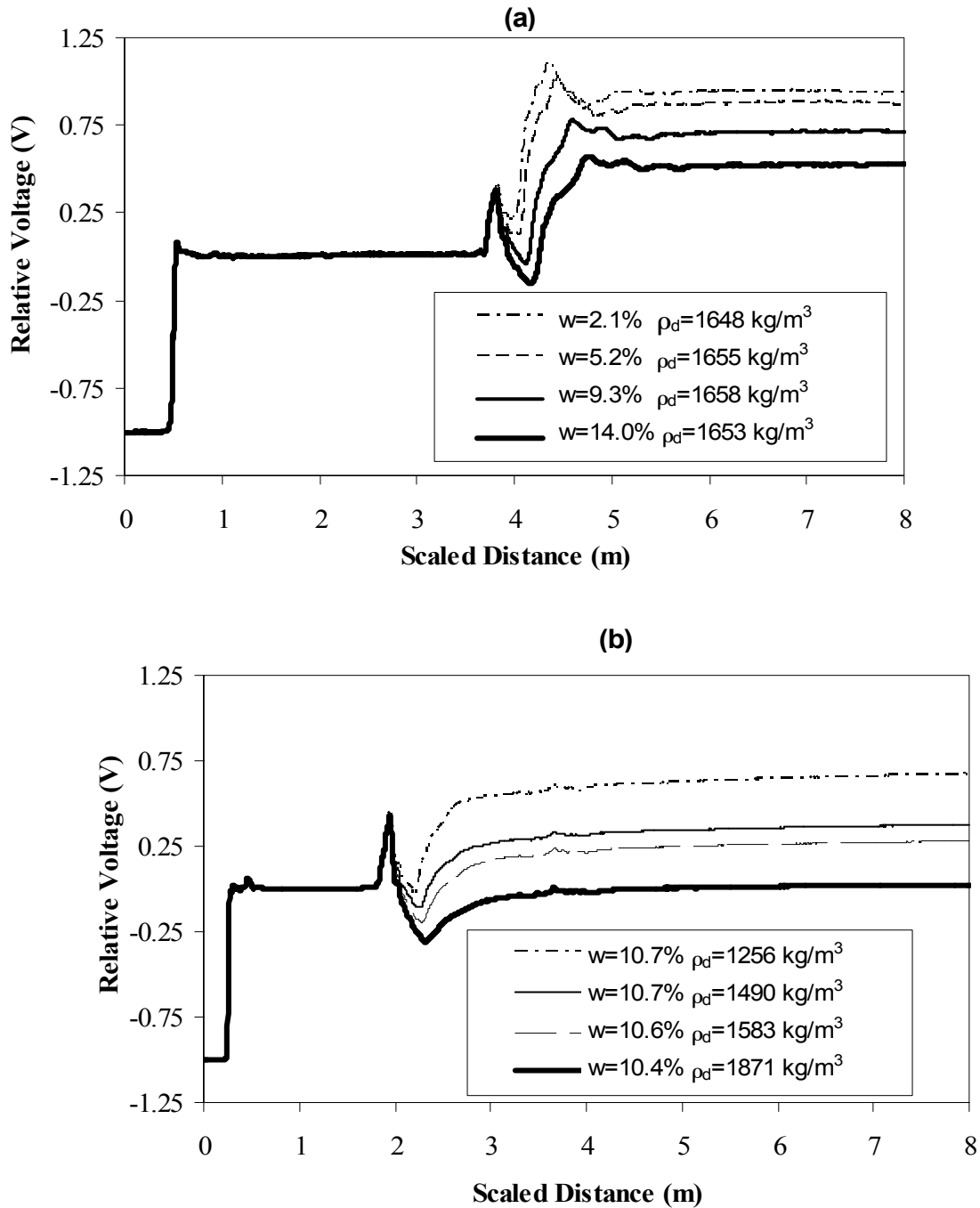


Fig. 6.1 Influence of Soil Properties on TDR Waveform: (a) Same Dry Density, Different Gravimetric Water Content; (b) Same Gravimetric Water Content, Different Dry Density

Various methods have been proposed (Topp et al., 1982; Baber and Allmaras, 1990) to pick the two reflection points from TDR waveforms among which the tangent line method is most widely used. As discussed in Chapter 4, the authors developed a robust algorithm using the concept of curvature to identify the reflection points for this study. The identified reflection points are then used to calculate soil apparent dielectric constant. Information on bulk soil electrical conductivity is also obtained from TDR long term signal level using Eq. 4-10.

This approach was proposed by Giese and Tiemann (1975) for analyzing dielectric behavior of thin samples. Topp et al. (1990) found that applying this approach for bulk soil electrical conductivity produced satisfactory results. The writers used this method for the measurement of the conductivity of water with various amounts of salts added to increased ionic conductivity. Results show a good linear relationship with conductivity measured with a bench conductivity meter (Fig.6.2). Equation 4-10 is used in the new method described in this chapter to obtain bulk soil electrical conductivity from TDR measurements.

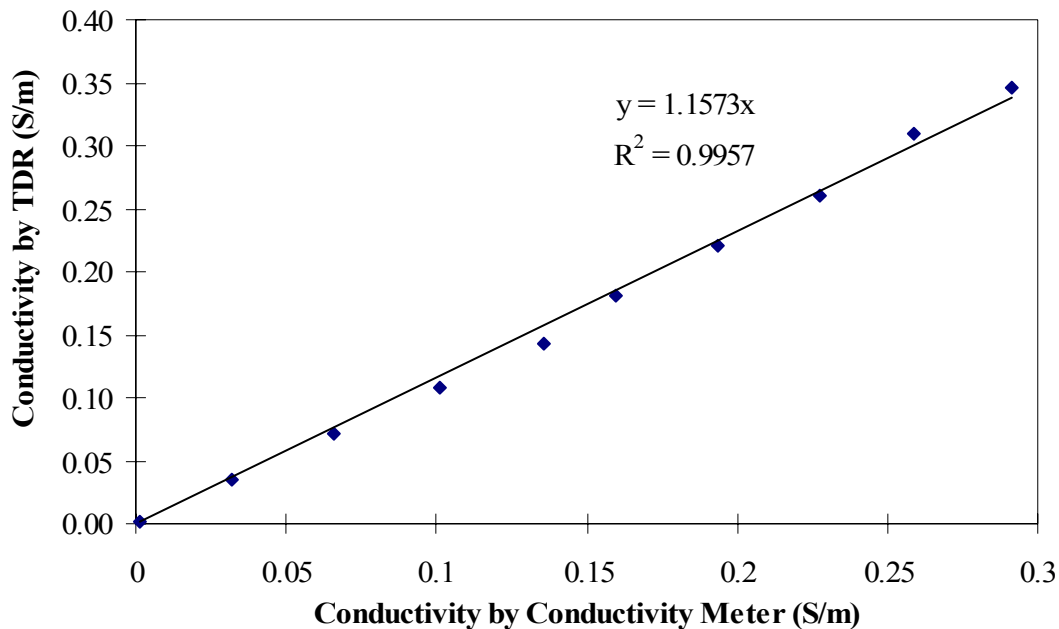


Fig. 6.2 TDR Measured Conductivity Versus Conductivity Meter Measurement

6.2.2 Calibration Relationship for Soil Apparent Dielectric Constant

Due to the large dielectric constant for water (around 80 at 20°C) in contrast to the relatively small dielectric constant for soil solids (around 3 to 5), it is possible to relate soil apparent dielectric constant to soil water content. The relationships are called calibration equations.

Topp et al (1980) showed that for soils with a wide range of mineral content, a single equation was adequate and was practically independent of soil bulk density, ambient temperature, and salt content. Their relation is now widely used as a calibration curve and is referred to as Topp's equation,

$$\theta = 4.3 \times 10^{-6} K_a^3 - 5.5 \times 10^{-4} K_a^2 + 2.92 \times 10^{-2} K_a - 5.3 \times 10^{-2} \quad (6-2)$$

This calibration equation has been confirmed by numerous authors on various soils and currently is the most widely used calibration equation for TDR applications.

However, it is observed that for organic soils, fine-textured soils, and clays, the dependency of K_a on θ differs from Topp's equation (Dobson et al., 1985; Dasberg and Hopmans, 1992; Roth et al, 1992; Dirksen and Dasberg, 1993). The deviation is attributed to soil density and texture (bound water) effects (Abdula et al 1988; Ponizovsky et al, 1999).

Experiments on eight different types of soils (Dirksen and Dasberg, 1993) indicate that the deviation from Topp's equation appears more due to density effects than to bound water effects. Jacobsen and Schjonning (1993) incorporated bulk dry density, percent clay content, and percent organic content to get an improved general calibration relation. They also showed that the improved accuracy in volumetric water content was mostly attributed to the dry density term.

Another popular type of calibration is based upon a linear relationship between $\sqrt{K_a}$ and θ (Herkelrath et al., 1991; Ferre et al., 1996; Malicki et al, 1996; Topp et al., 1996; Yu et al., 1997).

$$\theta = b\sqrt{K_a} + a \quad (6-3)$$

in which a and b are constants obtained by regression. Yu et al (1997) reported that the equation provides good fit to the data by Topp et al. (1980) when $a=0.1841$, $b=0.1181$. However, Eq. 6-3 does not account for soil density effects. A calibration equation incorporating density effects is proposed by Malicki et al. (1996)

$$\theta = \frac{K_a^{0.5} - 0.819 - 0.618\rho_b + 0.159\rho_b^2}{7.17 + 1.18\rho_b} \quad (6-4)$$

There also exists a calibration relationship based on theoretical polarization analysis of dielectric mixtures (De Looer, 1968) or semi-empirical dielectric mixing formulas (Birchak et al, 1974).

Two factors make it difficult to apply these calibration equations to geotechnical practice:

- 1) The calibrations are expressed in terms of volumetric water content and independent determination of dry density is needed to obtain gravimetric water content;
- 2) The improved calibrations accounting for bulk density effects are complex in form and hard to apply.

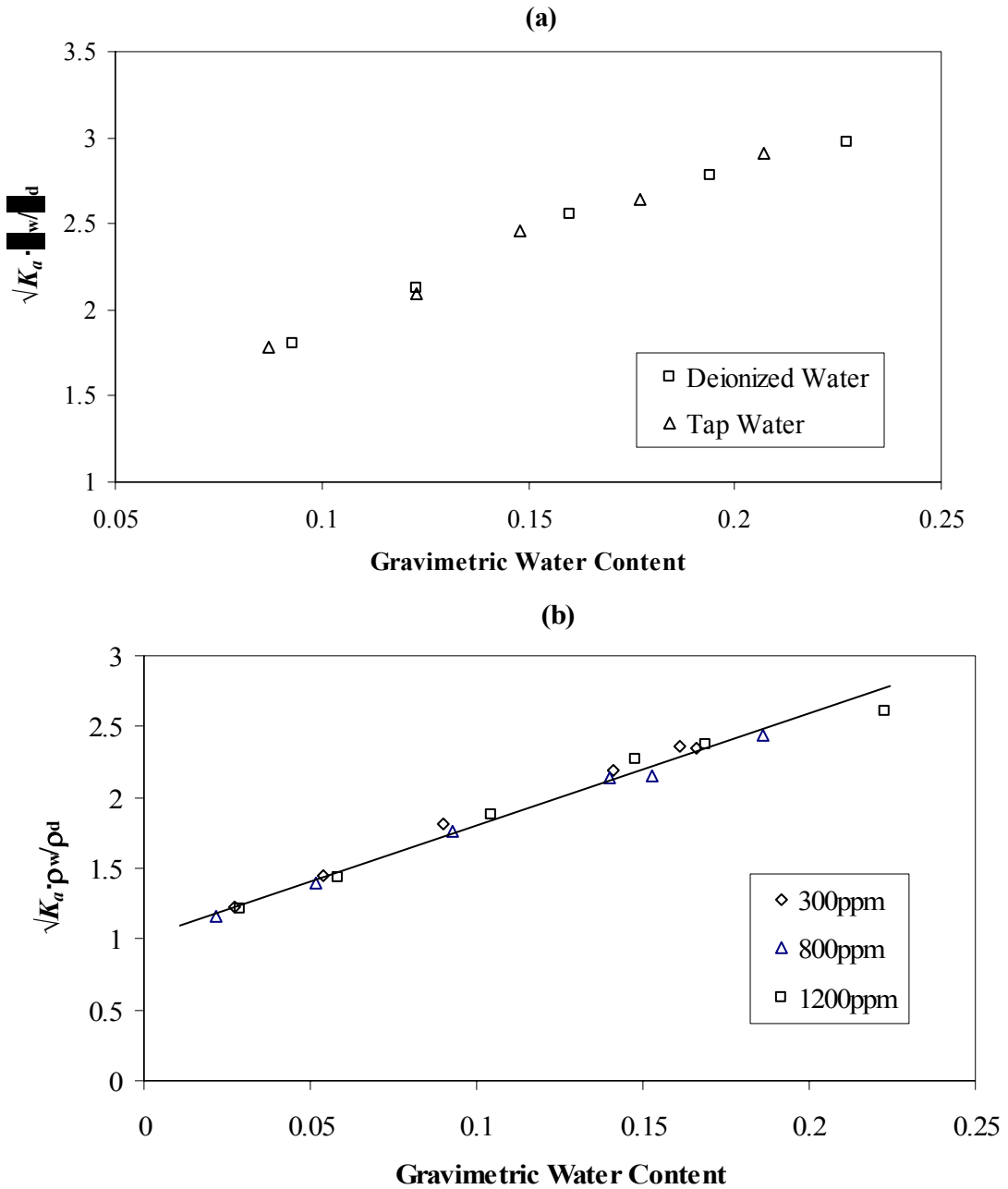
The study by Siddiqui (1995, 2000) utilized the concept of gravimetric water content in a calibration equation along with soil dry densities

$$\sqrt{K_a} \frac{\rho_w}{\rho_d} = a + bw \quad (6-5)$$

where a and b are soil specific calibration constants and w is the gravimetric water content. As discussed in Chapter 5, a is the $\sqrt{K_{a,s}}$ (refraction index of soil solids) normalized by soil dry density; b is $\sqrt{K_{a,w}}$ (refraction index of pore fluid) (Drnevich et al., 2002).

According to the procedure described in ASTM D6780 the calibration constants a and b are obtained in conjunction with the standard compaction test (ASTM D698 or ASTM D1557). Use of commonly accepted values for $K_{a,s}$ and extreme ranges of dry density show that the variation

of a is from 0.5 to 1.85. The typical value of $K_{a,w}$ is about 81 at 20°C which gives a value of b of approximately 9 (Drnevich et al. 2002). It is also observed that the calibration for dielectric constant is insensitive to pore-fluid conductivity for both sandy and clayed soils (Fig 6.3.)



A close inspection of this expression shows that it is consistent with the relationship obtained using volumetric mixing formulas (Lin, 1999).

6.2.3 Calibration Relationship for Bulk Soil Electrical Conductivity

Bulk soil electrical conductivity can be obtained from analysis of TDR waveforms by use of Eq. 4-10. The next task is to relate bulk soil electrical conductivity to soil physical properties.

Because soil is a three-phase system, factors influencing soil electrical conductivity include: porosity, degree of saturation, composition of pore water, mineralogy, soil structure, etc. General theoretical equations expressing the electrical conductivity as a function of all these factors is not available because of the inherent complexity of the soil-water system in most natural soils. However, a number of empirical equations and theoretical expressions based upon simplified models are available that gives satisfactory results for given conditions (Mitchell, 1993).

An important observation on bulk soil electrical conductivity from laboratory tests is that for a given soil water content, bulk electrical conductivity is proportional to soil pore fluid electrical conductivity. This leads to Archie's law (1942), in which bulk soil electrical conductivity is expressed as a function of pore fluid conductivity, porosity, degree of saturation etc. Conductivity by soil particles is ignored and thus the relationship is only applicable for coarse materials.

Rhoades et al (1976) developed an improved relationship based on a two-pathway model which took into consideration both the conduction by pore fluid and the conduction via surfaces of soil particles,

$$EC_b = T\theta EC_w + EC_s \quad (6-6)$$

where T is a geometric factor that has a linear relationship to volumetric water content, i.e. $T = a' + b'\theta$, in which a' , b' are empirical constants for a given soil. Thus the bulk soil electrical conductivity is a second order polynomial of volumetric water content, i.e.

$$EC_b = a'EC_w\theta^2 + b'EC_w\theta + EC_s \quad (6-7)$$

The expression shows good accuracy in relating soil volumetric water content and pore fluid conductivity to bulk soil electrical conductivity. The expression alone was used by Kalinski and Kelly (1993) to solve for soil volumetric water content from bulk electrical conductivity measurement on soils and gave satisfactory results.

However, this equation is inadequate for application to geotechnical engineering. First, it does not account for the effect of soil skeleton density. As seen from Eq 6-7, the conductivity of the soil solids is treated as a constant, which is inconsistent with the fact that the conductivity by the soil skeleton increases with the density of the material. Another problem for geotechnical applications is that conductivity is expressed in terms of volumetric water content.

In the expression for complex dielectric permittivity (Ramo et al. 1994), the electrical conductivity is included in its imaginary part. On the other hand, we can treat dielectric constant as the imaginary part of complex electrical conductivity (Sihvola, 1999). This implies that soil apparent dielectric constant and bulk soil electrical follows similar rules (White et al., 1994; Hilhorst, 2000). By this analogy, a calibration relationship for bulk soil electrical conductivity should be similar to that for soil apparent dielectric constant and can be expressed as:

$$\sqrt{EC_b} \frac{\rho_w}{\rho_d} = c + dw \quad (6-8)$$

where c and d are two soil specific calibration constants. This relationship was investigated by Feng (1999) and Lin (1999).

We may express Eq. 6-8 in terms of volumetric water content by substituting $\theta = w \frac{\rho_d}{\rho_w}$

$$\sqrt{EC_b} = c \frac{\rho_d}{\rho_w} + d\theta \quad (6-9)$$

and thus

$$EC_b = \left(c \frac{\rho_d}{\rho_w} + d\theta\right)^2 = \left(c \frac{\rho_d}{\rho_w}\right)^2 + 2c \frac{\rho_d}{\rho_w} d\theta + d^2\theta^2 \quad (6-10)$$

which is a second order polynomial for θ and is compatible with Rhoades's relation (Eq. 6-6).

Comparing the coefficient for second order term, we have

$$d = \sqrt{a' EC_w} \quad (6-11)$$

$$c = \sqrt{EC_s} \frac{\rho_w}{\rho_d} \quad (6-12)$$

Thus, d is a constant that includes the effect of both soil type and pore fluid properties. Similarly, c is a constant related to dry-density-normalized conductivity of the soil solids.

There are many advantages in using the calibration equation given by Eq. 6-8 including: 1) the relationship is expressed in terms of gravimetric water content and thus is more suitable for geotechnical applications; 2) the expression considers both conduction from pore water and from soil particles; 3) it accounts for the density of the soil skeleton on conductivity; and 4) the expression is simple in format and easy to apply.

Equation 6-8 is an important improvement over that observed by previous research. In a study on graphite-soil mixtures, White et al. (1994) observed that there is a reasonably good linear relationship between square root of bulk electrical conductivity and soil volumetric water content. Their data shows a systematic bias to the fitted line. The writers believe that this possibly is due to density effects and the correlation will be improved if density effects are accounted for by use of Eq. 6-8.

Equation 6-8, with data by Amenta et al. (2000) is plotted in Fig.6.5, These data originally were used to compare the accuracy of different models to estimate soil pore fluid conductivity from bulk electrical conductivity. Figure 5 shows that for a given pore fluid

conductivity, the square root of bulk electric conductivity has good linear relationship with gravimetric water content, with the slope of the calibration curve dependent upon the pore-fluid conductivity.

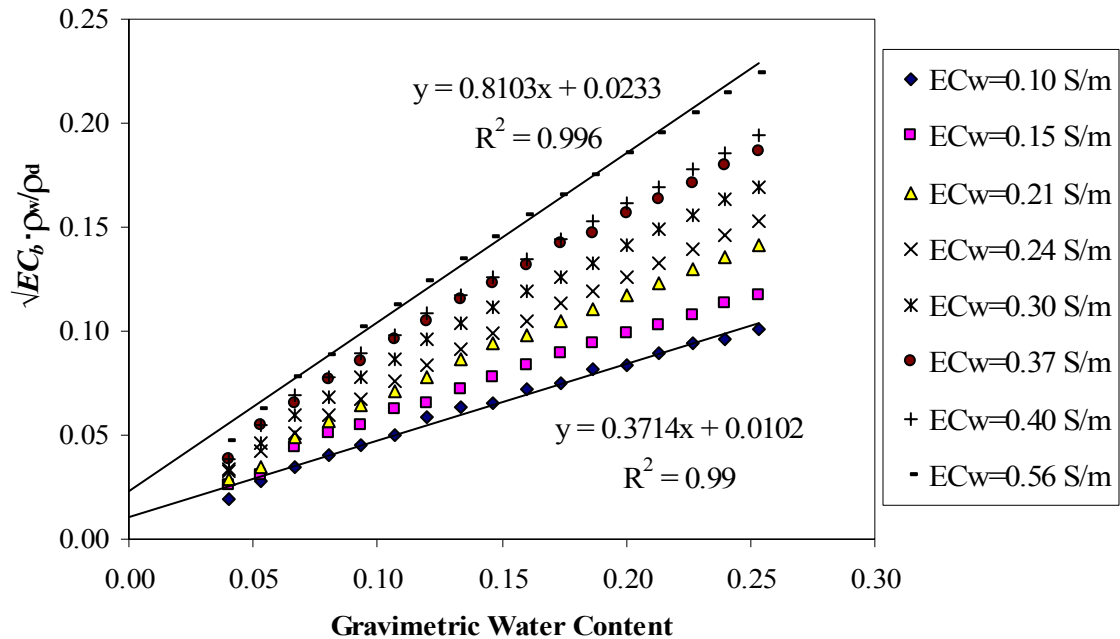


Fig. 6.4. Relationship between Bulk Electric Conductivity and Gravimetric Water Content at Given Pore Fluid Conductivity using Data by Amenta et al. (2000)

The constants c and d for Eq. 6-8 can be obtained in conjunction with obtaining the calibration constants, a and b for soil apparent dielectric constant (Eq. 4-10) while performing laboratory compaction tests. The calibration constants c and d are dependent on the conductivity of the pore fluid and will change if the pore fluid changes. In determining c and d , the pore fluid conductivity needs to be constant and within a range of 0.04~0.08 S/m and ordinary tap water is usually within this range. High pore fluid conductivity causes problems for determining K_a and low pore fluid conductivity results in poor accuracy for values of c and d .

6.2.4 The Soil Apparent Dielectric Constant - Bulk Electrical Conductivity Relationship

Soil apparent dielectric constant and bulk electrical conductivity are generally treated as two pieces of independent information obtained from the TDR waveform. Typically, these two pieces of information are applied separately, i.e. soil apparent dielectric constant is used to obtain soil water content while soil bulk electrical conductivity generally is used to estimate soil pore-fluid conductivity. However, these two parameters are related and their interrelationship can be utilized to simplify TDR measurements and make them more accurate.

From a theoretical point of view, soil apparent dielectric constant and bulk electrical conductivity are correlated since soil d.c. conductivity is contained in the imaginary part of soil complex permittivity (Ramo, 1994). Malicki et al. (1994) found a high degree of linear correlation between soil apparent dielectric constant and bulk soil electrical conductivity for a broad range of soil types. Based on a simplified analysis as well as on experimental verification with glass beads and 6 different kinds of soils, Hilhorst (2000) also found that there is a good linear relationship between soil apparent dielectric constant and bulk soil electrical conductivity.

We now have two independent equations, one for soil apparent dielectric constant (Eq. 4-10) and one for bulk soil electrical conductivity (Eq. 6-8), both of which are functions of water content and dry density. Hence, they must be related to each other. Combining Eqs. 4-10 and 6-8, we get

$$\sqrt{EC_b} = \frac{b \cdot c - a \cdot d}{b} \frac{\rho_d}{\rho_w} + \frac{d}{b} \sqrt{K_a} \quad (6-13)$$

Equation 13 can be simplified to

$$\sqrt{EC_b} = f + g \sqrt{K_a} \quad (6-14)$$

in which f and g are calibration constants related to soil type and pore-fluid conductivity.

Comparing Eq. 6-13 with Eq. 6-14, we see that slope of the line g in Eq. 6-14, equals d/b in Eq. 6-13. Since both b and d are related to pore-fluid properties, the value g must also be related to them. As we have seen, b is relatively independent of ionic conductivity and d is strongly related to the conductivity of the pore fluid, thus g is predominantly dependent upon

pore fluid conductivity, i.e. the slope of the line, g , changes systematically with pore fluid conductivity. A schematic plot of the Apparent Dielectric Constant – Electrical Conductivity calibration curves for different pore-fluid conductivities is shown in Fig.6. 5(a) where the square roots of both are plotted.

The Apparent Dielectric Constant – Electrical Conductivity calibration curve is useful for assessing the quality of a TDR measurement, e.g., values from a measurement showing large deviations from the corresponding calibration curve indicates a possible error in measurement such as caused by poor contact between the probe head and probe rods, gaps between the soil and the probe center rod, etc. Also, this calibration curve can be used to estimate the pore fluid conductivity. The most important use of the Apparent Dielectric Constant – Electrical Conductivity calibration curves is to adjust field measurements to obtain accurate values of water content and dry density as described subsequently.

6.2.5 Use of a Standard Pore Fluid to Calculate Soil Water Content and Dry Density

Given the calibration equations relating soil apparent dielectric constant and soil bulk electric conductivity to soil water content and dry density, it is natural to assume that we can obtain soil water content and dry density by simultaneously solving Eqs. 4-10 and 6-8 which gives

$$\rho_d = \frac{d\sqrt{K_a} - b\sqrt{EC_b}}{ad - cb} \quad (6-15)$$

$$w = \frac{c\sqrt{K_a} - a\sqrt{EC_b}}{b\sqrt{EC_b} - d\sqrt{K_a}} \quad (6-16)$$

However, water content and dry densities calculated by Eqs. 6-15 and 6-16 generally do not have satisfactory accuracy. Many factors can contribute to this inaccuracy, including random errors in dielectric constant and electrical conductivity measurements. The most significant source of

error is due to differences in pore fluid conductivity between calibration samples and field samples, i.e. the pore fluid conductivity is likely to be different from that used to obtain the calibration factors. As shown earlier, the influence of pore fluid conductivity on calibration constants for K_a is relatively insignificant.

Let us denote the calibration constants for electrical conductivity corresponding to the laboratory calibration test as c_0, d_0 and those corresponding to field test as c_1, d_1 . Obviously, c_1, d_1 need to be used in Eqs. 6-15 and 6-16 for calculating water content and dry density of the soil in the field. However, it is not practical to determine values of c and d for every conductivity likely to be encountered in the field. Our approach is to “adjust” the field situation so that the laboratory calibrations can be applied to it. By Eq. 6-12, the slope of electrical conductivity calibration curve (d -value) is proportional to square root of pore-fluid conductivity. Although pore-fluid properties in the field are unknown, we can use a systematic approach to adjust conductivity of the pore fluid in the field to the conductivity of the pore-fluid used in laboratory calibration tests, which we call the “standard pore fluid”. Suppose the calibration in laboratory is obtained with a pore fluid electrical conductivity (EC_w) of 0.08 S/m. A TDR test is done in the field with measured K_a and EC_b plotted as an open diamond in Fig.6. 5(a). There is a point with the same K_a value, but with a different EC_b value (indicated by solid diamond) that is located on the line from the laboratory calibration. As illustrated in Fig.6. 5(b), by projecting the point corresponding to the field measurement to the lab calibration line, e.g., $EC_w = 0.08$ S/m, we “replace” the sample tested in field with a sample having the same water content and dry density, but with pore fluid conductivity 0.08 S/m which equals to pore fluid conductivity used for laboratory calibration. Thus, calibration constants determined by laboratory tests are applicable to the “adjusted sample”, i.e. the dry density and water content of the “adjusted sample” can be solved using Eqs. (6-15) and (6-16) with the calibration constants from laboratory tests. Since the water content and dry density of the “adjusted sample” are the same as for the field sample, the values calculated for the “adjusted sample” apply to the field sample.

This adjustment can be made to any Apparent Dielectric Constant – Electrical Conductivity calibration line obtained from laboratory calibration. In the calibration process, we do not need to measure pore fluid conductivity, except that it should be kept constant for all calibration tests. Laboratory tests indicate that a pore fluid conductivity of 0.04~0.08 S/m works well, which is a range associated with ordinary tap water.

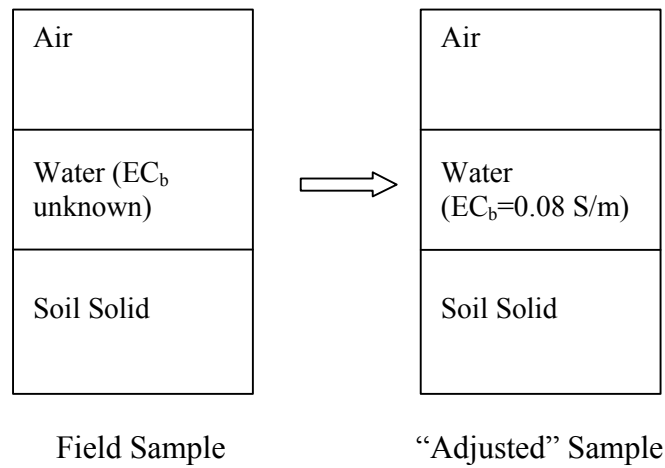
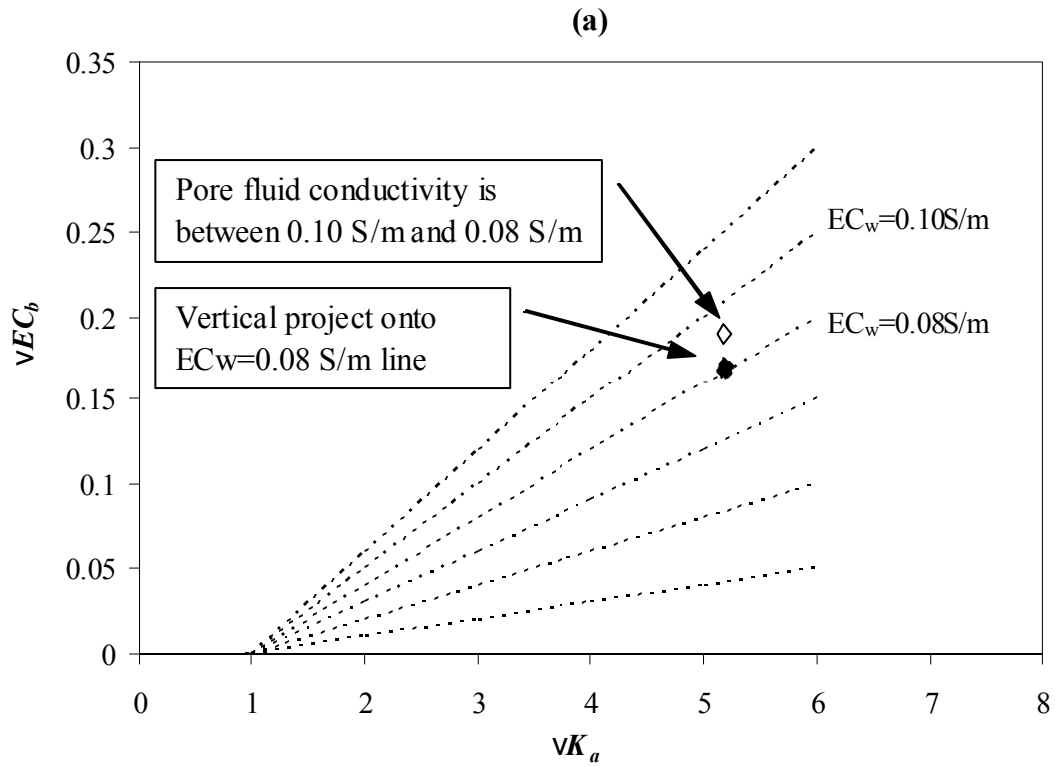


Fig. 6.5. Schema of “Adjustment” Process: (a) Vertical Projection to “Adjust” Field Measurement; (b) Phase Diagram of Field Sample and “Adjusted” Sample Represented by Points in Fig. 6. 5(a)

6.3 Application Procedure for One-Step Method

Equations 4-10, 6-8, and 6-14 provide the theoretical basis for the simplified One-Step Method. First, the field measurement of bulk soil electrical conductivity, $EC_{b,f}$, is “adjusted” to laboratory pore-fluid conductivity using calibration Eq. 6-14 and the soil apparent dielectric constant, $K_{a,f}$ giving $EC_{b,adj}$. The values of $K_{a,adj}$ and $EC_{b,adj}$ are then substituted into Eqs. 6-15 and 6-16 to obtain field gravimetric water content and dry density. The data reduction process is thus

$$\left. \begin{aligned} K_{a,adj} &= K_{a,f} \\ EC_{b,adj} &= (f + g \cdot K_{a,f})^2 \end{aligned} \right\} \Rightarrow \left\{ \begin{aligned} \rho_d &= \frac{d\sqrt{K_{a,adj}} - b\sqrt{EC_{b,adj}}}{ad - cb} \\ w &= \frac{c\sqrt{K_{a,adj}} - a\sqrt{EC_{b,adj}}}{b\sqrt{EC_{b,adj}} - d\sqrt{K_{a,adj}}} \end{aligned} \right. \quad (6-17)$$

where a, b, c, d, f , and g are calibration constants obtained from laboratory compaction tests.

The new One-Step Method for soil water content and dry density determination consists of laboratory calibration and field application.

Lab Calibration - For lab calibration, we obtain soil-specific calibration constants a, b, c, d, f , and g , which are related to soil type and pore-fluid properties. The laboratory calibration is performed in conjunction with standard compaction tests (ASTM D698 and ASTM D1557) using constant pore-fluid conductivity such as provided by tap water. Following compaction at a given water content, a central rod is driven into the mold using a plastic guide (Fig.6.6a). The MRP head is placed on the mold with the use of an adapter ring (Fig. 6.6(b)). The TDR reading is taken using with computer program called **PMTDR-SM**, which acquires the waveform and calculates K_a and EC_b . After taking the readings, soil in the mold is removed and placed into oven to obtain oven dry water content according to ASTM D2216.

The water content, dry density, K_a and EC_b from a series of compaction tests at different water contents are used to obtain calibration constants a, b, c, d, f , and g . The computer program **PMTDR-SM** has a built-in utility to calculate these calibration constants and place them into the

program for use in data reduction. An example of calibration for ASTM graded sand is shown in Fig. 6.7.



Fig. 6.6. Mold test procedures (a) Driving Central Rod through a guide placed on the mold (b) Multiple Rod Probe Head ready for making TDR measurements

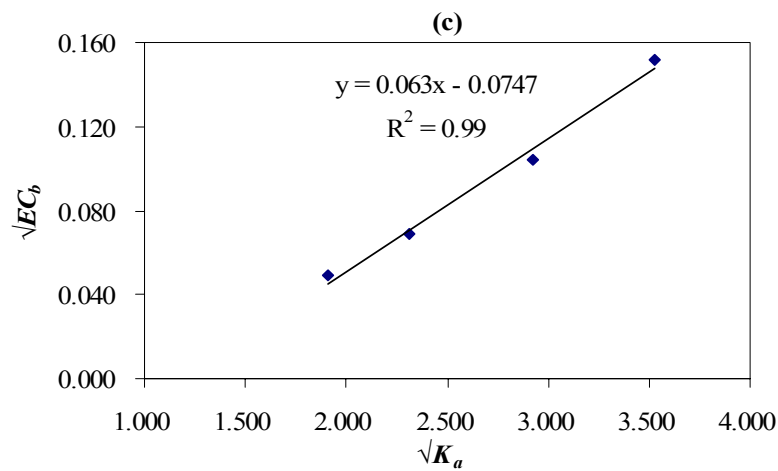
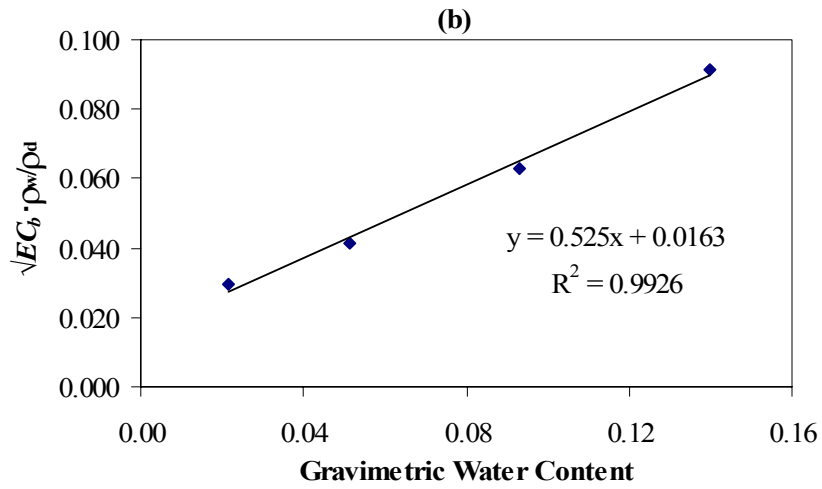
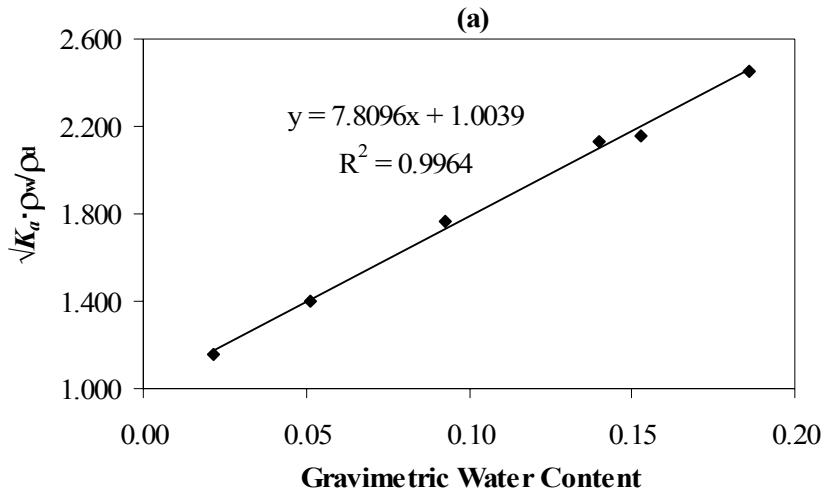


Fig. 6.7. An Example of Calibration on ASTM Graded Sand: (a) Calibration of K_a ; (b) Calibration of EC_b ; (c) Calibration of K_a and EC_b

Field test procedure – The field testing procedure and test apparatus for the One-Step Method is similar to those specified by ASTM D6780, **but omits** the steps of digging out the soil, compacting it in the mold, and running a second TDR test on the soil in the mold. In summary the process includes:

- 1) Level and smooth the soil surface and place the template on the surface
- 2) Drive four spikes into ground through holes in the guide template and remove template (See Fig.6.8a).
- 3) Seat MRP head on the four spikes (See Fig.6.8b).
- 4) Take a TDR reading to obtain $K_{a,f}$ and $EC_{b,f}$ using the ***PMTDR-SM*** program.

The program then uses the $K_{a,f}$ and $EC_{b,f}$ to get $K_{a,adj}$ and $EC_{b,adj}$ and calculates the field soil water content and dry density. Typically it takes about 3 to 4 minutes to do a field TDR test and obtain soil water content and dry density. This is much more time efficient than the earlier TDR test (ASTM D6780) and is comparable with the time required for nuclear tests.



Fig. 6.8 Field Test Procedures: (a) Spikes Being Driven through Template into Soil Surface; (b) Multiple Rod Probe Head on Spikes for Measurement

6.4 Temperature Compensation for the One-Step Method

Measured values of soil apparent dielectric constant and bulk electrical conductivity are somewhat temperature dependent and must be accounted for if temperatures of the soil in the field are more than +/- 5°C from the temperature of the soil during calibration.

Effects of temperature on soil apparent dielectric constant differ depending on the type of soil. Weast (1986) showed that the apparent dielectric constant of water, $K_{a,water}$, decreases linearly from a high of about 88 near freezing to about 70 for 50°C. Wraith and Or (1999) and others have noted that temperature effects for sandy soils behave similarly (but with reduced sensitivity) to temperature changes, but that clay soils exhibit the opposite behavior, i.e. K_a increases with temperature. Experiments by Drnevich et al. (2001) on a variety of soils, each with a range of water contents and density, determined temperature effects on the apparent dielectric constant. Based on this testing, they proposed adjusting the values of apparent dielectric constant from the TDR test at a given temperature to a standard temperature of 20°C. The adjusted values may be calculated from

$$K_{a,20^{\circ}C} = K_{a,T} \times TCF \quad (6-18)$$

Where TCF = Temperature Compensation Function

$$= 0.97 + 0.0015 T_{test,^{\circ}C} \text{ for cohesionless soils, } 4^{\circ}C \leq T_{test,^{\circ}C} \leq 40^{\circ}C$$

$$= 1.10 - 0.005 T_{test,^{\circ}C} \text{ for cohesive soils, } 4^{\circ}C \leq T_{test,^{\circ}C} \leq 40^{\circ}C$$

From Eq. 6-18 it can be seen that values of $K_{a,20^{\circ}C}$ will not exceed about ten percent for extremes in temperature covered by this equation. Considering Eq. 4-10, we see that water content is related to the square root of K_a and hence temperature effects on water content are relatively small. The authors suggest that temperature corrections are not needed for $15^{\circ}C \leq T_{test,^{\circ}C} \leq 25^{\circ}C$. Also, since the dielectric constant of ice has dramatically different properties from unfrozen water, the TDR method described herein does not apply to frozen soil.

On the other hand, observed effects of temperature on soil bulk electric conductivity is consistent for both cohesive and cohesionless soils (which is different from temperature effects on K_a) and include: 1) at given water content, bulk soil electrical conductivity increases with

temperature; 2) Compared with that for dielectric constant, the rate at which conductivity increases with temperature is more significant (e.g. 2% increase for each degree centigrade observed by Rinaldi and Cuestas (2002)); and 3) EC_b shows a linear variation with temperature for temperature ranges generally encountered in construction (Abu-Hassanein et al., 1996; Rinaldi and Cuestas, 2002).

There is a natural inclination to develop a temperature compensation function for bulk electrical conductivity (such as those proposed by Persson and Berndtsson (1998)) similar to that which was done for apparent dielectric constant as discussed above. While this approach seems obvious and straightforward, it is not necessary for the One-Step Method. A scheme to account for temperature effects in the One-Step Method can be explained by use of Fig.6. 9 where the $\sqrt{EC_b}$ is plotted versus $\sqrt{K_a}$ for different temperatures. The long-dashed lines correspond to the relationship at 20°C and the solid lines along the T axis represent the relationship at the temperature of the field test. The point $(EC_{b,T}, K_{a,T})$ is the data measured in the field, at temperature T . If the calibration for the $K_a - EC_b$ relationship was done at temperature T (denoted line 1 in the Fig.6. 9), adjustment to the standard pore-fluid conductivity is done as described previously. For this case, it is not necessary to make any temperature correction.

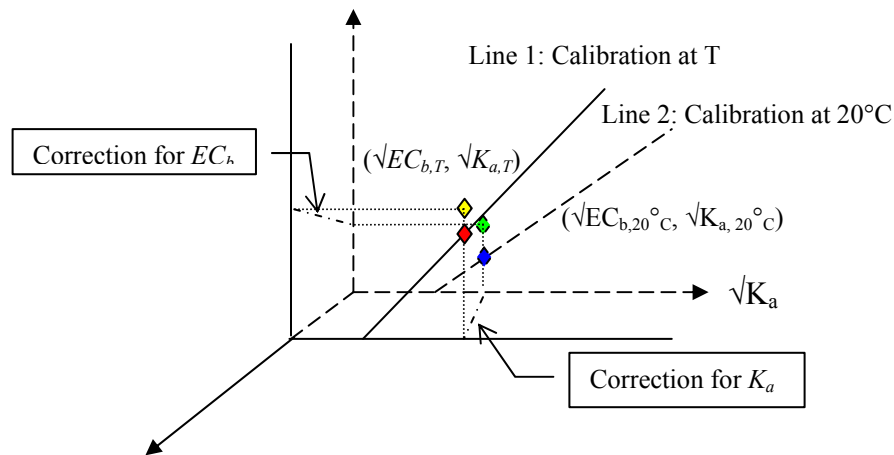


Fig.6. 9. Schematic Presentation of Temperature Correction for One Step Method

Now assume the calibration (denoted as Line 2 in Fig.6. 9) was conducted at room temperature (assumed to be 20°C). It is possible to correct for temperature effects on both K_a and EC_b independently (denoted by paths 2-2' and 3-3' in Fig.6. 9), with the corresponding point (denoted 1' with coordinates $(\sqrt{EC_{b,20^\circ\text{C}}}, \sqrt{K_{a,20^\circ\text{C}}})$) in the calibration plane for 20°C. Then, we can then apply the adjustment presented above, i.e. find point N' (with coordinates $([\sqrt{EC_{b,20^\circ\text{C}}}]_{\text{adj}}, \sqrt{K_{a,20^\circ\text{C}}})$) and make final computations using Eq. 6-17.

A closer look at the Fig. 6.9 indicates that the points 2', 1' and N' are located on the same vertical line. This means that given the calibration line at 20°C, we can find point N' by using point 2' alone. Thus, we only need to compensate for temperature effects on K_a using Eq. 6-18, i.e. correcting $K_{a,T}$ to $K_{a,20^\circ\text{C}}$ (points 2 to 2' in Fig.6.9) and then moving vertically to point N' which gives the values for making final computations using Eq. 6-17.

Tests were conducted on an ASTM graded sand to verify this adjustment for temperature effects. Standard compaction tests using ASTM D698 were conducted on the sand. The specimens were then sealed by plastic wrap and placed successively in rooms with controlled temperatures of 1°C, 7°C, 22°C, 30°C, and 40°C. TDR readings were taken after temperatures in the specimen stabilized. Afterwards, the entire soil specimen was oven-dried to determine soil water content by ASTM D2216.

Results of data reduction by this temperature compensation approach are shown in Fig.6.10 where the total density calculated from the results of the One-Step Method is compared to the Total Density by Direct Measurement. The data lie within +/- 3% which indicate this approach for temperature compensation provides satisfactory accuracy.

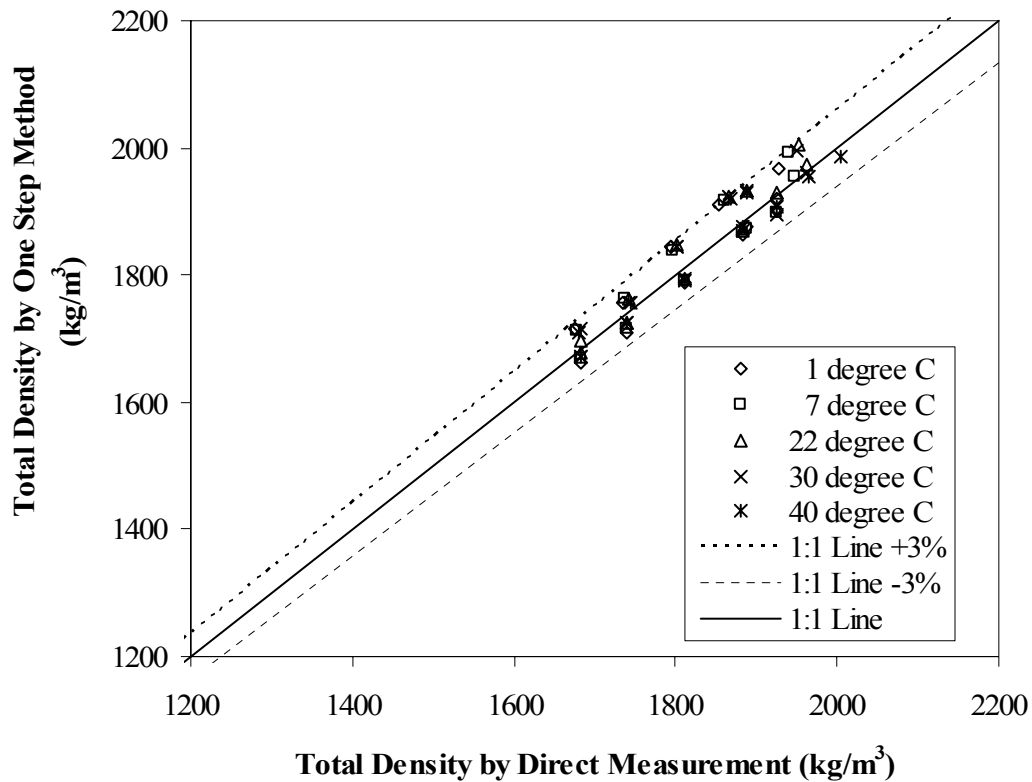


Fig. 6.10. Results by Simplified Temperature Correction Approach on ASTM Graded Sand

6.5 The One-Step Method for Testing Large Particles and Highly Conductive Soils

Coarse-textured soils, particularly those containing gravel or rock, occur at many sites. Work continues on studying the effects of testing large particle-sized materials. Based on preliminary tests, Siddiqui and Drnevich (1995) recommended that the TDR method can be used for soils where less than 30 percent of the sample by weight has particle sizes exceeding the 4.75-mm (No. 4) sieve and the maximum particle size passes the 19 mm (3/4-in.) sieve. This limitation is similar to the limitation associated with performing the conventional laboratory compaction test, ASTM D698, Method C. When testing large particles it is appropriate to use a mold with a larger diameter (such as used in ASTM D698 Method C) for calibration. This recommendation is to reduce soil volume-change effects caused by inserting the TDR probe rods (Yi, et al., (2001)). Results of testing on an Indiana 53 crushed stone (more commonly known as

Dense Graded Aggregate) are satisfactory as shown in Fig.6. 11. Additional work is continuing on improving the equipment and procedures for testing larger particle sizes.

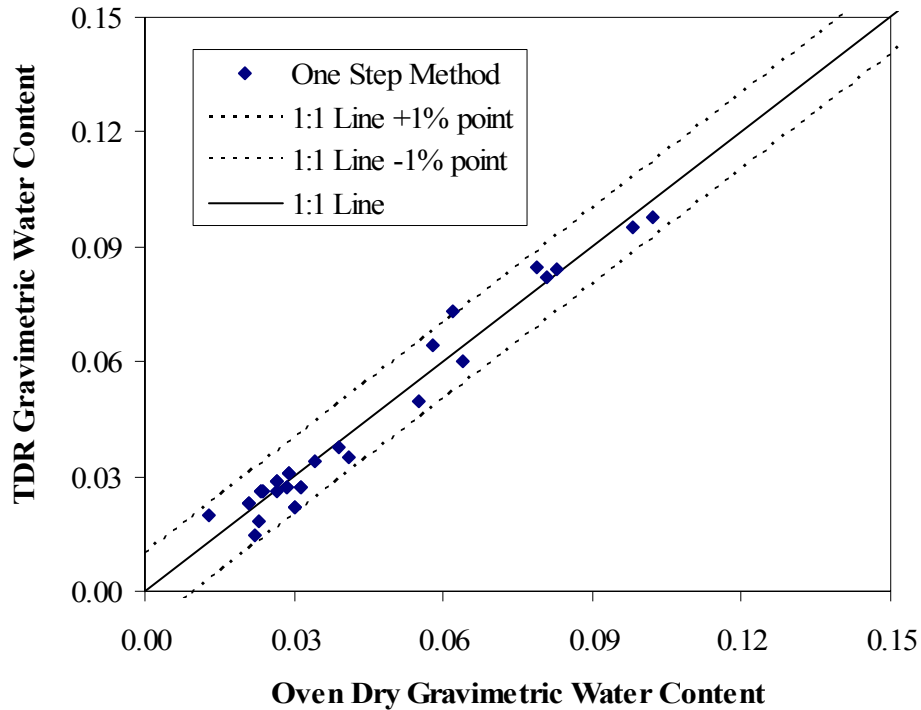


Fig. 6.11. Comparison of TDR Water Contents with Oven-Dry Gravimetric Water Contents for Testing on Indiana 53. (Results are typically accurate to within +/- 1 percentage point.)

For certain fine-textured soils such as fat clays at higher water contents, no significant second reflections are observed using a normal probe because the electrical energy is dissipated by high values of conductivity. For this special case it is possible to use an insulated center probe that has been properly calibrated. Drnevich et al, (2002) analyze this case and recommend procedures for use of an insulated center probe, but this masks the electrical conductivity, which means that the One-Step Method is not applicable. The writers are looking at ways to overcome this limitation. One approach that is under study is to transform the TDR signal to the frequency domain, strip off effects of apparatus and cables, and analyze the signal in the frequency domain. This approach was discussed by Feng, et al. (1999) and by Drnevich et al. (2001b) and work on it continues.

6.6 Typical Results

The One-Step Method for determining soil water content and dry density as described above was applied to data obtained from 192 laboratory and field tests. Accuracy of water content measurements is shown in Fig.6. 12 and that of dry density measurements is shown in Fig.6. 13. The data represent a variety of soils including dense-graded aggregate bases, sands, silts, clays, stabilized soils, and a low density mixed waste. From Fig.6. 12, water contents determined by the One-Step Method generally falls within ± 1 percentage points of oven-dry water contents while dry densities as shown in Fig.6. 13 generally falls within $\pm 3\%$ of the dry densities determined by direct measurement and oven dry water content. Both measurements provide sufficient accuracy for use in construction quality control. The One-Step Method makes the water content and dry density measurements on the same sample and appears to be applicable to a wide variety of soils commonly encountered in field.

A Beta Testing Program involving three State DOT's (Indiana, Florida, and New Jersey), two other universities (University of South Florida and Rutgers University), and two private firms (GAI Consultants and H.C. Nutting Company) is underway. Some of the data reported in Figs. 12 and 13 came from these participants.

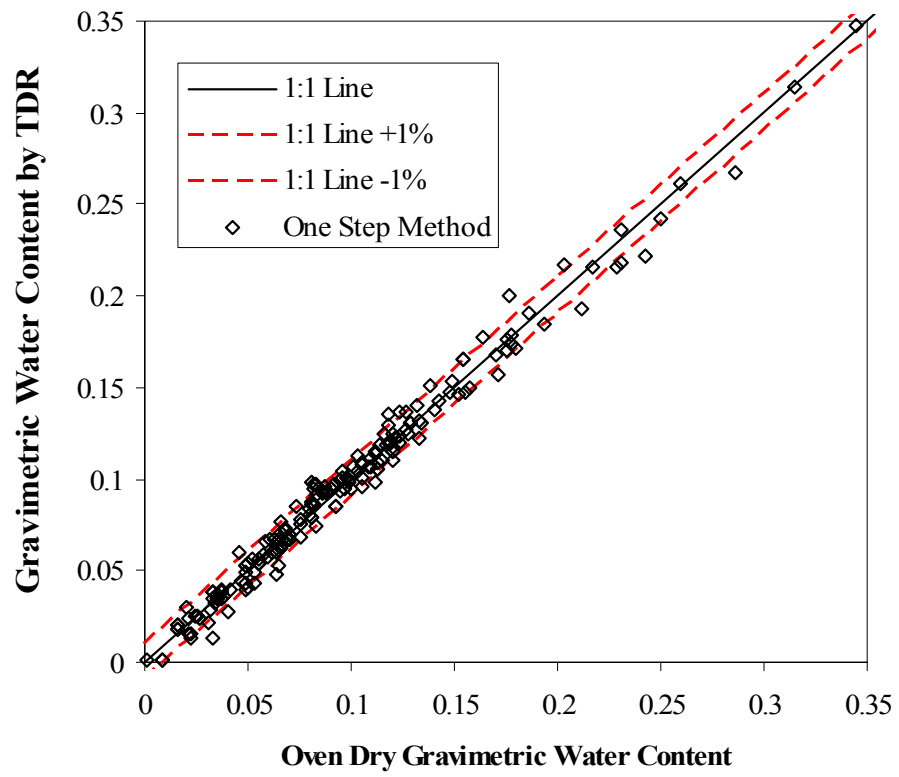


Fig. 6.12. Comparison of TDR Water Contents with Oven-Dry Gravimetric Water Contents. (Results are typically accurate to within +/-0.01)

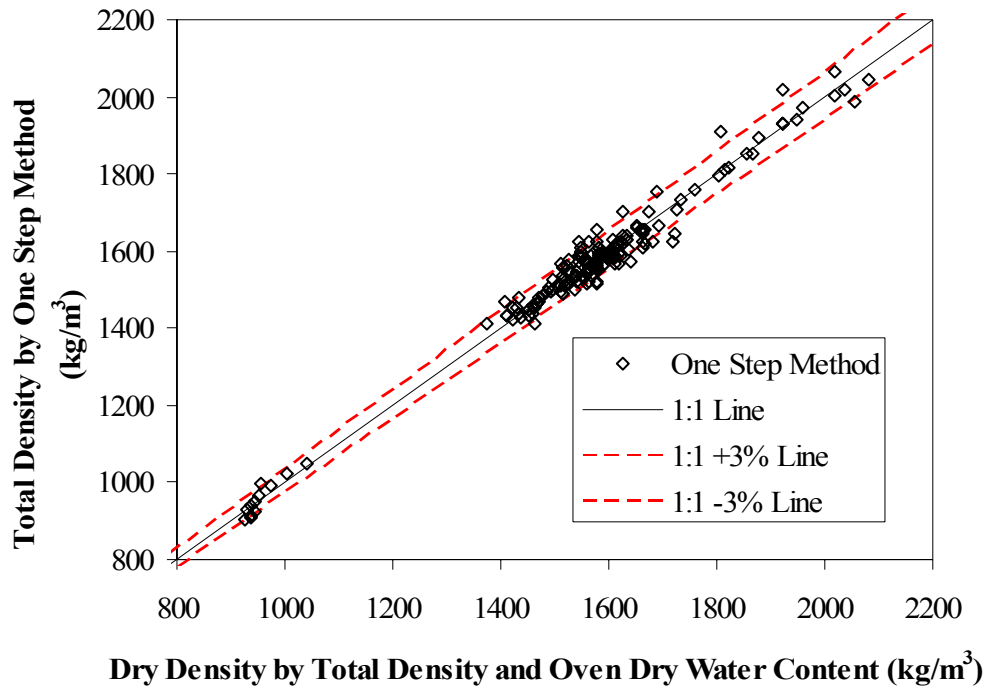


Fig. 6.13. Comparison of TDR Dry Density with Dry Density Determined from Total Density (direct measurement, sand cone, or nuclear) with Oven Drying for Water Content (Results are typically within +/- 3 percent.)

6.7 Conclusions

A One-Step Method for field determination of soil water content and dry density is presented in this chapter. The method is based upon simultaneous use of soil apparent dielectric constant and bulk soil electrical conductivity obtained from TDR measurements with specially designed probes on soil insitu or in a compaction mold. The method makes use of calibration equations for relating soil apparent dielectric constant and bulk soil electrical conductivity to soil water content and dry density. For a given soil, the electrical conductivity of the pore fluid may be different from that when calibration factors were obtained. To overcome this problem, a rational procedure is developed to adjust measured bulk electrical conductivity to a “standard” pore fluid, i.e. fluid used in obtaining the calibration factors (typically tap water). With the adjustment, laboratory calibration results apply to a wide range of field situations.

Laboratory calibration is conducted in conjunction with standard laboratory compaction tests, e.g. ASTM D698 and ASTM D1557, to obtain calibration constants for use in field tests. Field testing procedures follow only the first step of ASTM D6780. It is not necessary to excavate soil, compact it into a mold, weigh the mold, or do a TDR test in the mold. However, a test in the mold could be done in the field to validate the calibration factors. Effects of temperature on measurements made with the One-Step Method are studied and a simplified method to account for temperature effects gives satisfactory results. The calibration and field testing procedures have been automated with a program called *PMTDR-SM*. The One-Step Method only takes a few minutes to get values of water content and dry density, including the time to drive the probe rods.

Application of the One-Step Method to a wide variety of soil types shows satisfactory accuracy. The method is applicable to testing soils with relatively large particles, but calibration must use a larger diameter mold, e.g. ASTM D698, Method C. Currently, the method is not applicable to some highly conductive soils such as heavy clays at high water contents, where there is no clear reflection from the probe end.

Experience gained from on-going Beta Test program indicates the One-Step Method to be an accurate, fast and safe means to determine soil water content and dry density for purpose of compaction quality control.

7. Results from Purdue Working with Beta Partners

7.1 University of South Florida and Florida DOT

Two sets of Equipment were shipped to University of South Florida and Florida DOT, who teamed up in this Beta Test projects. These two Beta Partners, working together carried out a state-wide research program on typical sands used in Florida construction. Various kinds of sands were tested to obtain soil specific calibration constants a , b with the intention to obtain representative calibration constants. Research also was carried out to investigate the compaction energy effects on calibration and sensitivity of calibration constants a and b on measurement results. Recommendations were made by Professor Alaa Ashmawy and his student, Amr Sallam based on analysis on their testing results.

7.1.1 Experimental Results of Calibration Constants a and b of Sands around Florida

In order to ensure accuracy, two different operators performed the tests and, in selected cases, the test was performed by both of them to ensure consistent testing procedures. The final results are summarized in Table 7-1. According to Table 7-1, the mathematical average value for constants a and b were found to be 1.01 and 8.35, respectively.

Table 7-1. Values of Constants a and b for Various Florida Soil Types

Test	Description	Operator	USCS	AASHTO	a	b	Comment
1	Ottawa Sand	Amr	SP	A-1-b	1.22	11.68	Discarded
1-a	Ottawa Sand	Brian	SP	A-1-b	0.95	9.00	Accepted
1-b	Ottawa Sand	Both	SP	A-1-b	0.91	9.41	Accepted
Average					0.93	9.21	
2	Outside Lab	Amr	SP	A-3	1.00	8.20	Accepted
2-a	Outside Lab	Brian	SP	A-3	1.03	8.35	Accepted
Average					1.02	8.28	
3	MP-1	Amr	SP	A-1-b	0.93	8.78	Accepted
3-a	MP-1	Brian	SP	A-1-b	1.01	7.48	Accepted
3-b	MP-1	Brian	SP	A-1-b	0.98	8.21	Accepted
Average					0.97	8.16	
4	Sample # 515	Both	SP	A-3	1.05	8.19	Accepted
4-a	Sample # 515	Brian	SP	A-3	1.01	8.93	Accepted
4-a	Sample # 515	Brian	SP	A-3	1.03	8.73	Accepted

Test	Description	Operator	USCS	AASHTO	<i>a</i>	<i>b</i>	Comment
Average					1.03	8.62	
5	Sample # 2	Amr	SP	A-1-b	1.10	7.40	Accepted
5-a	Sample # 2	Both	SP	A-1-b	1.04	8.06	Accepted
Average					1.07	7.73	
6	Sample # 6944	Amr	SP	A-3	1.08	8.09	Accepted
6-a	Sample # 6944	Brian	SP	A-3	0.99	8.65	Accepted
Average					1.04	8.37	
7	Sample with # 6944	Brian	SP	A-1-b	0.99	8.80	Accepted
8	Sample # 6965	Both	SW	A-1-b	0.99	8.80	Study the effect of compaction
8-a	Sample # 6965	Both	SW	A-1-b	1.04	8.03	Study the effect of compaction
8-b	Sample # 6965	Both	SW	A-1-b	0.99	8.31	Study the effect of compaction
8-c	Sample # 6965	Both	SW	A-1-b	1.00	7.96	Study the effect of compaction
Average					1.01	8.28	
9	Sample with # 6965	Brian	SP	A-1-b	1.02	8.20	Accepted
10	Sample # 6974	Brian	SP	A-1-b	0.99	8.27	Accepted
11	Sample # 6978	Brian	SP	A-1-b	1.02	7.93	Accepted

The results of all tests are plotted on a single graph (Fig. 7.1). Values of 0.996 and 8.45 were determined for constants *a* and *b*, respectively. The correlation factor, or R-value, for the trend line used for all the data was 0.9837, indicative of a strong correlation.

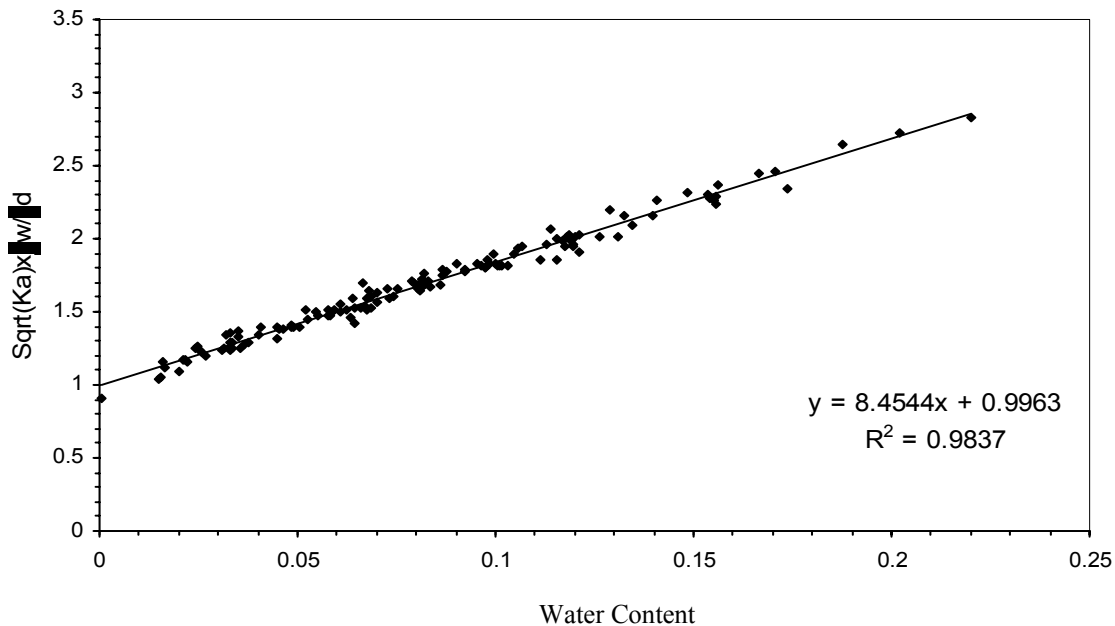


Fig. 7.1 Final Results of the TDR Tests in Mold for Various Soil Types

7.1.2 Effect of Compaction Energy on the Values of the Soil Constants a and b

In order to study the effect of compaction energy on the values of constants a and b , TDR tests must be performed at different compaction energies. A sample named 6944 has been chosen for this study. TDR tests were performed using different compaction efforts by varying the number of rod tamps, as summarized in Table (7-2).

Table 7-2 Different Tests Performed to Study the Effect of Compaction Energy

Case No.	Number of rod tamps per layer					
	Layer 1	Layer 2	Layer 3	Layer 4	Layer 5	Layer 6
1	5	6	7	8	9	10
2	10	11	12	13	14	15
3	20	21	22	23	24	25
4	30	31	32	33	34	35

For each case, the water content was determined four times to give an accurate value of water content. The results of the four tests are plotted in Fig. 7.2. From the figure, it can be

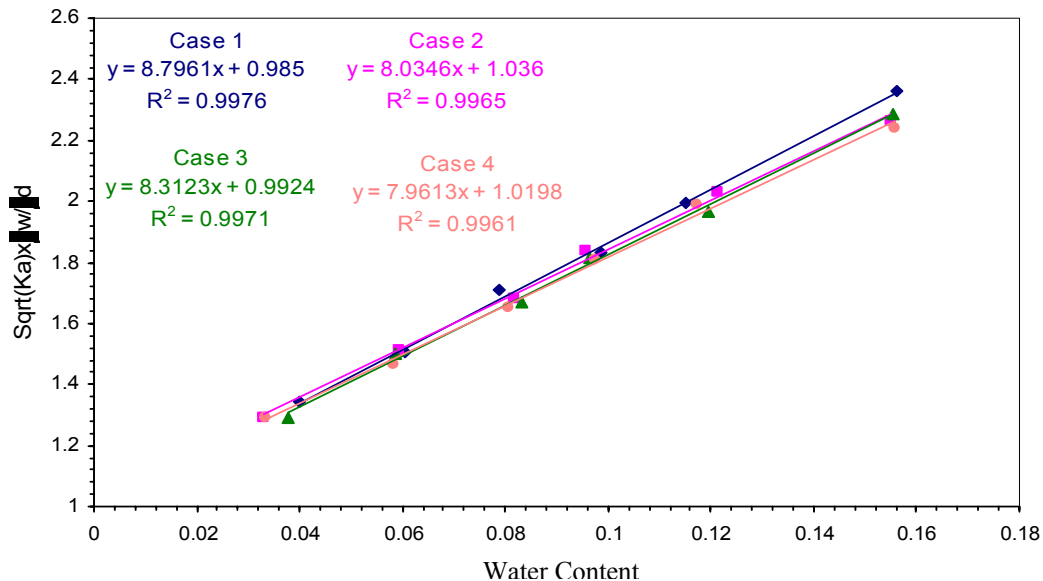


Fig. 7.2 Effect of Compaction Energy on Constants a and b .

concluded that constant b decreases slightly with increasing compaction energy, whereas

constant a exhibits an increasing trend. However, the difference between cases 2, 3, and 4 is insignificant. Therefore, it can be concluded that the compaction energy affects only slightly the value of constants a and b for the soils tested. It is recommended that the compaction energy associated with Case 3 be used to ensure consistent results.

7.1.3 Effects of the Accuracy of Constants a and b on the Resulting Moisture Contents

The study was based on Siddiqui and Drnevich (1995) normalized equation, Eq. 7-1. From the basic definitions and relations of Soil Mechanics, the dry density can be defined as:

$$\sqrt{K_a} \frac{\rho_w}{\rho_d} = a + bw \quad (7-1)$$

$$\rho_d = \frac{\rho_t}{(1+w)} \quad (7-2)$$

Substituting with ρ_d from Eq. (7-1) into Eq. (7-2):

$$\sqrt{K_a} \frac{\rho_w}{\rho_t} (1+w) = a + bw \quad (7-3)$$

Rearranging Eq. (7-3), we get:

$$w = \frac{K^* - a}{b - K^*} \quad (7-4)$$

Where K^* is defined as: $K^* = \sqrt{K_a} \frac{\rho_w}{\rho_t}$

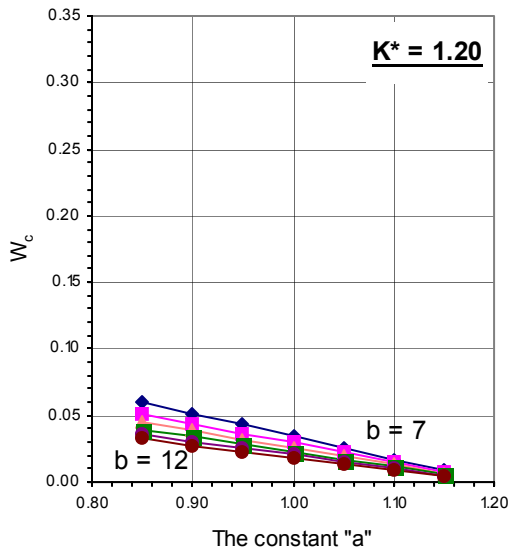
All the quantities defining K^* are presumed to be measured at a high accuracy. Therefore, no error is assumed to result from these quantities. In order to study the effect of

changing the constant a on the predicted value of moisture content, Eqn. (2-3) was used to calculate the water content from the assumed a values at different K^* and b values. The b values were varied from 7 to 12, whereas the K^* values were varied from 1.2 to 2.4. The results are summarized in Fig. 7.3 and table 7-3.

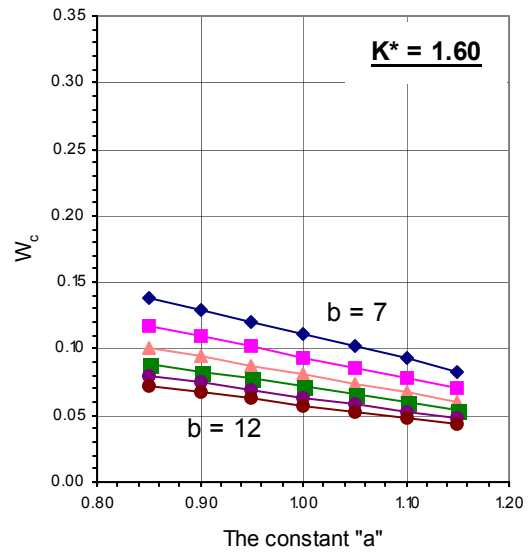
Table 7-3 Error Resulting from Changing the Constant a

Error range in a , ($b = 9$)	Change in the predicting moisture content in percentage			
	$K^* = 1.2$	$K^* = 1.6$	$K^* = 2.0$	$K^* = 2.4$
0.95 – 1.05	1.28	1.35	1.43	1.52
0.90 – 1.10	2.56	2.70	2.86	3.03

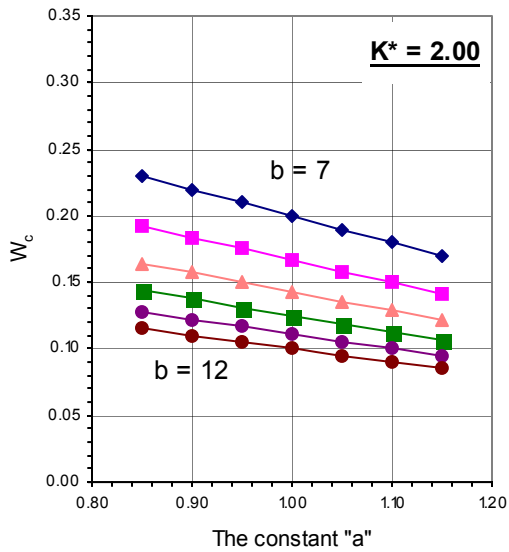
It is evident from Fig. 2.3 and table 2-5 that the predicted value of the moisture content does not change noticeably with changing the constant a in a range of 1 ± 0.05 . It is also clear that the change in the predicted value of the moisture content varies, depending on the value of K^* . This is logical because the effect of the constant a , as an intercept, has to be more predominant at lower values of moisture content.



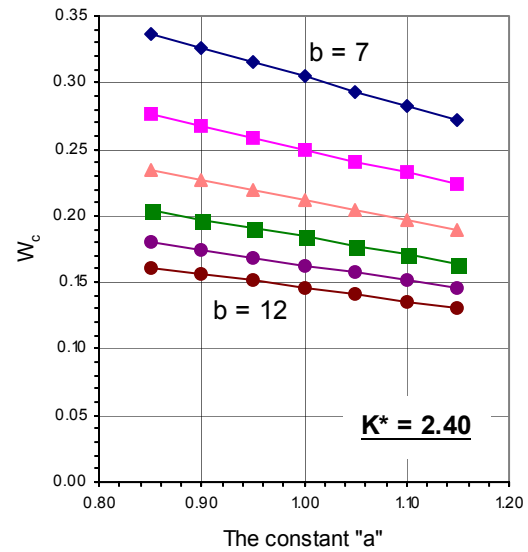
(a)



(b)



(c)



(d)

Figure 7.3 Error Resulting from Changing the Constant a on the Predicted Moisture Content

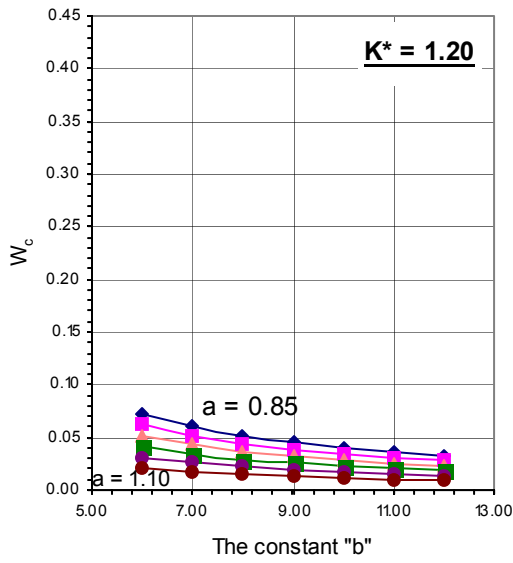
In order to study the effect of changing the constant b , the water content was calculated from the assumed b values at different K^* and a values. The a values were varied from 0.85 to 1.10, whereas the K^* values were varied from 1.2 to 2.4. The results are summarized in Fig. 7.4 and Table 7-4.

Table 7-4 Error resulting from Changing the Constant b

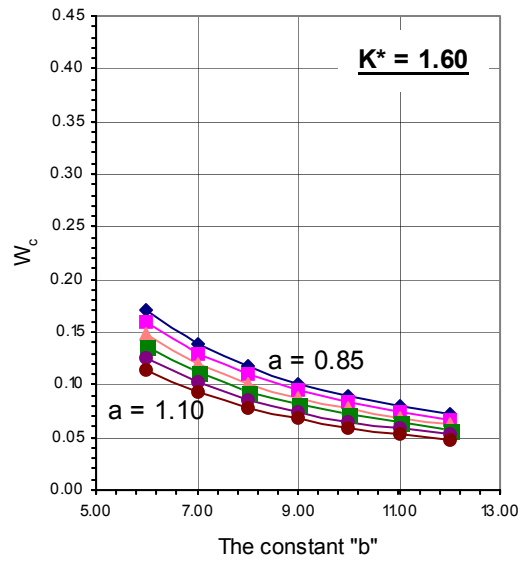
Error range in b , ($a = 1$)	Change in the predicting moisture content in percentage			
	$K^* = 1.2$	$K^* = 1.6$	$K^* = 2.0$	$K^* = 2.4$
8.0 – 10.0	0.67	2.23	4.16	6.82
7.0 – 11.0	1.41	4.73	8.89	14.15

The effect of changing the constant b was higher than the effect of changing the constant a . It can be seen from Fig. 7.4 and Table 7-4 that the predicted value of the moisture content changes noticeably with changing the constant b especially in a range of 9 ± 2.0 .

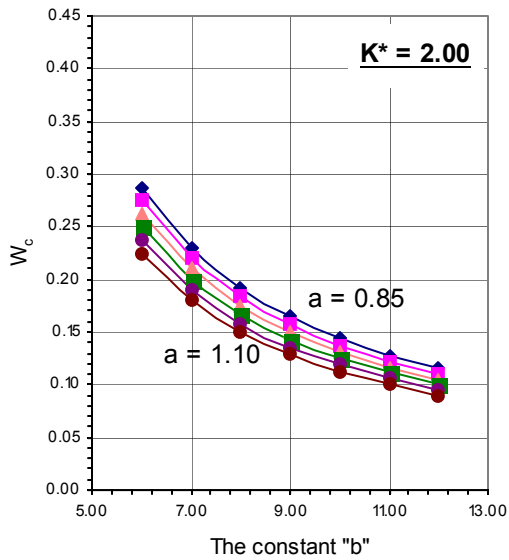
It is also clear that the change in the predicted value of the moisture content depends on the value of the K^* . The higher the K^* value, the higher the error in the predicted value of the moisture content. This is logical because the change in the predicted moisture content resulting from a change in the constant b , which is the slope of the straight line, is expected to be dramatic, especially at high water contents.



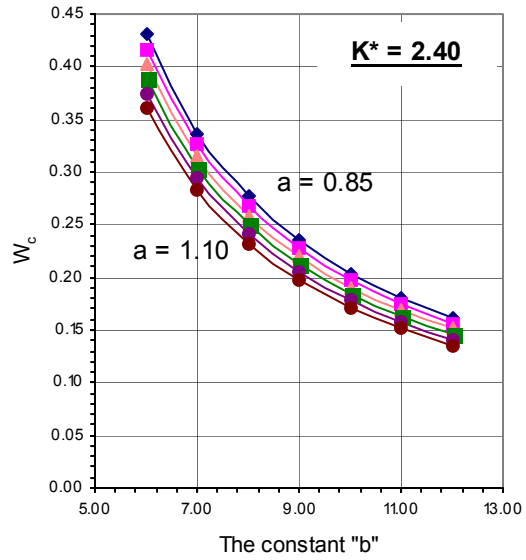
(a)



(b)



(c)



(d)

Figure 7.4 Results of Changing the Constant b on the Predicted Moisture Content

7.1.4 Accuracy of TDR Measurements

Various samples were prepared in a compaction mold to test the accuracy that TDR can attained using the default calibration constants identified. The results are presented in Table 2-5. In this table, soil type is identified by Unified Soil Classification System and AASHTO system. Oven dry water contents are used as the standard water content value to compare with TDR values. TDR measured dry density also is compared with standard dry density, which is calculated by measured total density and oven dry water content.

As can be seen from the Table 2-5, TDR measured water content is generally within 1% absolute difference compared with oven dry water content. TDR measured dry density is generally has a relative difference within 3% compared with dry density calculated from total density and oven dry water content.

7.1.5 Summary of Work by the University of South Florida Beta Partners

For the tested soils in this study, the value of the constant a ranges from 0.91 to 1.08 with an average value of 0.996. This value is considerably close to 1.00, the value proposed by Lin et al. (2000). The study also revealed that the value of the constant b ranges from 7.73 to 9.41 with an average value of 8.45. The value proposed by Lin et al. (2000) for the same parameter is 9.0. In practice, it is recommended based on this study to use a value of 1.00 for constant a and a value of 8.50 for constant b for sandy soils used in construction in Florida.

It is noted that most of the soil types included in this study, so far, were sandy soils. The USCS classification for these soil types was SP and SW. The AASHTO classification was A-1-b and A-3. Since no clayey or silty soil was used in this study, no recommendation is made about the values of constants a and b for these kinds of soils.

The effect of compaction energy on the resulting a and b constants was investigated. The TDR was performed on the same sample using different tamping energies and the resulting a and b values were calculated accordingly. This study revealed that the compaction energy slightly affects the values of the constant a and b . Based on the results, it is recommended to compact

the soil in six layers of 20 through 25 tamps for each layer. This energy level is enough to provide consistent results.

The effect of changing the constants a and b on the predicted moisture content has been studied. The study revealed that the predicted value of the moisture content does not change noticeably with changing the constant a and that the change in the predicted value of the moisture content does not depend on the value of K^* . The study also revealed that the predicted value of the moisture content changes more noticeably with changing the constant b . The level of change or “error” in the predicted value of the moisture content depends on the value of K^* . The higher the value of K^* , the higher the error in the predicted value of the moisture content. (Please refer to paper in appendix II for details)

Table 7-5 TDR Measured Results Using Default Settings versus Oven Dry Results

Sample	Date	USCS	AASHTO	Moisture content, %				Dry Density			
				Actual Value	TDR Value	Abs. Error	Norm. Error	Actual Value lb/ft ³	TDR Value lb/ft ³	Abs. Error lb/ft ³	Norm. Error, %
1	8/6/2002	SP	A-3	5.75	5.50	-0.25	-4.60	96.14	94.77	-1.37	-1.45
1-a	8/6/2002	SP	A-3	10.63	9.70	-0.93	-9.56	93.28	95.22	1.93	2.03
1-b	8/6/2002	SP	A-3	12.52	11.40	-1.12	-9.82	95.79	98.70	2.91	2.95
2	8/6/2002	SP	A-1-b	8.84	8.00	-0.84	-10.54	102.63	101.67	-0.96	-0.94
2-a	8/6/2002	SP	A-1-b	11.93	10.40	-1.53	-14.72	106.23	112.31	6.08	5.42
3	8/9/2002	SP	A-1-b	5.47	5.20	-0.27	-5.26	94.74	98.08	3.34	3.40
3-a	8/9/2002	SP	A-1-b	9.62	9.40	-0.22	-2.31	98.72	100.79	2.07	2.05
3-b	8/9/2002	SP	A-1-b	12.21	11.10	-1.11	-9.99	100.72	107.56	6.84	6.36
3-c	8/9/2002	SP	A-1-b	15.35	14.90	-0.45	-3.04	101.95	104.86	2.91	2.78
4	8/13/2002	SW-SM	A-1-b	13.95	14.50	0.55	3.82	104.16	106.12	1.95	1.84
4-a	8/13/2002	SW-SM	A-1-b	15.61	15.60	-0.01	-0.05	110.21	113.32	3.10	2.74
4-b	8/13/2002	SW-SM	A-1-b	14.73	14.40	-0.33	-2.32	109.72	107.36	-2.37	-2.20
5	8/15/2002	SP	A-3	8.23	8.90	0.67	7.57	93.94	94.65	0.71	0.75
5-a	8/15/2002	SP	A-3	10.70	12.00	1.30	10.85	96.58	96.30	-0.28	-0.29
5-b	8/15/2002	SP	A-3	12.12	12.60	0.48	3.82	99.24	102.32	3.08	3.01
5-c	8/15/2002	SP	A-3	16.89	17.80	0.91	5.11	102.29	97.80	-4.48	-4.58

7.2 GAI Consultants

A set of equipment was shipped to GAI Consultant in December, 2001. Results were obtained from field application of TDR technology to non-conventional materials such as LPC and Fly Ash. This greatly facilitated understanding of phenomena and extending application of TDR technology.

LPC is the acronym of LOW PERMEABILITY CEMENTITIOUS MATERIAL. This is a product composed of dewatered scrubber sludge, with additions of fly ash and lime to it. This produces a product that will become stable. Strength of LPC will vary based on many factors from the process used, coal being burnt, type and efficiency of scrubber and environmental conditioning. Typically this material is land filled, however this material has shown beneficial use qualities. The basic formula for the production of LPC can be changed to meet a particular engineered application. This is however limited by plant feed rate capability and cost. The factors that are varied are the amount of water left in the scrubber sludge, the amount of fly ash added and the amount of lime added. Presently the upper limit of the lime used by GAI Consultants stands at around 3%. GAI Consultants work with the product being produced or request changes in the formula being aware of the plants limitations. QA and QC becomes a very important regimented diligent practice when working with both fly ash and LPC since the product can change at any given time.

In addition to testing on LPC, GAI Consultant also carried out a trial study on ash called Harrison Fly Ash. The fly ash used in this trial study was surplus ash they had in house. The effort was to determine TDR capability with fly ash over a wide range of water contents. This was to reinforce the need to use a working range of water contents and the need for coated probes. At the higher water contents the return on the wave form was not well defined. This caused some problems in obtaining data for this material. This problem was overcome somewhat by increasing the density of the specimens at the higher water contents. Limited information is available for the particular ash: resource of the ash - Harrison Generating Station Clarksburg West Virginia. The coal used at this station comes in from approximately a 50 mile radius of the plant. The ash is a Type F fly ash.

There is not any specific data for the Harrison Fly Ash sample at hand. Much of work GAI has with particular ash has been environmental so there is little information on the mechanical properties of the ash. When a usability testing program is requested it is usually very basic and an empirical bench testing approach is implemented. The only information obtained on the ash is that most of the fly ash generate at Harrison is being land filled or injected back into the mines.

7.2.1 LPC material

7.2.1.1 Insulated Probe for Use in LPC Material

TDR was tried on LPC to measure both water content and dry density as it is found that the nuclear method gives significant errors in these soils. The TDR signal shows no obvious second reflection point using the field MRP probe due to high conductivity of this material. And thus, an insulated center probe was used in the LPC material to prevent energy loss and get clear TDR reflection signal. When incorporating the insulated center probe, a calibration is needed to account for the insulation effects.

Two different approaches were tried for the calibration process. The first is to adopt empirical approach, which treats the measured K_a by use of the insulated probe just as that measured by plain probes. And thus, calibration can be obtained just as for a normal soil. The calibration shows good linear relationship as indicated by Fig. 7.5 and Fig. 7.6. The calibration constants can then be used to make computation similar to those for plain probes. By using this approach, the soil specific a and b values includes the influence of insulation and thus can not be interpreted as discussed in Chapter 5. So it is not a surprise to learn that the value of a can be zero or even a negative value as shown in these figures.

Application of this approach indicates that for water content within the range used for calibration, the data shows good agreement compared with oven dry results. A problem arises for the situation where water content is very low. In this case, the calculated water content results using the calibration constants could be negative. The plot of data points measured on dry LPC shows a significantly deviation from that predicted by the calibration curve obtained in high moisture content (Fig.7.6). This is an indication that the behavior measured by insulated probe is different at high water content (and thus high conductivity) than that at low water

content (and thus low conductivity) (Fig. 7.8). This is also observed in a previous research by Mojid (2000) in studying the conductivity effects on TDR measurements using insulated center probe. In that study, it is found that insulated probe has different calibration for low conductive material and for high conductive materials.

Based on the different behavior measured on LPC at high versus low water content (conductivity), it is suggested that a single calibration curve can not cover the whole measurement range.

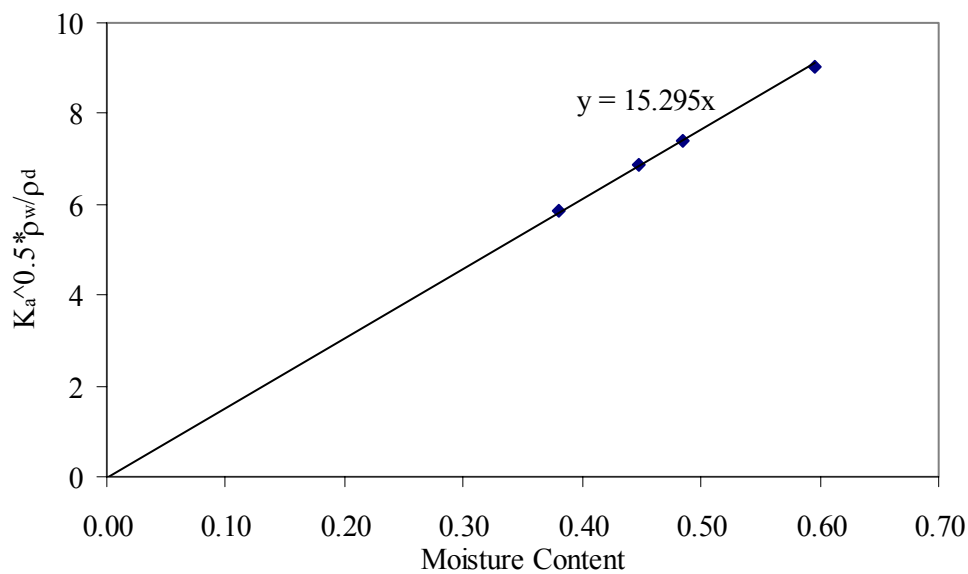


Fig. 7.5 Rostraver LPC *a* and *b* Constants Using an Insulated Probe (performed on Mar 22, 2002)

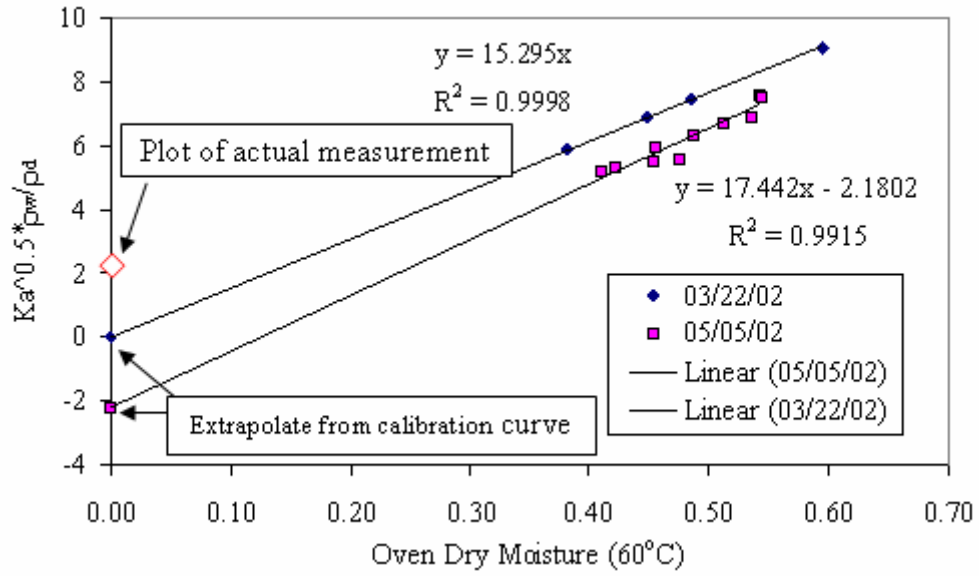


Fig. 7.6 Rostraver LPC a and b constant using insulated probe (performed on Mar 22, and May 05, 2002, respectively)

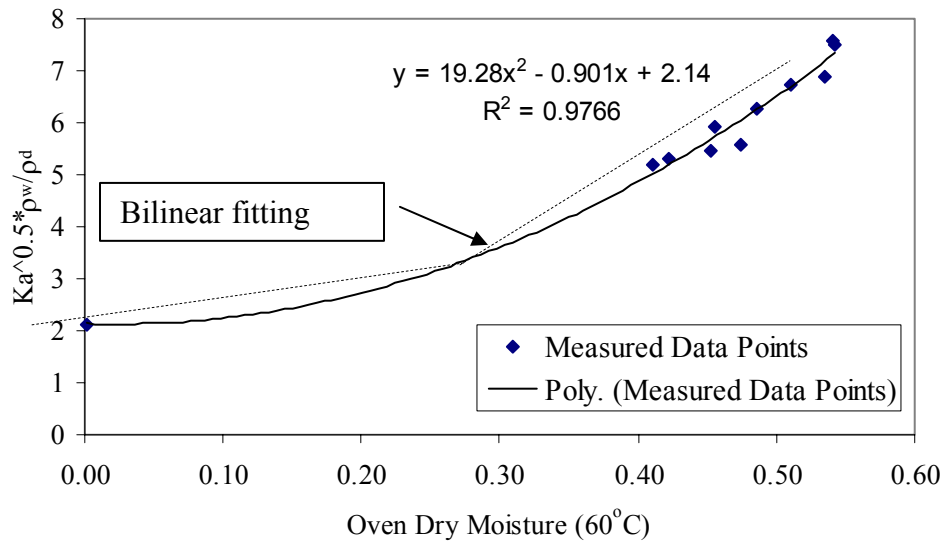


Fig. 7.7 Proposed bilinear calibration curve for LPC material using insulated probe

The second approach to calibration of an insulated probe is to use a more systematic approach. i.e. first calibrate for the insulated probe and convert the measured K_a . The K_a measured by insulated probe is first converted to one that will be measured by plain probe through the use of a calibration equation. The corresponding value measured by the plain probe is then used to calculate water content and density. The details on the theoretical basis and application procedures were discussed in Chapter 5.

Theoretically, this approach has a sound basis compared with the empirical approach discussed above. However, the results by applying this approach on LPC material is not as satisfactory as expected. An example of the calibration obtained by applying the insulated probe calibration equation is shown in Fig. 7.8. Although the calibration constants look more close to those expected for soils, the correlation coefficient is not as high as for regular soils. Several factors caused this behavior:

- a) Calibration materials used for calibration of the insulated probe is clean Ottawa sand; the water content range used for calibration is below 10%. Thus, the calibration might not be good for use in LPC, which has high water contents;
- b) As pointed out before, the insulated probe shows a significantly different response for materials with low conductivity versus material with high conductivity. For LPC, the material has very low conductivity at low water content and high conductivity at high water content (Fig. 7.9). As can be seen in Fig. 7.9, the final voltage level of TDR signal at water content of 0.5% is much higher than that at around 50% water content. This is an indication that the electrical conductivity of LPC at high water content is significantly larger than that at low water content.. And thus the response is believed to be different.

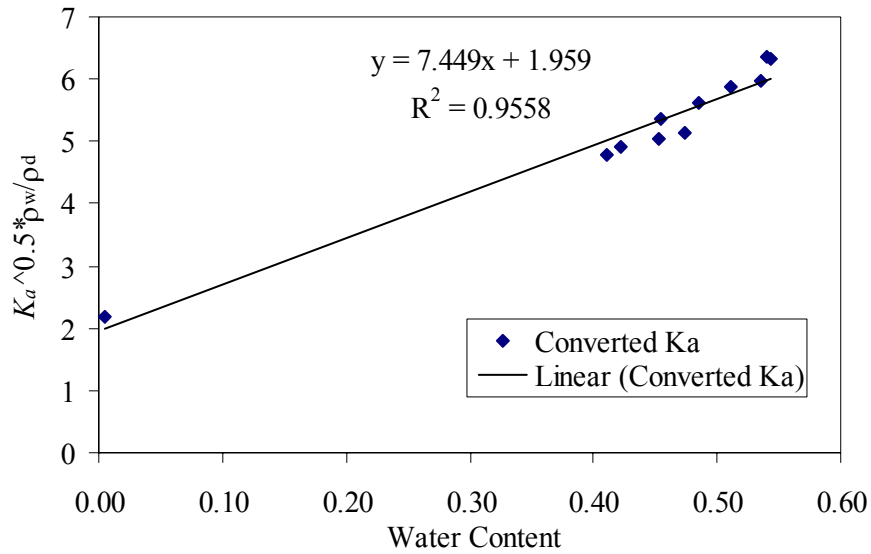


Fig. 7.8 Calibration for a and b using converted soil apparent dielectric constants

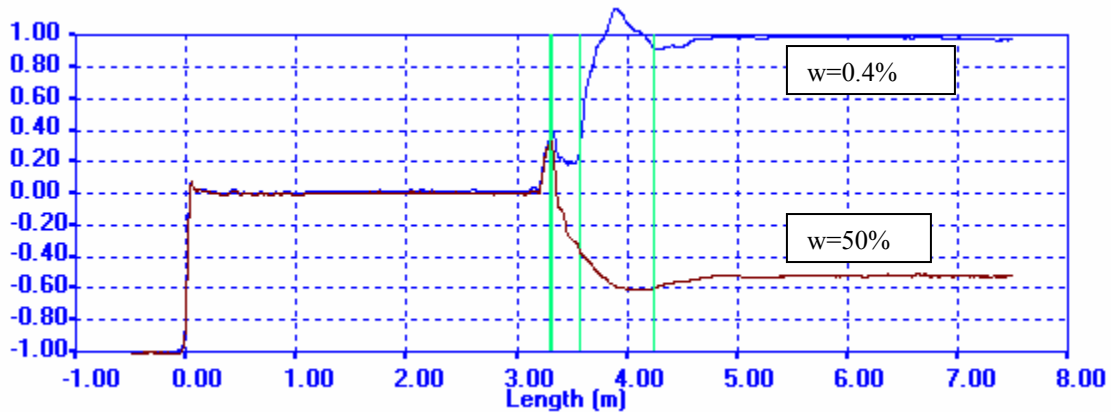


Fig.7.9 Difference in Conductivity of LPC at Low Water Content versus High Water Content

7.2.1.2 Calibration for LPC and Ash Materials Using a Shorter Probe

It was found that for TDR measurements in LPC, reflection points can be identified by using a shorter probe. A probe with total length of 14.6 cm (5.75 in.) and net length in the soil of 11.6 cm (4.57 in.) was used in conjunction with standard compaction mold to make the measurement. As shown in Fig. 7.9, using a short probe in LPC, it is possible to identify the 2nd reflection point and measure material apparent dielectric constant for water content up to around 50%.

LPC samples were prepared at incremental water content of around 5% and compacted into standard compaction mold to obtain compaction curves as well as make TDR measurements. The measured compaction curve is shown in Fig. 7.10, which is different from the compaction curve expected for conventional soil materials. As seen from Fig. 7.10, as water content increases, the dry density of LPC gradually increases. This behavior is characteristic of similar non-conventional materials such as fly ash, bottom ash, etc.

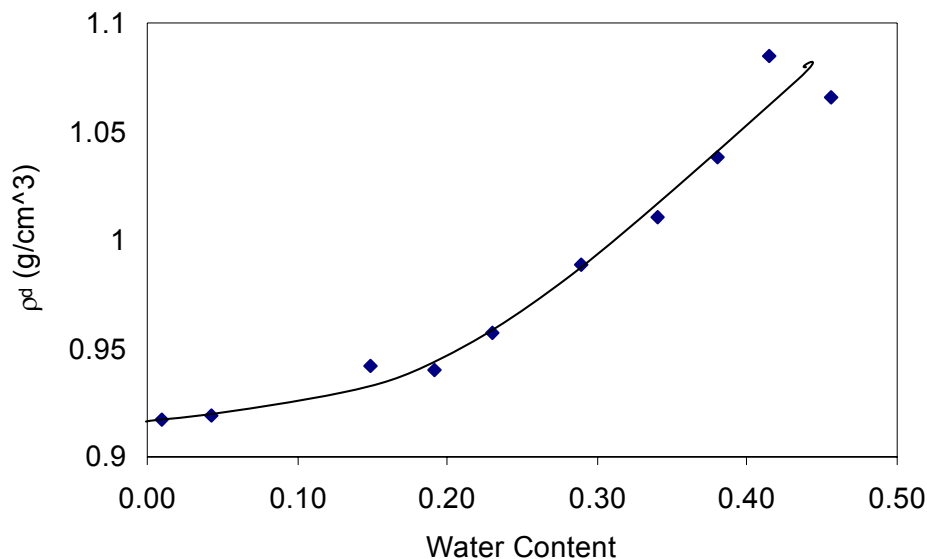


Fig. 7.10 Compaction Curve of LPC

Measured calibration curves of the apparent dielectric constants and bulk electrical conductivities of LPC are shown in Figs. 7.11 and 7.12, respectively. Both of them have relative high correlation coefficients. The calibration for dielectric constant is better than that of bulk electrical conductivity. This is attributed to the possibility of contact problems when making electrical conductivity measurement.

The high correlation coefficient of calibration for dielectric constant using short probe indicates that it is possible to achieve good measurement accuracy in water content and density measurement on LPC material using short plain probes. This is an advantage of TDR technology over the nuclear method in these non-traditional soils, which tend to have large errors in water content determination.

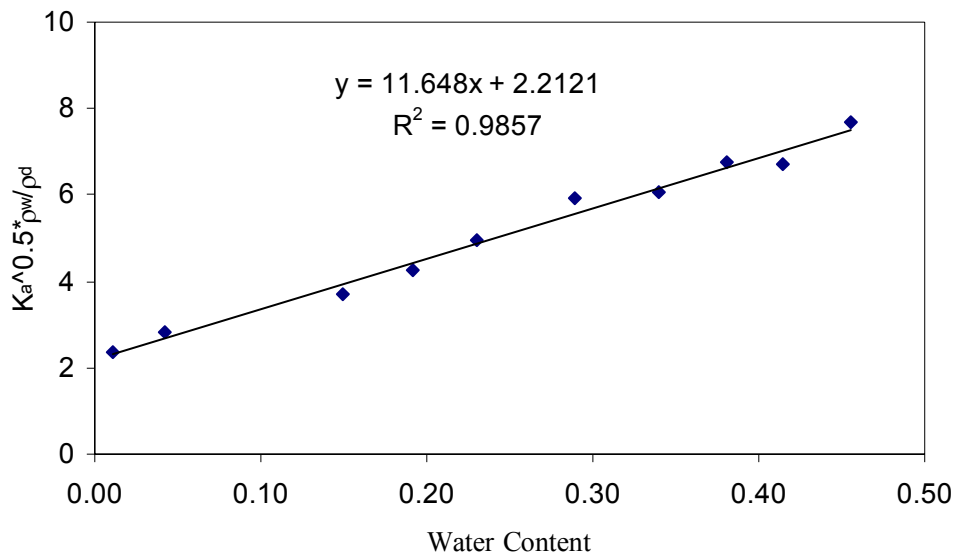


Fig. 7.11 Relationship between Apparent Dielectric Constant and Water Content Using Short Probes in a Standard Compaction Mold

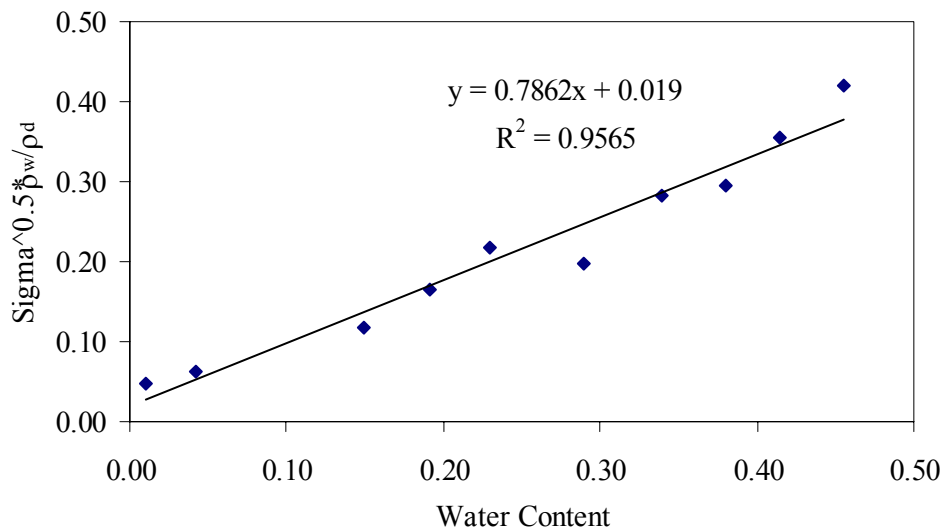


Fig. 7.12 Relationship between Electrical Conductivity and Water Content Using Short Probes in a Standard Compaction Mold

7.2.2 Experiments on Class C Fly Ash

Experiments also were conducted at Purdue on other non-traditional soils including Class C fly ash and bottom ash. (Typical components of Class C and Class F fly ash are listed in table 7-6. For Class C fly ash, it is found that a satisfactory TDR signal can be obtained using a short probe and thus a short probe was used to make TDR measurements. Results indicate that for bottom ash, no second reflection can be identified even using short probes. Thus, insulated probes have to be used for this material.

Table 7-6 Typical compositions of Class F and Class C ashes as defined by ASTM (1997).

Parameter	Class F	Class C
SiO ₂	54.90%	39.90%
Al ₂ O ₃	25.80%	16.70%
Fe ₂ O ₃	6.90%	5.80%
CaO	8.70%	24.30%
SO ₃	0.60%	3.30%
Moisture content	0.30%	0.90%
Loss on Ignition (LOI)(@750C)	2.80%	0.50%
Available alkalis as Na ₂ O	0.50%	0.70%
Specific gravity	2.34	2.67
fineness, retained on #325 mesh sieve	14%	8%

An effort was made to identify the causes of the high electrical conductivity in ash materials. Both tap water and deionized water were used in TDR measurements. The compaction curves of Class C fly ash using deionized water and tap water with standard

compaction energy are shown in Fig. 7.13. The shapes of compaction curves are close to each other, while the fly ash with tap water has slightly lower dry densities compared with that using deionized water.

Calibration curves for apparent dielectric constant and bulk electrical conductivity are shown in Fig. 7.14 and Fig. 7.15 respectively. From Fig. 7.14, it seems that the type of pore fluid does not have discernable effects on calibration of apparent dielectric constant. From Fig. 7.15, the calibrations for electrical conductivity are also close, while the calibration using tap water has relatively higher correlation coefficients. This is attributed the fact that the fly ash particles have high conductivity compared to the conductivity of water.

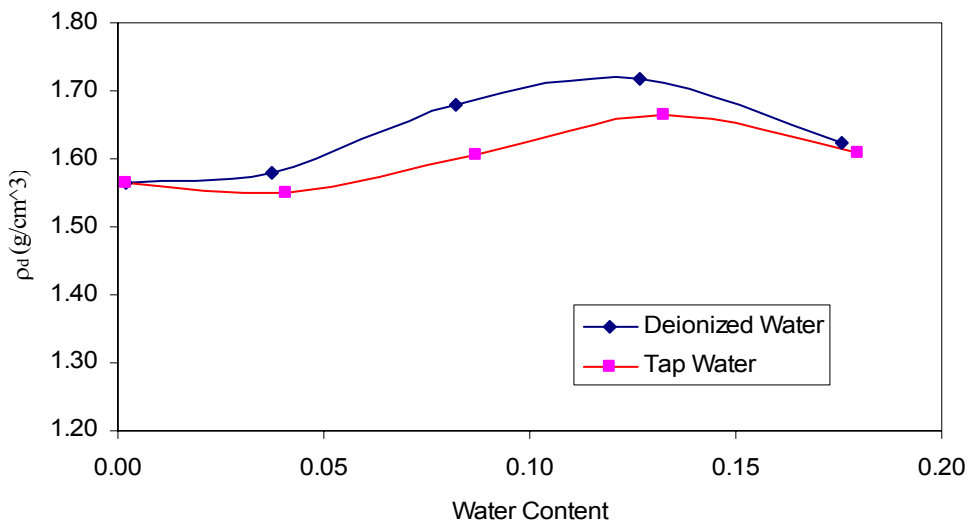


Fig. 7.13 Compaction Behavior of Class C Fly Ash Using Tap Water and Deionized Water

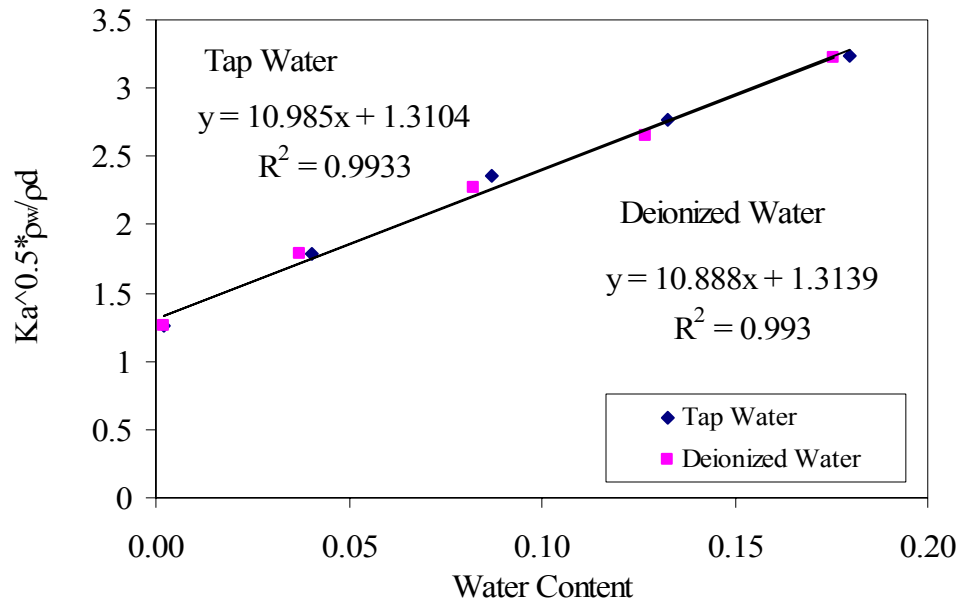


Fig. 7.14 Fly Ash Apparent Dielectric Constant Calibrations Using Tap and Deionized Water

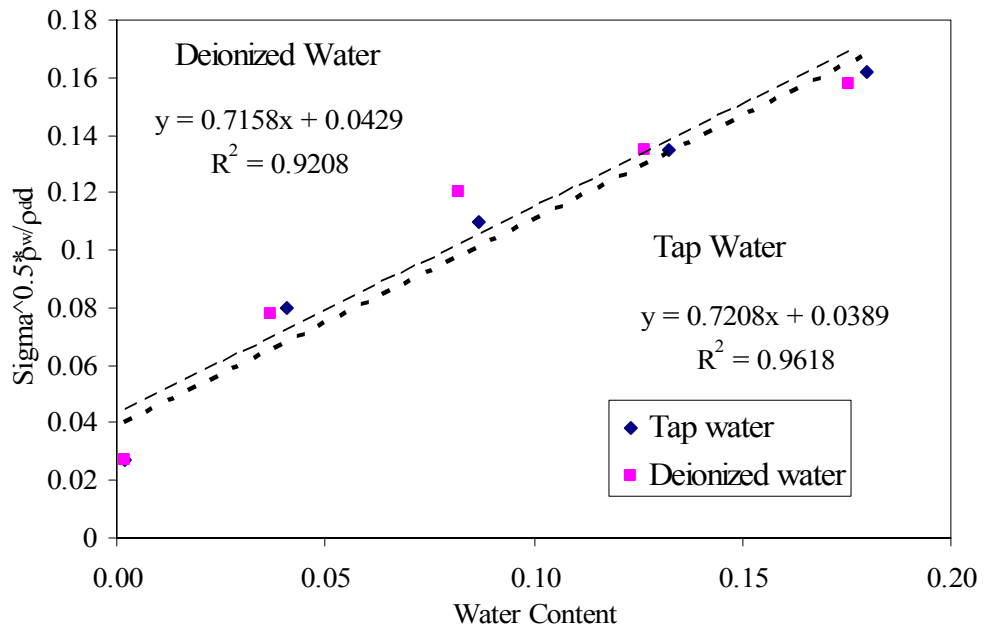


Fig. 7.15 Fly Ash Bulk Electrical Conductivity Calibrations Using Tap and Deionized Water

The high correlation coefficient in calibrations is an indication that TDR technology could attain good accuracy for water content and dry density measurement in Class C fly ash used in these tests.

7.2.3 Experiments on Harrison Fly Ash

Another group of tests were performed on Harrison Fly Ash using a plain probe. The calibration curve obtained on Harrison fly ash is shown in Fig. 7.16. The high value of correlation coefficient indicates that TDR technology gives good accuracy in testing this material. Results of dry density and water content determined by TDR compared with oven dry results are shown in Figs. 7.17 and 7.18, respectively. From the figures, water content generally falls within ± 0.01 of oven dry results while dry density is within ± 1 pcf of the density calculated by total density and oven dry water content.

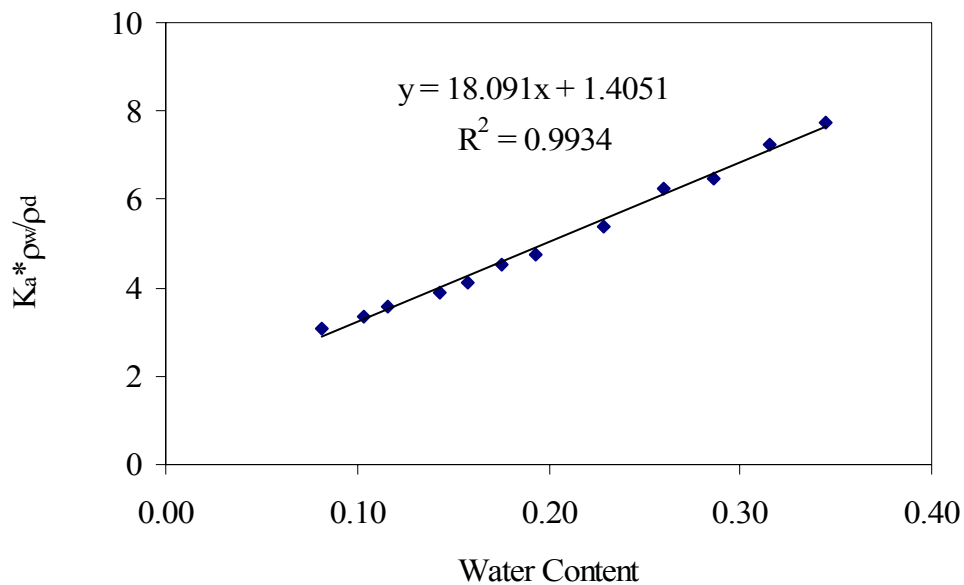


Fig. 7.16 Calibration Curve of Harrison Fly Ash

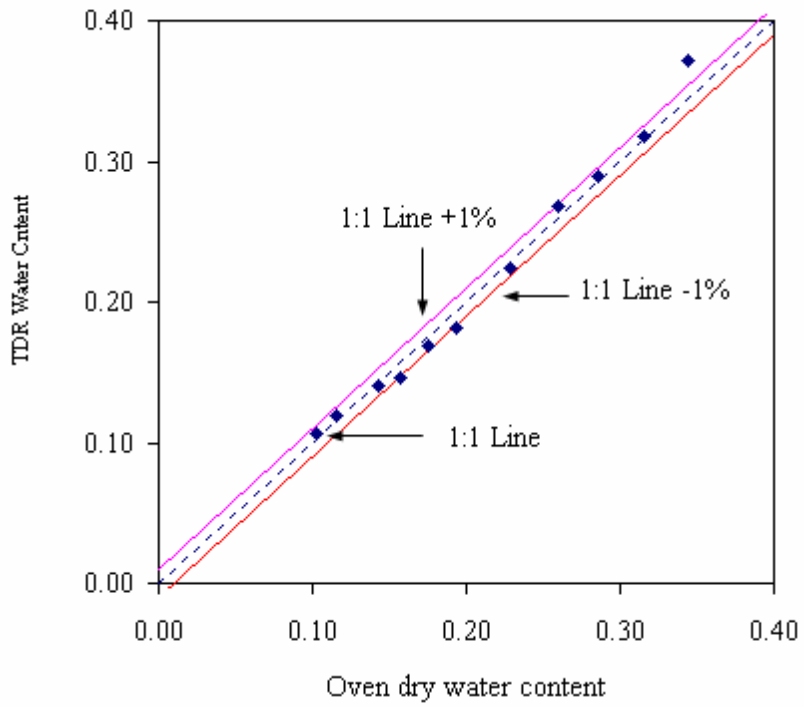


Fig. 7.17 TDR Water Content versus Oven Dry Water Content

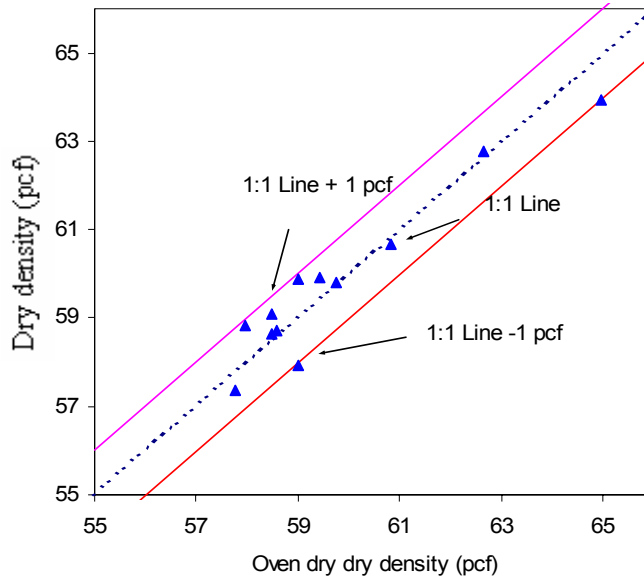


Fig. 7.18 TDR Dry Density versus Dry Density Calculated by Total Density and Oven Dry Water Content

7.2.4 Conclusions

Feedback, interaction, and data interchange with GAI Consultants, Inc. indicates that TDR can be used for quality control of non-traditional soils such as LPC and fly ash.

A short probe can be used to reduce energy loss and make valid TDR measurements on most of these materials. For materials with very high conductivities, the second reflection point can not be identified even with a short probe. In these cases, insulated probes can be used. Two approaches can be used for reducing data obtained by use of insulated probes. The first approach is an empirical approach which treats the dielectric constant measured by insulated probe just as that measured by conventional probe. Using this approach, the calibration constants obtained should be only applied for situations where the water content falls within the water content used for obtaining these calibration constants. Other water content range-dependent calibrations might need to be set up to cover the whole range.

Another approach to the calibration of insulated probes is more sophisticated. First, calibrate the insulated probes against plain probes. Then convert the dielectric constant measured by insulated probe to equivalent dielectric constant measured by plain probe using the calibration constants obtained. With the equivalent dielectric constant at hand, the remaining procedures are the same as that for a plain probe. To obtain good accuracy, attention needs to be paid to issues such as selection of calibration materials and properties of the high conductive materials under low and high water contents.

7.3 INDOT Sites

In support of INDOT Division of Research and INDOT Division of Materials and Tests, the Purdue TDR team carried out field tests at some of INDOT's construction sites. Part of the tests were conducted in conjunction with the added and heavily instrumented lane at the Division of Research site in West Lafayette. TDR tests were performed along side nuclear moisture/density tests performed by Alt and Witzig. This information provided a comparison to evaluate the accuracy of the TDR method and also helped to improve the TDR testing procedures.

In late January, 2003, the Purdue TDR research team was called upon by the Division of Materials and Tests working with the Greenfield District to assist with quality control problems at the I-70 relocation, measuring soil water content and dry density in lime stabilized soils. The INDOT personnel found that results by nuclear tests on these soils were not giving satisfactory results, especially for water content determination. The Purdue TDR method was tried at this site and preliminary results were deemed satisfactory.

7.3.1 INDOT Division of Research

TDR apparatus was used in the compaction quality control of compacted Subgrade soils and the base course of a new lane of test pavement constructed in the Fall of 2002 at the INDOT Division of Research. The subbase was silty clay glacial till and the pavement base material was made of crushed limestone Indiana 53's.

For the glacial till, standard compaction tests in conjunction with TDR calibration tests were performed to obtain TDR calibration constants. Both tap water and deionized water were used in the calibration process to study the influence of fluid type on calibration. The results are compared in Fig. 7.19. Compaction using deionized water creates a slightly higher optimum water content and lower maximum dry density compared with that using tap water.

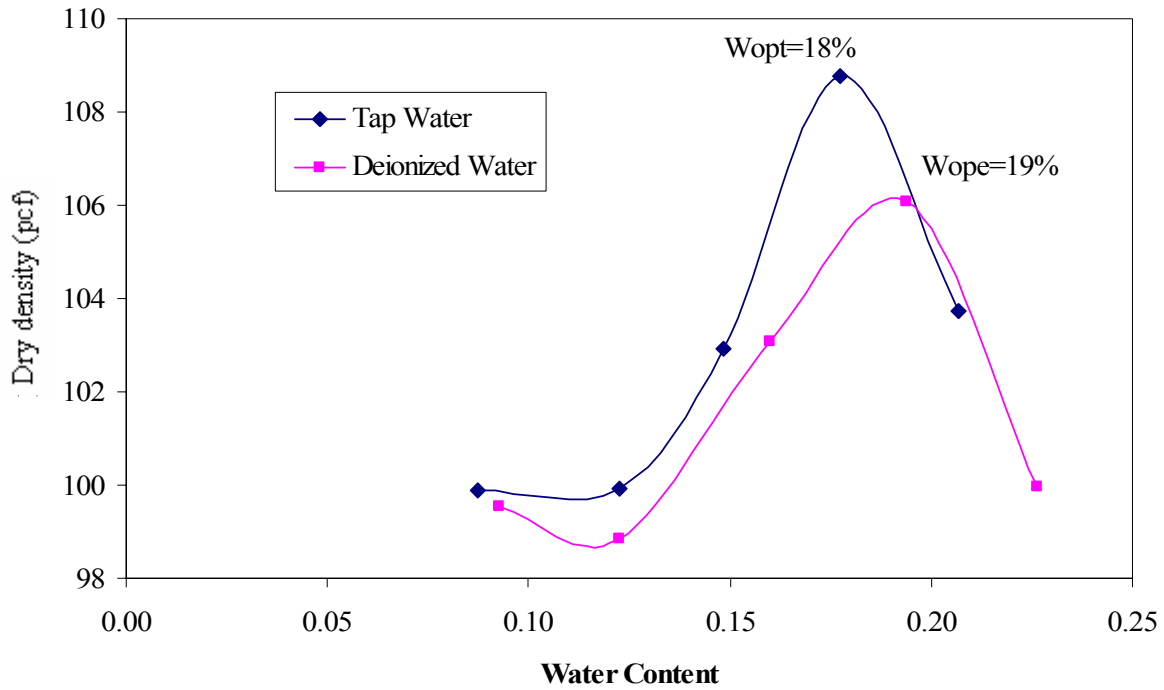


Fig. 7.19 Standard Compaction Curves of Glacial Till Subgrade Using Tap and Deionized Water for the INDOT, Div. of Research Test Pavement Site

TDR calibration curves for the glacial till with tap water and deionized water are shown in Fig. 7.20. From the figure we can see, the calibration curves for different pore fluids are close to each other and all data points essentially falls on the same line. There are no significant effects of pore fluids on the calibration constants for apparent dielectric constant.

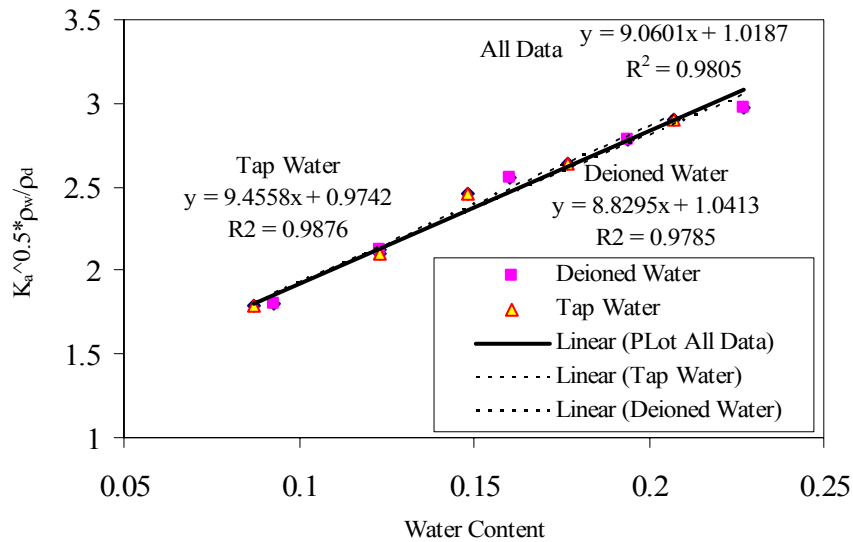


Fig. 7.20 Calibration Curves of Glacial Till using Tap and Deionized Water

The calibration constants obtained were used in field measurement to calculate soil water content and dry density and compared against the results by nuclear tests. The test program was carried out after the glacial till layer was compacted. To facilitate comparison, TDR tests were performed side by side with the nuclear tests at 14 locations. In several locations, soil samples were taken back to the lab to determine oven dry water contents. Results of water content and dry density comparisons are shown in Figs. 7.21 and 7.22, respectively. In both of these figures, TDR measured water content and dry density show similar trends to those from nuclear tests with locations along the pavement length. From Fig. 7.21, TDR measured water content seems to be closer to oven dry water content compared with nuclear results; while from Fig. 7.22, TDR measured dry density seems to be show less variation compared with nuclear results. The results measured by TDR seem to be more consistent with actual field condition considering the fact that the compaction of this layer was finished and thus the field density should be relatively consistent.

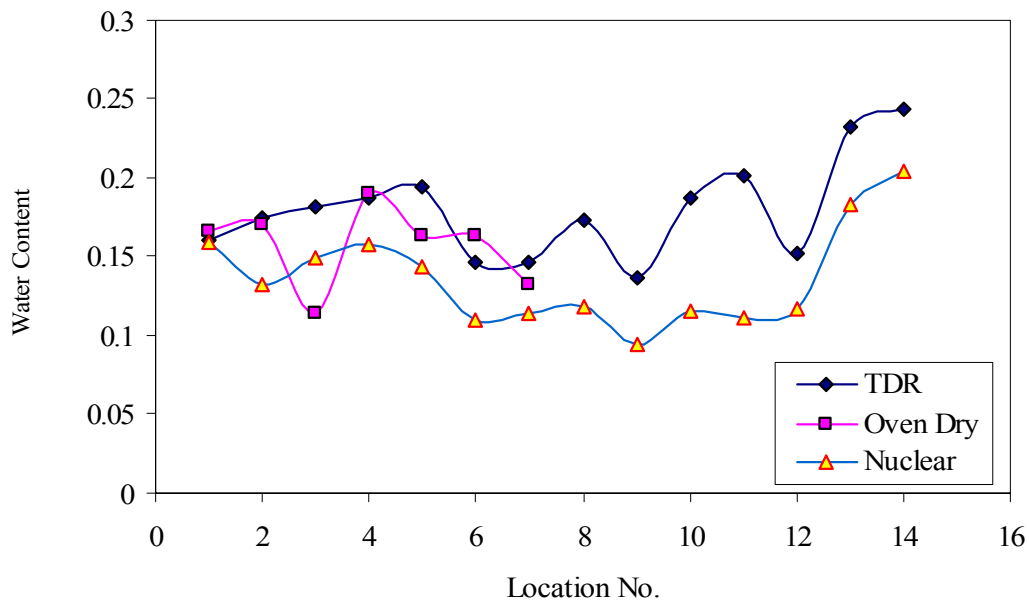


Fig. 7.21 Water Content versus Location by TDR, Nuclear and Oven Drying at INDOT Div. of Research Test Lane Site (Location 0 is on the East End of the Site.)

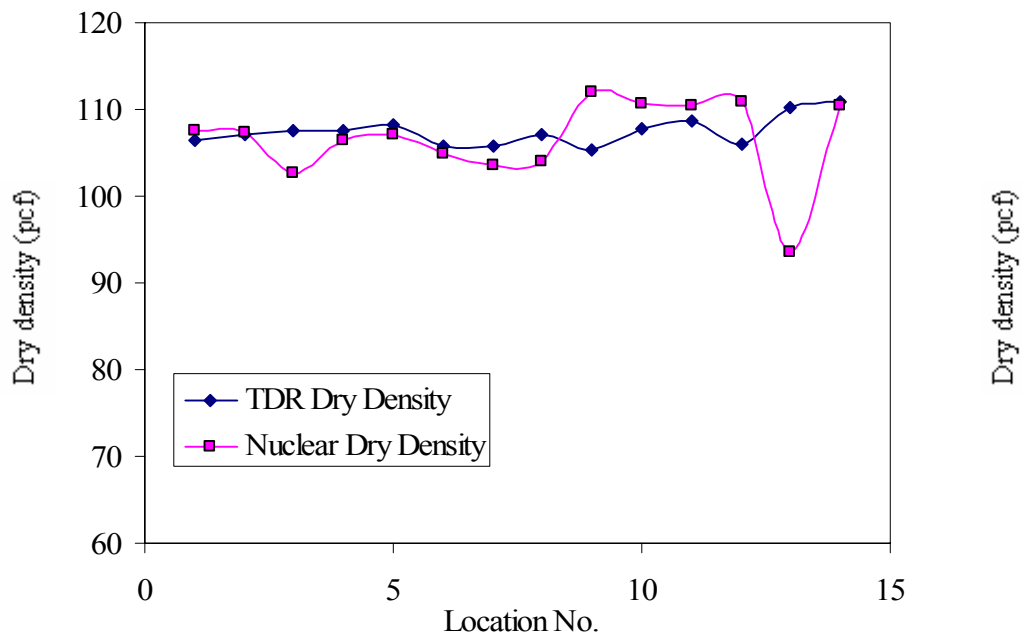


Fig. 7.22 Dry Density versus Location by TDR and Nuclear Method at INDOT Div. of Research Test Lane Site (Location 0 is on the East End of the Site.)

After the layer of glacial till was compacted, a base layer of **Indiana 53** was placed and compacted at this site. A sample was taken to the Purdue labs and compaction tests were performed using a standard compaction mold to obtain calibration constants. On the compaction curve (Fig. 7.23), dry density shows a gradual increase with increasing water content, which confirms the field observation that for this coarse-grained material, more compaction can be achieved at larger water contents.

As can be seen from Figs. 7.24, 7.25, and 7.26, calibrations for apparent dielectric constant and bulk electrical conductivity show good correlation coefficients, which is an indication that TDR can achieve good accuracy in testing this material. This was confirmed by field measurement results as shown in Fig. 7.27.

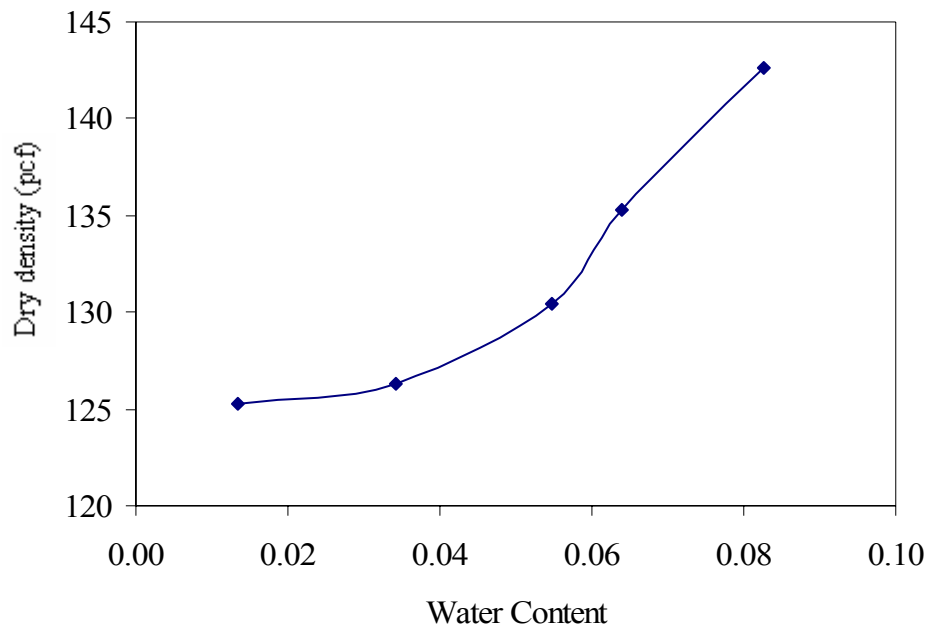


Fig. 7.23 Compaction Curve of Indiana 53 Used at INDOT, Div of Research Test Pavement Site

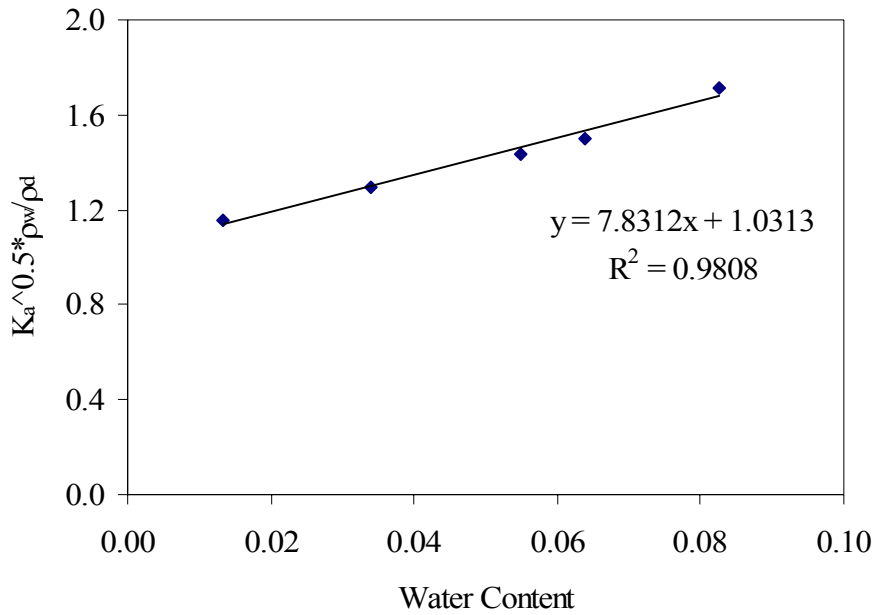


Fig. 7.24 Calibration of Apparent Dielectric Constant for Indiana 53 Used at INDOT, Div of Research Test Pavement Site

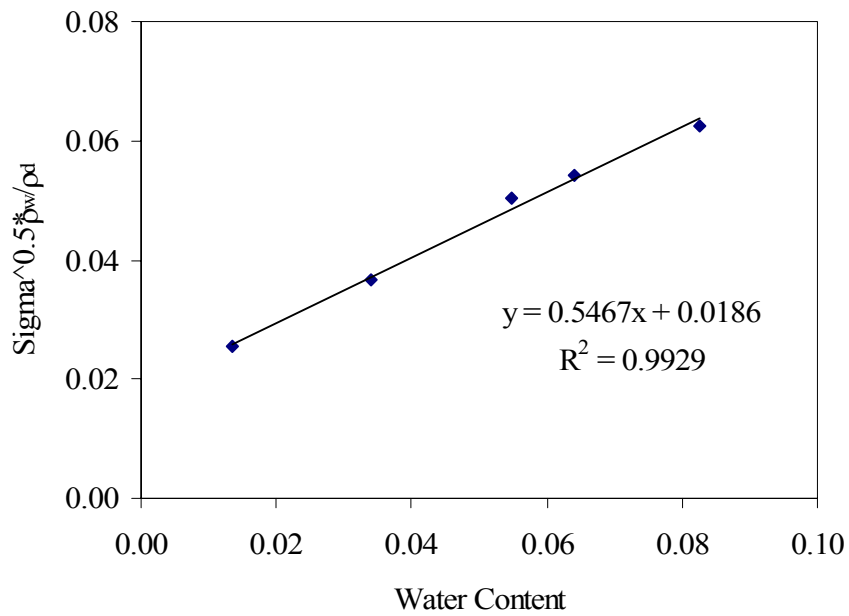


Fig. 7.25 Calibration of Bulk Electrical Conductivity for Indiana 53 Used at INDOT, Div of Research Test Pavement Site

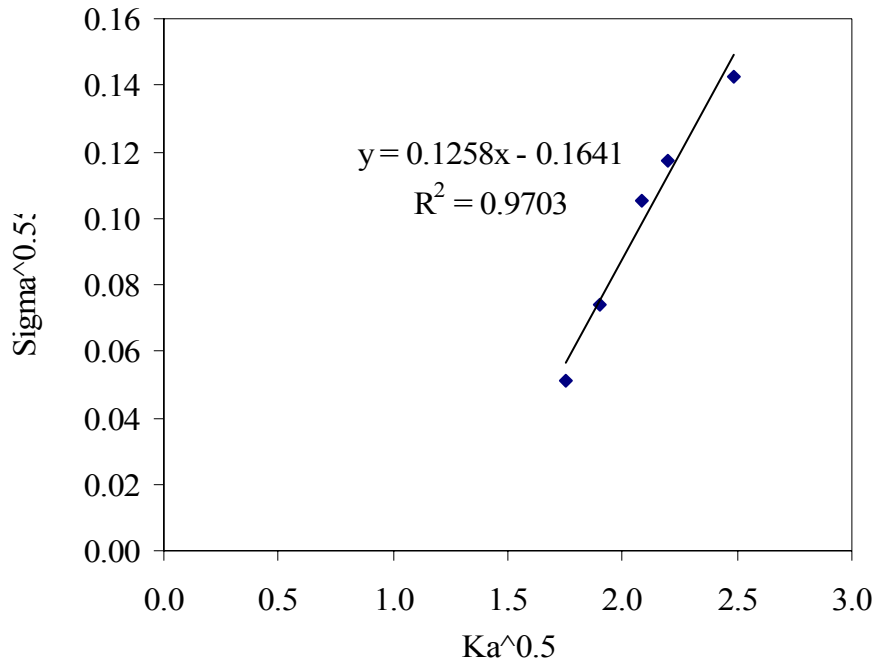


Fig. 7.26 Relationship between Apparent Dielectric Constant and Bulk Electrical Conductivity for Indiana 53 Used at INDOT, Div of Research Test Pavement Site

Results of using these calibration constants are shown in Fig. 7.27. Points denoted as “TDR” are the calculated results using all 5 data points obtained from laboratory calibration tests, while the points denoted as “4 point Cali” is the results using calibration constants obtained by using only the first 4 calibration points with relative lower water content (Fig. 7.28). As can be seen from Fig. 7.27, water content results follow the oven dry results, but the results using the 4 point calibration constants are closer to the moisture content determined by oven drying. The practical implication of this observation is that in the field application, the water content used for calibration should cover the field moisture range to achieve the best measurement accuracy.

In the study on INDIANA 53’s, it was discovered that although the water content measured by TDR is close to that measured by nuclear method. The dry density, however, is underestimated by TDR compared with nuclear results. This is attributed to the insufficient

compaction of Indiana 53 in the standard compaction mold in calibration tests. Mostly this is due to the relatively small diameter of compaction mold compared with the large particles of Indiana 53. The test was not in compliance with the specifications for particle size for ASTM D698. Based on these observations, it is recommended that a mold with larger diameter (such as 6 inch diameter mold) be used to perform the calibration tests.

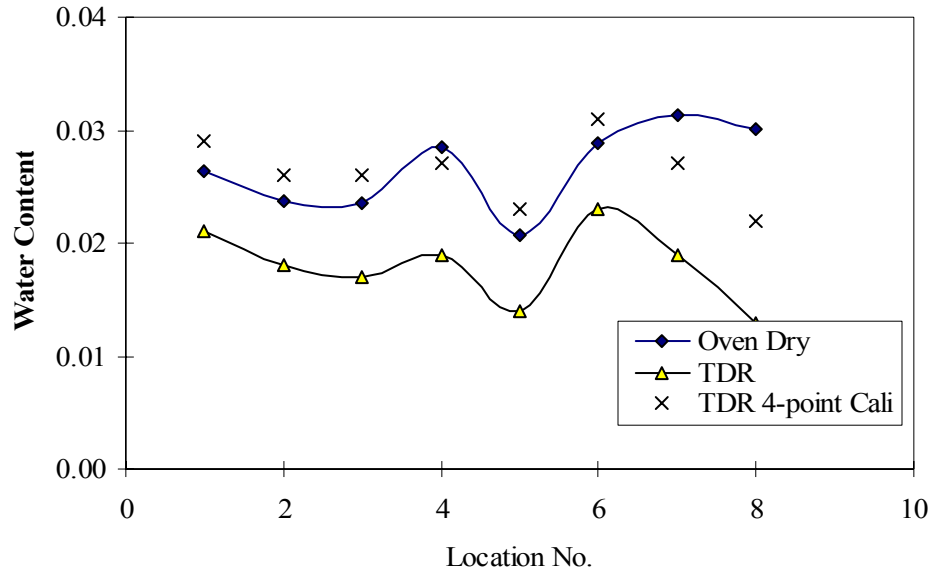


Fig. 7.27 TDR Measured Water Contents and Oven Dry Water Contents at INDOT Div. of Research Test Lane Site (Location 0 is on the East End of the Site.)

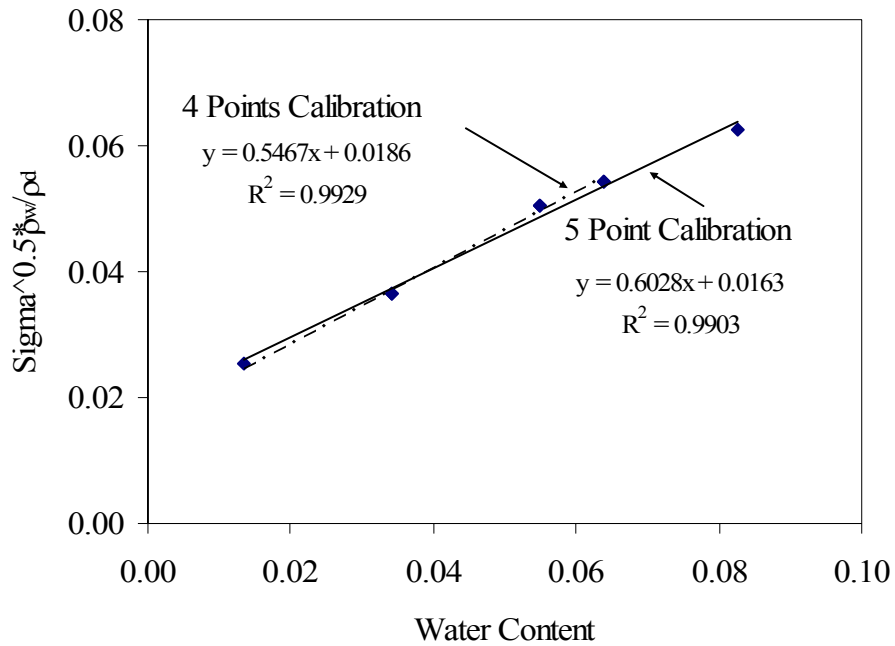


Fig. 7.28 Calibrations for Apparent Dielectric Constant Using All Five Data Points versus only Using First Four Points

7.3.2 I-70 Relocation Project near Indianapolis Airport

TDR technology was used by INDOT at the I-70 Relocation Project, where it was found that the nuclear method did not give good results for water contents. This was attributed to the fact that lime was used to treat the silty clay borrow soils at this site before they were compacted. Based on successful applications of TDR for LPC and fly ash materials, the TDR should work for these lime stabilized soils. The question to be answered was: how did the lime concentration affect TDR measurement results? A related question is: how to account for hydration process in lime stabilized soil? These questions needed to be addressed before the technology can be used with confidence.

Soil was sampled from the testing site, including virgin soil and lime stabilized soil. For lime stabilized soil, the percentage of lime used to stabilize soils ranged between 3%~6%.

TDR calibration tests were performed on the representative samples in conjunction with standard compaction tests. The standard compaction curves are shown in Fig. 7.29, the lime

stabilized soil has a larger optimum water content and lower dry density compared with the virgin soil. The calibration data for apparent dielectric constant for virgin soil and lime stabilized soil are shown in Fig. 7.30 where the calibration data points for virgin soil and lime stabilized soil locate approximately the same calibration line. This is an indication that the calibration constants a and b of apparent dielectric constant are insensitive of lime concentration.

On the other hand, as shown in Fig. 7.31, the calibration for bulk electrical conductivity, is strongly dependent on lime concentration. Where the lime concentration is just 3%~6%. The high sensitivity of calibration for bulk soil electrical conductivity also indicates that TDR is a potentially useful tool for monitoring lime concentration.

A monitoring function was developed and integrated into the PMTDR-SM program discussed in Chapter 4. The program was then used to monitor lime hydration process. Lime stabilized soil was first compacted into standard compaction using standard compaction energy. The central rod was installed and MRP head was seated on the adaptor ring. The automatic monitoring function of the computer program was activated to make continuous measurements at fixed intervals of time. The monitoring results are shown in Fig. 7.32. From Fig. 7.32, we can see the following phenomena:

- 1) Soil apparent dielectric constant is independent of lime hydration process;
- 2) Bulk soil electrical conductivity shows slightly decrease at the initial stage, which is indication of hydration process;
- 3) Bulk soil electrical conductivity stabilized in certain amount of time (about 8 hours in this case), which possibly indicates the end of hydration process.

The ability of TDR to discern these phenomena in lime stabilized soil makes TDR a potential useful tool for study of lime stabilized soil.

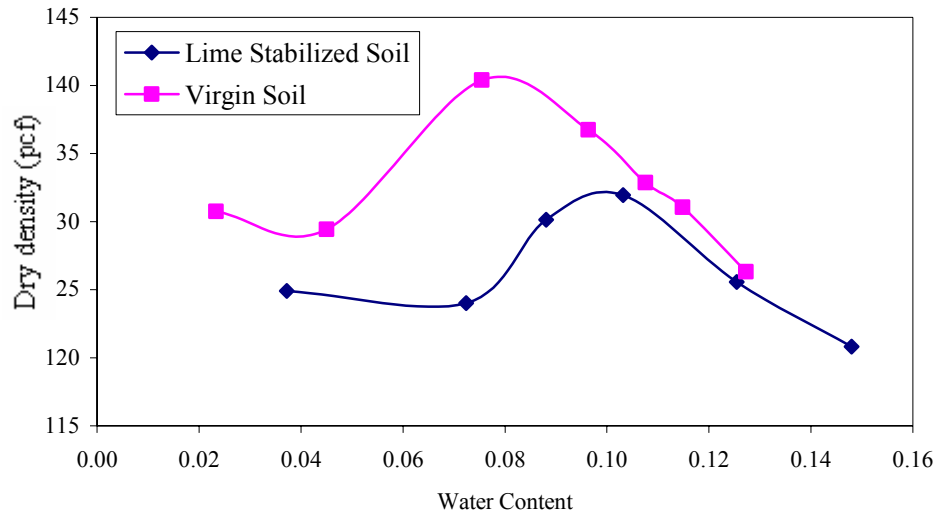


Fig. 7.29 Standard Compaction Curves for Virgin Soil and Lime Stabilized Soil (around 3~6% lime) for INDOT I-70 Relocation Site

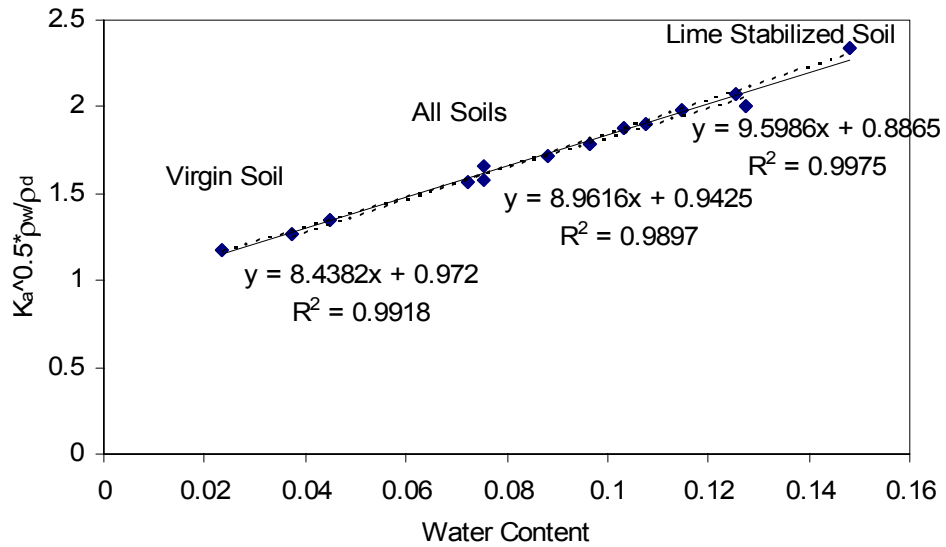


Fig. 7.30 Calibration Factor Determination for Apparent Dielectric Constant for INDOT I-70 Relocation Site

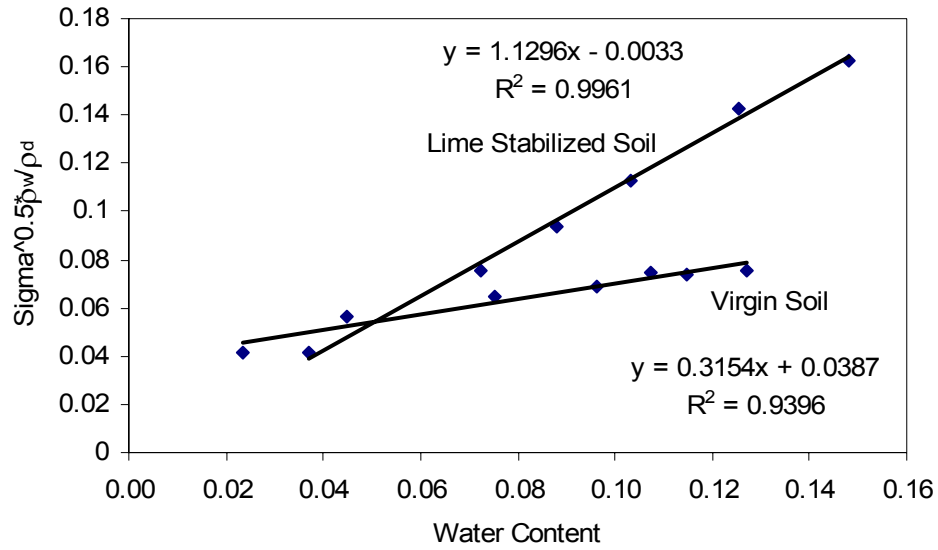


Fig. 7.31 Calibration for Bulk Electrical Conductivity for Soil from INDOT I-70 Relocation Site

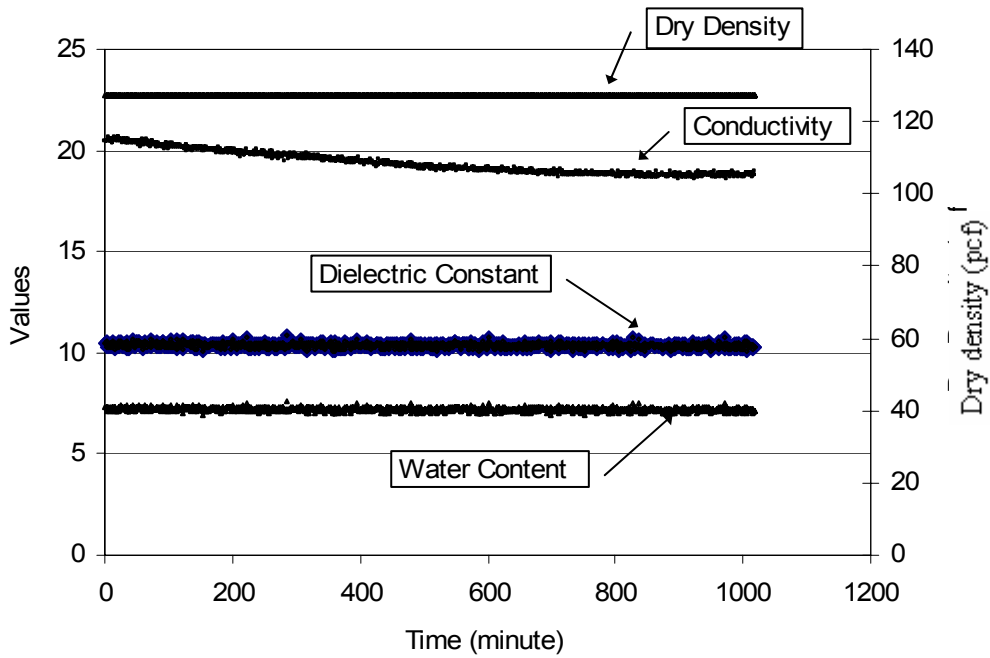


Fig. 7.32 Monitoring of Lime Hydration Process for Soil from INDOT I-70 Relocation Site

Additional calibrations for apparent dielectric constant were performed by technicians at INDOT I-70 field office, data points from these calibrations are put together on a single plot as

shown in Fig. 7.33, which has a good correlation coefficient. Based on the calibration data, calibration constants of $a = 0.89$ and $b = 9.60$ was recommended for use at this site.

Although the material types were not necessarily the same, the plot indicates that a “single” calibration constant might be applicable to measurement of similar materials in the field situations. This is an important observation made for field applications. The implication is that for certain projects or construction region, a project specific or regional specific calibration might be applied. This could save time and reduce the cost for repeated calibration efforts. It is a similar conclusion to that found for the sand soils in the State of Florida that were described earlier in this chapter.

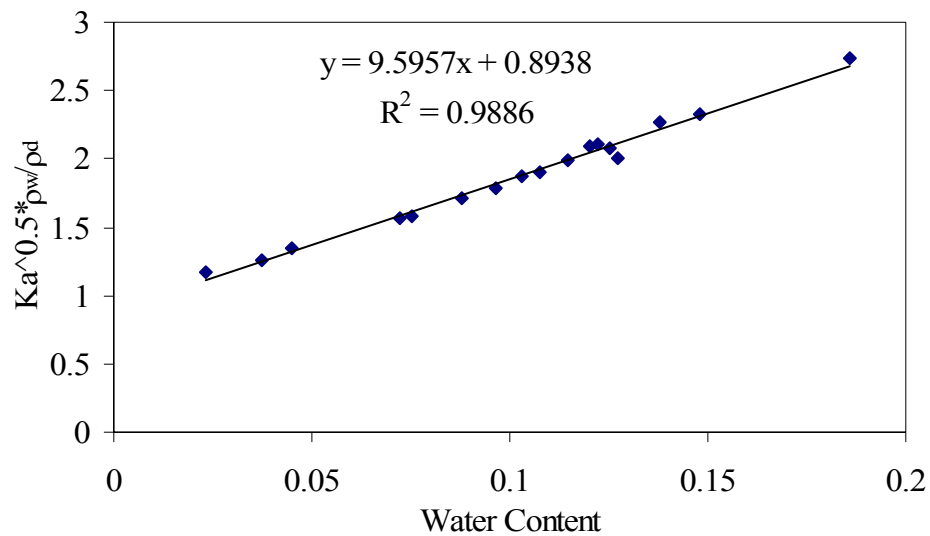


Fig. 7.33 Calibration of Apparent Dielectric Constant for Soils at the INDOT I-70 Site

Based on laboratory observation, a site specific application procedure was designed for the INDOT I-70 site for use with the lime stabilized soil. Field testing results compared with nuclear density and stove-top-cooked water contents (approximately following ASTM D????) are shown in Table 7-7. TDR measures both soil water content and dry density, while only the nuclear measurements for total density were used. The dry density was determined using nuclear total density and stove-top-cooked water content. As can be seen from the table, satisfactory

results are achieved using TDR compared with nuclear total density combined with the stove-top-cooked water contents.

Table 7-7 TDR Measured Water Content, Dry Density versus Results by Nuclear Total Density and Stove-Top-Cooked Water Contents for INDOT I-70 Soils

Total Density (pcf)		Dry Density (pcf)		Water Content		
Nuclear	TDR	Nuclear	TDR	Oven Dry	Nuclear	TDR
134.6	138.0	116.5	120.7	0.165	0.155	0.143
136.8	137.8	120.7	120.6	0.165	0.134	0.143
130.6	138.6	115.3	121.4	0.165	0.134	0.142
134.0	138.1	117.5	120.9	0.165	0.141	0.143
128.2	133.3	114.1	118.2	0.135	0.124	0.128
129.7	128.4	115.2	113.9	0.135	0.125	0.127
128.9	124.4	114.8	110.4	0.135	0.123	0.127
128.9	128.7	114.7	114.2	0.135	0.124	0.127
128.7	128.9	114.0	112.5	0.159	0.129	0.146
126.4	123.0	111.6	107.3	0.159	0.132	0.146
121.3	121.4	105.4	105.8	0.159	0.152	0.147
125.5	124.4	110.3	108.5	0.159	0.138	0.146

7.3.3 Summary of Findings from INDOT

Purdue TDR method can be applied for both cohesive soil and cohesionless soil and achieve satisfactory results. For cohesionless soil with large particles, mold with larger volumes must be used in calibration tests just as they must be used in regular compaction tests. The range

of water contents used for calibration should cover the range of expected field water contents to achieve better measurement accuracy.

Calibration constants for apparent dielectric constant are independent of lime concentration for lime content in 3%~6%. The bulk electrical conductivity as measured by TDR can be used to indicate lime hydration process. This makes TDR a useful tool for those non-conventional materials. Preliminary applications of TDR on these materials are satisfactory. Further research efforts are needed to refine the scheme of application.

7.4 H.C. Nutting Company

TDR tests were performed by H.C. Nutting Company on three projects. One project involved an ash material called Maxwell Silo ash, one involved a clayey soil called Brown County clay and one project is an airport site compaction project.

7.4.1 Maxwell Silo Ash

Calibration of Maxwell Silo Ash performed by H.C. Nutting is shown in Fig. 7.34. Results of measurement in the field using PMTDR program (refer to Chapter 4 for details on PMTDR program) are shown in Table 7-8. It can be seen from the table that the results at testing site No.3 are inconsistent with expected values. So the data was reanalyzed using PMTDR-RDR program. It was identified that the program PMTDR written by Campbell Scientific contained some errors. Recalculated results are shown in Tables 7-9 and Fig. 7.35. The results of both water content and dry density are promising. It is also identified that the inconsistent results on test No.3 are due to the abnormal signal (Fig. 7.36), which was possibly caused by poor contact between the probe head and the probe rods.

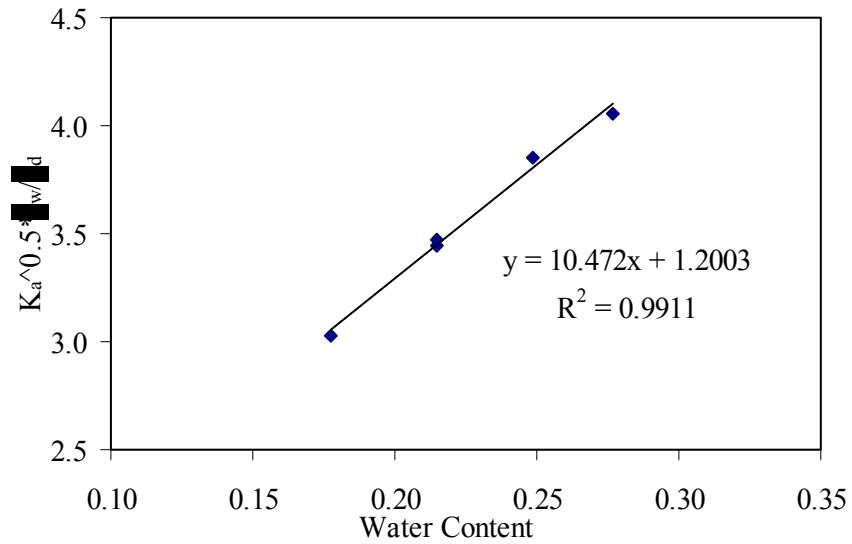


Fig. 7.34 Calibration of Maxwell Silo Ash

Table 7-8 Maxwell Silo Ash Data from HCN with PMTDR

(Note: Nuclear dry unit weight is calculated by nuclear total unit weight and oven dry water content)

Test No.	Dry Unit Weight (pcf)		Water Content			Total Unit Weight (pcf)
	Nuclear	TDR	Nuclear	TDR	Oven-Dry	Nuclear
1	78.1	94.8	18.8	21.3	22.6	95.8
2	70.9	71.5	20.8	26.6	24.9	88.6
3	76.6	8.7	19.1	11.2	23.6	94.7
4	73.8	72.8	20.3	26.0	23.4	91.1

Table 7-9. Maxwell Silo Ash Data Reanalyzed with PMTDR-RDR

(Note: Nuclear dry density is calculated by nuclear total density and oven dry water content)

Test No.	Dry Unit Weight (pcf)		Water Content			Total Unit Weight (pcf)	Total Unit Weight (pcf)
	Nuclear	TDR	Nuclear	TDR	Oven-Dry	TDR	Nuclear
1	78.1	81.3	18.8	21.2	22.6	99.7	95.8
2	70.9	71.5	20.8	26.6	24.9	89.3	88.6
3	76.6	*	19.1	*	23.6	*	94.7
4	73.8	74.4	20.3	25.2	23.4	91.8	91.1

* Abnormal data due to abnormal TDR signal (see Fig. 7.36)

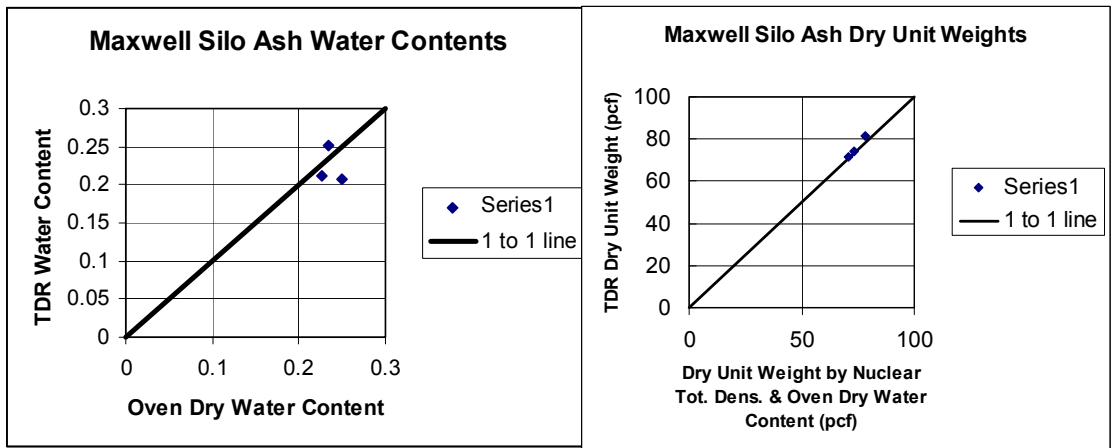


Fig. 7.35 TDR Measured Water Content and Dry Density of Maxwell Silo Ash

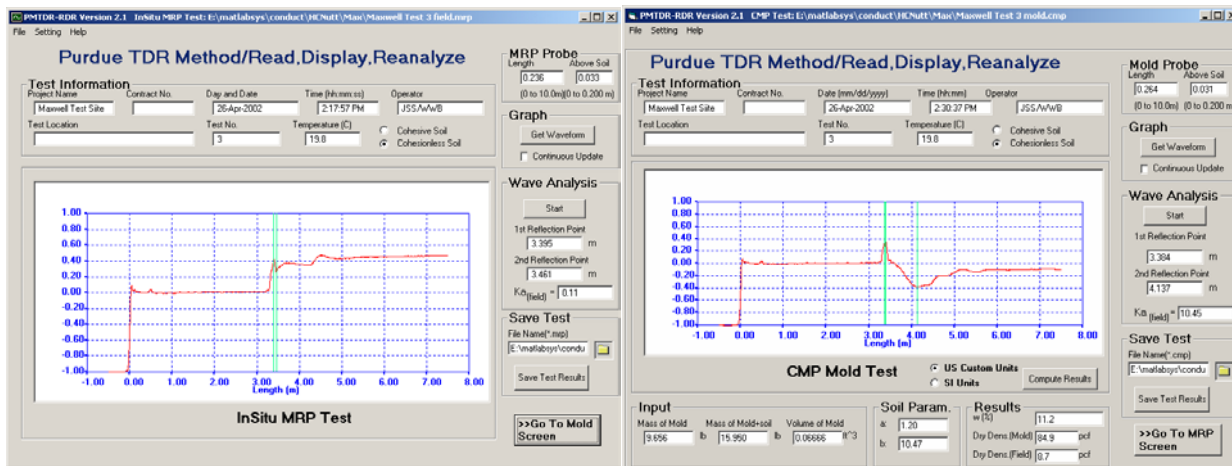


Fig. 7.36 Screen Dumps of the TDR Data for Test 3 on Maxwell Silo Ash

The good accuracy of results on this Maxwell Silo Ash by TDR further validated that TDR is a promising compaction quality control tool for these non-conventional materials.

7.4.2 Airport Site

At this site, H.C. Nutting made field measurements with the TDR apparatus using the program PMTDR-SM, the one-step method program. No tests were made in the TDR compaction mold, but buckets of soil and sealed bag samples of soil were obtained for each of the five test locations. Two of the buckets (Locations 3 and 8) and five of the bags were brought to Purdue for testing. Water contents were determined from the sealed bag samples by oven drying. They are given in column 2 of Table 7-12.

Nuclear test and driven cylinder tests were also performed by H.C. Nutting at 40 locations. It was found that except for 8 locations, the total densities by nuclear tests were significantly smaller than the results by driving cylinder tests. Detailed cause of this discrepancy is still under investigation.

The air-dried soils in the two buckets were combined, processed, and then compacted at different water contents with Modified Compaction energy following ASTM D1557 procedures. On each compacted specimen after weighing, a center rod was inserted and a TDR test was performed in the mold. The program PMTDR-SM was used. Afterwards, water contents were established by oven drying according to ASTM D2216. The compaction data and TDR data are

given in Table 7-10 and the compaction curve is given in Fig. 7.37. The maximum unit weight is about 122.4 pcf and it occurs at the optimum water content of about 13 percent.

Table 7-10 Compaction Data for Airport Site Soil

(Testing done by X. Yu at Purdue)

Test No.	Water Content	Dry Density (g/cm ³)	Dry density (pcf)	Ka	Sigma
1	0.077	1.860	116.1	8.90	23.03
2	0.129	1.962	122.4	15.85	40.19
3	0.179	1.901	118.6	22.35	70.71
4	0.208	1.738	108.4	22.89	69.77
5	0.181	1.844	115.1	21.65	69.23
Brown County Clay					
1	0.202	1.762	109.9	23.4	89

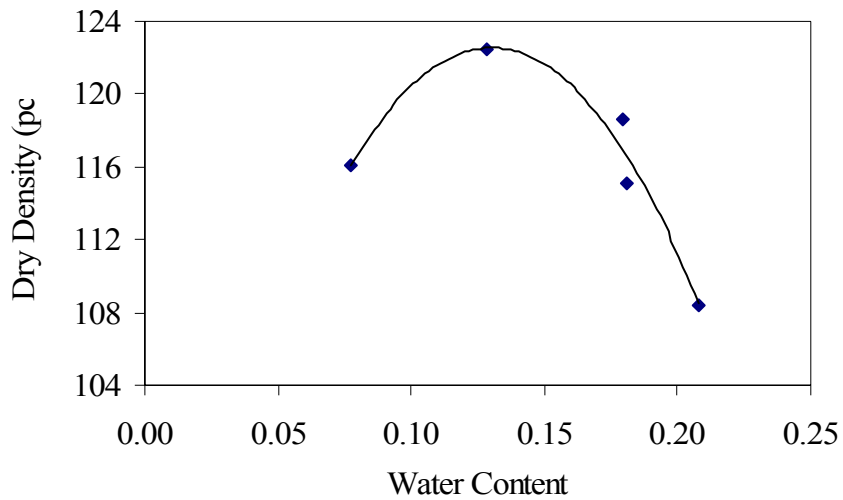


Fig. 7.37 Modified Compaction Test Results for Airport Soil.

(Testing done by X. Yu at Purdue)

Table 7-11 TDR Calibration Factors for Airport Soil

Parameter	Value
a	0.91
b	8.84
c	.0345
d	0.576
f	-0.0509
g	0.0662

The TDR Calibrations as done by the program PMTDR-SM are shown in Figs. 7.38 through 7.40. Calibration values obtained from these plots are summarized in Table 7-11. The single open-square data point in each of these three figures is for the Brown County Soil tested with Modified Compaction as will be described later. It appears to be similar to the Airport Site soil.

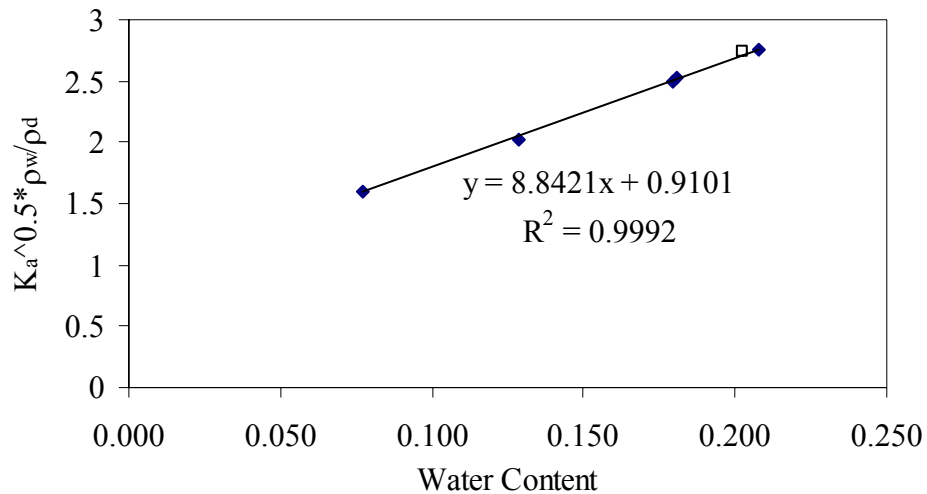


Fig. 7.38 Plot to Obtain Calibration Factors *a* and *b* for Airport Soil

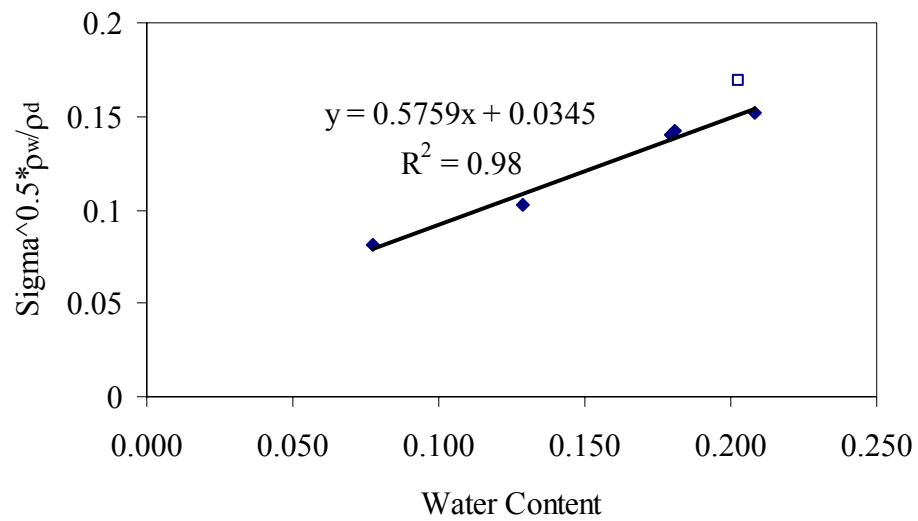


Fig. 7.39 Plot to Obtain Calibration Factors c and d for Airport Soil

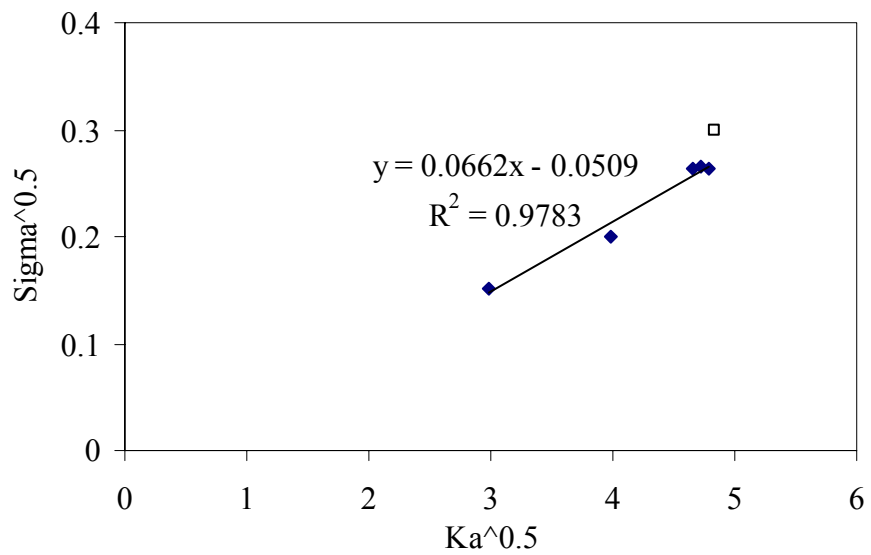


Fig. 7.40 Plot to Obtain Calibration Factors f and g for Airport Soil

Results from H.C. Nutting and Purdue tests are summarized in Table 7-12. Each row corresponds to a location at the Site. The column labeled *HCN Oven Dry* is the oven dry water contents determined by HCN and supplied to Purdue by Ron Ebelhar. The column labeled *Purdue Oven Dry* was obtained from tests done at Purdue on bag samples provided by H.C. Nutting on March 21st. The water contents and dry unit weights measured by the nuclear method were provided by H.C. Nutting. The *TDR* water contents and dry unit weights were calculated using the program *PMTDR-SM* (One-Step Method) with calibration factors determined at Purdue (Figs. 7.38 through 7.40 and Table 7-13) and with field TDR data files provided to us from H.C. Nutting.

Examination of the water content data in Table 7-12 shows the water contents determined by the nuclear device to be close to those from oven drying and the water contents by TDR One-Step Method to be lower by 2 to 5 percentage points

Examination of the unit weights in Table 7-12 indicates that those determined by the nuclear device are much lower than those determined by the TDR One-Step Method. Considering that the maximum dry unit weight from the Modified Compaction test was 122.4 pcf, the field dry unit weights by the nuclear method are only about 85% of the maximum dry unit weight while the dry unit weights by the TDR One-Step are on the order of 93% of the maximum dry unit weight. The latter seem more reasonable for a site where significant compaction took place. (In addition to this, as mentioned before, nuclear test and driven cylinder tests were also performed by H.C. Nutting at 40 locations. It was found that except for 8 locations, the total densities by nuclear tests were significantly smaller than the results by driving cylinder tests)

Table 7-12 Comparison of Results for Airport Site

Loc. No.	HCN Oven Dry	Purdue Oven Dry	Nuclear	TDR	Nuclear Dry Unit Weight	TDR Dry Unit Weight	Nuclear Total Unit Weight	TDR Total Unit Weight
5	0.243	0.232	0.204	0.171	102.8	116.2	123.8	136.1
6	0.241	0.233	0.227	0.182	98.4(pcf)	115.6	120.7(pcf)	136.6
7	0.180	0.178	0.193	0.163	106.0	116.3	126.3	135.3
8	0.200	0.189	0.201	0.143	106.1	117.3	127.4	134.1
3	0.193	0.203	0.209	*	103.5		125.1	

* Irregular field TDR waveform

7.4.2.1 Discussion of the Airport Site Results

Water Content – The data in Table 7-12 appears to indicate the water content measurements of the nuclear method are more accurate than those for the TDR method when comparing to the water contents measured by oven drying. However, one must consider that the TDR measures the average water content over the length of the spikes in the ground. If the water content near the soil surface was higher (lower) than that deeper beneath the surface the nuclear method might register a higher (lower) water content because it uses a back scatter method for water content determination. If the grab samples taken to the laboratory for oven drying were taken predominantly from near the surface, the corresponding oven-dried water contents might not represent the average water contents over the depth of soil covered by the TDR test.

Dry Densities (Unit Weights) – The nuclear device when the direct transmission mode is used, gives approximately average total density (unit weight) from the probe source to the surface. Dry density is determined by subtracting the mass of water per unit volume from the total mass per unit volume (total density). (The mass of water per unit volume is obtained by multiplying the volumetric water content by the density of water.) If the volumes over which the total density and water content are not the same, the calculated dry density will be in error if the water contents are not uniform over the depth of measurement. If the soil near the surface has higher water content than soil below it, then the average total density will be lower than the total density near the surface where the water content is higher. When the calculation is made for dry density, the obtained values will be lower than actual dry densities. The opposite will be true when the soil near the surface is dryer than the soil at depth. Here the nuclear dry densities will be higher than the actual dry densities.

In the TDR method, the dry density (unit weight) is calculated directly and is the average value over the depth of measurement, just as is the water content. Because the TDR measures the average values over the depth of measurement, results reported by this method could differ from those obtained by the nuclear method when water contents vary significantly with depth

near the soil surface. They also would vary from those obtained by oven drying if the sample taken for oven drying was not retrieved over the entire depth of the TDR test.

7.4.3 Brown County Soils

The original data taken in August, 2002 on Brown County soils seems to have problems. It is observed that TDR measured dry density is significantly smaller than that measured by nuclear tests. Efforts were spent on making analyses to identify the possible cause of this inconsistency.

The first item identified is the very low TOTAL UNIT WEIGHT in the TDR Compaction Mold (approx. 80 pcf), compared to the total density insitu (approx. 120 pcf). Specifically, the measured mass of mold plus soil is much lower than we normally encounter for this type of soil. (We typically see this value greater than 7500 grams while those recorded were around 6800 grams.) Based on this observation, it is suspected that there is something wrong when taking the mass of mold filled with compacted soil. One possible cause could be the scale was not leveled prior to making the measurements or that the scale was severely out of calibration. It is recommended that the scale be used to determine mass of the empty mold prior to filling it. The measured value should be very close to the value labeled on the mold. This forms a field calibration check on the scale.

Another explanation might be that the soil was placed into the mold in chunks with significant air gaps located within the soil. This possibility is supported by the fact that the measured apparent dielectric constant in the mold is much lower than what would expect for a soil with water content around 20%. The values of K_a were about half the values that would expect for this soil at this water content.

Additionally, the “compaction” curve associated with the calibration done by H.C. Nutting (See Fig. 7.41) doesn't look like an ordinary compaction curve. It is guessed that only hand compaction (10 or so tamps of the aluminum rod /lift with 6 lifts) was used. Even so, the curve should be concaved downward similar to one for standard compaction.

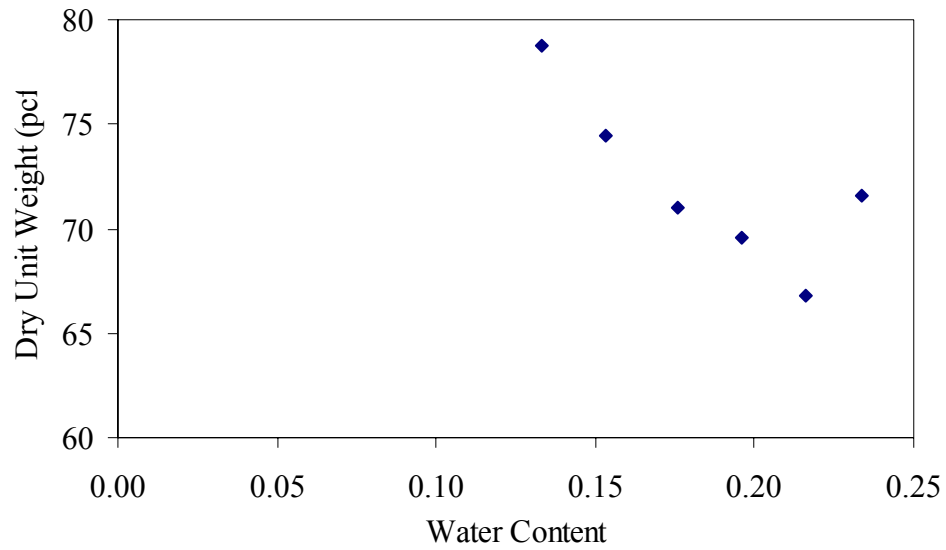


Fig. 7.41 Dry Density versus Water Content from TDR Calibration Tests by H.C. Nutting

It is interesting to note that the calibration equation resulting from this data (Fig. 7.42) gives a fairly straight line, although the intercept value is much lower than what would normally expect. (Many previous tests indicate that the values of a rarely below 0.7 and the values here are 0.40.) One reason for this is that the intercept for these data were obtained with all of the water contents between 13% and 23%. Extrapolation of the line back to the origin could account for most of this expected difference.

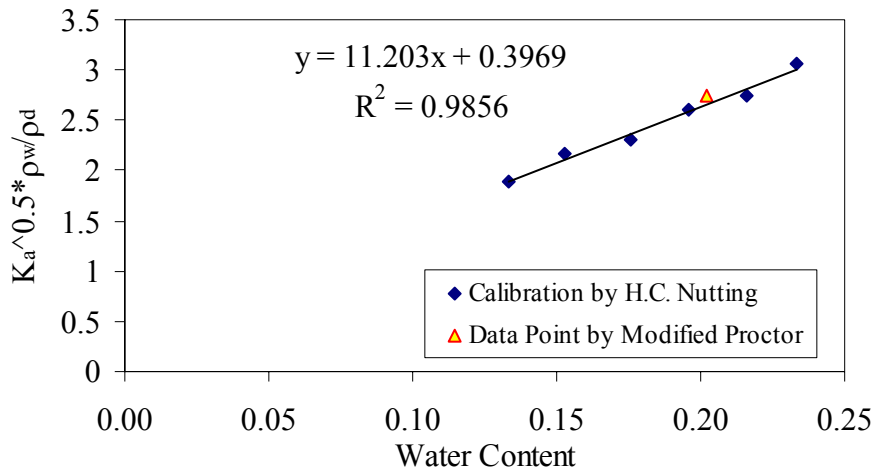


Fig. 7.42 Calibration Curve for Brown Country Clay from Calibration Test at H.C. Nutting
(The open triangle is the data done at Purdue with Modified Proctor energy.)

In Fig. 7.42, the point designated by an open triangle is from a test on the Brown County soil sent to Purdue. The point is measured using modified compaction effort on this soil. Note that the data point falls close to the line from the original HCN calibration. This would indicate that the calibration curve is not very sensitive to compaction energy.

According to the TDR Method developed in the prior research and incorporated into ASTM D6780, field values of dry density are obtained from dry density of the same soil in the mold determined from the measured total density and the TDR determined water content. The dry density is adjusted only by the difference in apparent dielectric constant measured in the field and in the mold as given by the equation below.

$$\rho_{d,field} = \rho_{d,mold} \sqrt{\frac{K_{a,field}}{K_{a,mold}}} \quad (7-5)$$

Since the soil is assumed to be at the same water content insitu as in the mold, total density in the field would be given by a similar equation (See Eq. 7-2).

$$\rho_{t,field} = \rho_{t,mold} \sqrt{\frac{K_{a,field}}{K_{a,mold}}} \quad (7-6)$$

Thus, if the total density in the mold is in error, and the K_a values measured are similar, the total and dry densities in the field also will be in error.

In summary, the most probable cause of the gross discrepancies between the TDR values and corresponding values from the nuclear method is inaccurate determination of the total density of the soil compacted in the mold during the field tests. From previous experience at Purdue, this total density with rod tamping is on the order of 85% to 90% of the total density insitu. The data obtained from HCN tests are on the order of 67%. As a result of this experience following recommendations are made for getting accurate and consistent results:

- a) The field scale calibration should be checked against a standard laboratory scale.
- b) The mass of the empty mold be determined prior to filling it as a field check on the scale calibration. The field measured value needs to be inserted into the appropriate data field in the PMTDR program. For the TDR molds of the Beta Test Program, this value should be about 4300 grams. If another mold is used, such as the Standard Compaction mold, its mass will have to be determined and appropriately inserted.
- c) The values for mold volume listed in the PMTDR program (1888 cm³ for the TDR mold, 944 cm³ for the Standard Compaction mold) need to be checked during each test that they are the correct values.

Suggestions for getting improved accuracy in field tests include:

- a) Remove the top inch or so of soil that may have dried or have become wet from recent rainfall before performing field density and water content measurements with either the nuclear method or the TDR method.

- b) Be sure the surface of the soil being tested is flat and smooth.
- c) When running the TDR test, be sure to drive the center spike last. This will minimize the forming of gaps adjacent to this spike. If after removing the template a small gap is observed around the center spike from drift of the spike from driving, fill it in with loose soil or redo the test at another location.
- d) Make sure that all spikes are driven to just touch the template. If one of the outside spikes is driven too hard, it will cause the other sides of the template to lift off the soil. This will introduce a source of error into the results because the “length above soil” will be different from that assumed in the data reduction.
- e) Check the TDR signal for good contact between MRP head and spikes (and ring on compaction mold). If the signal does not show the classic shape, move the MRP Head on the spikes or ring until that shape appears and does not change.
- f) Check the empty mold mass (weight) on the balance as a check of balance calibration. It should be the same as written on the mold. Be sure that this value also is entered correctly into the program.
- g) Check that proper mold volume is entered into the program. If the TDR mold is used, that volume should be 1888 cm³ and if a Standard Compaction mold is used, that volume should be 944 cm³.
- h) Check that the proper total length of spikes is entered into the program. Also check that the correct length above soil also is entered into the program.

7.4.4 Summary of H.C. Nutting Tests

Feedback and results obtained from H.C. Nutting indicate that TDR is applicable for non-conventional soils such as fly ash, which further validated the discoveries of other Beta partners.

Results from tests on Brown County Clay and the airport site by H.C. Nutting were also analyzed. It is found that one step method provided better results on soil dry density while the results of water content is lower than oven drying results. Cause of the abnormal results obtained on Brown County Clay was also investigated. Based on the investigation, recommendations were made to obtain more accurate test results.

7.5 Rutgers University

Rutgers University plan was to evaluate the device on a landfill cover consisting of amended dredge and treated MSW ash. The construction for this fill has been postponed until August 2003 and they will be using TDR device in parallel with sand-cone and Nuclear gage tests. They anticipate completing the work by October 2003 and getting their results to Purdue around that time. Except in laboratory evaluation, no field application of TDR has been used by Rutgers University at this time.

The information obtained in the future from Rutgers University will be added as an addendum to this report and/or included in external publications..

8. Suggestions for Further Implementation

The focus of this research project was to begin the implementation process, through a Beta Test Program, by refining and improving the technology, establishing an ASTM Standard, introducing soil practitioners to this new method, and to obtain data on a wide variety of soils. This Beta Test program helped verify the accuracy, improve the testing procedure, and refine the testing equipment. Feedback from Beta Test Partners provided very important information on the accuracy of this testing method and will be incorporated in the future revision of the ASTM D6780 *Standard Method for Measurement of Soil Water Content and Dry Density by Time Domain Reflectometry*. An important discovery in this research was a simplified One-Step Method. Preliminary conclusions from field evaluations are that the One-Step Method is both fast and accurate.

Efforts were spent on automation of the testing procedures and on creation of a reference database. These will greatly facilitate the application of this technology into geotechnical engineering practice.

This research also indicates that TDR technology can be used for non-conventional materials such as fly ash and lime stabilized soil, where current state-of-art nuclear tests fail to provide reliable measurements.

In addition to use in compaction quality control, the newly discovered One-Step Method can also be used for long term monitoring of earthwork performance. The implementation procedures of TDR technology for field quality control and long-term monitoring are summarized below.

8.1 Improvements to Support Implementation of the Original TDR Method

Several important improvements in the testing procedure occurred during this project. They include:

- 1) Procedures for compacting soil into the mold, for calibration or for field tests, should ensure that the soil is uniform and that no large voids occur anywhere in the mold. While the accuracy of the method is relatively insensitive to the density of the soil in the mold, it is sensitive to the presence of large voids. Hence, more compaction energy is better than too little compaction energy when compacting the soil in the mold, especially for cohesive soils that may have clumps.
- 2) The size of the compaction mold could be reduced for testing most materials. From previous research, the recommended mold had the same diameter but twice the height of a standard compaction mold. The primary reason for this selection was to provide a volume large enough to accommodate all of the soil excavated from the zone enclosed by the spikes in the insitu test. This research shows that accurate measurements can be made where the length is only one-half that of the previously recommended lengths. The shorter length is especially helpful in highly conductive soils and allows the use of a standard compaction mold with a non-metallic base plate. It also makes the equipment less expensive, more portable, and easier to accept among practitioners.
- 3) Results from the Beta Tests indicate that calibration factors a and b for apparent dielectric constant may be relatively constant. For example, a single set of values ($a = 1$; and $b = 8.50$) appear to be valid for Florida sands used in highway construction. Similar results may be likely for other regional soils.

8.2 Laboratory Tests to Establish Soil Parameters for the One-Step Method

For the One-Step Method, calibration is required to obtain the soil specific constant a , b , c , d , f , and g . Soil specific calibration tests are recommended for applying this One-Step Method, unless the user has experience with a soil and is confident that there are no variations that would influence the soil specific constants.

Calibration is using standard compaction tests (ASTM D698 or ASTM D1557) and a standard compaction mold with a non-metallic base. For soils with predominantly

large particles, a mold with larger diameter such as 6 inch is recommended to improve the accuracy of calibration.

Procedures of the calibration are:

- 1) Prepare the soil at water contents that cover the range of water contents expected for TDR field tests, using ordinary tap water;
- 2) Compact soil into the mold using standard compaction energy designated by ASTM D698 or ASTM D1557;
- 3) After compaction for each water content, drive the center rod through the rod guide into the soil (Fig. 8.1), place the adaptor ring on the mold, seat MRP head on the ring (Fig. 8.2), and take a TDR reading to obtain the apparent dielectric constant (K_a) and bulk electrical conductivity (EC_b);



Fig. 8.1 Driving the Central Rod through the Rod Guide Placed on Mold



Fig. 8.2 Placement of the MRP Head on the Mold using the Adaptor Ring

- 4) After taking the readings, soil in the mold is removed and oven dried according to ASTM D2216 to obtain the oven-dried water content;
- 5) Information on soil water content (w), dry density (ρ_d), dielectric constant and electrical conductivity are used to obtain soil specific calibration constants a, b, c, d, f , and g .

An example data reduction is shown in the following Fig. 8.3. The intercept and slope of a line fitting $\sqrt{K_a} \frac{\rho_w}{\rho_d}$ versus w provide constants a and b , respectively; c and d are the intercept and slope, respectively, of a line fitting $\sqrt{EC_b} \frac{\rho_w}{\rho_d}$ versus w ; and f and g are intercept and slope, respectively, of a line fitting $\sqrt{EC_b}$ versus $\sqrt{K_a}$. Thus, from Fig. 8.3 (a), $a = 1.00$ and $b = 7.81$; from Fig. 8.3 (b), $c = 0.0163$ and $d = 0.525$; and from Fig. 8.3 (c), $f = -0.0747$, and $g = 0.063$.

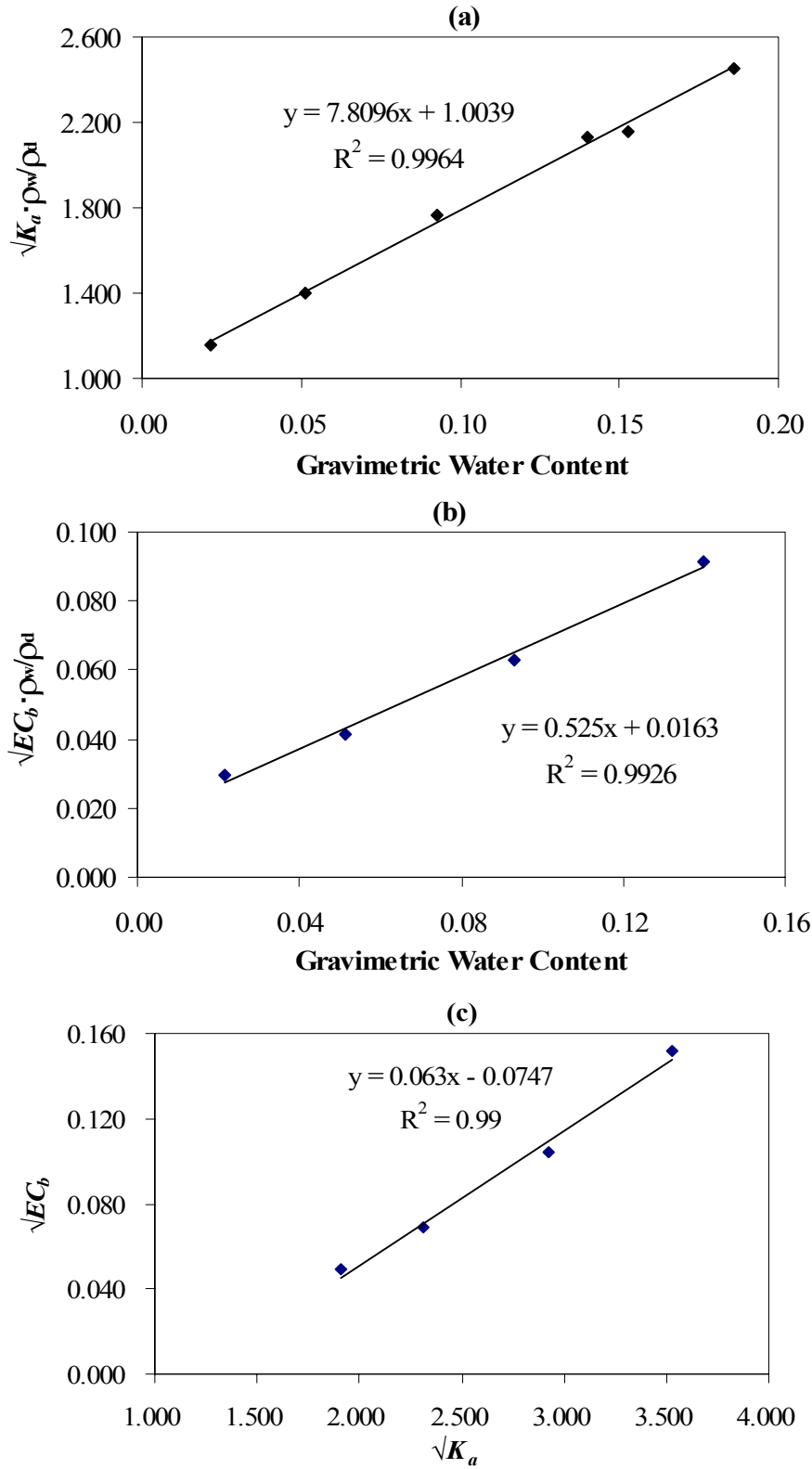


Fig. 8.3 An Example of Calibration on ASTM Graded Sand: (a) Calibration of K_a ; (b) Calibration of EC_b ; (c) Calibration of K_a versus EC_b

The data reduction and curve fitting process can be done with spread sheet or the computer module provided within the PMTDR-SM program. Please refer to the PMTDR-SM Operation Manual for the details about data reduction using the computer program.

Note: Since conductivity measurement is used for analysis, there needs to be good contact between the adapter ring and mold and between the MRP head and adapter ring. Soil residue needs to be cleaned up before installing the adapter ring, placing the MRP head on the ring, and making the measurement.

8.3 Quality Control in Construction Operations with the One-Step Method

The field testing procedure and test apparatus for the One-Step Method is similar to those specified by ASTM D6780, **but omits** the steps of digging out the soil, compacting it into the mold, and running a second TDR test on the soil in the mold. In summary the field testing procedure includes:

- 1) Level and smooth the soil surface and place the template on the surface
- 2) Drive four spikes into ground through the holes in the guide template and remove template (See Fig. 8.4a).
- 3) Seat MRP head on the four spikes (See Fig. 8.4b).
- 4) Take a TDR reading to obtain $K_{a,f}$ and $EC_{b,f}$ using the PMTDR-SM program (See Fig. 8.5).

The program then uses the $K_{a,f}$ and $EC_{b,f}$ to get $K_{a,adj}$ and $EC_{b,adj}$ and calculates the field soil water content, w , and dry density, ρ_{dry} . Typically it takes about 3 to 4 minutes to do a field TDR test and obtain soil water content and dry density, which is much less time compared with the conventional Purdue TDR test (ASTM D6780). It is comparable to the time required for nuclear tests.

(a)



(b)



Fig. 8.4 Field Test Procedures: (a) Spikes Being Driven through Template into Soil Surface; (b) Multiple Rod Probe Head on Spikes for TDR Measurement

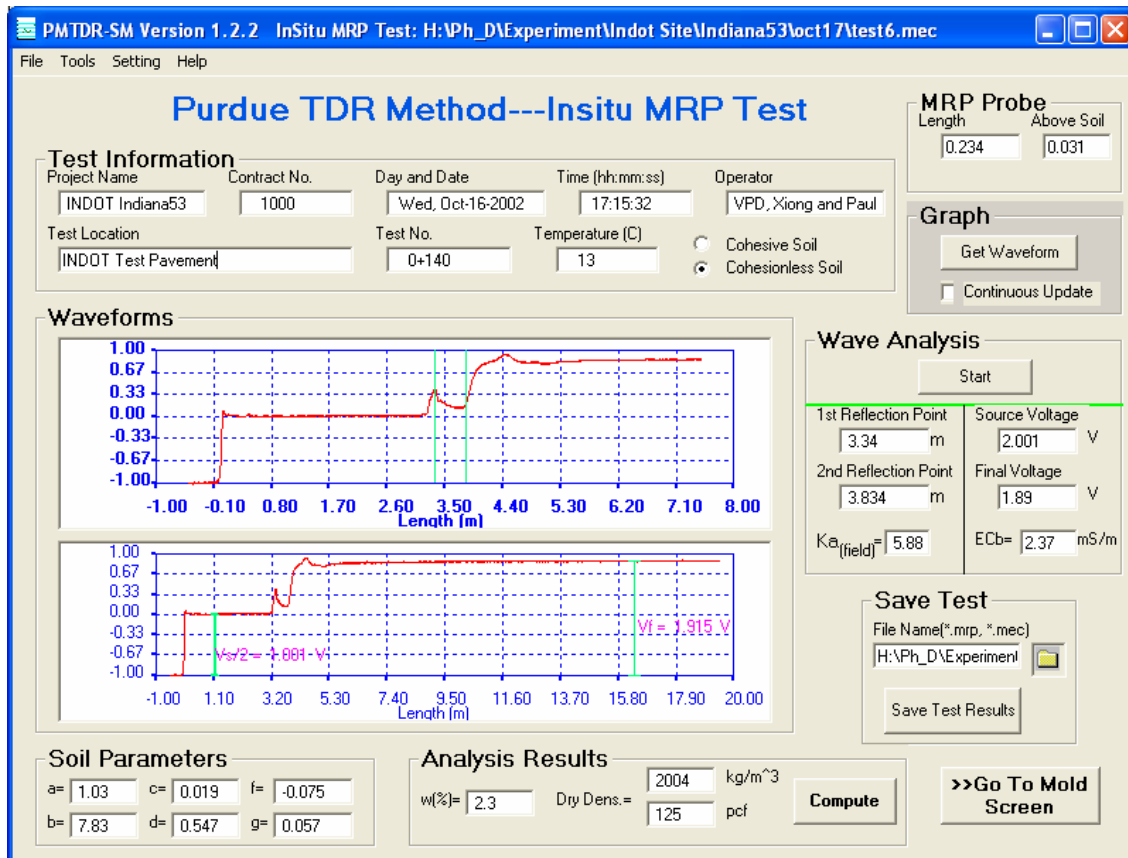


Fig. 8.5 Program to Obtain TDR Waveform and Determine Water Content and Dry Density for One-Step Method

8.4 Monitoring Performance

The nondestructive characteristics of One-Step Method make it ideal for field monitoring of earthwork performance. Procedures for monitoring performance are similar to that used for field compaction quality control. For example, it is possible to observe the changes in water content and dry density with time, including the effects of rainfall, drying, traffic loads, and vibrations. When materials that hydrate are present, it is possible to monitor the hydration process and, hence, establish when the hydration process is essentially complete.

8.5 Movement of the Technology to the Market Place

8.5.1 Discussions with Potential Firms to Manufacture, Market, and Service the TDR Method

Since the fall of 2002, the PI, working with Kannan Grant of Purdue's Office of Technology Commercialization, has been in discussion with two firms about manufacturing, marketing, distributing, and servicing this technology. One of the firms has visited Purdue to see the equipment and will be returning again in May 2003. The other firm has been sent a set of equipment and is independently evaluating its performance before discussions continue. It is likely that arrangements will be made during the summer of 2003 with one or both of these firms.

8.5.2 Interaction with the Management 451 Class in the Krannert School of Business to Obtain Marketing Plans

In the spring 2003 semester, the PI interacted with the instructor of **Management 451 – Managerial Policy**. He provided a lecture on the Purdue TDR Method and worked over the semester with six student teams of five-to-seven students each on their semester projects. Each team took a slightly different aspect of marketing the Purdue TDR Method. Some focused on the potential market for this product, others focused on whether the process should be handled by a “start-up” company or by an establish firm. Still others looked at the potential markets for a combination of TDR for soil and TDR for concrete. The TDR Team and Kannan Grant observed the final presentations of these groups and received their final written reports. As one might expect, a variety of recommendations came forth, with some teams making different recommendations from others. However, all teams concluded that the Purdue TDR Method needs to be marketed very soon before others enter the market with similar technology, U.S. Patents notwithstanding.

9. Recommendations for Future Research

TDR has been applied in geotechnical engineering for years, mostly for volumetric water content estimation. However, most applications of this technology directly or indirectly originated from research conducted in one of the agriculture sciences. They typically do not account for material density nor do they account for temperature effects in measuring water content and measurement of dry density was not even considered. The research in this, and previous projects, developed a systematic approach to calculating both gravimetric water content and dry density of the soil that included adjustments for effects of temperature on the apparent dielectric constant. This research project developed a new one-step method that makes use of both apparent dielectric constant and bulk electrical conductivity. At this writing, the one-step method is less than a year old. Nearly all previously data acquired with the process that made use of only the apparent dielectric constant could be reanalyzed with the one-step method. This provided the basis for the conclusions drawn for the new method. Because the one-step method makes use of measured bulk electrical conductivity in addition to apparent dielectric constant, a whole new realm of possibilities emerged for use of this method in testing civil engineering materials. Apparent dielectric constant measurements are relatively independent of the pore fluid conductivities, but bulk electrical conductivity measurements are very strongly affected by the chemical composition of the pore fluid. Furthermore, when the composition of the pore fluid changes the bulk electrical conductivity can accurately measure that change. Specifically, bulk electrical conductivity is very sensitive to amounts of additives to soils such as fly ash, bentonite, cement, and lime. Additionally, when some of these additives cause hydration to occur, bulk electrical conductivity measurements can accurately monitor the hydration process. The computer program PMTDR-SM and the measurement probes developed in this research allows for easily monitoring apparent dielectric constant and bulk electrical conductivity with time for extended periods (days, weeks, or longer).

9.1 Application of TDR for Regional Soils

The Beta partners currently involved in this research mostly are located in the eastern part of the United States. While TDR tests were performed in this project on soils which are representative of a variety of soil types, the applicability of TDR for the other regional soils,

especially those in the western part of the United States, needs to be further investigated. A few examples of these regional soils include caliche in Nevada, collapsing soils and volcanic ash in Arizona, non-plastic silts in California, etc. Investigations of TDR on these regional soils are important as the soils might have distinct electrical properties resulting from their specific origin and environment. Besides, the regional soils are frequently encountered and widely used in the civil engineering practice of these regions, and thus, research on this topic have important engineering implications. Research on regional soils can be implemented by involving the state DOTs and FHWA. FHWA can act as the bridge between the DOTs to provide communication channels.

9.2 Stabilized Soils

9.2.1 Chemically Stabilized Soils

Chemically modified soils typically include, but are not limited to: cement, fly ash and lime stabilized soils. For chemically stabilized soils, the amount of stabilization depends not only on the amount of stabilizing material added, but also on the nature of the soil being stabilized, the presence of moisture, temperature, and time after adding the chemical and mixing. The TDR method developed in this research can easily monitor the stabilization process as described in Chapter 8. A preliminary study conducted on using TDR for lime stabilized soil reveals that soil dielectric behavior is not influenced by lime concentration while bulk soil electrical conductivity shows strong dependency on lime concentration. It has also been observed that hydration process causes change in electrical conductivity which can be monitored using TDR technology. These phenomena were also observed by our research project partners. These not only indicate that TDR can be used to obtain soil water content and dry density of these non-traditional soils, but also has the potential to provide additional information such as lime or ash concentration. Also, the potential exists to relate the TDR measurements to strength and deformation properties directly. This could be an especially practical application.

Other methods of measuring water content and density on these soils, such as the nuclear method cannot monitor chemical processes and may give erroneous information on water content because the chemical additives cannot be systematically accounted for as they are in the TDR method. The TDR application to these chemically modified soils will be proposed as part of a

future research program. Research results will generate application guidelines for applying TDR technologies compaction and quality control for chemically modified soils.

9.2.2 Mechanically Stabilized Soils

In some cases, additives such as asphalt or asphalt emulsions are mixed with granular soils as a means of stabilizing them. After mixing, the soils are compacted in place. The TDR methods developed herein also could be useful for monitoring the density, water content, and asphalt content of these stabilized soils. A preliminary test on hot-mixed asphalt shows that TDR measurements can be accurately made, but are very temperature dependent. Hence, if temperature is measured, the density and asphalt content could be measured using TDR. Once the asphalt is cooled, the addition of moisture to the asphalt could be monitored with TDR. Much more research is needed to develop the detailed procedures.

9.3 Other Civil Engineering Materials

9.3.1 Asphalt

Application of TDR technology to other civil engineering materials is important for research and engineering practice. One of these materials is asphalt. Like earthwork compaction, compaction quality of asphalt is also needed to be inspected before it is regarded as satisfactory. The difference between asphalt and soil is that water is not present in hot-mixed asphalt, but there is asphalt binder which affects the dielectric constant and electrical conductivity. The currently used methods for asphalt quality control include the nuclear method in the back scatter mode and drilling to take cores, which is time consuming, expensive, and destructive. Also, there is a trend toward using other non-destructive methods such as falling weight deflectometer tests that allow for back-calculating the moduli of soil layers.

Several impedance based products have been marketed to measure asphalt compaction quality. Initial feedback is that they are not very accurate. All of these methods actually are based on TDR principles, although the configuration is not the same (the probe does not extend into the compacted asphalt). The field probe consisting of disposable spikes could be driven into freshly compacted asphalt and the MRP probe head placed on these spikes to make a measurement that is an average over the length of the spikes. Besides, the spike configuration

can be used for performing cross-hole tests. Accelerometers can be attached to make shear wave speed measurements with one spike acting as the exciter and the others acting as receivers. The density information together with wave speed can then be used to calculate low strain shear modulus, which is an important parameter for pavement design and construction. Preliminary investigation indicates that low strain shear modulus can be obtained with good accuracy. With further investigation, the experience obtained from TDR research can be transferred into the research on asphalt compaction control.

9.3.2 Concrete

Two items are of special importance in quality control of concrete, the water-cement ratio at the time of mixing and the compressive strength at a specified time after placement.

Quality control of concrete strength is generally performed after the hydration process is nearly completed. Mechanical tests on test cylinders are used to measure strength at specified times after placement, e.g. 7 days, 28 days, etc. If the strength meets specifications, everything is fine; otherwise, the concrete has to be removed at great expense and loss of time.

The water-cement ratio at the time of mixing has very strong influence on the strength of concrete. The advantage of measuring water-cement ratio to control the concrete quality is that it can be performed before the hydration takes place. The TDR procedures developed in this research measure the dielectric constant and the bulk electrical conductivity of the material in a known volume. Research has shown that hydrated (bound) water behaves significantly different from free water in a mixture such as concrete. In the process of hydration free water reacts with the cement particles and becomes hydrated. Preliminary tests indicate that this process can be accurately monitored with time by use the probes and TDR one-step method measurement systems developed in this research. Research also indicates that the apparent dielectric constant is most affected by the amount of free water in the mixture while the bulk electrical conductivity is most affected by the amount of cement in the mixture. Considering this, it should be possible to use these TDR – measured values on freshly mixed concrete to estimate the water cement ratio. If this turns out to be valid and accurate, water-cement ratio of fresh concrete could be determined in about a minute after placing the freshly mixed concrete.

Work by other researchers indicates that bulk electrical conductivity of curing concrete is very closely related to the compressive strength of the concrete. Preliminary TDR tests at Purdue on cylinders of concrete show that accurate, repeatable measurements of both apparent dielectric constant and bulk electrical conductivity are easy to obtain. In these tests, a thermocouple was inserted into the concrete and temperatures were measured along with the apparent dielectric constant and bulk electrical conductivity. Additional experiments were made to determine temperature effects on these readings by placing the TDR instrumented cylinders in an oven and in a refrigerator, allowing for temperature equilibration, and then monitoring the changes of apparent dielectric constant and bulk electrical conductivity with temperature. Indications from these tests are that the TDR measurements, along with temperature can accurately characterize the hydration process, and hence be good indicators of compressive strength. It is likely that accurate predictions of seven-day and twenty-eight-day strengths may be possible in less than one day.

A presentation on these concepts, along with some of the preliminary data was made to the Midwest Concrete Consortium on May 2, 2003. Reactions to the presentation were very favorable and the group is looking to find support for definitive research on this topic. Should this research on TDR provide an accurate and reliable method for measuring the water-cement ratio of fresh concrete and be able to predict long-term compressive strength, it would be a major contribution to the state of practice in concrete technology.

9.4 Future Research in the Frequency Domain

The TDR technologies developed as part of this and previous projects shows exceptional potential for measuring physical properties of soil, especially water content and dry density. All of the work described in this report makes use of measurements in the time domain. Work by Drnevich et al. (2001) sponsored by the JTRP indicates that even more information may be obtained if the time domain signals are transformed to the frequency domain. For example, the real component of the electrical permittivity at a frequency of 1 GHz is relatively independent of bound water and hence can give an accurate measure of free water in a mixture. Values at lower frequencies along with those at 1 GHz could indicate the amount of water in a mixture and hence give information on particle sizes. A proposal for conducting TDR-based frequency domain

research on soils was submitted to the National Science Foundation in September 2002. The proposal was for a two-year project and requested a budget of \$200,000. It received a “Highly Recommended for Funding” rating but funding is pending NSF budget allocations.

9.5 Summary of Recommendation for Future Research

The equipment, procedures, and software developed as part of this and prior projects provides a powerful and accurate tool for studying the behavior of, and controlling quality of soils, modified soils, and other civil engineering materials. Of particular significance is the ability to non-destructively monitor subtle changes with time due to chemical processes or environmental changes. This and prior projects supported by INDOT through the Joint Transportation Research Program at Purdue gives Purdue a leadership role in this technology. It is important for this leadership be maintained by continuing the work in hopefully all of the topics listed above.

10. Summary and Conclusions

The Purdue TDR Method is a new technology for measuring water content and density of soil, which are two important indicators for earthwork compaction quality control. The technology is proving to be accurate, non-hazardous, and efficient. This Beta Testing project involves field testing on a broad spectrum of soils. The test results validated that Purdue TDR method is an accurate and robust method for compaction quality control. Based on feedback from field practice, many improvements were made in the testing procedure and testing equipment. These facilitate field performing of TDR testing and increase robustness of the equipment, and improve the accuracy of the results.

An ASTM standard based on the Purdue TDR method was approved and was designated ASTM D6780 in spring, 2002. This provides standardized procedures to perform this test and will promote application of Purdue TDR method in field practice. Results from this project have obtained supplementary information for refining the standard in the future. These include the information on the accuracy for ASTM D6780 as well as refinement for the testing procedure.

In the Beta Testing projects, results from TDR testing were compared with existing technologies and the results established a substantive database for the precision and bias statements needed for standardization. Given good calibration, absolute error of the Purdue TDR method for water content measurement is found to be ± 0.01 and relative error of Purdue TDR method for dry density determination is $\pm 3\%$. Both of these accuracies meet the requirement for field applications.

Research discoveries in the Beta Test project lead to the One-Step Method for soil water content and dry density determination, which simplifies the field application procedures. This was made possible by incorporating the bulk electrical conductivity information in addition to the apparent dielectric constant that was used before. Research efforts were spent in creating, evaluating and refining the one step method for soil water content and dry density measurement, including investigating and documenting the theoretical basis for this new testing procedure, studying the accuracy of the method by analysis on previous test data, experimental studying the temperature effects on the data analysis process, and creating and updating PMTDR-SM (Purdue

Method TDR-Simplified Method) program for automating the testing process and calculating the water content and dry density. Overall results provided by this one-step method for both water content and dry density are satisfactory, but more extensive testing will be required to develop confidence in its use. A U.S. Patent application has been filed for the One-Step Method.

Software programs were continuously refined during this project. The installation package and manual for operating these programs were generated. The One-Step Method can be used for insitu measuring soil water content and dry density with time to monitor changes such as occur with vibration, weather changes, and hydration. A module for implementation of automatically monitoring behavior with time was incorporated into the program.

Besides application for conventional soils, Purdue TDR method is found applicable for non-conventional materials as well. Preliminary results on fly ash, lime-stabilized soil, LPC, etc, indicates that TDR technology applies to these materials and gives reliable results for most situations. Further investigation into this topic is recommended in the future.

Acknowledgements

The authors wish to acknowledge the enthusiastic support and creative ideas of the Study Advisory Committee for these projects. The members are: Mr. Peter Capon (Rieth Riley Construction), Mr. Donald Johnson (FHWA), Mr. Thomas Kuhn (Kuhn Construction), Sam Mansukhani (FHWA), Dr. Tommy Nantung (INDOT), Mr. Wes Shaw (INDOT), Mr. Firooz Zandi (INDOT), and Mr. Nayyar Zia (INDOT). The interaction with the Beta Test Partners continues to be of great value for advancing this technology. The authors greatly acknowledges: Dr. Alaa Ashmawy and Mr. Amr Sallam (U. of South Florida), Dr. David Horhota (FDOT), Dr. Kulanand Jha (INDOT), Mr. Barry Newman, Mr. Dennis Nebiolo, and Mr. Robert Cimarolli (GAI Consultants), Mr. Ronald Ebelhar and Mr. Jason Sanders (H.C. Nutting Company), and Dr. Ali Maher and Dr. Nenad Gucunski (Rutgers University). Dr. James Bilskie, Chief Soil Scientist for Campbell Scientific was a great source of help with the TDR electronics and programs. The authors are most appreciative of the leadership provided by Dr. Kumares Sinha (Director of the JTRP), Donald Lucas (retired Chief Engineer, INDOT), Firooz Zandi (former Acting Chief Engineer), and Rick Smutzer (Chief Engineer). The authors wish to acknowledge the dedicated work on this project of graduate assistants: Jie Zhang, Quanghee Yi, and Weiyi Ma. Project personnel enjoyed exceptional service from Karen S. Hatke (Program Manager, JTRP). Finally, the authors are most appreciative of FHWA/INDOT/JTRP for the support of this project.

References

1. Abdulla, A.A., Mohammed, A.A., Al-Rizzo, H.M. (1988). "The Complex Dielectric Constant of Iraqi Soils as a Function of Water Content and Texture," *IEEE Transactions on Geoscience and Remote Sensing*, Vol. 26, No. 6, pp. 882-885.
2. Abu-Hassanein, Z., Benson, C., and Blotz, L. (1996). "Electrical Resistivity of Compacted Clays," *Journal of Geotechnical and Geoenvironmental Engineering*, Vol. 122, No. 5, pp. 397-406.
3. Amente, G., Baker, J. M. and Reece, F. C. (2000). "Estimation of Soil Solution Electrical Conductivity from Bulk Soil Electric Conductivity in Sandy Soils," *Soil Sci. Soc. Am. J.*, Vol. 64, pp. 1931-1939.
4. ASTM D698 (2002). "Standard Test Methods for Laboratory Compaction Characteristics of Soil Using Standard Effort", *Annual Book of Standards*, American Society for Testing and Materials, Vol. 04.08, pp. 78-88.
5. ASTM D2216, (2002). "Standard Test Method for Laboratory Determination of Water (Moisture) Content of Soil and Rock by Mass," *Annual Book of Standards*, American Society for Testing and Materials, Vol. 04.08, pp.218-222.
6. ASTM D6780, (2003). "Standard Test Method for Water Content and Density of Soil in Place by Time Domain Reflectometry (TDR)," *Annual Book of Standards*, American Society for Testing and Materials, Vol. 04.09, pp. 1311-20.
7. Baker, J. M. and Allmaras, R. R. (1990). "System for Automating and Multiplexing Soil Moisture Measurement by Time-Domain Reflectometry", *Soil Sci. Soc. Am. J.*, Vol. 55, pp. 1-6.
8. Benson, C. H. and Bosscher, P. J. (1999), "Time-Domain Reflectometry (TDR) in Geotechnics: A Review, Nondestructive and Automated Testing for Soil and Rock Properties", *ASTM SPT 1350*, W. A. Marr, C. E. Fairhurst, eds., American Society for Testing and Materials, West Conshohocken, PA.
9. Birchak, J. R., Gardner, C. G., Hipp, J. E. and Victor, J. M. (1974), "High Dielectric Constant Microwave Probes for Sensing Soil Moisture," *Proc. IEEE*, Vol.62, pp. 93-98.
10. Dalton, F. N., "Development of Time Domain Reflectometry for Measuring Soil Water Content and Bulk Soil Electrical Conductivity, Advances in Measurement of Soil Properties: Bring Theory into Practice", Topp, G.C. et al., eds, *Soil Sci. Soc. Am.*, Madison, WI, SSSA Sp. Pub. 30, pp. 143-167.
11. Dalton, F. N., Herkelrath, W. N., Rawlins, D. S., and Rhoades, J. D. (1984), "Time-Domain Reflectometry: Simultaneous Measurement of Soil Water Content and Electrical Conductivity with a Single Probe", *Science*, Vol. 224, pp. 989-990.
12. Dasbirg, S., Hopmans, J.W. (1992), "Time-Domain Reflectometry Calibration for Uniformly and Non-uniformly Wetted Sandy and Clayey Loam Soils", *Soil Sci. Soc. Am. J.*, Vol. 56, pp. 1341-1345.

13. De Loor, G. P. (1968), "Dielectric Properties of Heterogeneous Mixtures Containing Water", *J. Microwave Power*, Vol. 3, No. 2, pp. 67-73.
14. Dirksen, C., Dasberg, S. (1993), "Improved Calibration of Time-Domain Reflectometry Soil Water Content Measurements", *Soil Sci. Soc. Am. J.*, Vol. 57, pp. 660-668.
15. Dobson, M.C., Ulaby, F.T., Hallokainen, M.T., El-Rayes, M.A. (1985), "Microwave Dielectric Behavior of Wet Soil. Part II: Dielectric Mixing Models", *IEEE Trans. Geosci. Remote Sensing* GE 23, pp. 35-46.
16. Drnevich, V.P., Yu, X., Lovell, J., and Tishmack, J.K. (2001a), "Temperature Effects On Dielectric Constant Determined By Time Domain Reflectometry," *TDR 2001: Innovative Applications of TDR Technology*, Infrastructure Technology Institute, Northwestern University, Evanston, IL, September, 10 p.
17. Drnevich, V. P., Lin, C. P., Yi, Q., Yu, X. and Lovell J. (2001b), "Real-Time Determination of Soil Type, Water Content and Density Using Electromagnetics", Report No.:FHWA/IN/JTRP-2000-20, *Joint Transportation Research Program, Indiana Department of Transportation* - Purdue University, August, 288 p. (http://rebar.ecn.purdue.edu/jtrp/final_report/spr_2201_final_form1700.pdf)
18. Drnevich, V.P., Yu, X., and Lovell, J. (2002), "A New Method for Water Content and Insitu Density Determination", *Proceedings of the Great Lakes Geotechnical and Geoenvironmental Conference*, Toledo, Ohio, May, 15 p.
19. Feng, W., Lin, C.P., Drnevich, V.P., Deschamps, R.J. (1998), "Automation and Standardization of Measuring Moisture Content and Density Using Time Domain Reflectometry", Final Report, *Joint Transportation Research Program, Indiana Department of Transportation* - Purdue University, Sept.
20. Feng, W., Lin, C. P., Deschamps, R. J., Drnevich, V. P. (1999), "Theoretical Model of Multisection Time Domain Reflectometry Measurement System", *Water Resource Research*, Vol. 35, No. 8, pp. 2321-2331.
21. Ferre, P.A., Rudolph, D.L., Kachanoski, R.G. (1996), "Spatial Averaging of Water Content by Time Domain Reflectometry: Implications for Twin Rod Probes with and without Dielectric Coating", *Water Resource Research*, Vol. 32, pp. 271-279.
22. Giese, K. and Tiemann, R. (1975), "Determination of the Complex Permittivity from Thin Sample Time Domain Reflectometry: Implications for Twin Rod Probes with and without Dielectric Coatings", *Water Resource Research*, Vol. 32, pp. 271-279.
23. Herkelrath, W.N., Hamburg, S.P., Murthy, F. (1991). "Automatic, Real-Time Monitoring of Soil Moisture in a Remote Field Area with Time Domain Reflectometry", *Water Resource Research*, Vol. 27, pp. 857-864.
24. Hilhorst, M.A. (2000), "A Pore Water Conductivity Sensor", *Soil Sci. Soc. Am. J.*, Vol. 64, pp. 1922-1925.

25. Jacobsen, O.H., Schjonning, P. (1993), "A Laboratory Calibration of Time Domain Reflectometry for Soil Water Measurement Including Effects of Bulk Density and Texture", *Journal of Hydrology*, Vol. 151, pp. 147-157.
26. Kalinski, R.J. and Kelly, W.E. (1993), "Estimating Water Content of Soils from Electrical Resistivity", *Geotechnical Testing Journal, GTJODI*, Vol. 16, No. 3, pp. 323-329.
27. Lin, C. P. (1999), "Time Domain Reflectometry for Soil Properties", *Ph.D. Thesis*, School of Civil Engineering, Purdue University, West Lafayette, IN.
28. Malicki, M.A, Walczak, R. T., Koch, S. and Fluhler, H. (1994), "Determining Soil Salinity from Simultaneous Readings of its Electrical Conductivity and Permittivity using TDR", In. Proc. Symp. on TDR in Environmental, Infrastructure and Mining Applications, Evanston, IL. *Spec. Publ. SP. 19-94*, U.S. Dept. of Interior Bureau of Mines, Washington D.C., pp. 328-336.
29. Malicki, M.A., Plagge, R., Roth, C.H. (1996), "Improving the Calibration of Dielectric TDR Soil Moisture Determination Taking into Consideration the Solid Soil", *Eur. J. Soil Sci.*, Vol. 47, pp. 357-366.
30. Mitchell, J.K. (1993), *Fundamentals of Soil Behavior*, 2nd edition, John Wiley & Sons, Inc.
31. Noborio, K. (2001), "Measurement of Soil Water Content and Electric Conductivity by Time Domain Reflectometry: A Review", *Computers and Electronics in Agriculture*, Vol. 31, pp. 213-237.
32. Persson, M. and Berndtsson, R. (1998), "Texture and Electrical Conductivity Effects on the Temperature Dependency in Time Domain Reflectometry", *Soil Sci. Soc. Am. J.*, Vol. 62, pp. 887-893.
33. Ponizovsky, A.A., Chudinova, S.M., Pachepsky, Y.A. (1999), "Performance of TDR Calibration Models as Affected by Soil Texture", *Journal of Hydrology*, Vol. 218, pp. 35-43.
34. Ramo, S., Whinnery, J. R., and Van Duzer, T. (1994), *Fields and Waves in Communication Electronics*, 3rd ed., John Wiley, New York.
35. Rhoades, J.D., Raats, P.A., Prather, R.J. (1976), "Effects of Liquid Phase Electrical Conductivity, Water Content, and Surface Conductivity on Bulk Soil Electrical Conductivity", *Soil Sci. Soc. Am. J.*, Vol. 40, pp. 651-655.
36. Rinaldi, A.V. and Cuestas, A.G. (2002), "Ohmic Conductivity of a Compacted Silty Clay", *Journal of Geotechnical and Geoenvironmental Engineering*, Vol. 128, No. 10, pp. 824-835.
37. Roth, C.H., Malicki, M.A., Plagge, R. (1992), Empirical Evaluation of the Relationship Between Soil Apparent Dielectric Constant and Volumetric Water Content as the Basis for Calibrating Soil Moisture Contents by TDR", *Journal of Soil Science*, Vol. 43, pp. 1-13.

38. Siddiqui, S.I. and Drnevich, V.P. (1995), "A New Method of Measuring Density and Moisture Content of Soil Using the Technique of Time Domain Reflectometry," Report No.: FHWA/IN/JTRP-95/9, *Joint Transportation Research Program, Indiana Department of Transportation - Purdue University*, February, 271 p.
39. Siddiqui, S.I., Drnevich, V.P. and Deschamps, R.J., (2000). "Time Domain Reflectometry Development for Use in Geotechnical Engineering," *Geotechnical Testing Journal, GTJODJ*, Vol. 23, No. 1, March, pp. 9-20.
40. Sihvola, A.H., (1999), *Electromagnetic Mixing Formulas and Applications*, London: Institution of Electrical Engineers, c1999.
41. Timlin, D.J. and Pachepsky, Y.A. (1996), "Comparison of Three Methods to Obtain the Apparent Dielectric Constant from Time Domain Reflectometry Wave Traces", *Soil Sci. Soc. Am. J.* , Vol. 60, pp. 970-977.
42. Topp, G. C., Davis, J. L. and Annan, A. P. (1980), "Electromagnetic Determination of Soil Water Content: Measurements in Coaxial Transmission Lines", *Water Resource Research*, Vol. 6, No. 3, pp. 574-582.
43. Topp, G. C., Davis, J. L., Annan, A. P. (1982), "Electromagnetic Determination of Soil Water Content Using TDR: II. Evaluation of Installation and Configuration of Parallel Transmission Lines", *Soil Sci. Soc. Am. J.*, Vol. 46, pp. 678-684.
44. Topp, G.C., Yanuka, M., Zebchuk, W. D., and Zegelin, S. (1988), "Determination of Electrical Conductivity Using Time Domain Reflectometry: Soil and Water Experiments in Coaxial Lines", *Water Resource Research*, Vol. 24, No. 7, pp. 945-952.
45. Topp, G.C., Watt, M., Hayhoe, H.N. (1996), "Point Specific Measurement and Monitoring of Soil Water Content with an Emphasis on TDR", *Can. J. Soil Sci.*, Vol. 76, pp. 307-316.
46. Waith, M.J. and Or, Dani, (1999), "Temperature Effects on Soil Bulk Dielectric Permittivity Measured by Time Domain Reflectometry: Experimental Evidence and Hypothesis Development", *Water Resource Research*, Vol. 35, No.2, pp. 361-369.
47. Weast, R.C. (1986), *CRC Handbook of Chemistry and Physics*, 67th ed., CRC Press.
48. White, I., Zegelin, S. J., Topp, G.C. (1994), "Effect of Bulk Electric Conductivity on TDR Measurement of Water Content in Porous Media", *Symposium and Workshop on Time Domain Reflectometry in Environmental, Infrastructure, and Mining Applications*, Northwestern University, Evanston, Illinois.
49. Yanuka, M., Topp, G.C., Zegelin, S., and Zebchuk, W.D. (1988), "Multiple Reflection and Attenuation of Time-Domain Reflectometry Pulses: Theoretical Considerations for Application to Soil and Water", *Water Resource Research*, Vol. 7, pp. 939-944.

50. Yi, Q., Drnevich, V.P., and Lovell, J. (2001), "Effects of Particle Size Distribution on the Purdue TDR Method with Rock and Silty Clay Soil," *TDR 2001: Innovative Applications of TDR Technology*, Infrastructure Technology Institute, Northwestern University, Evanston, IL, September. 12 p
51. Yu, C., Warrick, A., Conklin, M., Young, M. and Zreda, M. (1997), "Two and Three Parameter Calibrations of Time Domain Reflectometry for Soil Moisture Measurement", *Water Resource Research*, Vol. 33, No. 10, pp. 2417-2421.

Appendix I. Notation

- a = intercept of calibration line for soil apparent dielectric constant
 a' = empirical constant for Rhoades' two-pathway model
 \bar{a} = intercept of calibration line using volumetric water content
 b = slope of calibration line for apparent dielectric constant
 b' = empirical constant for Rhoades' two-pathway model
 \bar{b} = slope of calibration line using volumetric water content
 c = intercept of calibration line for bulk soil electrical conductivity
 d = slope of calibration line for bulk soil electrical conductivity
 EC_b = bulk soil electrical conductivity
 $EC_{b,f}$ = adjusted bulk soil electrical conductivity
 $EC_{b,adj}$ = field measured bulk soil electrical conductivity
 $EC_{b,T^\circ C}$ = bulk soil electrical conductivity at temperature T ($^\circ C$)
 EC_w = electrical conductivity of water
 EC_s = electrical conductivity of soil solids
 f = intercept of calibration line for bulk soil electrical conductivity-soil apparent dielectric constant
 g = slope of calibration line for for bulk soil electrical conductivity-soil apparent dielectric constant
 K_a = soil apparent dielectric constant
 $K_{a,f}$ = field measured soil apparent dielectric constant
 $K_{a,adj}$ = adjusted soil apparent dielectric constant
 $K_{a,w}$ = apparent dielectric constant of water
 $K_{a,s}$ = apparent dielectric constant of soil solids
 $K_{a,T^\circ C}$ = soil apparent dielectric constant at temperature T ($^\circ C$)
 L_a = apparent length from length scaled TDR waveform
 L_p = length of probes in soil
 T = temperature ($^\circ C$)
 TCF = temperature compensation factor
 w = soil gravimetric water content
 σ = bulk electrical conductivity (see also EC_b)
 θ = soil volumetric water content
 ρ_d = soil dry density
TDR = Time Domain Reflectometry
PMTDR = Purdue Method TDR (Original program developed by Campbell Scientific)
PMTDR-RDR = Purdue Method TDR-Read, Display, Recalculate (Program used for ASTM D6780 procedures)
PMTDR-SM = Purdue Method TDR-Simplified Method (One-Step Method)
MRP = Multiple Rod Probe

APPENDIX II.

Comparison of PCTDR and PMTDR with CSI 605 Probe

Weiyi Ma¹

(Edited by Xiong Yu and V.P. Drnevich, May 2003)

In partial fulfillment of CE597

Supervisor: Dr. Vincent P. Drnevich

School of Civil Engineering

Purdue University

October 30, 2002

¹ Research Assistant, School of Civil Engineering, Purdue University

A2.1. Introduction

Time Domain Reflectometry (TDR) is an established technique for measuring soil water content, bulk electrical conductivity, and rock mass deformation. The CSI605 probe (shown in Fig. A2.1) is manufactured by Campbell Scientific, Inc. It is widely employed in geotechnical engineering to measure the insitu volumetric water content using the TDR100 Time Domain Reflectometer, also manufactured by Campbell Scientific, Inc. PCTDR software provided by Campbell Scientific (Fig. A2-2) is used to control the TDR100 from a personal computer. The software can display a waveform obtained from the TDR100 to help setting up the device and in troubleshooting. PCTDR utilizes several calibration functions to calculate bulk electrical conductivity and volumetric water content. However, the TDR system composed of the PCTDR software, the TDR100, and the CSI605 probe is designed for use in agricultural science and water resources. Accuracy of this technique when being applied in geotechnical engineering needs to be verified.

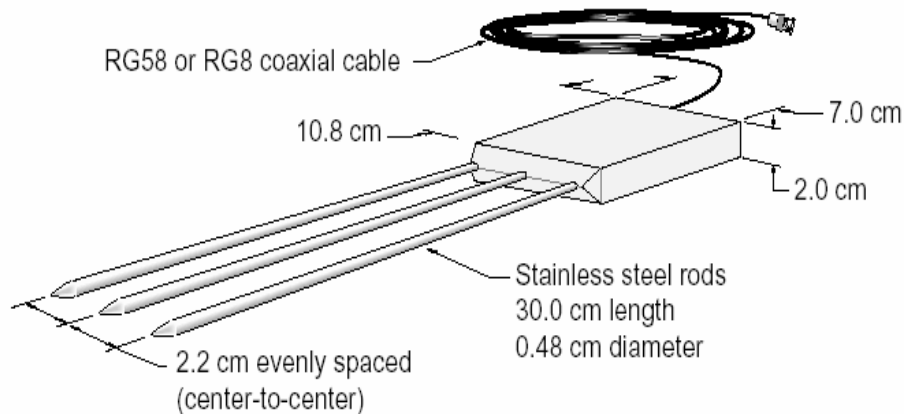


Fig. A2.1. CSI 605 Probe by Campbell Scientific, Inc.

PMTDR-RDR software (see Fig. A2.3) is a Windows-based program designed by Xiong Yu² for the automation of TDR measurements of both soil gravimetric moisture contents and densities using the method developed by the TDR research group at Purdue University.

² Research Assistant, School of Civil Engineering, Purdue University

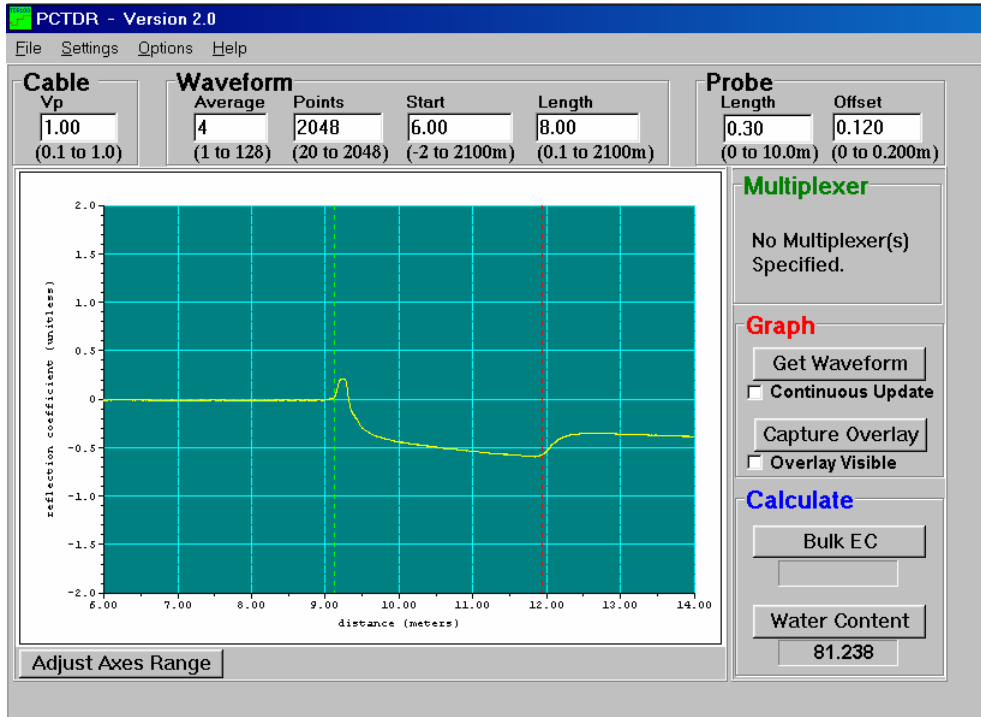


Fig. A2.2. PCTDR Sample Screen

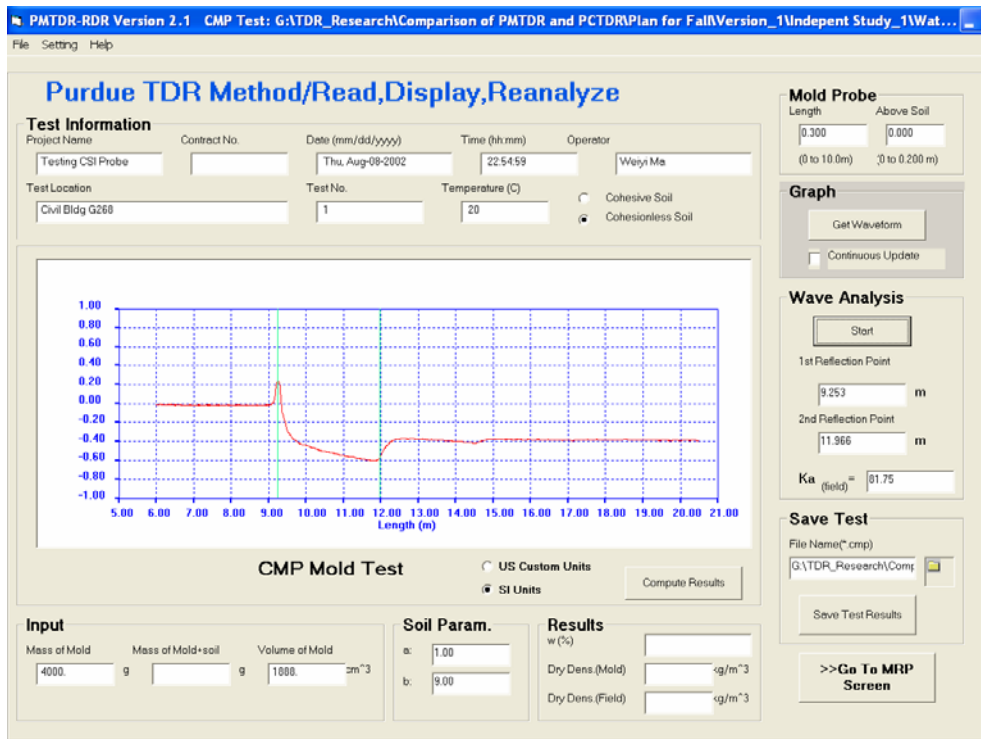


Fig. A2.3. PMTDR-RDR Sample Screen

The feasibility of making TDR measurements using the PMTDR-RDR program in place of the PCTDR program was studied in two phases. The first phase studied the possibility of using the PMTDR-RDR program with the CSI605 probe to make measurements in soil compacted with low compaction energy level (simulating soils with low density as encountered in agriculture and water resources). The second phase studied TDR tests in well compacted soil (simulating soil with high density as encountered in geotechnical engineering). In each of these two phases, comparisons of PMTDR-RDR program with the PCTDR program were made by comparing the measured values of volumetric water content and dielectric constant using the two programs. Topp's equation (Topp et al. (1980)) was employed in the PCTDR program for measuring volumetric water content and a user-defined function was used for measuring dielectric constants, K_a .

A2.2. Equipment

The following equipment was used: TDR100, personal computer (loaded with PMTDR-RDR and PCTDR programs), CSI 605 probe, Purdue TDR equipment³, sprayer, pan, 12 inch plastic mold, cans, rag, etc. (See Figs. A2.4 and Fig. A2.5 for details)

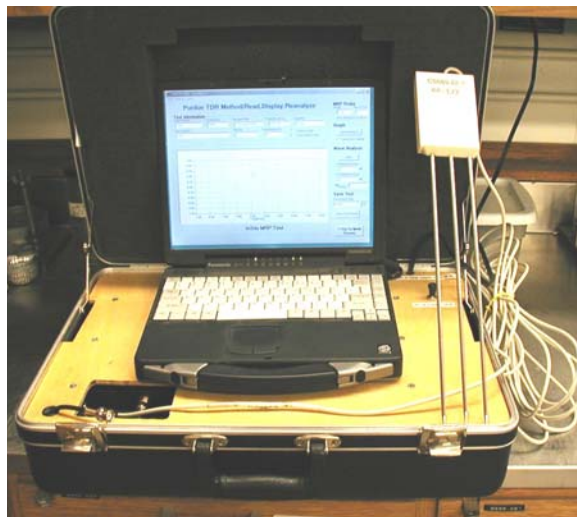


Fig. A2.4. Case Containing TDR100 and Computer, CSI 605 Probe

³ See ASTM D6780 for details.



Fig. A2.5. Hand Tools and Equipment Used

A2.3. Experimental Procedures

The CSI605 probe was tested with the PMTDR-RDR and PCTDR software in three different materials: tap water, Ottawa silica sand, and a glacial till soil provided by the INDOT Division of Research. Tests were run in both water and Ottawa silica sand contained in a 12 inch plastic mold to calibrate the CSI605 probe. The probe was slightly inclined to ensure that it is fully embedded (Fig. A2.6). After completing the calibration procedures, tests were run on the glacial till obtained from the INDOT Division of Research to complete both planned test phases.



Fig. A2.6. Fully Embedded CSI 605 Probe

A2.3.1. Tests on Tap water

Water has an established dielectric constant of around 81 at room temperature. Thus tap water was tested to check the accuracy of algorithms used by PCTDR and PMTDR-RDR. The procedures used to make TDR tests in tap water were listed as follows.

- 1) Fill the 12 inch plastic mold with tap water.
- 2) Insert the rods of the CSI probe completely into the water.
- 3) Take TDR readings using the programs PMTDR-RDR and PCTDR.

Figs. A2.7 and A2.8 shows the analysis using PMTDR-RDR and PCTDR programs. These figures indicate that the second reflection point located by PCTDR and PMTDR-RDR are close to each other (shown in Figs. A2.7 and A2.8 as Point 2). However, the first reflection points identified are different. PCTDR selected the point with largest first derivative (Point 1 in Fig. A2.7) as the first reflection point. The distance between the first and second reflection points include the length of the measurement probe head, which was subsequently subtracted in calculating dielectric constant. PMTDR-RDR program selected the local maximum point as the first reflection point. The distance between first and second reflection points are directly used to calculate dielectric constant. The dielectric constant of water obtained by PCTDR is 81.2, that obtained by PMTDR-RDR is 81.7, which are close to each other and expected values. Thus, although different algorithms are used by these programs, the results are comparable.

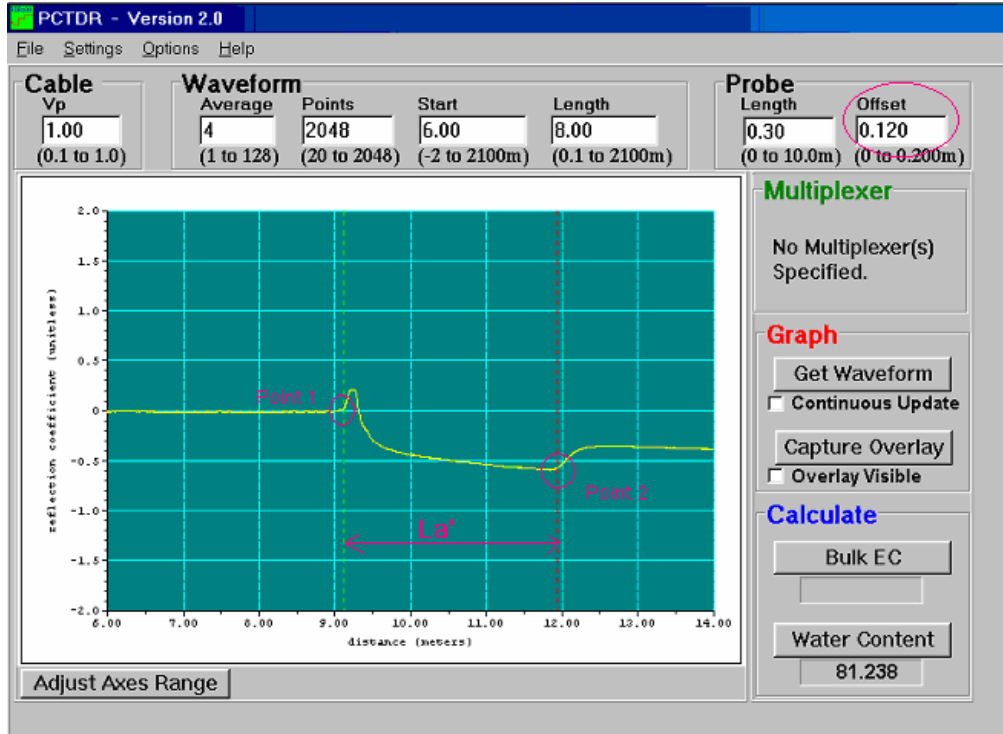


Fig. A2.7. Algorithms of PCTDR to determine K_a

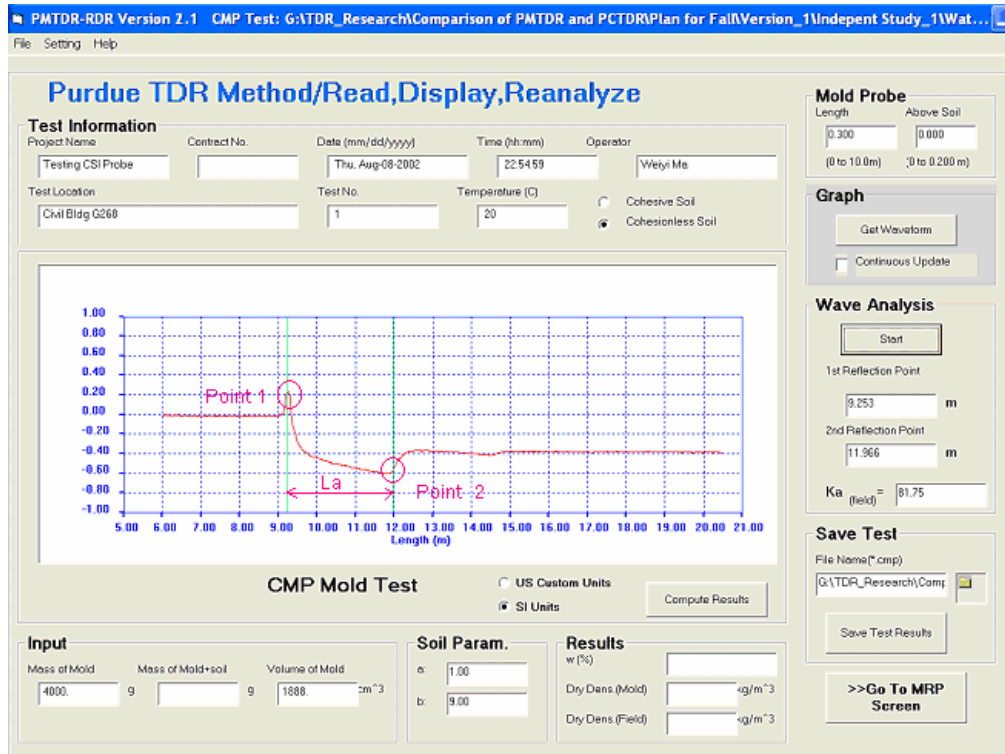


Fig. A2.8 Algorithms of PMTDR-RDR to determine K_a

A2.3.2. Tests on Ottawa silica sand

Tests on tap water indicated that PMTDR-RDR can be used with CSI probe in place of PCTDR. Additional tests were conducted on Ottawa sand were conducted mostly to obtain soil calibration constants and further validate this observation. Tests were performed both in 12 inch plastic mold and 9 inch compaction mold. The procedures for these tests are described below:

- 1) Tests in 12 inch plastic mold.
 - i) Fill the plastic mold full with dry sand.
 - ii) Insert the CSI probe entirely into the dry sand (Shown in Fig. A2.6 above).
 - iii) Get the readings by PMTDR-RDR and PCTDR, respectively.
 - iv) Fill the plastic mold with tap water slowly until the sand is saturated, measuring the amount of water added and measuring the change in mass of the soil, water, and container after filling. Do not touch the CSI probe in the process.
 - v) Run PMTDR-RDR and PCTDR again with CSI probe in the saturated sand.

Results of calibration constants obtained are shown in figure 9 below.

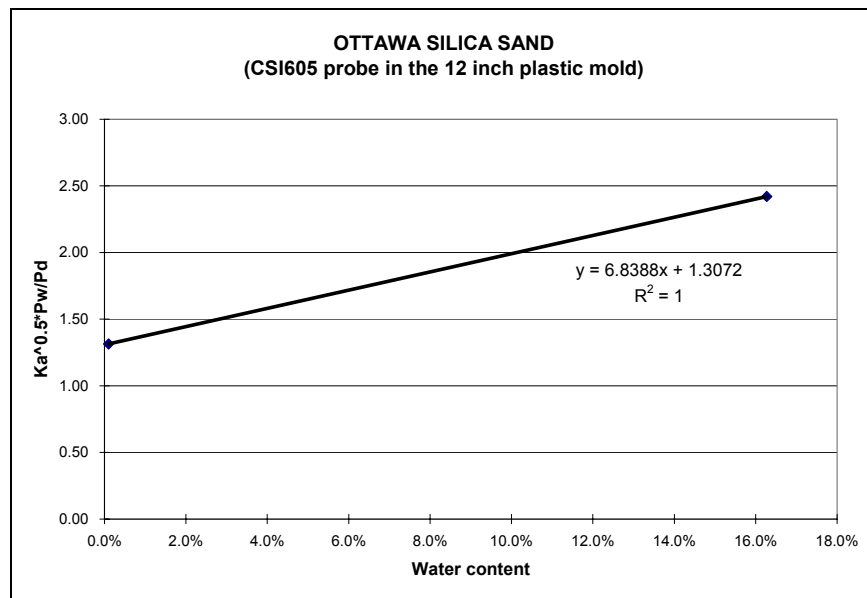


Fig. A2.9. Calibration Parameters a and b for Ottawa Silica Sand in the 12-inch Plastic Mold

- 2) Tests in modified standard compaction mold
 - i) Run test on the same dry sand using Purdue TDR Method using the mold probe and record the readings.
 - ii) Fill the mold with tap water slowly until the sand is saturated, keep the central rod untouched during this process.
 - iii) Take TDR readings by PMTDR-RDR (Shown in Fig. A2.10 below)



Fig. A2.10 TDR Test in a 4.0-in Diameter by 9-in. High Metal Compaction Mold

A2.3.3. Tests on the Glacial Till from the INDOT Research Division

Soil was sampled from the INDOT, Division of Research test pavement location. Atterberg limit tests, hydrometer tests and standard compaction tests were performed to characterize the soil. The soil was classified as silty clay (A-6 according to ASSHTO).

Before performing TDR tests, the soil was first air-dried in the laboratory. Soil clumps that would not pass the No. 4 sieve were broken up before tests. Two phases of tests were performed on this soil to verify the feasibility of using PMTDR-RDR program together with CSI probe for both agriculture and geotechnical purposes. Procedures of tests are outlined below:



Fig. A2.11 Soil from INDOT that Passed No.4 Sieve

A2.3.4. Phase I—Study the Feasibility of Using PMTDR-RDR with the CSI605 Probe in Soil Compacted with Low Energy (simulating low density soil in agriculture).

Tests were conducted at low densities both in a 6-in. diameter by 12-in. high plastic mold using the CSI probe and in a 4.0-in.diameter by 9-in. high metallic mold using Purdue TDR probes. Results of calibration factors and calculated water contents were compared.

Procedures for TDR tests in 6-in. diameter by 12-in. high plastic mold using the CSI probe:

- i) Fill the plastic mold with soil by 9 lifts (30 blows per lift) using hand compaction.
- ii) Insert the CSI605 probe entirely into the soil.
- iii) Take TDR readings with the two programs PMTDR-RDR and PCTDR
- iv) Pull out the CSI605 probe and put the soil sample into 110 °C oven for

12 hours to determine oven-dry water content.

Results of gravimetric water content measured by PMTDR-RDR were converted into volumetric water content and compared with the results by PCTDR.

The procedures used for conducting TDR Tests in the 4.0-in. diameter by 9-in. high metal mold were similar to those described above except for the mold size and use of the Purdue TDR mold probe. The tests were performed in parallel with the tests performed above using the same prepared soil.

A2.3.5. Results from Phase I—Study the feasibility of using PMTDR-RDR with the CSI605 probe in soil under low energy compaction (simulating soil in agriculture).

1) Compaction behavior

Results of compaction obtained using low compaction energy were shown in Table A2.1 and Fig. A2.12. The compaction curves obtained in 12 inch plastic mold and 9 inch metallic mold show similar behavior

Table A2-1. Low Energy Hand Compaction, (9 lifts, 30 blows per lift) in Test Phase I

6-in. Dia. by 12-in. Plastic Mold With CSI605 Probe		4-in. Dia. by 9-in. TDR Mold with Purdue TDR Probe	
$\rho_d (kg / m^3)$	$GWC_{oven-dried}$	$\rho_d (kg / m^3)$	$GWC_{oven-dried}$
1308.1	4.4%	1373.2	4.4%
1460.7	6.1%	1472.3	6.1%
1384.6	8.4%	1407.0	8.2%
1237.5	10.9%	1304.6	10.9%
1193.0	11.5%	1210.3	11.5%
1147.4	16.3%	1178.5	15.7%
1212.2	18.4%	1192.7	18.7%

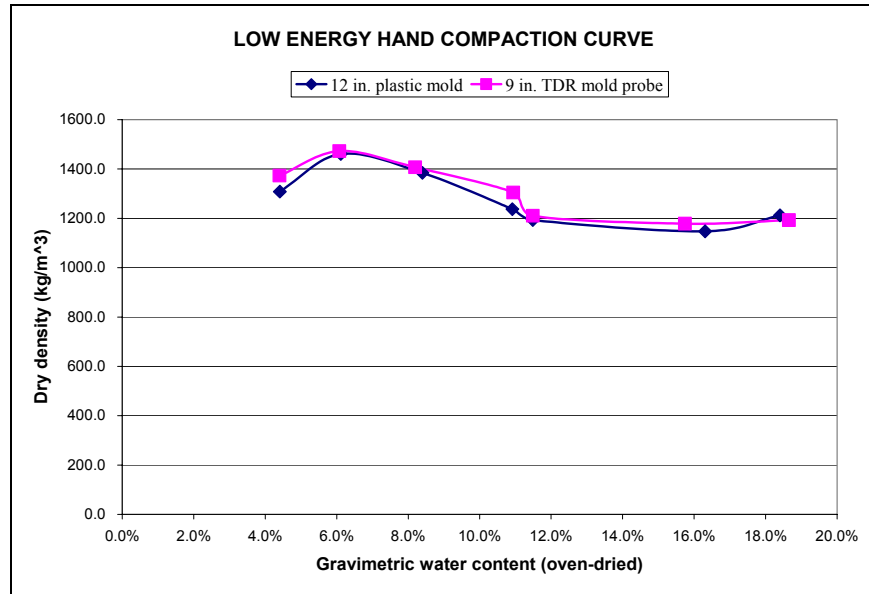


Figure A2.12 Low Energy Hand Compaction Curves of INDOT Soil

A2.3.6. Calibration factors obtained using CSI probe and Purdue TDR probes.

Soil dielectric constants measured with the CSI probe and Purdue TDR probes together with water content and dry density were shown in Table A2-2 and Table A2-3 below. The data were used to calculate calibration factors *a* and *b* as shown in Figs. 13 and 14.

Table A2.2. Data for Calibration Factors *a* and *b* for INDOT Soil with Low Energy Hand Compaction Using 4-in. Dia. by 9-in. High TDR Mold with Purdue TDR Probe

$K_{a, PMTDR-RDR}$	$\rho_d (kg / m^3)$	$\sqrt{K_a} \times \rho_w / \rho_d$	$GWC_{oven-dried}$
4.27	1373.2	1.50	4.4%
5.15	1472.3	1.54	6.1%
6.49	1407.0	1.81	8.2%
7.22	1304.6	2.06	10.9%
6.57	1210.3	2.12	11.5%
8.40	1178.5	2.46	15.7%
11.24	1192.7	2.81	18.7%

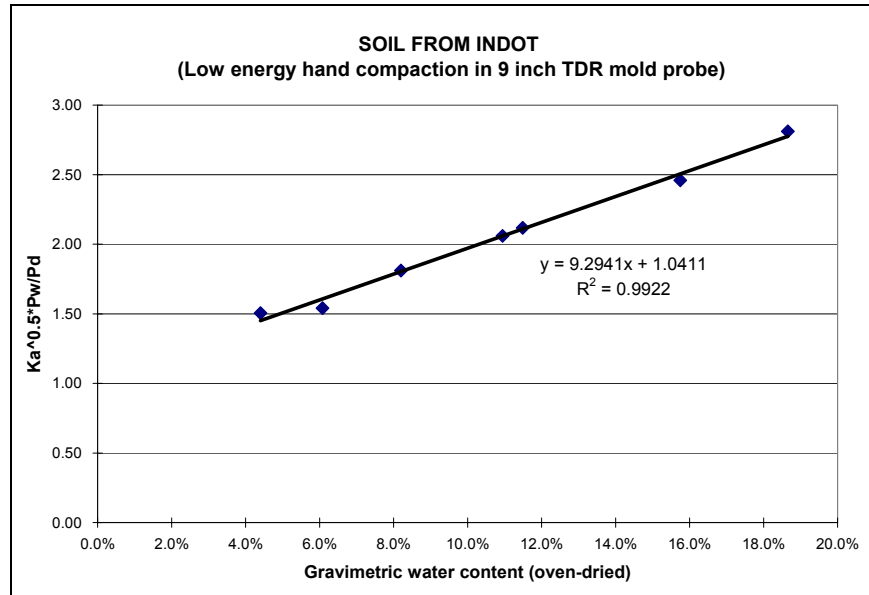


Fig. A2.13. Plot to Determine Calibration Parameters a and b for INDOT Soil in the 4-in. Dia. by 9-in. TDR Mold with Purdue TDR Probe

Table A2.3. Data for Determination of a and b for INDOT Soil under Low Energy Hand Compaction from PMTDR-RDR with 6-in. Dia. by 12-in. Plastic Mold with CSI605 Probe

$K_{a,RDR+CSI}$	ρ_d (kg / m ³)	$\sqrt{K_a} \times \rho_w / \rho_d$	$GWC_{oven-dried}$
4.06	1308.1	1.54	4.4%
5.26	1460.7	1.57	6.1%
6.86	1384.6	1.89	8.4%
6.49	1237.5	2.06	10.9%
6.41	1193.0	2.12	11.5%
8.93	1147.4	2.60	16.3%
11.43	1212.2	2.79	18.4%

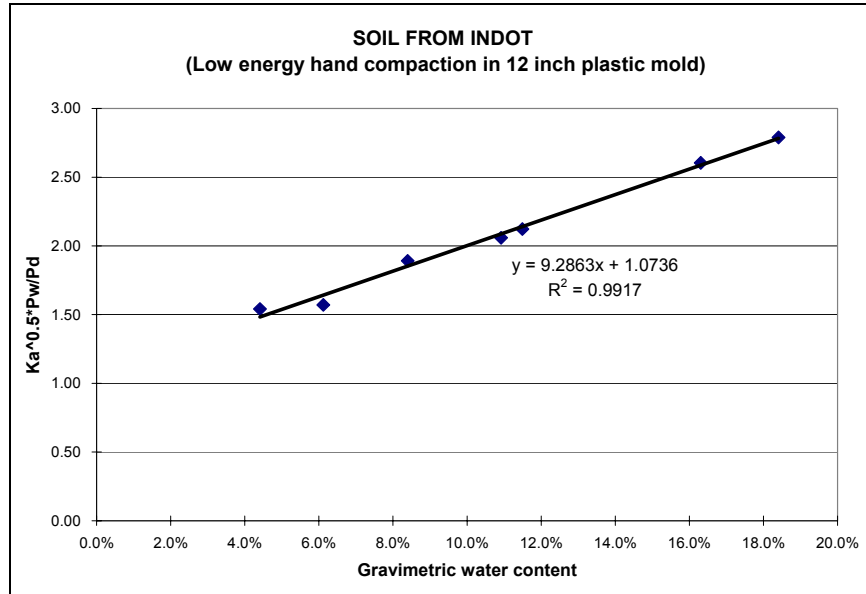


Fig. A2.14. Plot to Obtain Calibration Parameters a and b for INDOT Soil under Low Energy Hand Compaction in the 6-in. Dia. by 12-in. High Plastic Mold with CSI605 Probe

Results of soil calibration factors a and b obtained using low compaction energy are summarized in Table A2-4 from which it is obvious that the calibration factors are essentially the same. This indicates that Purdue TDR software can be used with the CSI 605 probe.

Table A2-4. Calibration Factors a and b Obtained from Low Energy Hand Compaction for INDOT Soil

Description	a	b
PMTDR-RDR w/ CSI605 probe, 12" plastic mold	1.07	9.29
Standard calibration procedure, 9" TDR mold probe	1.04	9.29

A2.3.7. Results of Water Contents

The calibration factors obtained above were used to calculate soil gravimetric water content using Purdue TDR theory and compared with that by oven dry. The measured gravimetric water content were also converted into volumetric water content and compared

with the results measured by PCTDR.

Comparison of results of gravimetric water content measured by TDR and oven dry were presented in Table A2-5 and in Figs. A2.15 and A2.16. The experimental results indicate that PMTDR-RDR, used together with CSI605 probe, obtained fairly good results of gravimetric water content compared with that by the oven-dry method.

Table A2-5. The comparison of gravimetric water contents from oven-dry method and those by PMTDR-RDR program with CSI605 probe

GWC _{oven-dried}	GWC _{software}	GWC _{calibrated}	
	PMTDR-RDR	Case I ⁴	Case II ⁵
6.1%	6.8%	6.0%	5.6%
8.4%	10.3%	9.3%	8.5%
10.9%	12.0%	11.0%	10.6%
11.5%	12.7%	11.7%	11.3%
16.3%	18.3%	17.0%	16.6%
18.4%	21.3%	18.8%	19.4%

GWC_{oven-dried} — Gravimetric water content obtained by oven-drying method (ASTM D2166)

GWC_{software} — Gravimetric water content obtained from software (PMTDR-RDR). PMTDR-RDR program generated these results with its default settings ($a=1$, $b=9$).

GWC_{calibrated} — Gravimetric water content calibrated by using a and b values from calibration tests described above.

⁴ Calibration parameters a and b were obtained from compaction in PMTDR mold probe.

⁵ Calibration parameters a and b were obtained from compaction in 12 inch plastic mold with CSI605 probe.

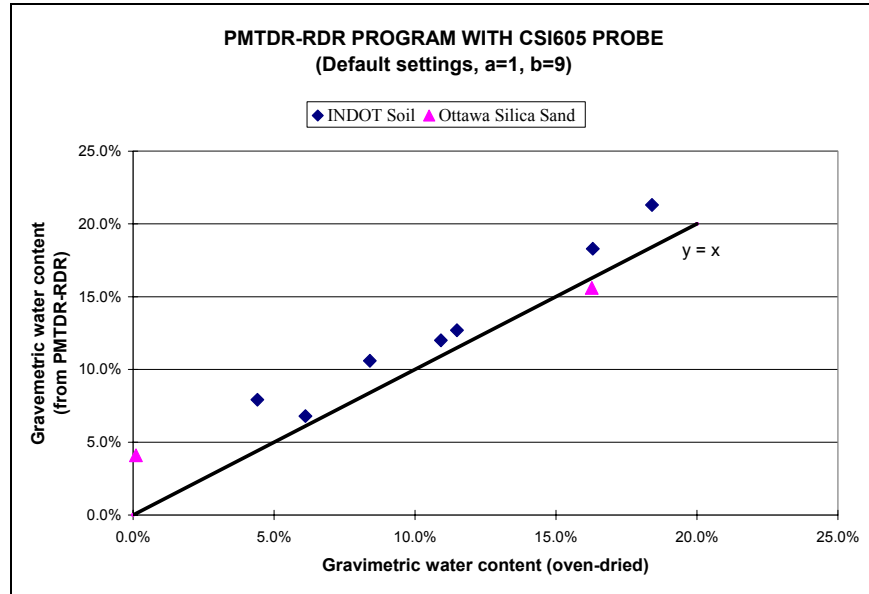


Fig. A2.15 Gravimetric Water Content from PMTDR-RDR with CSI 605 Probe Using Default Calibration Factors ($a=1$, $b=9$)

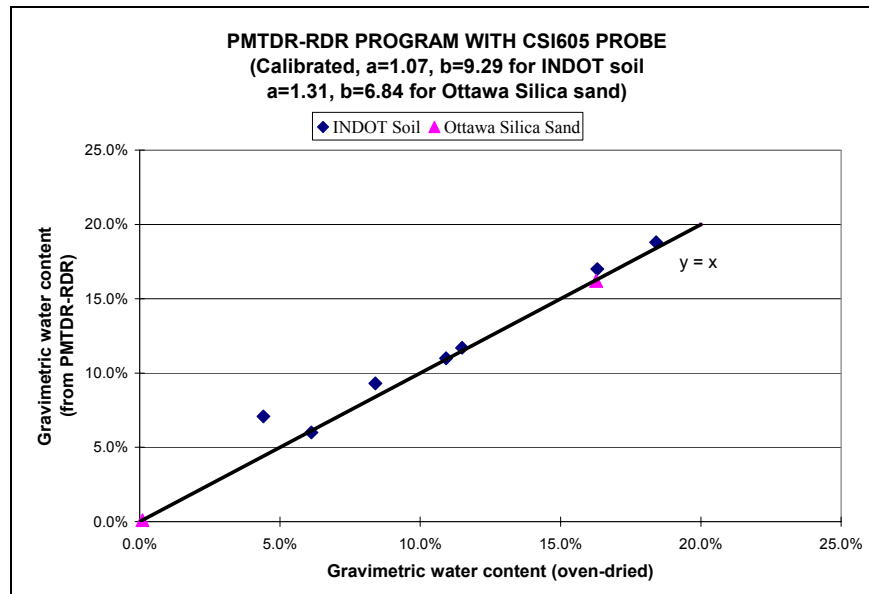


Fig. A2.16 Gravimetric Water Content from PMTDR-RDR with CSI 605 Probe Using INDOT Soil Calibration Factors ($a=1.07$, $b=9.929$)

Gravimetric water contents measured by PMTDR-RDR and CSI probe in 12 inch plastic mold using Purdue TDR theory were converted into volumetric water content and compared with the results of volumetric water content measured by PCTDR using Topp's equation. The results are compared in Fig. A2.17. The results indicate that for soil with low density, the program PMTDR-RDR together with the CSI 605 probe achieved similar accuracy as the program PCTDR with the CSI 605 probe in measuring volumetric water content.

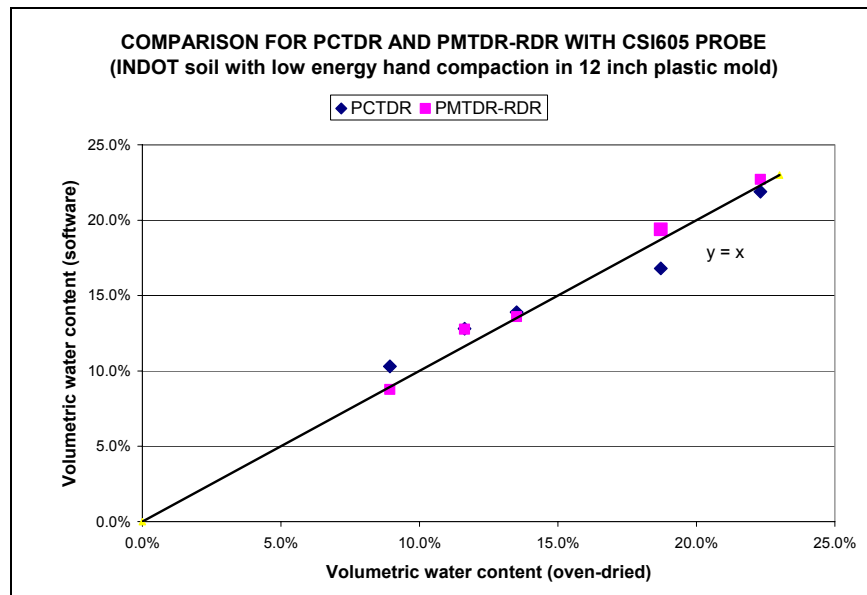


Fig. A2.17. Comparison of Volumetric Water Contents from Different Software with the Oven-Dried Method for Low Energy Hand Compaction of INDOT Soil

A2.4. Phase II—Evaluation of the Accuracy of PCTDR with CSI605 Probe in Soil with High Dry Density (simulating soil used in typical geotechnical engineering applications).

Tests were also performed on soil compacted with relative high compaction energy to verify the applicability of PMTDR-RDR and CSI probe for geotechnical engineering purposes. Procedures for conducting these tests are:

- i) The 12 inch plastic mold was filled with soil in 9 lifts using hand compaction of 60 blows per lift

- ii) After the first soil layer in the 12 inch plastic mold was compacted. The CSI605 probe was inserted with a slant into it with slant angle of 5° to ensure full embedment.
- iii) Compact the other 8 lifts around the CSI 605 probe rods and screed the top of soil flat.
- iv) Take TDR readings using PMTDR-RDR and PCTDR.
- v) Convert volumetric water contents measured by PCTDR to gravimetric water contents and compare with the result by PMTDR-RDR.
- vi) Remove the CSI605 probe from mold and place soil into a 110 °C oven for 12 hours to determine the water content.

A2.4.1. Calibration factors

Data used to obtain calibration factors a and b using PMTDR-RDR and the CSI 605 probe under high compaction energy were shown in Table A2-7. Plots to obtain a and b are shown in Fig. A2.18, in which we obtain $a=1.09$ and $b=7.07$.

Table A2-7. Data to Calculate a and b for INDOT Soil under High Energy Hand Compaction from PMTDR-RDR with CSI 605 probe

$K_{a,RDR+CSI}$	$\rho_d (kg / m^3)$	$\sqrt{K_a} \times \rho_w / \rho_d$	$GWC_{oven-dried}$
4.06	1496.7	1.59	7.2%
5.26	1413.2	1.91	11.5%
6.86	1490.1	2.03	13.5%

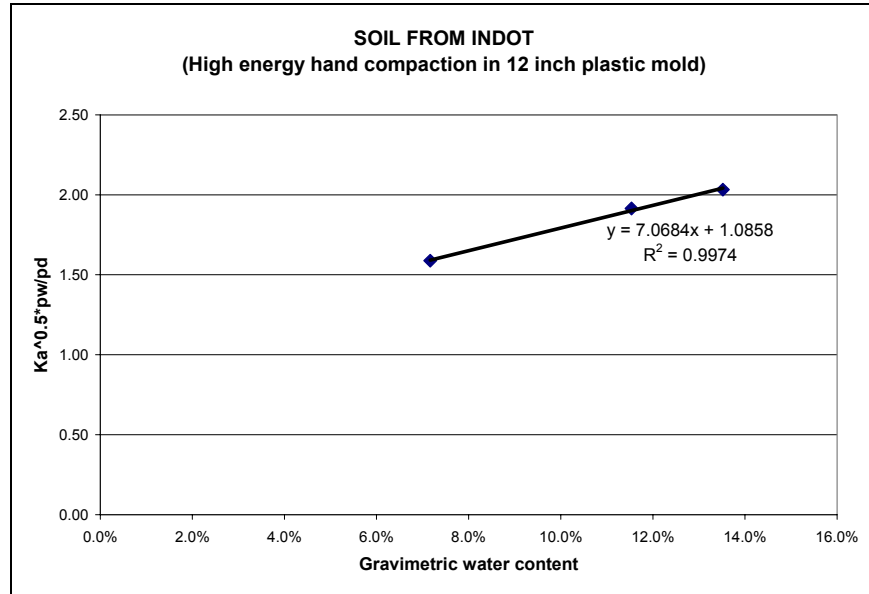


Fig. A2.18. Plots to Obtain Calibration Parameters a and b for INDOT Soil in the 6-in. Dia. by 12-in. High Plastic Mold (high energy hand compaction)

A2.4.2. Results for Volumetric Water Content

TDR measured volumetric water contents were compared with volumetric content calculated by oven dry gravimetric water content and soil density. Results of comparison were shown in Table A2-8 and Fig. A2.19.

Table A2-8⁶. The Comparison of Volumetric Water Content by Different Programs

VWC _{oven-dried}	VWC _{software}					
	PCTDR	Bias _{PCTDR}	Relative Bias _{PCTDR}	PMTDR	Bias _{PMTDR}	Relative Bias _{PMTDR}
10.7%	11.7%	1.0%	9.1%	10.5%	0.2%	2.2%
16.3%	15.1%	1.2%	7.4%	16.5%	0.2%	1.3%
20.1%	17.5%	2.6%	13.1%	19.9%	0.3%	1.4%
Average		1.6%	9.9%		0.2%	1.6%

⁶ Refer to the explanation of Table A2-6. for the terms in this table.

Table A2-8 and Fig. A2.19 indicate that results of volumetric water content measured by PMTDR-RDR using CSI probe and Purdue TDR theory have better accuracy than the results by the PCTDR program. This was attributed to the fact that Purdue TDR theory accounts for density effects in the calibration equation.

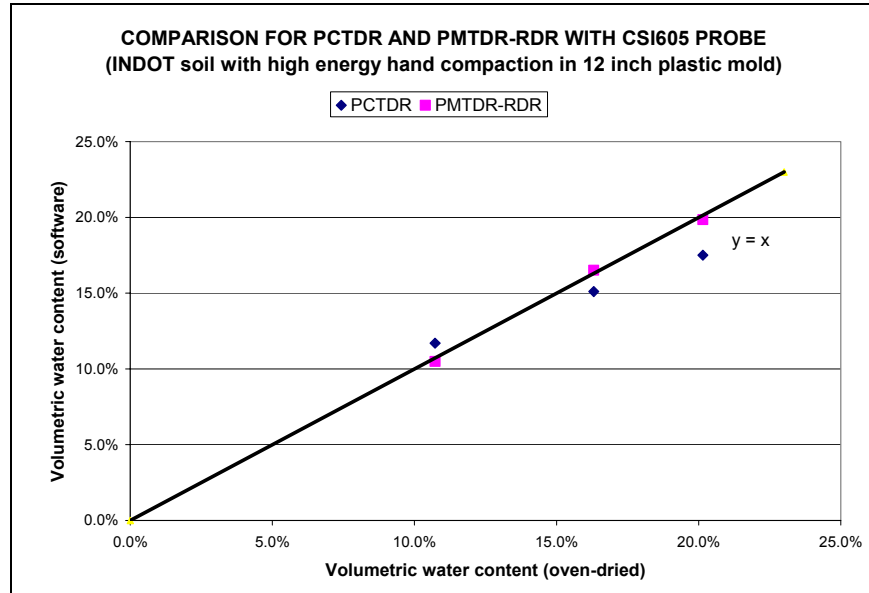


Fig. A2.19. Comparison of Volumetric Water Contents from PCTDR and PMTDR-RDR software with the Oven-Dried Method (High Energy Hand Compaction)

A2.5. Conclusions

From the experiments and analysis above, the following conclusions are obtained:

- 1) The algorithm for determining apparent dielectric constant used by PMTDR-RDR has similar accuracy with that used by PCTDR.
- 2) Preliminary results indicate that the Purdue TDR theory and software may be used with the CSI 605 probe to measure soil volumetric water content. The results of volumetric water contents measured by Purdue TDR theory were comparable to that measured by PCTDR for soil with low densities. For soils with high density, the

results of volumetric water contents calculated with the Purdue TDR theory and the program PMTDR-RDR have better accuracy than those calculated by PCTDR because the Purdue TDR Method accounts for soil density.

REFERENCES

1. ASTM D2216, (2002). "Standard Test Method for Laboratory Determination of Water (Moisture) Content of Soil and Rock by Mass," *Annual Book of Standards*, American Society for Testing and Materials, Vol. 04.08, pp.218-222.
2. ASTM D6780, (2003). "Standard Test Method for Water Content and Density of Soil in Place by Time Domain Reflectometry (TDR)," *Annual Book of Standards*, American Society for Testing and Materials, Vol. 04.09, pp. 1311-20.
3. ASTM D698 (2002). "Standard Test Methods for Laboratory Compaction Characteristics of Soil Using Standard Effort", *Annual Book of Standards*, American Society for Testing and Materials, Vol. 04.08, pp. 78-88.
4. Xiong Yu (2002). Help file of PMTDR-RDR program.
5. Campbell Scientific, Inc. (2000). Help file of PCTDR program.

APPENDIX III.

DATABASE MANAGEMENT SYSTEM DESIGN¹

Introduction

A database management system (DBMS) was designed by the University of South Florida, one of the Beta partners, and was delivered for use to the Purdue. The database system intends to provide storing of data and information obtained from Beta Test program and to provide easy access to this information for future references. Criteria set for design the DBMS are simplicity, ease of use, and robustness.

Compared to the traditional system management by file processing, the database approach has several advantages. Some of these benefits are program-data independence, minimal data redundancy, improved data consistency, improved data quality, and improved data accessibility and responsiveness. In this project, a Microsoft Access 2000 was developed based on various considerations, including commercial availability and portability. The database consists of one form, which includes agency information. The rest of the data are entered in a logical sequence as sub-forms. The database development process and database structure are described below.

Database Development Process

In general, the database development process passes through various development phases as follows:

1. *Conceptual Data Modeling*: This includes i) planning, where the relationships among the entities and the data hierarchy are established, and ii) analysis, where the data model is conceived.
2. *Logical Database Design*: During this stage, the nature and specifications of the data are determined, and the normalization of the design is performed.
3. *Physical Database Design and Creation*: The database management system is selected, and the database structure is organized and stored in the computer.

¹ This report was generated by Dr. Alaa Ashmawy, U. of South Florida, a Beta Testing Partner, August 2002.

4. *Database Implementation*: The programs for processing the database are coded, tested, and installed, and the data are loaded from the existing sources and tested.
5. *Database Maintenance*: The structure of the database is added, deleted, or changed in order to be consistent with the business needs.

Data Model

Microsoft Access relies on the relational data model, which relies on Tables or “relations” to store the data. These tables are linked through so-called “foreign keys” which identify the relationship between the data entities in a database. The relational model is flexible in that it allows for future expansion of the database and inclusion of additional elements as needed. The data model consists of the following three components:

Data Structure

Data are organized in tables, which consist of a known number of named columns and as many unnamed rows as needed to store the data. Table A3-1 shows an example of the table “Compaction”, where compaction data related to this study are stored. The table *attributes* are Comp ID, Lab Test ID, Sample Number, Date, Time, Technician, Dry Density, Labcomp filename, and moisture content. The table contains 19 rows of data corresponding to 19 different compaction tests.

In the relational model, each table must have a *primary key* that uniquely identifies each row in the table. In table A3-1, the primary key is Comp ID, in this case a number automatically assigned by the software. A *foreign key*, Lat Test ID, serves as the link between this entity and a related entity in another table. In this example, each set of compaction data in the Compaction table is related to a specific lab test in another table through this foreign key. Table A3-2 shows a part of the Agency table, where basic information about the performing agency (e.g. FDOT) is stored. Grain size distribution data are stored in GSD (Table A3-3). Table A3-4 shows the Lab table, where lab data is stored, and Table A3-5 shows a part of the PMTDR table, where the main bulk of the TDR test data is saved.

Table A3-1 Compaction Table with Sample Data

CompID	LabTestID	Sample_Number	Date	Time	Technician	Dry_Density	LabCMP_filename	Moisture
3	8		26-May-1998	10:54:54 AM	Feng, Lin, Vogel	1687	Geotechnical\TDR Data\Lin\Rev_Lin\tdrtest\REV_M1\rev_M1_1_1	3.84
4	12	M1_1_2	26-May-1998	11:06:47 AM	Feng, Lin, Vogel	1864	Geotechnical\TDR Data\Lin\Rev_Lin\tdrtest\REV_M1\rev_M1_1_2	3.76
5	13	M1_1_3	26-May-1998	11:48:10 AM	Feng, Lin, Vogel	1960	Geotechnical\TDR Data\Lin\Rev_Lin\tdrtest\REV_M1\rev_M1_1_3	3.82
6	14	M1_1_4	26-May-1998	11:48:10 AM	Feng, Lin, Vogel	2121	Geotechnical\TDR Data\Lin\Rev_Lin\tdrtest\REV_M1\rev_M1_1_3	3.65
7	15		26-May-1998	10:54:54 AM	Feng, Lin, Vogel	1687	Geotechnical\TDR Data\Lin\Rev_Lin\tdrtest\REV_M1\rev_M1_2_1	3.84
8	16		26-May-1998	10:54:54 AM	Feng, Lin, Vogel	1687	Geotechnical\TDR Data\Lin\Rev_Lin\tdrtest\REV_M1\rev_M1_2_2	3.84
9	17		26-May-1998	10:54:54 AM	Feng, Lin, Vogel	1687	Geotechnical\TDR Data\Lin\Rev_Lin\tdrtest\REV_M1\rev_M1_2_3	3.84
10	18		26-May-1998	10:54:54 AM	Feng, Lin, Vogel	1687	Geotechnical\TDR Data\Lin\Rev_Lin\tdrtest\REV_M1\rev_M1_2_4	3.84
11	19		26-May-1998	10:54:54 AM	Feng, Lin, Vogel	1687	Geotechnical\TDR Data\Lin\Rev_Lin\tdrtest\REV_M1\rev_M1_3_1	3.84
12	20		26-May-1998	10:54:54 AM	Feng, Lin, Vogel	1687	Geotechnical\TDR Data\Lin\Rev_Lin\tdrtest\REV_M1\rev_M1_3_2	3.84
13	21		26-May-1998	10:54:54 AM	Feng, Lin, Vogel	1687	Geotechnical\TDR Data\Lin\Rev_Lin\tdrtest\REV_M1\rev_M1_3_3	3.84
14	22		26-May-1998	10:54:54 AM	Feng, Lin, Vogel	1687	Geotechnical\TDR Data\Lin\Rev_Lin\tdrtest\REV_M1\rev_M1_3_4	3.84
15	23		26-May-1998	10:54:54 AM	Feng, Lin, Vogel	1687	Geotechnical\TDR Data\Lin\Rev_Lin\tdrtest\REV_M1\rev_M1_4_1	3.84
16	24		26-May-1998	10:54:54 AM	Feng, Lin, Vogel	1687	Geotechnical\TDR Data\Lin\Rev_Lin\tdrtest\REV_M1\rev_M1_4_2	3.84
17	25		26-May-1998	10:54:54 AM	Feng, Lin, Vogel	1687	Geotechnical\TDR Data\Lin\Rev_Lin\tdrtest\REV_M1\rev_M1_4_3	3.84
18	26		26-May-1998	10:54:54 AM	Feng, Lin, Vogel	1687	Geotechnical\TDR Data\Lin\Rev_Lin\tdrtest\REV_M1\rev_M1_4_4	3.84
19	27		26-May-1998	10:54:54 AM	Feng, Lin, Vogel	1687	Geotechnical\TDR Data\Lin\Rev_Lin\tdrtest\REV_M1\rev_M1_5_1	3.84

Table A3-2 A Part of Agency Table with Sample Data

Agency ID	Agency_Name	Contract_Number	Street_Address_1	Street_Address_2	City	Zip	State	Country	Phone_Number	Extension	Fax_Number	Email_Address
11	Geotech. Engr. (Dnevich)		Geotechnical Engineering,	Purdue University	West Lafayette	47906	IN	U.S.A.	(765) 494-5029	0000	(765) 496-1364	dnevich@purdue.edu

Table A3-3 GSD Table with Sample Data

LabTestID	Grain_Size	Sieve_Number	Percent_finer
12	0.075	200	0.413
13	0.075	200	0.413

Table A3-4 Lab Table with Sample Data

LabTestID	PMTDRID	Lab_Name	Supervisor	Sample_ID	Visual_Manual	Visual_Manual_Date	Visual_Manual_Tech	LL	PL	G_s	Atterberg_Date	Atterberg_Tech	GSD_date	GSD_Tech	USCS	Comment	AASHTO
8	13	Geotech. Lab	VPD	M1_1_1						2.76	26-May-1998		26-May-1998	Feng, Lin, Vogel	SM-SC		
12	15	Geotech. Lab	VPD	M1_1_2						2.76	26-May-1998		26-May-1998	Feng, Lin, Vogel	SM-SC		
13	16	Geotech. Lab	VPD	M1_1_3						2.76	26-May-1998		26-May-1998	Feng, Lin, Vogel	SM-SC		
14	17	Geotech. Lab	VPD	M1_1_4						2.76	26-May-1998		26-May-1998	Feng, Lin, Vogel	SM-SC		
15	22	Geotech. Lab	VPD	M1_2_1						2.76	26-May-1998		26-May-1998	Feng, Lin, Vogel	SM-SC		
16	23	Geotech. Lab	VPD	M1_2_2						2.76	26-May-1998		26-May-1998	Feng, Lin, Vogel	SM-SC		
17	24	Geotech. Lab	VPD	M1_2_3						2.76	26-May-1998		26-May-1998	Feng, Lin, Vogel	SM-SC		
18	25	Geotech. Lab	VPD	M1_2_4						2.76	26-May-1998		26-May-1998	Feng, Lin, Vogel	SM-SC		
19	26	Geotech. Lab	VPD	M1_3_1						2.76	26-May-1998		26-May-1998	Feng, Lin, Vogel	SM-SC		
20	27	Geotech. Lab	VPD	M1_3_2						2.76	26-May-1998		26-May-1998	Feng, Lin, Vogel	SM-SC		
21	28	Geotech. Lab	VPD	M1_3_3						2.76	26-May-1998		26-May-1998	Feng, Lin, Vogel	SM-SC		
22	29	Geotech. Lab	VPD	M1_3_4						2.76	26-May-1998		26-May-1998	Feng, Lin, Vogel	SM-SC		
23	30	Geotech. Lab	VPD	M1_4_1						2.76	26-May-1998		26-May-1998	Feng, Lin, Vogel	SM-SC		
24	31	Geotech. Lab	VPD	M1_4_2						2.76	26-May-1998		26-May-1998	Feng, Lin, Vogel	SM-SC		
25	32	Geotech. Lab	VPD	M1_4_3						2.76	26-May-1998		26-May-1998	Feng, Lin, Vogel	SM-SC		
26	33	Geotech. Lab	VPD	M1_4_4						2.76	26-May-1998		26-May-1998	Feng, Lin, Vogel	SM-SC		
27	34	Geotech. Lab	VPD	M1_5_1						2.76	26-May-1998		26-May-1998	Feng, Lin, Vogel	SM-SC		

Table A3-4 Lab Table with Sample Data

PMTDRID	AgencyID	Project_Name	Project_Number	Test_Number	Location_Description	State	County	Longitude	Latitude	Operator
13	11	Compaction of Mixture Soil 1-5		M1-1-1	Laboratory	IN	U.S.A.			Feng, Lin, Vogel
15	11	Compaction of Mixture Soil 1-5		M1-1-2	Laboratory	IN	U.S.A.			Feng, Lin, Vogel
16	11	Compaction of Mixture Soil 1-5		M1-1-3	Laboratory	IN	U.S.A.			Feng, Lin, Vogel
17	11	Compaction of Mixture Soil 1-5		M1-1-4	Laboratory	IN	U.S.A.			Feng, Lin, Vogel
22	11	Compaction of Mixture Soil 1-5		M1-2-1	Laboratory	IN	U.S.A.			Feng, Lin, Vogel
23	11	Compaction of Mixture Soil 1-5		M1-2-2	Laboratory	IN	U.S.A.			Feng, Lin, Vogel
24	11	Compaction of Mixture Soil 1-5		M1-2-3	Laboratory	IN	U.S.A.			Feng, Lin, Vogel
25	11	Compaction of Mixture Soil 1-5		M1-2-4	Laboratory	IN	U.S.A.			Feng, Lin, Vogel
26	11	Compaction of Mixture Soil 1-5		M1-3-1	Laboratory	IN	U.S.A.			Feng, Lin, Vogel
27	11	Compaction of Mixture Soil 1-5		M1-3-2	Laboratory	IN	U.S.A.			Feng, Lin, Vogel
28	11	Compaction of Mixture Soil 1-5		M1-3-3	Laboratory	IN	U.S.A.			Feng, Lin, Vogel
29	11	Compaction of Mixture Soil 1-5		M1-3-4	Laboratory	IN	U.S.A.			Feng, Lin, Vogel
30	11	Compaction of Mixture Soil 1-5		M1-4-1	Laboratory	IN	U.S.A.			Feng, Lin, Vogel
31	11	Compaction of Mixture Soil 1-5		M1-4-2	Laboratory	IN	U.S.A.			Feng, Lin, Vogel
32	11	Compaction of Mixture Soil 1-5		M1-4-3	Laboratory	IN	U.S.A.			Feng, Lin, Vogel
33	11	Compaction of Mixture Soil 1-5		M1-4-4	Laboratory	IN	U.S.A.			Feng, Lin, Vogel
34	11	Compaction of Mixture Soil 1-5		M1-5-1	Laboratory	IN	U.S.A.			Feng, Lin, Vogel

Data Integrity

The data model includes some integrity constraints to ensure accuracy of data when they are inserted or manipulated. These are known as entity integrity, or operational constraints. Examples include the field format (e.g. numeric vs. text), numeric format of numbers (e.g. number of decimals), field lengths (e.g. zip code length), and range constraints for parameter values.

Database Design and Relationships

The database can be divided into 5 parts: Agency, PMTDR, Lab, Compaction, and GSD. The relationships between these tables are described as follows:

- Each agency could have zero, one, or more PMTDR records, whereas each PMTDR record must belong to exactly one Agency.
- Each PMTDR record could have zero, one, or more Lab records associated with it, but each Lab record is related to only one PMTDR record.
- Each Lab record could have zero, one, or more GSD records, whereas each GSD record has to be related to exactly one Lab record.
- Each Lab record could have zero, one, or more Compaction records, but each Compaction record belongs to only one Lab record.

Figure A3.1 shows the database design elements, and Fig. A3.2 shows the developed database schema.

Data Access and Display

In order to display and store the data in a user-friendly manner, forms were created as a front-end interface for processing the data in each table. The main form was the Agency form, and other forms were incorporated as sub-forms within the main form. Both Compaction and GSD forms were introduced as tabs from within the Lab form, as shown in Fig. A3.3. Function buttons were

used to facilitate routine operations such as browsing the records, adding new records, delete existing records, duplicating entities, searching, saving, and printing.

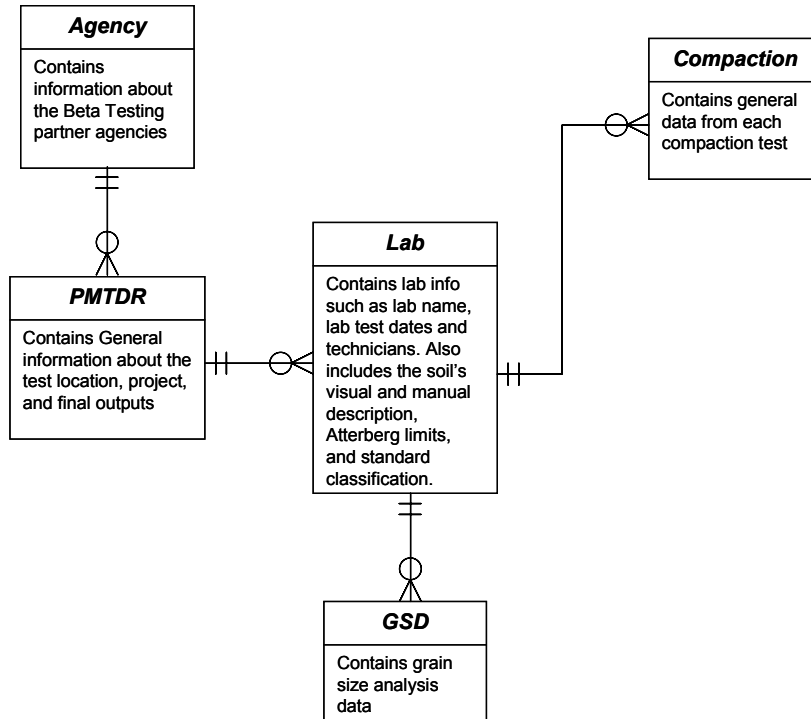


Fig. A3.1 Database Design Elements

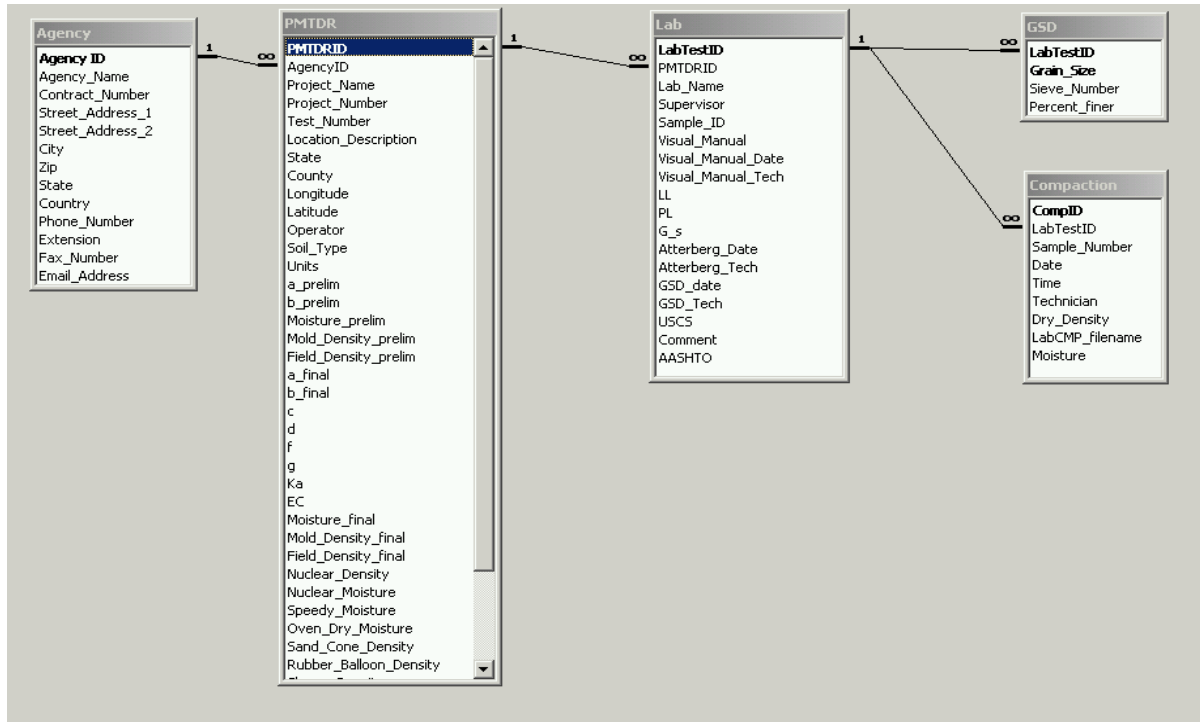


Fig. A3.2 Database Schema

Agency Name				Contract Number		
Geotech. Engr. (Dnevich)						
Street Address - Line 1		Street Address - Line 2		City	State	Zip
Geotechnical Engineering.		Purdue University		West Lafayette	IN	47906
Phone Number		Extension	Fax Number	Email Address		
(765) 494-5029		0000	(765) 496-1364	dnevich@purdue.edu		

Agency ID: 11

PMTDR

Agency ID	Project Name	Project (contract) Number	Test Number	Operator
11	Compaction of Mixture Soil 1-1		M1-1-1	Feng, Lin, Vogel

Location Description
Laboratory

State	County	Longitude	Latitude
IN	U.S.A.		

File Name and Path for MRP
File Name and Path for CMP

Soil Type	Original Units	Unit	Nuclear Density	Sand-Cone Density
Cohesionless	SI	c	kg/m ³	kg/m ³
Preliminary "a" Value	Final "a" Value	d	Nuclear Moisture Content	Rubber-Balloon Density
1	0.972		kg/m ³	kg/m ³
Preliminary "b" Value	Final "b" Value	f		Drive-Cylinder Density
9	8.015			kg/m ³
Preliminary Moisture Content	Final Moisture Content	g	Speedy Moisture Content	Sleeve Density
%	%		%	kg/m ³
Preliminary Mold Density	Final Mold Density	Ka		Other Density
kg/m ³	kg/m ³			kg/m ³
Preliminary Field Density	Final Field Density	EC	Oven-Dry Moisture Content	Actual Density
kg/m ³	kg/m ³	μS/cm	3.84 %	1750 kg/m ³

PMTDR ID: 13

LABORATORY

PMTDR ID	Laboratory Name	Supervisor	Sample ID
13	Geotech. Lab	VPD	M1_1_1

Visual-Manual Tests Date
Visual Manual Classification
Visual-Manual Technician

Atterberg Test Date	GSD date	Specific Gravity
26-May-1998	26-May-1998	2.76
Atterberg Test Technician	GSD Technician	Comments
	Feng, Lin, Vogel	
Liquid Limit	Plastic Limit	USCS
		SM-SC
AASHTO		

Lab Test ID: 8

GSD COMPACTION

LabTestID	Sample Number	Date	Time	Technician
8				
File Name and Path for Laboratory CMP	Dry Density	Moisture Content		
	kg/m ³	(%)		

Record: 2 of 2

Fig. A3.3 Database interface